

LOW SYMMETRY Pincer Ligands Designed for Applications
in Coordination Chemistry and Catalysis

by

Khrystyna Herasymchuk

Bachelor in Science, Chemistry

Ryerson University, Toronto, Ontario, Canada 2012

A thesis presented to Ryerson University

In partial fulfillment of the

Requirements for the degree of

Master of Science

In the Program of

Molecular Science

Toronto, Ontario, Canada 2014

© Khrystyna Herasymchuk 2014

AUTHOR'S DECLARATION FOR ELECTRONIC SUBMISSION OF A THESIS

I hereby declare that I am the sole author of this thesis. This is a true copy of the thesis, including any required final revisions, as accepted by my examiners.

I authorize Ryerson University to lend this thesis to other institutions or individuals for the purpose of scholarly research.

I further authorize Ryerson University to reproduce this thesis by photocopying or by other means, in total or in part, at the request of other institutions or individuals for the purpose of scholarly research.

I understand that my thesis may be made electronically available to the public.

LOW SYMMETRY Pincer Ligands Designed for Applications in Coordination Chemistry and Catalysis

Master of Science, 2014

Khristyna Herasymchuk

Molecular Science

Ryerson University

ABSTRACT

Pincer ligands are monoanionic, tridentate binding molecules that have been used in coordination chemistry as efficient homogeneous and heterogeneous catalysts (*i.e.* as transition metal complexes). The focus of this work lies in the synthesis, characterization and coordination chemistry of a series of novel asymmetric potentially monoanionic NN'N'', NN'C and NN'P type pincer ligands with amide functionality derived from the skeleton of 2-(2'-aniliny)-4,4-dimethyl-2-oxazoline. Modular approach to this synthesis has been developed through an alkyl halide intermediate, in addition to the substrate-dependent alternative pincer syntheses, which are also described. The coordination chemistries of Pd and Ni, as well as the potential application of these pincer complexes in metal mediated catalysis of aldehyde allylation reactions will be explored. Moreover, a number of Pd(II) pincer complexes have been successfully synthesized and structurally characterized and these results are likewise described.

ACKNOWLEDGMENTS

It has been four years, and five summers since I have met Dr. Gossage and was fortunate to work under his supervision. I would like to begin by thanking him for his mentorship and friendship, his true support and motivation during the course of this thesis, as well as some great giggles along the way.

I would also like to thank Dr. Koivisto and Dr. Viirre for their help, motivation, support and contribution to my work. Both of you are extraordinary chemists and educators and I feel so fortunate to have been your student.

A sincere thanks goes to Dr. McWilliams and Dr. Wylie for taking their time to read my thesis and help me make it even better. My gratitude extends to Dr. Foucher, Dr. Wylie and Dr. Gossage for their pivotal role in my career growth. As they opened their doors to a student volunteer all those summers back. It is thanks to you that I am where I am today.

Now onto the life-long friendships that have been *synthesized* during the course of this work and my studies at Ryerson. Michelle, friend, you have been there for me even when no other friend was, always caring, supporting and cheering me on all the way. You are truly the greatest friend one can ask for! I would like to also mention Jennifer, who has been working alongside with me and has helped me tremendously. You are the most humble and selfless person I know! How can I forget about the biggest distraction (yes, you beat Michelle) – Shane (*a.k.a.* Robin), thanks for your friendship and keeping the lab “safe”. I want to thank Jeffrey, Tamara, Alina, Maryam, Mahroo, Grace, Aman, Billy, Devin, Nande and Jon for your friendship and support. Shout out to KHN202, KHE211 and KHE322C – the friendliest environment and grads! Thank you all for being simply amazing people!

Special thank you goes out to the most important person in my life, Dima, whose love and support means the world to me. Thank you for always being there for me!

To my parents,

Марії і Павлу

TABLE OF CONTENTS

ABSTRACT	III
ACKNOWLEDGMENTS	IV
DEDICATION	V
TABLE OF CONTENTS	VI
LIST OF FIGURES	VIII
LIST OF SCHEMES	IX
LIST OF TABLES	X
LIST OF ABBREVIATIONS	XI
CHAPTER 1.0 – INTRODUCTION.....	1
1.1 Pincer ligands and complexes	1
1.1.1 Oxazoline-containing pincer ligands and their complexes	3
1.1.2 Asymmetric pincer complexes in catalysis.....	4
1.2 PREVIOUS WORK	13
1.3 THESIS OBJECTIVE.....	14
CHAPTER 2.0 – LIGANDS	16
2.1 AMINO ACID ROUTE	16
2.2 MODULAR APPROACH	18
2.2.1 Synthesis of Pincers 3b-3j	20
2.2.2 Synthesis of 3k	23
2.2.3 Synthesis of 3l : a carbene-pincer precursor	25
2.2.4 Synthesis of 3m and 3m•oxide	26
2.2.5 Synthesis of 3n	27
2.3 CHIRAL DERIVATIVES	28
CHAPTER 3.0 – COMPLEXES	30
3.1 PALLADIUM COMPLEXES	30

3.1.1 <i>NNN type pincer complexes</i>	30
3.1.2 <i>NNC type pincer complex</i>	32
3.1.3 <i>NNP type pincer complex</i>	34
3.2 ATTEMPTS AT THE SYNTHESIS OF NICKEL COMPLEXES	36
3.2.1 <i>NNN type pincer complexes</i>	36
3.2.2 <i>NNC type pincer complex</i>	37
3.2.3 <i>NNP type pincer complex</i>	37
CHAPTER 4.0 – CATALYSIS	39
4.1 ALLYLATION OF ALDEHYDES.....	39
CHAPTER 5.0 – EXPERIMENTAL	43
5.1 GENERAL	43
5.2 LIGANDS	44
5.3 PALLADIUM COMPLEXES	63
5.4 CATALYSIS	76
CHAPTER 6 – CONCLUSION AND FUTURE WORK	77
CHAPTER 7 – APPENDIX	78
7.1 NMR SPECTRA	78
7.3 X-RAY CRYSTALLOGRAPHY	143
CHAPTER 8 – REFERENCES	177

LIST OF FIGURES

Figure 1.1 Classification of ligands (L = ligand, M = metal atom).....	1
Figure 1.2. General depiction of a pincer ligand, where M = metal, L = ancillary ligand and X, Y = linking atoms for A (E = E'), for B (E = E') and C (E ≠ E').....	3
Figure 1.3 Structure of oxazoline (4,5-dihydro-2-oxazoline).....	4
Figure 1.4 Structures of [PdCl ₂ (2-ethyl-2-oxazoline) ₂] (D) and 1,3-bis-(4,4-dimethyl-2-oxazoliny)benzene (E).....	4
Figure 1.5 Asymmetric Ru and Os pincer complexes.	6
Figure 1.6 Ru complex with NNC pincer ligand.....	7
Figure 1.7 Asymmetric NNC pincer complexes with Ru, Rh, Pd and Au	9
Figure 1.8 Pd(II) complex with NNC pincer type ligand.....	10
Figure 1.9 Ru(II) complex with NNP pincer ligand.....	12
Figure 1.10 Synthesis of PNN Ru complex (O).	12
Figure 1.11 Structures of NNN pincer ligand (P) and Cu NNN pincer complex (Q)	14
Figure 1.12 κ^4 -PNN'O pincer-like complexes with an amide moiety.....	14
Figure 1.13 Classification of NN'L type pincer complex (M = metal, L = ligand)	15
Figure 2.1 X-ray crystal structure of 2 (on the left; solved by Alan Lough) and calculated (DFT) structure of 2 at the B3LYP: 6-311++G** theory level (on the right)	19
Figure 2.2 X-ray crystallographic structure of 3m•oxide (Solved by Laura R. Fernández).	27
Figure 2.3 X-ray crystal structure of 6 (Solved by Robert A. Gossage).....	29
Figure 3.1 Crystal structures of 9a (left) and 9h (right) solved by Laura R. Fernández	31
Figure 3.2 The comparison of the ¹ H NMR spectra for 3l and 9l	33
Figure 3.3 Select ¹ H chemical shifts for 3m•oxide and 9m , depicting splitting effect ...	35

LIST OF SCHEMES

Scheme 1.1	The evolution of pincer definition	2
Scheme 1.2	Transfer hydrogenation of ketones catalyzed by F and G	6
Scheme 1.3	Catalytic transformations using Ru NNC pincer complex, H	8
Scheme 2.1	Synthesis of NNN type pincer ligand using 1 and amino acids	16
Scheme 2.2	Synthesis of NNN type pincer ligand from <i>N,N</i> -dimethylglycine	16
Scheme 2.3	Synthesis of compound 2 – pincer precursor	18
Scheme 2.4	Synthesis of NNN type pincer ligands through a modular approach	21
Scheme 2.5	Synthesis of an extended pincer NNNO, 3k , from <i>N</i> -methylaminoethanol	24
Scheme 2.6	Synthesis of NNC pincer ligand, 3l from 1-benzylimidazole	25
Scheme 2.7	Synthesis of NNP pincer ligand, 3m , from potassium diphenylphosphide	26
Scheme 2.8	Synthesis of 3n from 1	28
Scheme 2.9	Synthesis of the chiral derivatives, 6 and NNN type pincer ligand, 7	28
Scheme 3.1	Synthesis of Pd-NNN pincer complexes, 9a-e and 9g-k	30
Scheme 3.2	Synthesis of Pd-NNC pincer complex, 9l	32
Scheme 3.3	Synthesis of Pd-NNP pincer complex, 9m	34
Scheme 3.4	Synthesis of Ni-NNC type pincer complex from 3l ligand	37
Scheme 3.5	Synthesis of Ni-NNP pincer complex	38
Scheme 4.1	Bis(allyl)palladium in catalysis.	39
Scheme 4.2	Allylation of <i>para</i> -substituted benzaldehydes catalyzed by 9b	40
Scheme 4.3	A proposed mechanism for the allylation of aldehydes	42

LIST OF TABLES

Table 1.1 Heck and Stille cross-coupling reactions catalyzed by M	11
Table 1.2 Transfer hydrogenation of ketones catalyzed by NNP Ru complex (O)	13
Table 1.3 Esterification of primary alcohols catalyzed by Ru NNP complex (O)	13
Table 2.1 IR spectrum analysis for NNN type pincer ligands.....	17
Table 2.2 Experimental and calculated hydrogen bond lengths and angles for 2	19
Table 2.3 Select ¹ H NMR chemical shifts and yields for 2 , 3a-3m•oxide , 6 and 7	22
Table 2.4 Protection of the hydroxyl group on the <i>N</i> -methyaminoethanol	23
Table 2.5 Select literature and experimental ³¹ P NMR chemical shifts for PNN pincer .	26
Table 3.1 Synthesis of Ni-NNN type pincer complex from 3e ligand	36
Table 4.1 Pd-NNN pincer complex-catalyzed allylation of select aldehydes	41
Table 4.2 Comparison of ¹ H NMR chemical shifts for aldehyde allylation reaction	41

LIST OF ABBREVIATIONS

B3LYP	Becke 3 Lee Yang Parr
CDCl₃	Chloroform-d ₁
DCC	<i>N,N'</i> -Dicyclohexylcarbodiimide
DCFC	Dry-column flash chromatography
DCM	Dichloromethane
DFT	Density functional theory
DMAP	4-Dimethylaminopyridine
DME	Dimethoxyethane
DMTMM	4-(4,6-Dimethoxy-1,3,5-triazin-2-yl)-4-methylmorpholinium chloride
Et	Ethyl
Et₂O	Diethyl ether
Et₃N	Triethylamine
EtOH	Ethanol
h	Hour(s)
IR	Infrared
LDA	Lithium diisopropylamide
Me	Methyl
MeCN	Acetonitrile
Mp	Melting point
<i>n</i>BuLi	Butyllithium
NHC	<i>N</i> -Heterocyclic carbene
NMR	Nuclear magnetic resonance
Ph	Phenyl
R_f	Retardation factor
RT	Room temperature
S_N2	Bimetallic nucleophilic substitution
SPS	Solvent purification system
<i>t</i>BuOK	Potassium <i>tert</i> -butoxide

THF	Tetrahydrofuran
TLC	Thin layer chromatography
TMSCI	Trimethylsilyl chloride
TOF	Turnover frequency

CHAPTER 1 – INTRODUCTION

1.1 PINCER LIGANDS AND COMPLEXES

Even though coordination compounds have existed for a long time, it was not until the late nineteenth century that Alfred Werner proposed the octahedral structures for Co(III) complexes, and as such pioneered this area of study. He was awarded the Nobel Prize in chemistry for his work on coordination compounds in 1913 and has since been referred to as the “Father of Coordination Chemistry”.^{1,2} In coordination chemistry, **ligand** can be defined as an ion or molecule bound to a metal atom through a coordinating bond, forming a **coordination complex**. This bond is due to an electron pair donation from the ligand to the metal. In contrast, a **chelating ligand** has two or more points of attachment to the metal centre. Ligands can also be described as mono-, bi-, tri-, tetra-, penta- and hexadentate, having one through six atoms of attachment, respectively (see **Figure 1.1**).³

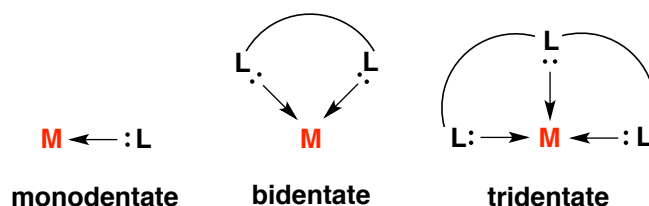
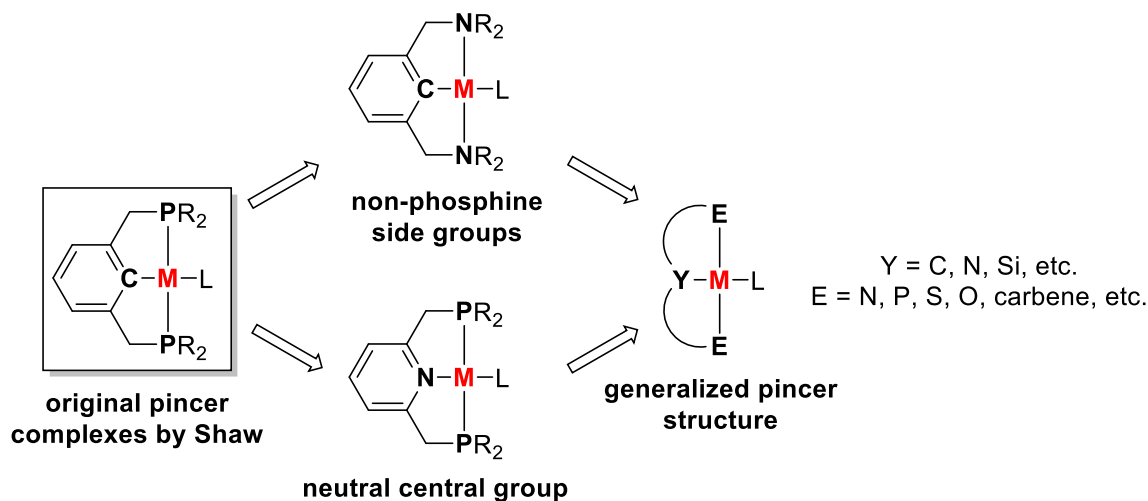


Figure 1.1 Classification of ligands (L = ligand, M = metal atom).

Over the years chelating ligands have been of much interest and use for catalytic purposes.^{4,5} An important class of chelate chemistry is comprised of pincer ligands and their complexes. Ever since the original PCP type pincer ligand was reported by Molton and Shaw in 1976⁶ (**Scheme 1.1**) – pincer complexes have become prominent as homogeneous and heterogeneous catalysts in both organic synthesis and materials

science.⁷⁻¹² But it was not until late 1980s that this class of ligands received the name of the ‘pincer’, a term coined by the pioneer in the field – Gerard van Koten.

Pincers can be defined as tridentate ligands with one formal anionic coordinating atom and two neutral coordinating atoms binding to a central atom in typically a *mer* configuration.^{13,14} Over the years, this definition has been broadened (**Scheme 1.1**), and the scope of pincer chemistry has been extended to encompass various coordinating atoms (e.g., P, N, S, O).¹ To control the property of a metal centre, the pincer ligand framework can be modified with respect to both steric and/or electronic features. This has led to the development of a large number of different types of pincer ligands. The coordination modes of pincer ligands in complexes have been found to be L_3 , L_2X , LX_2 , and X_3 (where L = neutral atom and X = anionic atom)¹⁵



Scheme 1.1 The evolution of the pincer definition.

Depending on the character of the coordinating atoms on the pincer ligand, each individual M-ligand interaction can either be reinforced or competed against. For example, having σ -donating or π -accepting phosphanyl groups on a PCP pincer can either reinforce or compete against a σ -donating central aryl moiety – this provides a

certain level of control over the dipolar nature of the pincer complex.¹⁶ The unique qualities of pincer ligands include: their typical high thermal stability, as well as imparting a greater reactivity to transition metal complexes versus those without pincer-type ligands.¹⁶⁻¹⁸

From the onset of the pincer chemistry, the research focus lied on the ECE type pincer ligands with the central position having an anionic C_{ipso} , (part of the phenyl ring), with two identical *ortho* substituents (**A**, **Figure 1.2**).¹⁹ Lately the research into pincer chemistry led to investigations of non-carbon monoanionic framework²⁰ with two *ortho* moieties having different substituents, as well as having different E donor atoms all together, giving it C_1 point group symmetry (**B** or **C**, **Figure 1.2**). The manipulation of a pincer ligand with respect to its structure is an endless endeavour.

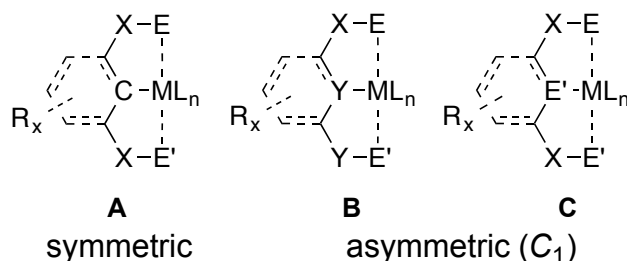


Figure 1.2. General depiction of a pincer ligand, where M = metal, L = ancillary ligand and X, Y = linking atoms for **A** ($E = E'$), for **B** ($E = E'$) and **C** ($E \neq E'$).²¹

1.1.1 Oxazoline-containing pincer ligands and their complexes

The oxazoline, a subclass of oxazoles, is a five-membered heterocyclic organic compound with O and N atoms connected through an sp^2 hybridized C atom (**Figure 1.3**).¹³ It plays an important role in transition metal chemistry, since oxazoline-based ligands have been investigated extensively in recent years and show great number of applications in homogeneous catalysis.²²

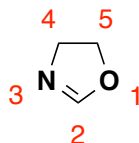


Figure 1.3 Structure of the oxazoline (4,5-dihydro-2-oxazoline) showing the typical numbering scheme.

Metal complexes formed with oxazoline moieties, combined with phosphorus, nitrogen or oxygen as donor atoms, often showcase interesting electronic properties associated with catalysis.²² For example, it has also been shown that Pd complexes containing oxazoline moiety (**D**, see **Figure 1.4**) have demonstrated oxidatively robust systems with respect to applications in cross coupling reactions.²³

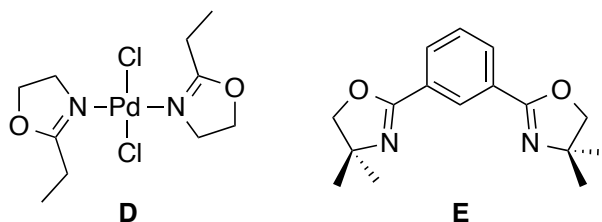


Figure 1.4 Structures of $[\text{PdCl}_2(2\text{-ethyl-2-oxazoline})_2]$ (**D**) and 1,3-bis-(4,4-dimethyl-2-oxazoliny)benzene (**E**).

Incorporation of an oxazoline moiety into pincer ligands has also been investigated. Coordination of pincer ligand **E** (**Figure 1.4**) and its derivatives has been studied with Pt and Pd metals, showcasing successful application in catalysis of carbon-carbon bond forming reactions.²⁴⁻³⁰

1.1.2 Asymmetric pincer complexes in catalysis

Since asymmetric pincer ligand complexes have gained the spotlight in the scientific community, their catalytic activity has been of great interest. Some of the reactions that they were found to catalyze include: ethylene polymerization, hydrogenation, transfer hydrogenation, dehydrogenation or oxidation (of alcohols), cyclopropanation, and such

cross-coupling reactions such as the Kumada (coupling of an organic halide and Grignard reagent), Suzuki (coupling of an organic halide and boronic acid), Heck (coupling of an organic halide and an alkene) and Stille (coupling of an organo halide and organotin) coupling reactions.³¹⁻³⁶

Transition metal pincer complexes have also shown great potential in stoichiometric and catalytic reactivity,^{19,37} however, chiral complexes have been investigated less because the auxiliary ligands have been responsible for the enantioselectivity in catalysis.⁷ Pincer complexes also exhibit high thermal stability and interesting properties of robustness, which make them even more desirable for homogeneous catalysis.³⁷

The environmental aspect of any chemical transformation is greatly affected by the amounts and types of reagents used. That is why the use of catalyst is preferred over the use of stoichiometric amounts of reagents.³⁸

One of the most important reactions involved in producing chiral alcohols is the asymmetric reduction of ketones. So far, Ru, Rh, Ir and Os complexes have been synthesized and successfully applied in ketone hydrogenation and transfer hydrogenation reactions. For Ru catalyzed process, the presence of an -NH₂ group is crucial for the catalysis and formation of Ru-H hydride, this relationship can be described as a *metal-ligand bifunctional catalysis*.³² Based on this find, Baratta *et al.* have developed new Ru (and Os) complexes with chiral asymmetric NNC pincer ligands that carry an -NH₂ functionality. The presence of the σ metal-carbon bond in these complexes has been shown to prevent catalyst deactivation and at the same time ensures high stability and productivity. During catalysis the Ru pincer complex is formed *in situ*, and hence had to be isolated separately to study in detail.³⁹

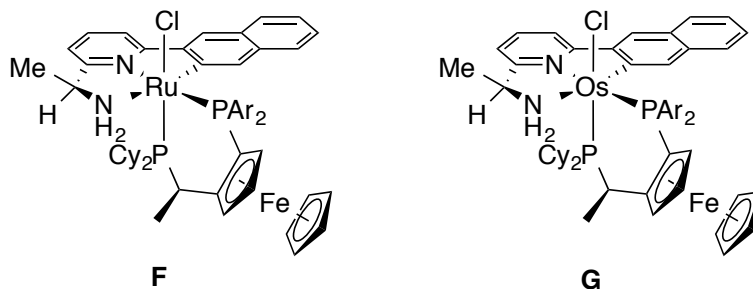
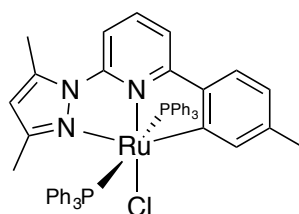


Figure 1.5 Asymmetric Ru and Os pincer complexes.

Preliminary catalytic study of Ru and Os complexes identified complex **F** and **G** as the most suitable candidates for further catalytic investigation. Transfer hydrogenation of ketones catalyzed by **F** and **G** showed promising results (**Scheme 1.2**), where ketones have been reduced to their secondary alcohol forms with 80-99% conversion, 92-99% ee and TOF ranging from 1.9 to $26 \times 10^4 \text{ h}^{-1}$ for **F** and 93-99% conversion, 90-99% enantioselectivity and TOF ranging from 5.1 to $90 \times 10^4 \text{ h}^{-1}$ for **G**. However, attempts at the reduction of sterically demanding ketones revealed low alcohol conversions of only up to 20%. Overall, both Ru and Os NNC complexes used in transfer hydrogenation of ketones proved to be effective catalysts, with **G** having the greatest percentage conversion(s) and TOF.³⁹

Scheme 1.2 Transfer hydrogenation of ketones catalyzed by **F** and **G**.



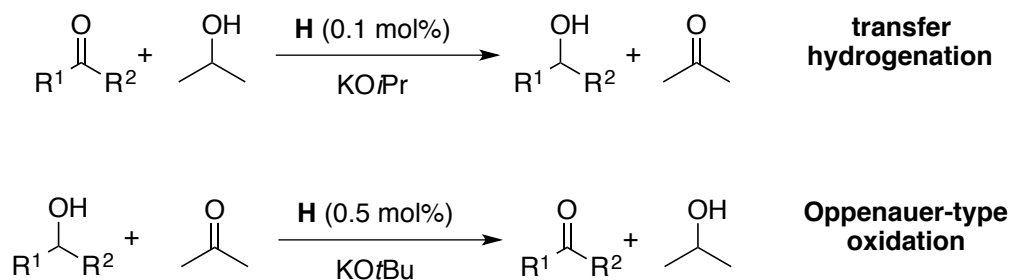
H

Figure 1.6 Ru complex with NNC pincer ligand

The complex **H** was characterized using NMR spectroscopy, and it was shown through a $^{31}\text{P}\{^1\text{H}\}$ NMR spectrum that the two PPh_3 are magnetically identical and are positioned *trans* to each other because of a singlet observed at $\delta_{\text{p}} = 26.4$ ppm. The complex was also characterized using X-Ray crystallography and was shown to have a neutral molecular structure with the NNC ligand in nearly a planar tridentate orientation.⁴⁰

The transfer hydrogenation of ketones was carried out in 2-propanol under a nitrogen atmosphere in the presence of 0.1 mol% of the catalyst, **H** (see **Scheme 1.3**). A variety of substituted ketones were transformed, including substituted acetophenones, aliphatic cyclic and acyclic ketones. Overall, the conversion of the ketones was observed to be greater than 98% within 1 min with TOF values of up to $18 \times 10^4 \text{ h}^{-1}$. The ketones with electron-withdrawing substituents on the aryl rings had a higher rate of reaction, whereas *ortho* substituted ketones had a reduced reaction rate due to the steric considerations. It should be noted that no transfer hydrogenation is observed in the absence of a base.⁴⁰

The Oppenauer-type oxidation is a widely used method for production of carbonyl compounds without using stoichiometric amounts of oxidants. Similar to the transfer hydrogenation reactions above, the secondary alcohols undergo dehydrogenative oxidation with **H** (0.5 mol%) with *t*BuOK (10 mol%) in refluxing acetone (**Scheme 1.3**).



Scheme 1.3 Catalytic transformations using Ru NNC pincer complex, **H**.

The oxidation of alcohols was successfully carried out from 1 min to 3 h, averaging at conversions greater than 97% and with TOF values of up to $1.2 \times 10^4 \text{ h}^{-1}$. This catalytic activity represents one of the best reported to date.⁴⁰

The coordination of the Ru, Rh, Pd and Au with NNC pincer ligands was reported to work through Lin's method of transmetallation.³⁸ Reacting the NNC pincer ligands with Ag_2O in DCM – produced a silver(I) intermediate complex. With the addition of each appropriate metal precursor to the reaction solution directly, allowed for the complexes **I** – **L** to be formed in excellent yields (>90 %). Upon coordination of the ligands, a new chiral centre is introduced in all of the complexes (**Figure 1.7**), and the coordination of Ru is completely stereospecific.³⁸

Catalytic behaviour of **I** was tested on a hydrogenation reaction of diethyl citraconate and diethyl 2-benzylidenesuccinate. All the catalysts show high enantioselectivity and activity for the hydrogenation of diethyl 2-benzylidenesuccinate, the enantioselectivity is low with respect to the desired enantiomer, even though activity is high for the diethyl citraconate substrate.³⁸

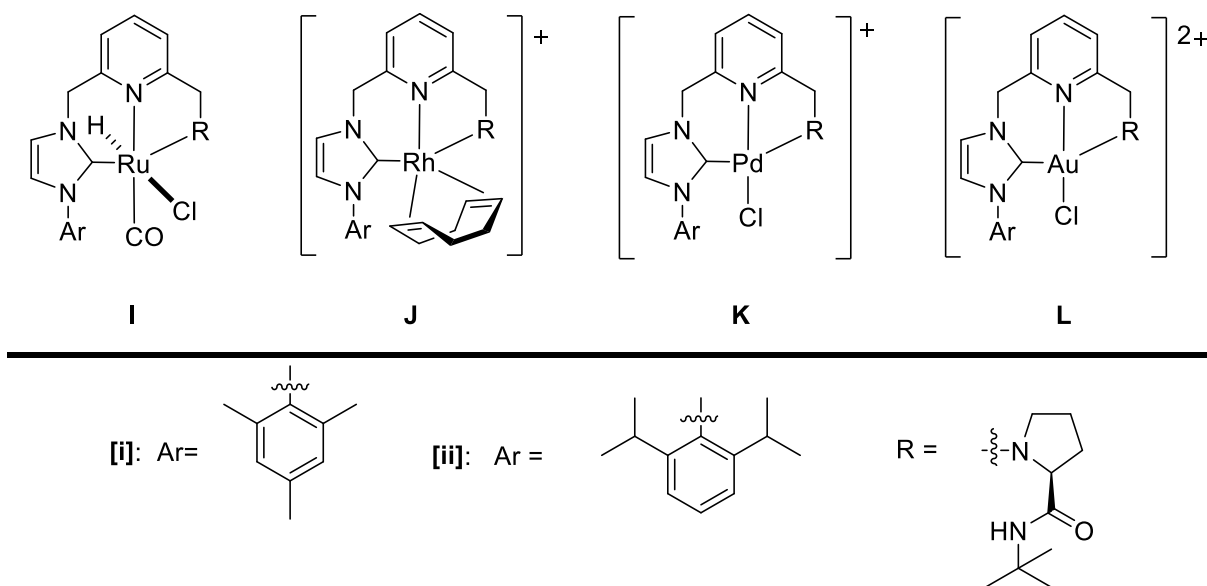


Figure 1.7 Asymmetric NNC pincer complexes with Ru, Rh, Pd and Au.

Prior to the synthesis of NNC Ru complexes (**I**), Boronat *et al.* looked at the chemistry of the NNC pincer type ligand of Rh (**J**), Pd (**K**) and Au (**L**).⁴¹ Catalytic activity of Rh complexes (**J**[i-ii]) was tested on hydrogenation of olefins, exhibiting high TOF but very low enantioselectivity for diethyl itaconate hydrogenation. Whereas, hydrogenation of diethyl 2-benzylidene succinate was successfully catalyzed by **J**[i] with good enantioselectivity of 82% for the *S* stereoisomer and **J**[ii] with excellent enantioselectivity (99%) for the *R* isomer. However, the reaction rates are much lower.⁴¹ Catalytic activity of **K**[i] and **K**[ii] was also tested on the hydrogenation of olefins as well. Just like with Rh and Au, the reaction rate is higher for the hydrogenation of both diethyl itaconate and diethyl 2-benzylidene succinate catalyzed by **K**[i], however the enantioselectivity with respect to the *S* isomer is again very low. On the other hand, **K**[ii] shows superior enantioselectivity for the *R* form with moderate reaction rate(s) for the hydrogenation of diethyl 2-benzylidene succinate.⁴¹

When the catalytic activity of **L[i]** and **L[ii]** was tested on hydrogenation of olefins, both Au complexes (**L[i-ii]**) showed great enantioselectivity in hydrogenation of diethyl 2-benzylidene succinate with moderate reaction rates. However, the reaction rate(s) observed for diethyl itaconate hydrogenation was much higher for both of the Au catalysts, but the enantioselectivity was very low.⁴¹

Previous attempts at the synthesis of anionic isoindoline based NNC Pd complex resulted in a neutral NNC pincer. Broring *et al.* reported Pd complex coordinated to an anionic NNC pincer ligand (**M**, **Figure 1.8**) and its first application in catalysis.⁴²

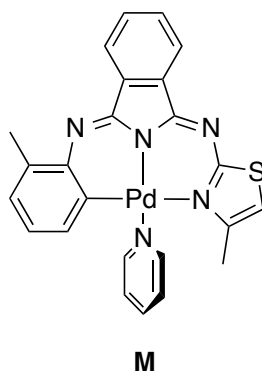


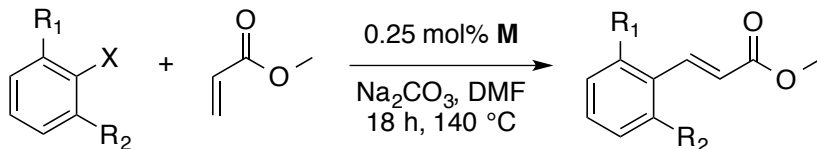
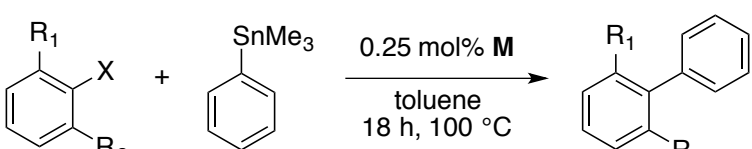
Figure 1.8 Pd(II) complex with an NNC pincer type ligand.

Complex **M** was characterized by both 1D and 2D NMR spectroscopy as well as X-ray crystallography, all supporting the proposed structure. The X-ray structure suggests an almost perfect square planar geometry around Pd and an unanticipated helical twist of the 2-tolyl ligand.⁴²

The catalytic activity of complex **M** was tested on Heck and Stille cross-coupling reactions; for comparison purposes Pd(OAc)₂ was used as a standard (**Table 1.1**). When **M** was used in Heck cross-coupling reaction – the reactivity of the reaction decreases with X = I > X = Br > X = Cl as expected (with yields of 96%, 33% and 1%, respectively). With an increase in steric hindrance (*i.e.* changing the substrates from R₁

= R₂ = H to R₁ = R₂ = Me) the yield of the reaction decreased from 96% to 78%, respectively. The same pattern was observed in the catalysis of Stille cross-coupling reaction. Moreover, steric hindrance effect was well-defined, the change in substrate (R₁ = R₂ = H to R₁ = R₂ = Me) yielded products from 40% to 20%.⁴²

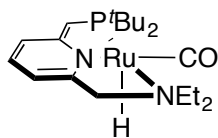
Table 1.1 Heck and Stille cross-coupling reactions catalyzed by **M**

Substrate	Yield (%)	TON	TOF (min ⁻¹)
<i>Heck coupling</i>			
			
R ₁ =R ₂ =H, X=I	73 ^a	297	0.27
R ₁ =R ₂ =H, X=I	96	385	0.36
R ₁ =R ₂ =H, X=Br	33	133	0.12
R ₁ =Me, R ₂ =H, X=I	98	392	0.36
R ₁ =R ₂ =Me, X=I	78	315	0.29
<i>Stille coupling</i>			
			
R ₁ =R ₂ =H, X=I	23 ^a	89	0.09
R ₁ =R ₂ =H, X=I	40	154	0.16
R ₁ =R ₂ =H, X=Br	39	153	0.15
R ₁ =Me, R ₂ =H, X=I	35	135	0.14
R ₁ =R ₂ =Me, X=I	20	78	0.08

^a Pd(OAc)₂ as the catalyst;

Dehydrogenation reactions are coupling reactions that can produce amides, imines, esters and ketones with elimination of H₂. These reactions have been studied extensively, and have been shown to be successfully catalyzed by Ru complexes with NNP or PNP pincer ligands as part of their structure; in some cases in the presence of catalytic amounts of base.^{43,44} Li and Zeng were able to propose the mechanism for the

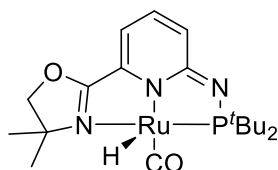
dehydrogenative coupling of alcohols with amines catalyzed by NNP-Ru(II) hydride complex (**N**, **Figure 1.9**) through density functional theory (*i.e.* DFT) calculations.⁴³



N

Figure 1.9 Ru(II) complex with NNP pincer ligand.

Other mechanistic studies showed that addition of base is unnecessary in hydrogenation/dehydrogenation reactions if an NNP Ru hydrido complex is used. An example of such complex, **N**, is an excellent catalyst for a vast amount of hydrogenation reactions, the coupling of alcohols and amines and the splitting of water into hydrogen and oxygen gas.⁴⁴



O

Figure 1.10 Synthesis of PNN Ru complex, **O**.

The NNP Ru pincer complex, **O** (**Figure 1.10**) was used in catalytic transfer hydrogenation reactions (**Table 1.2**) exhibiting product yields of up to 99%. It was later tested on the esterification of primary alcohols (**Table 1.3**) giving the desired product in as high as 99% yield. As with transfer hydrogenation reactions, esterification of alcohols is catalyzed in the absence of a base.⁴⁵

Table 1.2 Transfer hydrogenation of ketones catalyzed by NNP Ru complex (**O**).

$ \begin{array}{c} \text{O} \\ \parallel \\ \text{R}^1-\text{C}-\text{R}^2 \end{array} + \begin{array}{c} \text{OH} \\ \\ \text{CH}_3-\text{CH}-\text{CH}_3 \end{array} \xrightarrow[\text{iPrOH}]{\text{Catalyst (1.0 mol\%)}} \begin{array}{c} \text{OH} \\ \\ \text{R}^1-\text{CH}-\text{R}^2 \end{array} + \begin{array}{c} \text{O} \\ \parallel \\ \text{CH}_3-\text{C}-\text{CH}_3 \end{array} $		
Entry	Ketone	Yield (%)
5	cyclohexanone	99
6	cyclohexanone	91
7	2-hexanone	94
8	2-heptanone	91
9	acetophenone	74

^a1.0 mol% KO^tBu was added; Conditions:
in 1 mL of *i*PrOH at 40 °C.

Table 1.3 Esterification of primary alcohols catalyzed by Ru NNP complex (**O**).

$ \begin{array}{c} \text{R}-\text{CH}_2-\text{OH} \end{array} \xrightarrow{\text{catalyst}} \begin{array}{c} \text{O} \\ \parallel \\ \text{R}-\text{C}-\text{O}-\text{CH}_2-\text{R} \end{array} + 2 \text{H}_2 $					
Entry	Cat. (mol%)	Alcohol	T (°C)	Time (h)	Yield (%)
1	0.3	1-butanol	118	12	99
2	0.3	1-pentanol	138	12	97
3	0.1	1-hexanol	160	24	98
4	0.5	1-phenylmethanol	160	12	94

The examples detailed above give a strong background portfolio that clearly shows that metal-pincer complexes have great potential as asymmetric catalysts and stoichiometric promoters.

1.2 PREVIOUS WORK

Gossage *et al.* previously reported the synthesis of the formally C₁-symmetric amide pincer ligand (**P**, **Figure 1.11**) through the *in situ* chlorination of picolinic acid and its reaction with 4,4-dimethyl-2-(*o*-aniliny)-2-oxazoline.⁴⁶

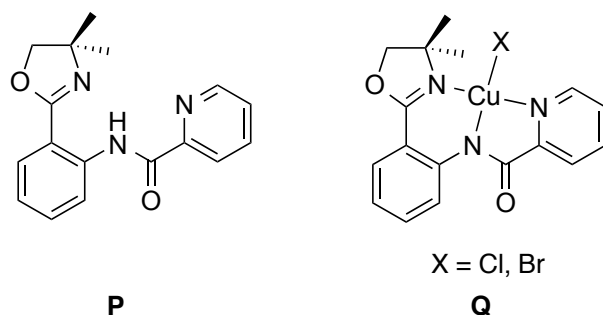


Figure 1.11 Structures of NNN pincer ligand (**P**) and Cu NNN pincer complex (**Q**).

The coordination chemistry of **P** with Cu centres (**Q**, **Figure 1.11**) has been studied in the Gossage group with the purpose of applying these complexes in catalysis such as the Henry reaction.⁴⁷ To our knowledge, the use of the amide moiety in the chelating ligands (**N**, as a monoanionic coordinating atom) has only been reported by Durran *et al.* in 2010 (**R**, **Figure 1.12**).⁴⁸ The synthesis and complexation of the tetradentate ligands and their complexes with Pt(II), Pd(II) and Ni(II) were studied.⁴⁸

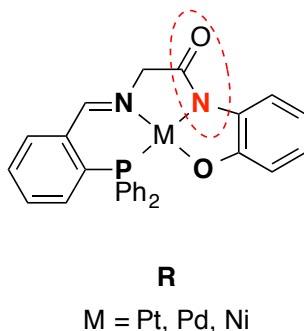


Figure 1.12 κ^4 -PNN'O pincer-like complexes with an amide moiety.

1.3 THESIS OBJECTIVE

The objective of this work lies in the design of the asymmetric pincer ligands of the NNN, NNC and NNP types (shown in **Figure 1.13**). The study of the coordination chemistry of these ligands with Pd and Ni metals as well as the application of the synthesized pincer complexes in catalysis will be explored. These monoanionic pincer

ligands coordinate in a square planar fashion with Pd and Ni. Catalytic investigations into their activity in C-C bond forming reactions will be explored.

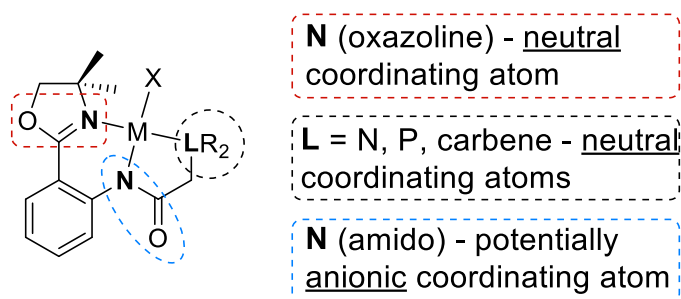
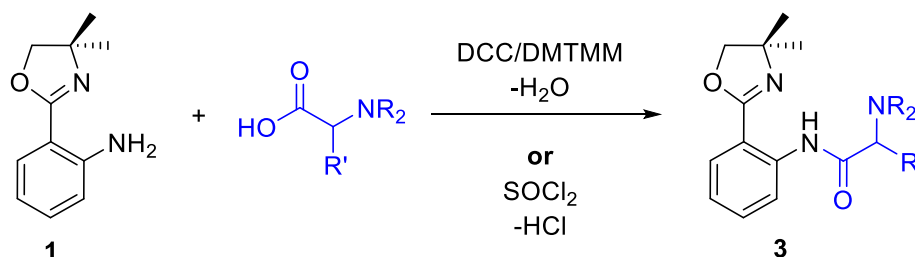


Figure 1.13 Classification of NN'L type pincer complex (M = metal, L = ligand).

CHAPTER 2 – LIGANDS

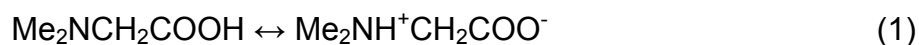
2.1 Amino acid route

Conversion of compound **1** into the respective pincer ligand was initially proposed to take place through an amide coupling with an appropriate amino acid. The formation of the amide bond could be attained either through the use of peptide coupling agents (*i.e.* DCC or DMTMM) or through the formation of an acyl chloride (**Scheme 2.1**).^{50,51}

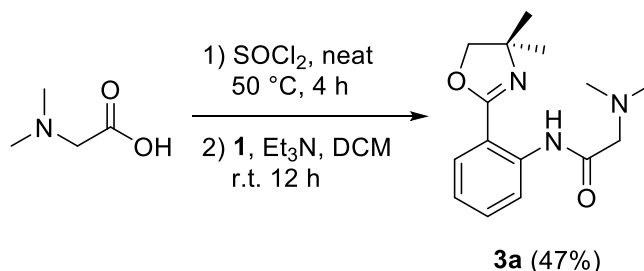


Scheme 2.1 Synthesis of NNN type pincer ligand using **1** and amino acids.

A more accessible route to pincer ligand synthesis was needed due to the prominent Zwitterionic effect of amino acids in aqueous solvents, their reactivity in non-polar organic solvents decreases substantially (equation 1) (*i.e.* Zwitterion – an overall neutrally charged molecule having both positive and negative charges).^{52,53}



The magnitude of the tautomeric equilibrium for *N,N*-dimethylglycine is completely solvent dependent, and in most protic and aprotic polar solvents it exists in the Zwitterion form.⁵²



Scheme 2.2 Synthesis of NNN type pincer ligand from *N,N*-dimethylglycine.

We previously showed that carboxylic group on the *N,N*-dimethylglycine can be transformed into the acyl chloride form using excess thionyl chloride under the neat conditions (**Scheme 2.2**).⁵⁴ After the reaction of an amino acid and the thionyl chloride at 50 °C, the excess thionyl chloride was removed and the resulted yellow solid compound, *in situ* generated *N,N*-dimethylglycinoyl chloride, was consequently reacted with compound **1** (primary amine) in the presence of Et₃N in DCM, which produced the desired pincer ligand, **3a** (**Scheme 2.2**). The structure of this product was analyzed by IR, ¹H and ¹³C NMR spectroscopy, and elemental analysis to successfully support the formula.⁵⁴ From the IR spectrum, the presence of a secondary amide (N-H) and an amide carbonyl (C=O) stretch/bend were observed and support the presence of the amide bond (**Table 2.1**).

Table 2.1 IR spectrum analysis for NNN type pincer ligands.

Assignment	3a	3b	3g	3h	Literature (cm ⁻¹) ³³
C=O stretch ^a	1677	1686	1683	1683	1680
N-H bend ^b	1645	1641	1636	1643	1640

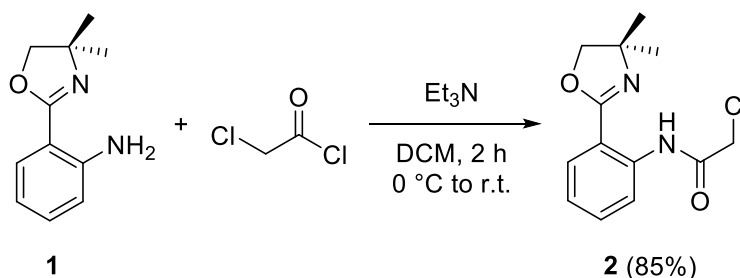
^a Amide carbonyl; ^b Secondary amide;

Thirteen unique chemical shifts were observed in the ¹³C NMR spectrum, agreeing with the formulation. From the ¹H NMR data, two singlet shifts were observed for the methylene groups (δ_{H} = 4.05 and 3.16 ppm) and two for the equivalent methyl groups (2.39 and 1.41 ppm) integrating for 2 and 6 protons each, respectively. Four protons were also observed in the aromatic region (in the range from 7.07 to 8.84 ppm) with a distinct proton shift at 12.80 ppm for the proton on the amide (-NH) (see **Table 2.3**). The synthesis of highly functionalized pincer ligands using this route might be problematic, since the amino acid derivative would have to be exposed to harsh conditions when

reacted with thionyl chloride, because thionyl chloride is extremely reactive and corrosive. Hence, a new synthetic strategy was devised.

2.2 MODULAR APPROACH

The need for the synthesis of easily accessible asymmetric pincer ligands led to the proposed use of 2-chloroacetyl chloride, as a building block to synthesize compound **2** – a pincer precursor. 2-Chloroacetyl chloride is often used in organic chemistry to introduce amide bonds (by reacting through the acyl chloride) into a structure, thus providing a functionalizable end group (*i.e.* a chloromethyl group).⁵⁵



Scheme 2.3 Synthesis of compound **2** – pincer precursor.

Upon the addition of 2-chloroacetyl chloride to **1** in the presence of Et₃N, the reaction mixture was stirred in DCM at room temperature (RT) for 2 h. The desired product, **2** (**Scheme 2.3**), was obtained, upon gravity filtration and solvent evaporation, in 85% as an orange coloured crystalline solid. It was analyzed by X-ray crystallography (**Figure 2.1**, left), elemental analysis and ¹H and ¹³C NMR spectroscopy. Both ¹H and ¹³C NMR supported the proposed structure of **2**. Two singlet shifts were observed for the methylene groups (4.21 and 4.07 ppm) and one for the two equivalent methyl groups (1.41 ppm) integrating for 2 each and 6 protons, respectively. Four protons were also observed in the aromatic region (in the range from 7.13 to 8.74 ppm) with a distinct

proton shift at 13.05 ppm for the amide proton (-NH). Twelve unique carbon environments were observed in the ^{13}C NMR and supported the structure of **2**.

From the crystallographic study of **2** (**Figure 2.1**, left), hydrogen bonding was reported for the amide hydrogen between both N and Cl atoms on the oxazoline ring (2.03 Å) and on the chloromethyl group (2.468 Å), respectively (**Table 2.2**). Since crystal structures represent the molecule in the solid state, a DFT calculation was performed on **2** (**Figure 2.1**, right) to determine the theoretical behaviour of the compound in the gas phase, and to serve as a training exercise to familiarize oneself with the theoretical calculations using molecular modeling software.

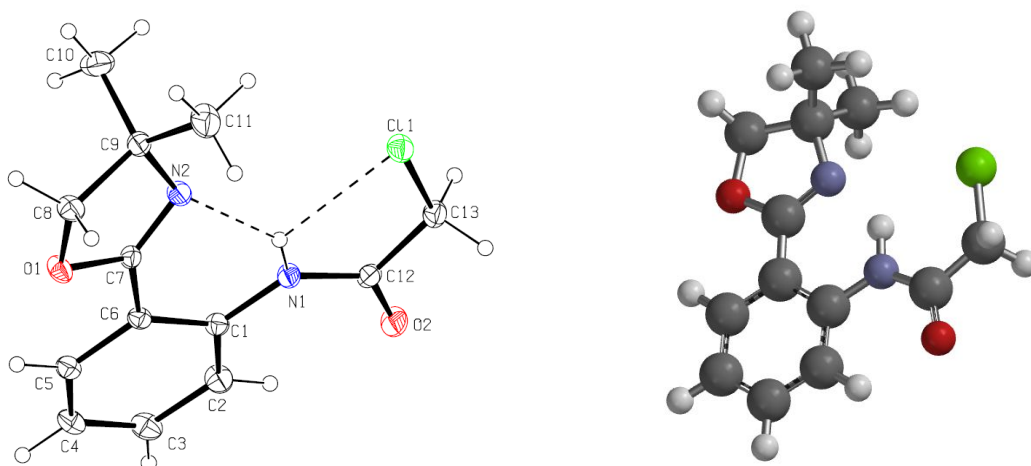


Figure 2.1 X-ray crystal structure of **2** (left; solved by Alan Lough) and calculated (DFT) structure of **2** at the B3LYP: 6-311++G** level of theory using Spartan'10 (right).

Table 2.2 Experimental and calculated hydrogen bond lengths and angles for **2**.

D-H...A	N(1)-H...N(2)	N(1)-H...Cl(1)	D-H...A	N(1)-H...N(2)	N(1)-H...Cl(1)
<(DHA) [°] ^a	138.4	112.5	D(H...A) [Å] ^a	1.86	2.521
<(DHA) [°] ^b	138.9	118.9	D(H...A) [Å] ^b	2.03	2.468

^a calculated value (DFT); ^b experimental value (crystal structure)

The calculated angles and bond lengths for the three atoms involved in the above-mentioned hydrogen bonding hydrogen agreed with the crystal structure values (see **Table 2.2**). The calculation was done at B3LYP with 6-311++G** basis set, with the

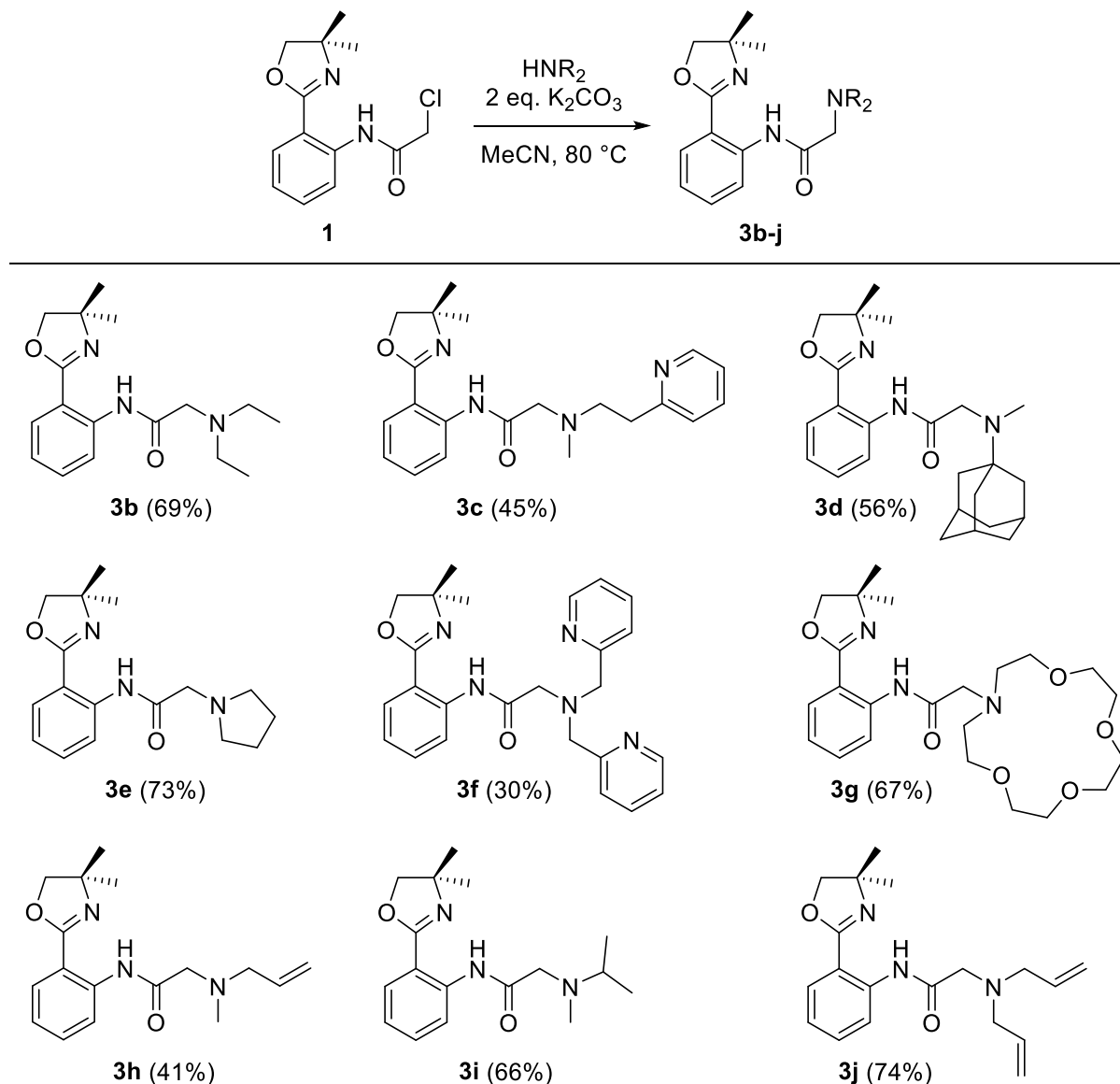
geometry of the structure being in agreement with the crystal structure (**Table 2.2**); it should be mentioned that the structure of **2** was optimized several times starting from different geometrical orientations and hence Figure 2.1 (right) represents one of the likely gas phase configurations.

2.2.1 Synthesis of Pincers **3b-3j**

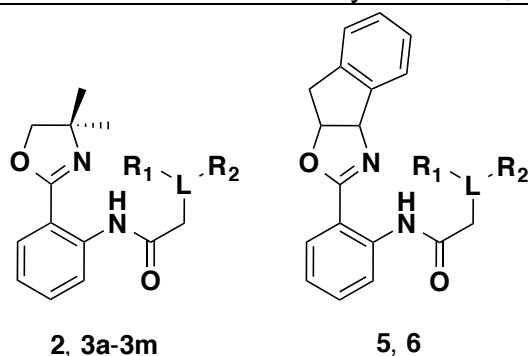
As previously stated, compound **2** was theorized to be a useful precursor for a modular synthetic approach, wherein this alkyl halide (**2**) can be reacted with selected secondary amines in the presence of the base to produce the desired pincer products.⁵⁵ The reaction between a secondary amine and an alkyl halide can be classified as a nucleophilic substitution reaction (*i.e.* S_N2 reaction).⁵⁰ Therefore, the compounds **3b-3j** were synthesized by reacting **2** with the appropriate secondary amine in the presence of K₂CO₃ as the base, according to **Scheme 2.4**.

Pincer ligands **3b-3j** were thus synthesized in moderate to good yields, ranging from 30% to 74% (see **Table 2.3**). After the purification (see Section 5.2), the compounds were successfully analyzed by ¹H and ¹³C NMR spectroscopy, as well as elemental analysis to support the proposed structures. Compounds **3b**, **3g** and **3h** were also analyzed by IR spectroscopy, confirming the presence of the amide bond through the presence of the typical C=O stretch and N-H bend absorption frequencies (see **Table 2.1**). The conversion of **2** into the appropriate pincer ligand product can be easily observed by a distinct proton NMR chemical shift of the amide (13.05 ppm for **2**; see **Table 2.3**) functionality which shifts upfield for compounds **3a-3j** (**Table 2.3**). The shift observed can be explained in terms of the increase in the strength of the hydrogen bonding (or an electronically donating interaction) between the H (on the amide) and N

(of the tertiary amine) in **3a-3j** due to the lone pair of electrons on the latter N atom; in comparison to the hydrogen bonding between the H (on the amide) and Cl (on the chloromethyl) as found in the crystal structure of **2** (**Figure 2.1**). Hence, shielding of the –NH proton is observed in **3a-3j**. Chiral derivatives, **6** and **7**, were also synthesized and are discussed in **Section 2.3**.



Scheme 2.4 Synthesis of NNN type pincer ligands through a modular approach.

Table 2.3 Select ^1H NMR chemical shifts and yields for **2**, **3a-3m•oxide**, **5** and **6**.

Compound	L	R ₁ group	R ₂ group	-NH shift (ppm)	Yield (%)
2	Cl	-	-	13.05	85
3a	N	Me	Me	12.80	47
3b	N	Et	Et	12.64	69
3c	N	Me	2-Ethylpyridine	12.65	45
3d	N	Me	Adamantyl	12.24	56
3e	N	Pyrrolidine	-	12.47	73
3f	N	Picolyl	Picolyl	12.57	30
3g	N	5-Crown	-	12.52	67
3h	N	Me	Allyl	12.71	41
3i	N	Me	<i>i</i> Pr	12.63	66
3j	N	Allyl	Allyl	12.61	74
3k	N	Me	EtOH	12.22	88
3l	C	-	-	12.96	57
3m•oxide	P	Ph	Ph	12.43	55
6	Cl	-	-	12.98	86
7	N	Et	Et	12.54	55

Functionalization of **3b-3j** pincer ligands was achieved by using secondary amines: diethylamine (**3b**), 2-(2-methylaminoethyl)pyridine (**3c**), *N*-methyl-*N*-adamantylamine (**3d**), pyrrolidine (**3e**), 2,2'-dipicolylamine (**3f**), 1-aza-15-crown-5 (**3g**), *N*-allyl-*N*-methylamine (**3h**), *N*-isopropyl-*N*-methylamine (**3i**), diallylamine (**3j**). Compounds **3c** and **3f** were designed with an extended pincer motif – with the potential for the picolyl functional groups to chelate to a metal centre(s); increasing the coordination number to at least four for **3c** and potentially five for **3f**. An extended pincer ligand, **3f**, can also be efficiently applied in homo- or heterobimetallic coordinating systems. Copper can be

one of the potential candidates for a bimetallic study on **3f**; Brown *et al.* recently showed a successful coordination and application of Cu with an *N,N*-bis(2-picolyl)benzamide ligand in methanolysis reactions, for example.⁵⁶

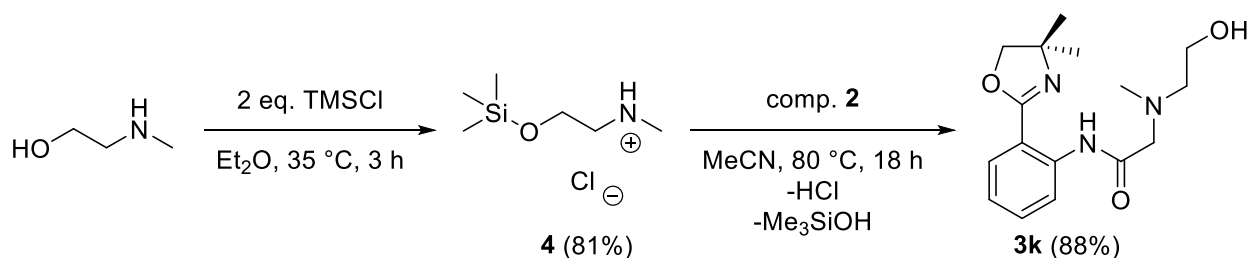
2.2.2 Synthesis of **3k**

Pincer **3k** was also synthesized since it contains an extended motif and therefore, having the potential to coordinate to the metal centre through four atoms (three N atoms and an O of the hydroxyl group). The synthesis of **3k** followed the same procedure as for the **3b-3j**, however prior to that the hydroxyl group on *N*-methylaminoethanol had to be protected due to its reactivity. Several protection reactions were performed on *N*-methylaminoethanol to protect the hydroxyl group (**Table 2.4**).

Table 2.4 Protection of the hydroxyl group on the *N*-methylaminoethanol.

Trial	Protecting group	Additive	Solvent	Product
1	Ac ₂ O	DMAP	DCM	NO
2	TMSCl	Et ₃ N	Et ₂ O	NO
3	HMDS	D,L-Aspartic acid	MeCN	NO
4	TMSCl	–	Et ₂ O	YES

Unsuccessful trials using acetic anhydride (Ac₂O) with catalytic amounts of *N,N*-dimethylaminopyridine (DMAP),⁵⁷ or hexamethyldisilazane (HMDS) with D,L-aspartic acid as a catalyst⁵⁸ to protect hydroxyl group on the *N*-methylaminoethanol resulted in unsuccessful outcomes (**Table 2.4**). The use of trimethylsilyl chloride (TMSCl) in combination with Et₃N in Et₂O also did not produce successful results in protecting the hydroxyl group.⁵⁹ However, it has been recently shown that in the presence of 2 eq. of TMSCl in Et₂O and in the absence of the base (Et₃N), the *N*-methyl-2-((trimethylsilyl)oxy)ethan-1-aminium chloride (**4**) was isolated in 81% yield. This material can be successfully used to synthesize an appropriate pincer, **3k** (**Scheme 2.5**).⁶⁰



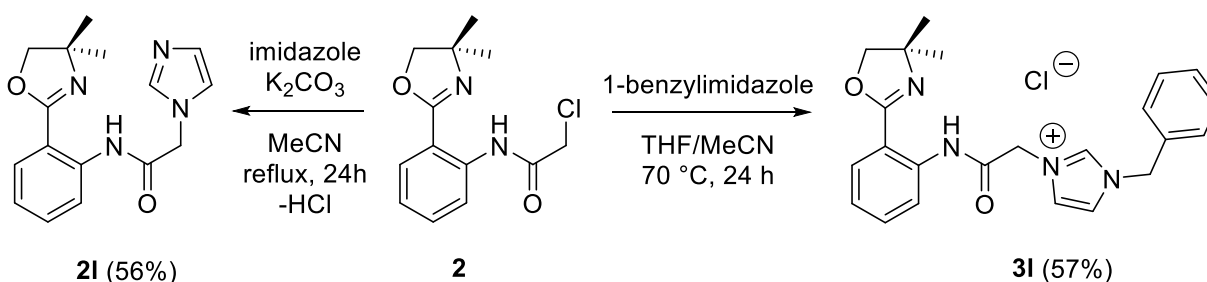
Scheme 2.5 Synthesis of an extended pincer NNNO, **3k**, from *N*-methylaminoethanol.

Compound **4** was isolated and successfully characterized by elemental analysis and ^1H and ^{13}C NMR spectroscopy. From the ^1H NMR spectrum, a resonance integrating for 9 protons appears as a singlet at 0.14 ppm, which suggested the presence of the $-\text{SiMe}_3$ group on the O atom. The two chemical shifts at 3.08 and 3.93 ppm appeared as triplets and integrated for 2 protons each. The identity of the product, as a chloride salt, was confirmed by the presence of the broad shift at 9.43 ppm integrating for 2 protons; a chemical shift which is indicative of the $-\text{NH}_2$ group.⁶¹

With the *in situ* formation of **4**, compound **3k** was synthesized in only 12% after purification by the column chromatography. However, after the isolation of **4** and an optimization study was later performed by Jennifer Huynh⁶⁰ and, of the reaction shown in **Scheme 2.5**, yields of up to 88% are achievable (**Table 2.3**). Compound **3k** was successfully characterized by elemental analysis and ^1H and ^{13}C NMR spectroscopy. As in pincers **3a-3j** an indicative $-\text{NH}$ chemical shift was observed at 12.22 ppm for **3k** — an upfield shift compared to the starting material (13.05 ppm; see **Table 2.3**). The close proximity of the alcohol group on the N atom to the amide proton could create the shielding effect, explaining the observed phenomena.

2.2.3 Synthesis of **3I**: a carbene-pincer precursor

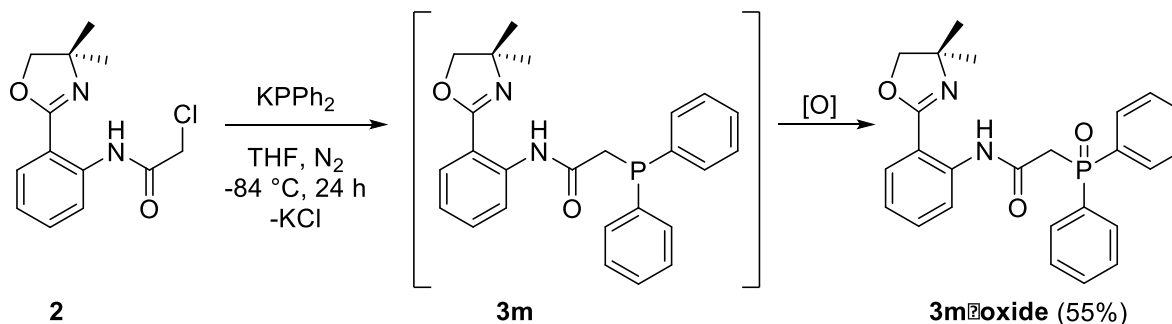
1-Benzylimidazole⁶² was synthesized by reacting imidazole hydrochloride with benzyl bromide in the presence of K₂CO₃ in MeCN. Pure compound was isolated in 42% yield as an off-white coloured waxy solid. ¹H NMR analysis of 1-benzylimidazole agreed with the literature.⁶² The synthesis of NNC type pincer ligand, **3I**, from 1-benzylimidazole and **2** in THF:MeCN (15.0:3.0 mL ratio) resulted in successful isolation of the desired product in 57% yield as a yellow wax (**Scheme 2.6**). The low solubility of 1-benzylimidazole in THF was resolved by the addition of a small amount of MeCN. The compound, **3I**, was successfully analyzed by elemental analysis, ¹H and ¹³C NMR spectroscopy. The resonance observed at 12.96 ppm is representative of the –NH on the amide (**Table 2.3**). The proton appeared to be more deshielded in comparison to NNN pincers (**3a-3k**), which can be due to the absence of the hydrogen bonding or other interactions between the hydrogen on the amide and the imidazole moiety. Alternatively, **2I** was synthesized from **2** as described in **Scheme 2.6**, as the precursor for **3I**. However, the yield for the reaction to synthesize **2I** (56%) did not introduce any benefits into increasing the overall yield for **3I**; hence it was not investigated further.



Scheme 2.6 Synthesis of NNC pincer ligand **3I** and a precursor **2I**.

2.2.4 Synthesis of **3m** and **3m•oxide**

The synthesis of NNP type pincer ligand, **3m•oxide**, was accomplished by reacting **2** with equimolar THF solution of potassium diphenylphosphide (KPPh₂) under nitrogen atmosphere for 24 h (**Scheme 2.7**).



Scheme 2.7 Synthesis of NNP pincer ligand, **3m**, from potassium diphenylphosphide.

The work-up of this reaction involved gravity filtration of the KCl, formed as the by-product. By exposing the sample to air and moisture, **3m** is readily converted to **3m•oxide** and was isolated in 55% yield (**Table 2.3**). This transition was monitored by ³¹P NMR, where **3m** and **3m•oxide** displaying chemical shifts at -15.77 ppm and 28.48 ppm, respectively. During the first experimental trial of this reaction, diphenylphosphine oxide (O=PPh₂H; Ph = phenyl) and diphenylphosphine (HPPh₂) were both observed in the reaction mixture δ_p = 21.54 ppm and -40.39 ppm, respectively (**Table 2.5**). The literature values were in agreement within experimental error, with these observations.⁶³⁻⁶⁴

Table 2.5 Select literature and experimental ³¹P NMR chemical shifts for PNN pincer.

Compound	Lit. chemical shift (ppm)	Exp. chemical shift (ppm)
KPPh ₂	-9.8 ⁶⁵	-
HPPh ₂	-42.1 ⁶⁴	-40.39
O=PPh ₂ H	21.9 ⁶³	21.54
3m	-	-15.77
3m•oxide	-	28.48

Compound **3m•oxide** was analyzed by X-ray crystallography (**Figure 2.2**) supporting the proposed structure and showcasing that there was no interaction between the

hydrogen on the amide and the phosphorus in the solid state. Also, a molecule of water was coordinated to the oxygen on the phosphine oxide. **3m•oxide** was also characterized by ^1H and ^{13}C NMR supporting the structure of the compound (see **Table 2.3**).

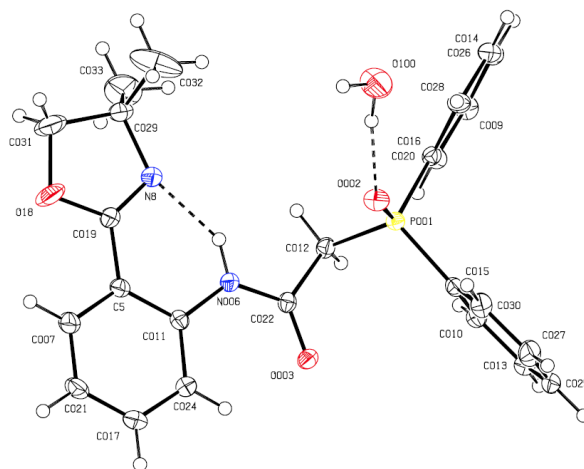
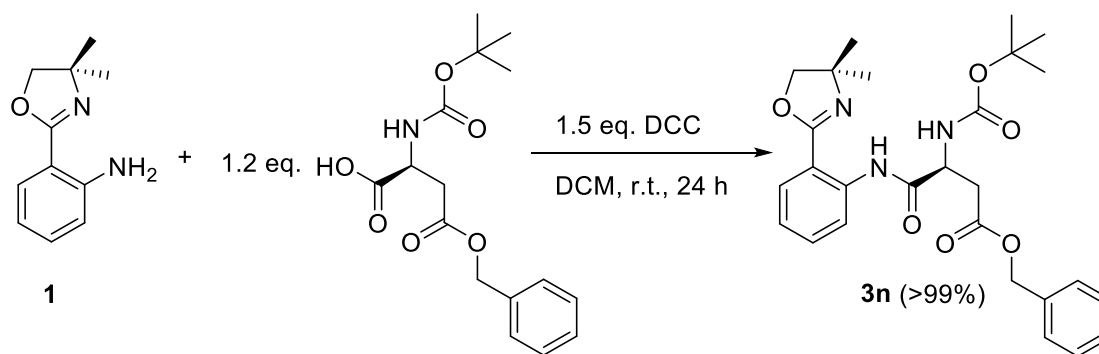


Figure 2.2 X-ray crystallographic structure of **3m•oxide** (Solved by Laura R. Fernández).

2.2.5 Synthesis of **3n**

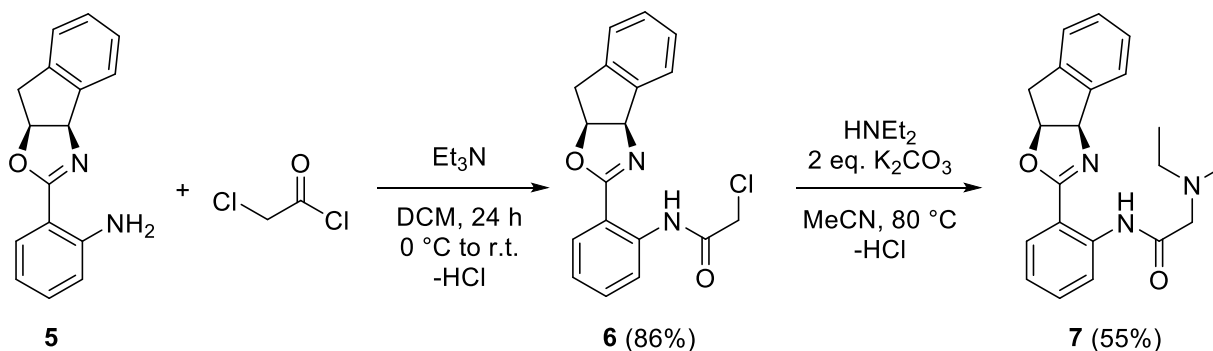
An NNN pincer derivative from **1** and Boc-*L*-aspartic acid 4-benzyl ester was synthesized using 1.5 eq. DCC (a peptide coupling agent) in DCM (**Scheme 2.8**). Upon aqueous work-up the compound was obtained in >99% yield as pale yellow wax. Elemental analysis and ^1H and ^{13}C NMR spectroscopy supported the compounds' identity. The interest into the development of this particular pincer is its unique applicability. Deprotecting the Boc and the benzyl groups on **3n**, deprotects the amine and carboxylic acid functional groups, which can then be covalently bonded to peptides. Combining this pincer ligand with peptides could yield interesting sensor-type molecules.



Scheme 2.8 Synthesis of **3n** from **1**.

2.3 CHIRAL DERIVATIVES

A chiral derivative of **2** was synthesized and isolated in 86% yield following the same procedure: from 2-chloroacetyl chloride and **5** (synthesized as per **1**⁴⁹) in DCM (see **Scheme 2.9**). Peachy-coloured crystalline compound was analyzed by elemental analysis, x-ray crystallography and ¹H and ¹³C NMR spectroscopy. Based on the orientation of the molecule (**Figure 2.3**), just as in the solid state of compound **2**, it appeared that hydrogen bonding was observed for the amide hydrogen between both, the N on the oxazoline and the Cl on the chloromethyl group. From the crystal structure it was also determined that **6** exists as a single *R*, *S* stereoisomer.



Scheme 2.9 Synthesis of the chiral derivatives, **6** and NNN type pincer ligand, **7**.

The reaction of **6** with diethylamine in the presence of K₂CO₃ in MeCN yielded crude **7** in 55% yield, which was analyzed by ¹H NMR. Even after recrystallization, small

amounts of starting material (**6**) were still observed; this suggests a slow decomposition of the product. A singlet observed at 12.54 ppm was indicative of the proton on the amide (**Table 2.3**) and the $-\text{CH}_2$ and $-\text{CH}_3$ of the ethyl group on the amine were observed in the spectrum at 1.14 ppm and 2.75 ppm as triplet and quartet respectively, having matching J values of 7.2 Hz. These observations concluded that the product present in majority was indeed the desired chiral NNN pincer ligand.

Any attempt at functionalizing **6** with 1-benzylimidazole (as for **3l**) or KPPH_2 (as for **3m**) to yield chiral NNC or NNP type pincer ended with unsuccessful results.

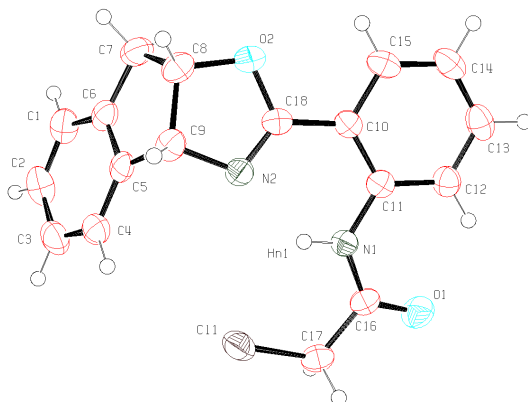


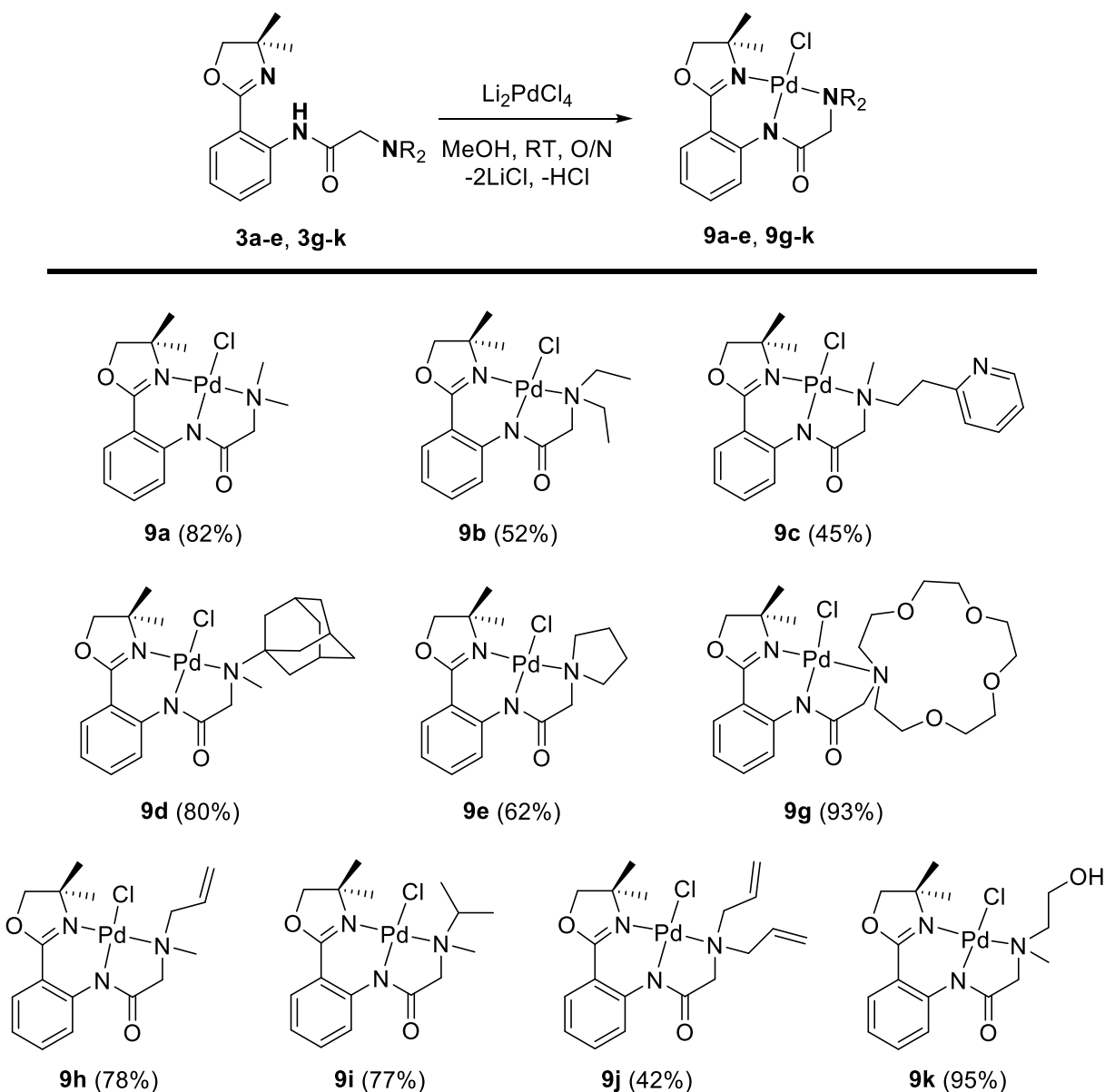
Figure 2.3 X-ray crystal structure of **6** (Solved by Robert A. Gossage).

CHAPTER 3 – COMPLEXES

3.1 PALLADIUM COMPLEXES

3.1.1 NNN type pincer complexes

Complexation of NNN type pincer with Pd metal was accomplished using previously reported method of coordination as described by Decken *et al.* This uses a methanolic solution of Li_2PdCl_4 , as Pd source, at RT (**Scheme 3.1**).⁴¹



Scheme 3.1 Synthesis of Pd-NNN pincer complexes, **9a-e** and **9g-k**.

A solution of Li_2PdCl_4 was prepared from stoichiometric amounts of LiCl and PdCl_2 refluxed in MeOH ;⁴¹ upon the dissolution of the starting materials the reaction was complete and the Pd precursor solution is ready to use. When Li_2PdCl_4 was added to a yellow coloured solution of an NNN pincer ligand (*i.e.* **9a-e** or **9g-k**) in MeOH , the reaction solution turned bright orange in colour almost instantaneously. All resulting Pd-NNN complexes, aside from **9c**, were purified by redissolving the compound in DCM and filtering the mixture (an orange solution with fine pale coloured precipitates) through a thick layer of Celite. In contrast, **9c** was purified using preparative TLC (100% acetone as eluent). All compounds were isolated as either waxy solids or powders, bright yellow to orange in colour, and isolated in yields ranging from 42% to 98%.

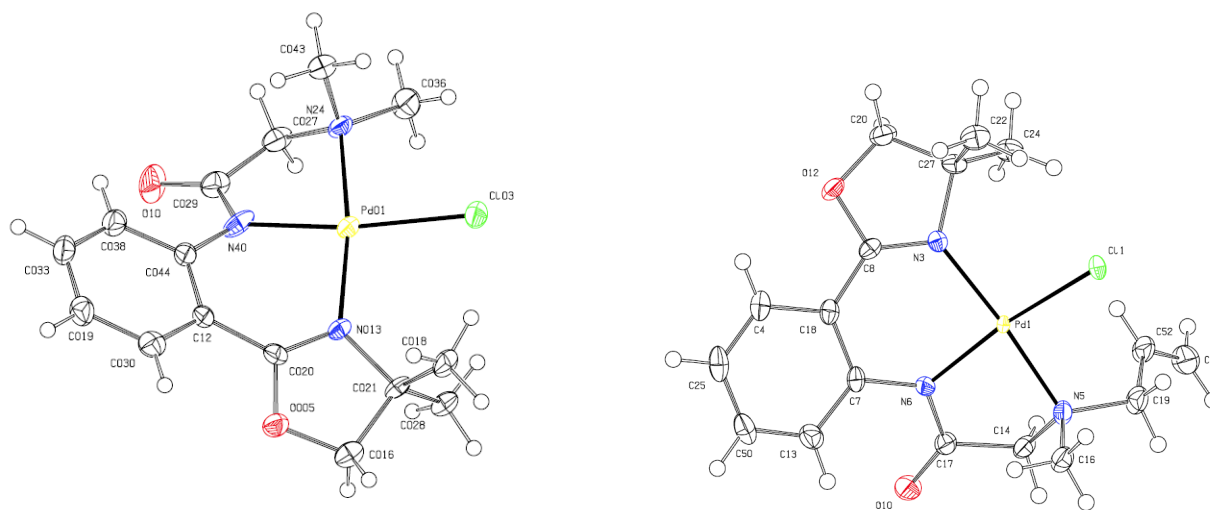


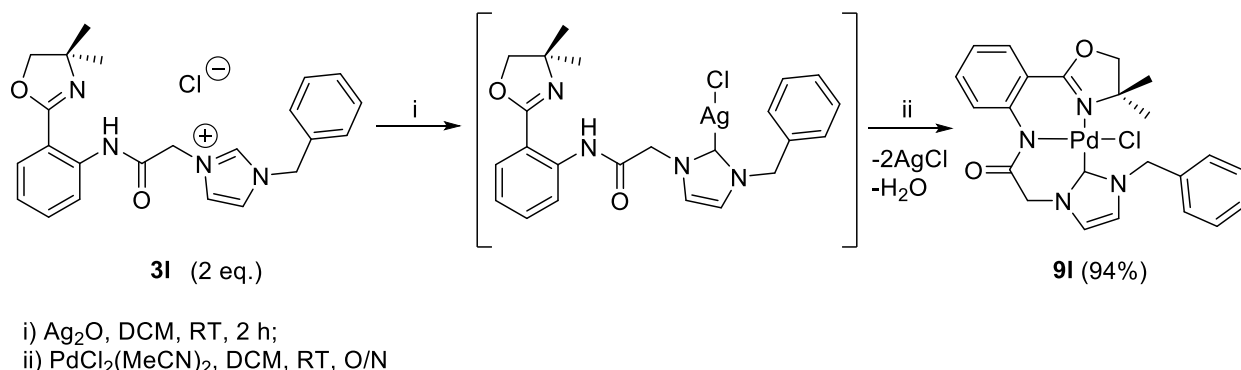
Figure 3.1 Crystal structures of **9a** (left) and **9h** (right) solved by Laura R. Fernández.

Suitable crystals for the complexes **9a** and **9h** were grown to be analyzed by X-ray crystallography (**Figure 3.1**, left and right respectively). Both of the complexes showed a distorted square planar orientation of the ligated atoms around the metal centre. The Pd atom has a coordination number of 4 in both cases and an assigned oxidation state of +2. The NNN pincer ligands indeed proved to behave as monoanionic ligands, being

deprotonated at the amide position during the reaction, as shown previously for Pd complex with ligand **P**.⁴¹ Aside from the X-ray crystallography analysis, all Pd-NNN complexes were characterized by elemental analysis and *via* ¹H and ¹³C NMR spectroscopy. Proton chemical shifts for methyl and methylene functional groups moved downfield due to the electron withdrawing effect of the metal centre, upon complexation.⁶⁶ The chemical shifts of the aromatic protons were not considerably affected by complexation. From ¹³C NMR, all of the structures for Pd complexes, **9a-e** and **9g-k**, support a stoichiometry of Pd:NNN:Cl = 1:1:1. Note that one H has been lost from the free NNN ligand in all cases (**Scheme 3.1**).

3.1.2 NNC type pincer complex

Over the last decade *N*-heterocyclic carbenes (NHCs) have shown promising results in catalysis and specifically in cross-coupling reactions. Hence, NHC-containing ligands have been studied extensively for the design and use of carbene containing catalysts.⁶⁷⁻⁶⁹ The NHC ligand is considered a strong σ -donor and weak π -acceptor, which in turn improves the catalytic activity due to the increase in electron density on the metal centre.⁷⁰



Scheme 3.2 Synthesis of Pd-NNC pincer complex, **9I**.

A Pd-NNC complex was synthesized through Lin's method of transmetallation using silver(I) oxide (Ag_2O) as the transmetallating agent.⁶⁹ Ligand **3I** was stirred with Ag_2O in DCM for 2 h and then the reaction mixture was filtered through Celite. Bis(acetonitrile)palladium(II) dichloride ($\text{PdCl}_2(\text{MeCN})_2$) was added to the pale yellow filtrate, and the reaction solution turned bright yellow/orange within a few minutes, suggesting complexation (**Scheme 3.2**). Even though not isolated in this case due to its low stability, the syntheses of silver(I), gold(I) and copper(I) carbene intermediates have been previously reported.⁷¹⁻⁷² The protocols used here directly parallel those studies.⁶⁹⁻

72

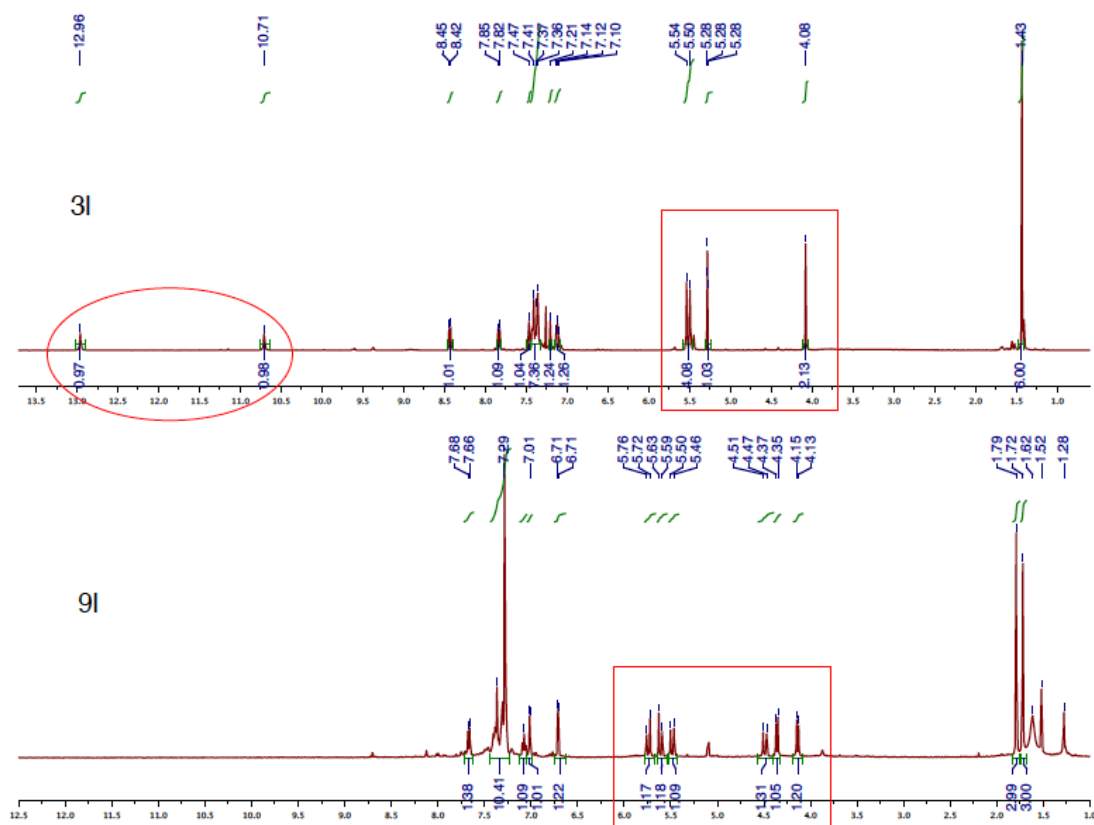


Figure 3.2 The comparison of the ^1H NMR spectra for **3I** and **9I**.

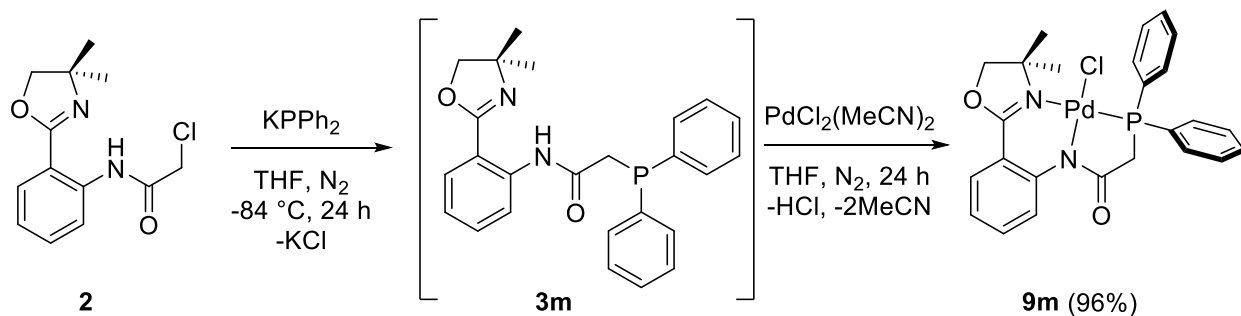
The investigation into the coordination of complex **9I** using ^1H NMR spectroscopy suggests that coordination of Pd to the carbene precursor did take place. This evidence

includes the observed chemical shifts for the amide proton ($-\text{NHC}=\text{O}$) at 12.96 ppm and the imidazole proton ($-\text{NR}_2\text{CHNR}'_2-$) at 10.71 ppm that are present for the carbene precursor (circled, **Figure 3.2**). Both of these resonances are absent for the isolated complex. The second order effect was also observed for all three methylene groups, which appeared as singlets at 4.08 ppm, 5.50 ppm and 5.54 ppm on the ligand molecule, **3l**. This suggests that those protons reside in different environments and are magnetically inequivalent (**Figure 3.2**).

3.1.3 NNP type pincer complex

Asymmetric pincer ligands containing soft donor atom, such as phosphorus, have also been of much interest with respect to catalysis applications for a wide variety of chemical transformations.⁷³

A Pd-NNP pincer complex was therefore prepared in two steps. Due to the facile oxidation of **3m** to **3m•oxide**, NNP pincer ligand **3m** was synthesized and used *in situ* following the procedure outlined in **Section 2.2.1**. The THF solution with **3m** was cannula transferred to a MeCN solution of $\text{PdCl}_2(\text{MeCN})_2$ and the resulting mixture stirred for 24 h (**Scheme 3.3**) at RT. After this time, the solution was gravity filtered and the solvent was then removed *in vacuo*. The crude sample of **9m** was retrieved in 96% yield, and appeared dark orange in colour.



Scheme 3.3 Synthesis of Pd-NNP pincer complex, **9m**

However, preparative TLC was used to further purify the compound for complete characterization (elemental analysis and ^1H , ^{13}C and ^{31}P NMR spectroscopy).

From the ^{31}P NMR spectrum, single resonance was observed with a chemical shift of 50.45 ppm, in contrast to the free ligand that was observed at -15.77 ppm, suggesting only one phosphorus environment present.

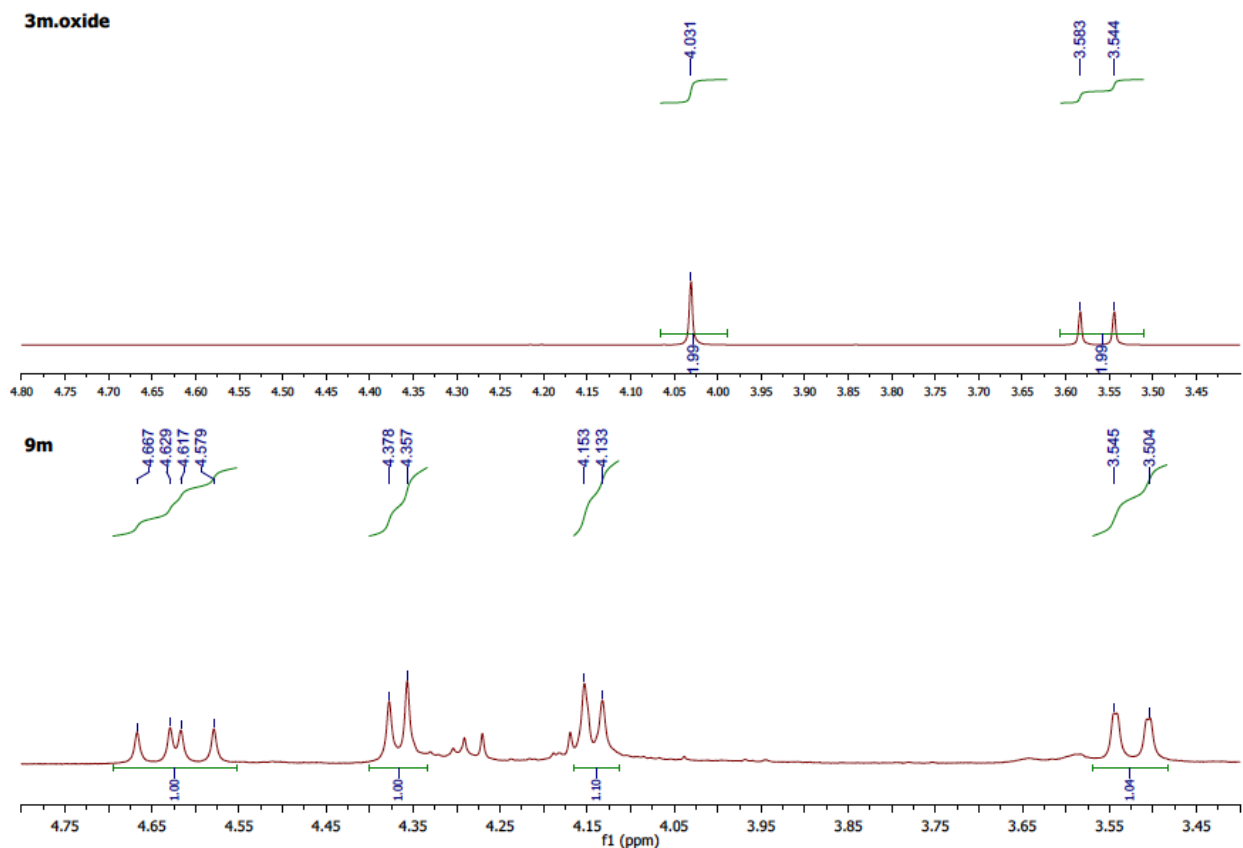


Figure 3.3 Select ^1H chemical shifts for **3m•oxide** and **9m**, depicting splitting effect.

From the ^1H NMR spectrum, a second order effect for the methylene groups ($-\text{CH}_2-$) can be observed for **9m**, where in comparison to **3m•oxide** they were observed as singlet and a doublet (coupled to $^{31}\text{P}\{^1\text{H}\}$, $J = 15.6$ Hz) (see **Figure 3.3**).

3.2 ATTEMPTS AT THE SYNTHESIS OF NICKEL COMPLEXES

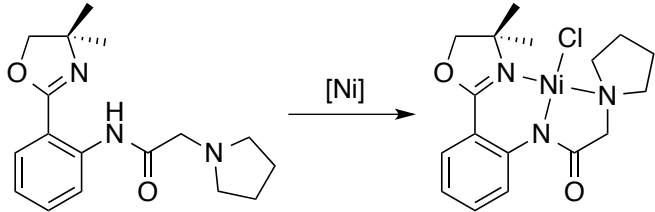
3.2.1 NNN type pincer complexes

Both academic and industrial research has witnessed an immense progress in the use of nickel complexes as catalysts in polymerization and cross-coupling type reactions.⁷⁴⁻

⁷⁵ For this reason, the investigation into employing NNN, NNC and NNP type pincer ligands, presented in this work, was performed in coordination chemistry with Ni.

Gao and co-workers reported Ni-NNN pincer-like complexation using $\text{NiCl}_2 \cdot 6\text{H}_2\text{O}$ in ethanol (with or without the base) or $\text{NiCl}_2(\text{DME})$ and lithium diisopropylamide (LDA) as the base in THF.⁷⁴ However, following these reaction conditions with **3e** pincer ligand did not yield any desired product. In fact, upon reaction work-up, which consisted of gravity filtration and Et_2O wash, the resulted yellow waxy compound was found to be the free ligand (entries 1-4, **Table 3.1**). Peters and coworkers reported coordination of their monoanionic NNN type pincers with Ni through $\text{NiCl}_2(\text{DME})$ precursor in the presence of Et_3N in THF.⁷⁵ Entry 5 (**Table 3.1**) depicts the unsuccessful trial with **3e** pincer ligand.

Table 3.1 Synthesis of Ni-NNN type pincer complex from **3e** ligand.

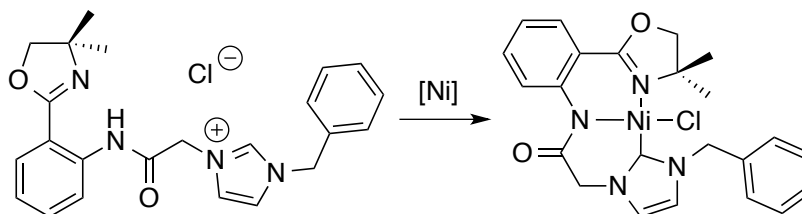


Entry	[Ni]	Solvent	Base	Time	Temperature/Atmosphere
1	$\text{NiCl}_2 \cdot 6\text{H}_2\text{O}$	EtOH	-	12 h	RT/air
2	$\text{NiCl}_2 \cdot 6\text{H}_2\text{O}$	EtOH	$t\text{BuOK}$	12 h	RT/air
2	NiCl_2DME	THF	LDA	O/N	RT/ N_2
3	NiCl_2DME	THF	LDA	18 h	RT/ N_2
5	NiCl_2DME	THF	Et_3N	19 h	60 °C/ N_2

The theorized molecular geometry of the diamagnetic Ni-NNN pincer complex was square planar, the colour of which had to be red. However, the reaction solutions for all of the trials (**Table 3.1**) did not change the colour in the course of the reaction and remained green.

3.2.2 NNC type pincer complex

The synthetic route for Ni-NNC pincer complex was employed from the synthesis of **9l**, through Lin's method of transmetallation using silver(I) oxide (Ag_2O) as the transmetallating agent.⁶⁹ Ligand **3l** was stirred with Ag_2O in DCM for 2 h and then the reaction mixture was filtered through Celite. Bis(triphenylphosphine)nickel(II) dichloride ($\text{NiCl}_2(\text{PPh}_3)_2$) was added to the pale yellow filtrate, and the reaction solution turned dark green instantaneously (**Scheme 3.4**). Unfortunately, this trial was unsuccessful in producing a Ni-NNC complex, once again yielding light yellow wax – characterized as the free ligand.

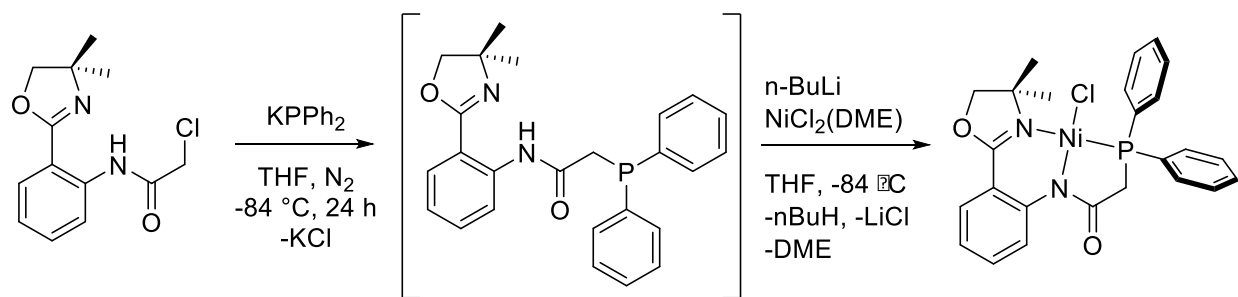


Scheme 3.4 Synthesis of Ni-NNC type pincer complex from **3l** ligand.

3.2.3 NNP type pincer complex

A trial reaction, investigating the synthesis of Ni-NNP complex from **3m** and NiCl_2DME precursor in the presence of *n*-BuLi (to deprotonate the amide hydrogen), was followed from the reaction conditions reported by Liu and co-workers (**Scheme 3.4**).⁷⁶ First, **3m** was treated with *n*-BuLi and then this solution was added to the suspension of

NiCl₂DME in THF. The colour of the reaction solution was pale green, and after solvent evaporation, blue waxy compound resulted in having minimal solubility in CDCl₃ or benzene-d₆. Unfortunately, as previously shown with NNN and NNC type ligands, the complexation and characterization with NNP ligand was also unsuccessful. In contrast to Pd – Ni chemistry appeared to be more air/water sensitive and if the paramagnetic complexes are formed – the characterization by x-ray crystallography is required.



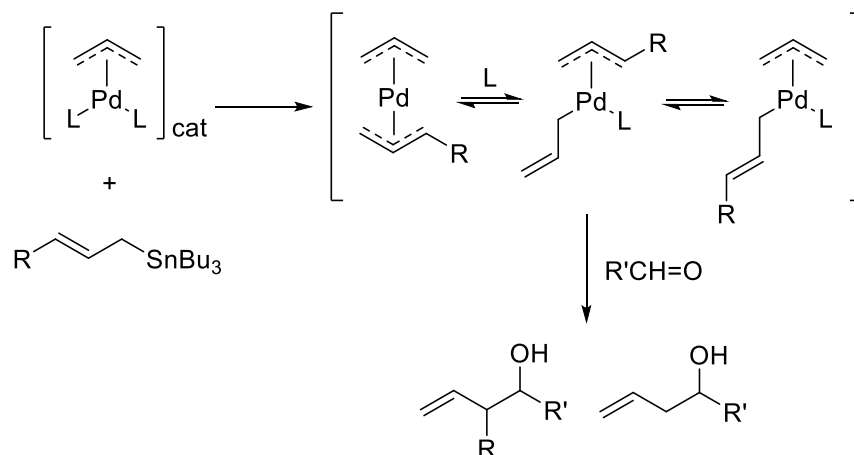
Scheme 3.5 Synthesis of Ni-NNP pincer complex from **3m** ligand.

Due to these presumed stability issues and time constraints, further Ni chemistry in this regard was abandoned.

CHAPTER 4 – CATALYSIS

4.1 ALLYLATION OF ALDEHYDES

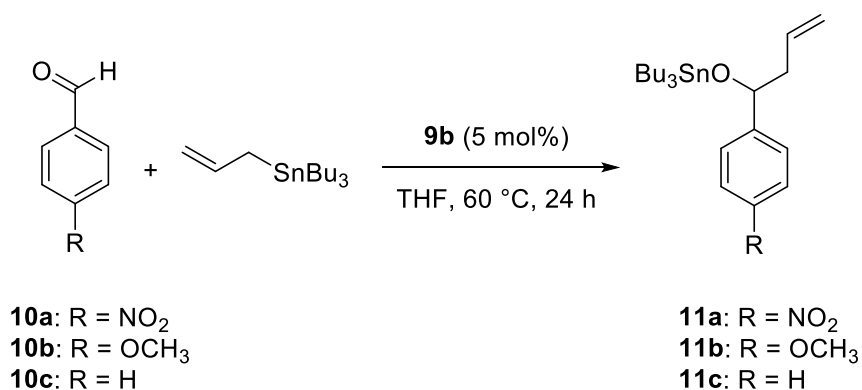
Allylic substitution reactions catalyzed by palladium complexes have become an important set of transformations in modern organic chemistry.⁷⁷⁻⁸¹ The first series of reports on allylation of aldehydes and imines catalyzed by bis(allyl)palladium species was published by Yamamoto and coworkers in 1996, where the allyltributyltin was the source of the allyl group.⁸² However, there are two inherent drawbacks with using bis(allyl) complexes. First, the difficulty in controlling the regioselectivity when the two allylic group have different substituents (**Scheme 4.1**). And secondly, allyl-allyl coupling can occur before the reaction with a desired electrophile.



Scheme 4.1 Bis(allyl)palladium in catalysis.⁷⁸

Szabó and co-workers theorized using palladium pincer complexes for the allylation of electrophiles, and the monodentate anionic ligand would undergo transmetalation. The pincer ligand to metal bond (that is trans to the Pd-allyl bond) would enhance the nucleophilicity of the allyl fragment.⁸³ So far, the application of the carbon electrophiles in these types of reactions remains unexplored.⁸⁴

Palladium pincer complexes have been considered to be attractive complexes in catalytic applications. Some of the features supporting that argument include: 1) their stability, even during a catalytic transformation the pincer ligand remains tightly bound to the metal centre for the entire duration of the reaction; 2) due to the strong coordination of the pincer, there is only one coordination site, *trans* to the anionic atom, providing restriction with respect to catalytic sites on palladium; 3) Oxidation state of palladium in pincer complexes is +2 under ambient conditions, upon reduction of the metal atom – ligand dissociates from the metal. Hence, the oxidation state of +4 is attainable but only under elevated temperatures (over 120 °C).^{78,85}



Scheme 4.2 Allylation of *para*-substituted benzaldehydes catalyzed by **9b**.

A preliminary study into the allylation reaction was studied with three *para*-substituted benzaldehydes (**10a-c**) and allyltributyltin (as the allyl group source) catalyzed by previously described Pd-NNN pincer complex, **9b**. To each of the aldehydes, a solution of **9b** in THF was added following the addition of 1.2 equiv. of allyltributyltin. The reaction solution was stirred in air at 60 °C. After 24 h the reaction solution still appeared yellow in colour (suggesting no catalyst decomposition) and the solvent was allowed to evaporate. The resulting yellow waxy compounds were characterized using ¹H NMR spectroscopy to determine the % conversion (see **Table 4.1** and **Figure A62**).

Both benzaldehyde and *p*-nitrobenzaldehyde showed high conversion to the desired product (entries 1 and 5, **Table 4.1**) with the aldehyde peak not present. *p*-Methoxybenzaldehyde was converted in 76% (entry 3, **Table 4.1**). However, even though an unreacted aldehyde was observed in the spectrum, there was no unreacted allyltributyltin compound present. This could be due to an error in the amounts of the reagents added when the reaction was set-up.

Table 4.1 Pd-NNN pincer complex-catalyzed allylation of select aldehydes.

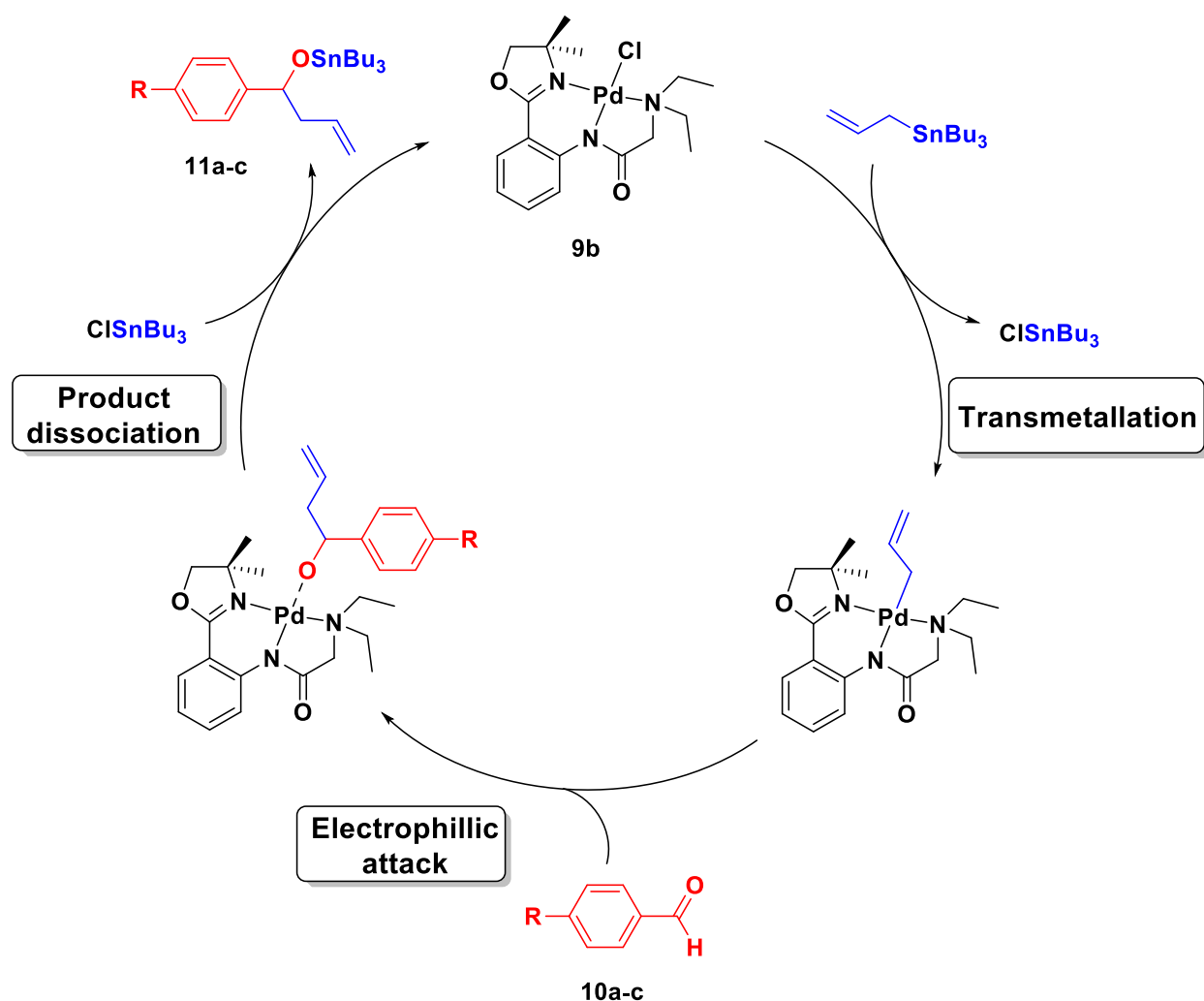
Entry	R	Yield (%) ^a
1	NO ₂	99
2 ^b	NO ₂	0
3	OCH ₃	76
4 ^b	OCH ₃	0
5	H	99
6 ^b	H	0

^a not isolated yields (determined from ¹H NMR); ^b no catalyst used;

As stated previously, the reaction studied in **Scheme 4.2** has been of a preliminary interest. So far in literature, only Pd pincer complexes with symmetric PCP type ligands have shown progress in these types of catalytic transformations.⁸⁶ Herein we demonstrated asymmetric Pd-NNN type pincer complex as a successful catalyst. **Table 4.2** outlines the chemical shifts for the allylation of aldehydes reaction. It should be noted that no acidic work-up or product isolation took place.

Table 4.2 Comparison of ¹H NMR chemical shifts for aldehyde allylation reaction.

10a	11a	10b	11b	10c	11c
10.16	-	9.91	-	10.02	-
8.39	8.22	7.86	7.28	7.87	
8.07	7.55	7.02	6.88	7.61	7.50-7.25
AllylSnBu ₃		3.91	3.81	7.51	
5.95	5.80	AllylSnBu ₃		AllylSnBu ₃	
4.79	5.19	5.95	5.80	5.95	5.82
4.65	4.88	4.79	5.13	4.79	5.14
1.79	2.53	4.65	4.69	4.65	4.74
		1.79	2.50	1.79	2.52



Scheme 4.3 A proposed mechanism for the allylation of aldehydes.

DFT calculations,⁸⁶ show that the mechanism of this catalytic process involves transmetalation step to happen first on a relatively electron poor palladium centre. The electrophilic attack happens at the γ -position of the allyl group in the second step. This is driven by electronic (not steric) factors. And as the final step, product dissociation and catalyst regeneration happens. Importantly, no change in oxidation state of palladium takes place during the three steps of the catalytic process (**Scheme 4.3**).

CHAPTER 5 – EXPERIMENTAL

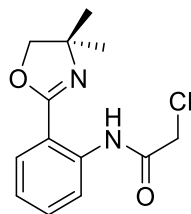
5.1 GENERAL

All reactions were carried out under ambient atmosphere conditions unless otherwise stated. All chemicals were purchased commercially. All of the reagents were used without further purification. Solvents used for reactions were supplied by an mBraun Solvent Purification System (SPS) or in commercial bottles (Aldrich), none of which were further purified. Compounds **1** and **5** were synthesized according to literature⁴⁹. NMR experiments were recorded on a Bruker Avance II 400 using CDCl₃ (chloroform-d₁) at 400 MHz (¹H), 162 MHz (³¹P) and 100 MHz (¹³C) at RT. In all spectra, chemical shifts were adjusted to the solvent peak (7.26 ppm for CHCl₃ for ¹H and 77.16 ppm for CDCl₃ for ¹³C). Melting points were determined using Fisher Scientific melting point apparatus with the maximum temperature of 300 °C. The values provided for melting point are uncorrected. IR spectra were obtained on Perkin Elmer Spectrum One using KBr disks for solid compounds and NaCl disks for liquid/oil compounds. SiliCycle Thin Layer Chromatography (TLC) plates (thickness: 250 μm) were used for TLC characterization; visualization was obtained under UV light irradiation. Some of the products (as specified) were purified by dry-column flash chromatography (DCFC). The general procedure included the sample being adsorbed onto silica (~3 g) followed by rotary evaporation. Then, a 100 mL sintered glass funnel was packed with clean silica (~12 g) and then topped with the compound-adsorbed silica sample. Fractions were collected individually by applying vacuum. Each fraction consisted of total 25 mL of the solvent mixture, starting from 25 mL of hexanes and increasing the polarity by adding 1 mL of EtOAc with each consecutive fraction (e.g. fraction #2: 24 mL of hexanes and 1

mL of EtOAc). Theoretical calculations were performed on Spartan'10 at B3LYP: 6-311++G** level of theory.

5.2 LIGANDS

2-Chloro-*N*-(2-(4,4-dimethyl-4,5-dihydrooxazol-2-yl)phenyl)acetamide (2)



Molecular weight: 266.72 g mol⁻¹

The solution of **1** (1.70 g, 8.90 mmol) and triethylamine (1.86 mL, 13.3 mmol) in DCM (25 mL) was placed into an ice bath and stirred for 15 min. 2-Chloroacetyl chloride (0.78 mL, 9.8 mmol) was then added dropwise over the period of 5 min to the stirring solution. Upon the completion of addition, the contents of the reaction vessel were stirred for 2 h at RT. Over that period of time, the colour of the solution changed from yellow to orange and finally to deep red; a pale pink precipitate was also noted. After 2 h, the dark red solution was gravity filtered and the filtrate was left to evaporate overnight (fumehood). Dark brown crystals formed and were then washed with Et₂O (20 mL), resulting in an orange solution and a black-coloured precipitate. The mixture was gravity filtered. Following solvent removal the product was isolated as orange crystalline solid (2.02 g, 85% yield; pure): Mp 97-99 °C; *R*_f = 0.62 (hexanes-EtOAc, 4:1).

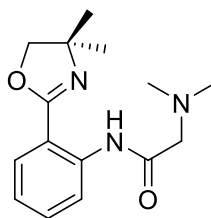
IR (KBr): 2953, 1675, 1639, 1609, 1589, 1535, 1450, 1355, 1303, 1057, 1046, 959, 776, 690 cm⁻¹.

^1H NMR (400 MHz, CDCl_3): δ = 13.05 (s, 1 H), 8.74 (dd, J = 1.2 Hz, J = 8.8 Hz, 1 H), 7.85 (ddd, J = 0.4 Hz, J = 2.0 Hz, J = 8.0 Hz, 1 H), 7.47 (dddd, J = 0.4 Hz, J = 2.0 Hz, J = 7.6 Hz, J = 8.8 Hz, 1 H), 7.13 (ddd, J = 1.2 Hz, J = 7.6 Hz, J = 8.0 Hz, 1 H), 4.21 (s, 2 H), 4.07 (s, 2 H), 1.41 (s, 6 H).

^{13}C NMR (100 MHz, CDCl_3): δ = 165.9, 161.6, 139.2, 132.4, 129.1, 123.3, 120.0, 114.5, 78.1, 68.2, 43.7, 28.6.

Anal. Calcd for $\text{C}_{13}\text{H}_{15}\text{ClN}_2\text{O}_2$: C, 58.54; H, 5.67; N, 10.50%. Found: C, 58.40; H, 5.55; N, 10.44%.

***N*-(2-(4,4-Dimethyl-4,5-dihydrooxazol-2-yl)phenyl)-2-(dimethylamino)acetamide (3a)**



Molecular weight: 275.35 g mol $^{-1}$

Thionyl chloride (8.81 mL, 121 mmol) was added to *N,N*-dimethylglycine (0.50 g, 4.85 mmol) in a 50 mL round-bottom flask. The orange-coloured mixture was heated to 50 °C and stirred for 4 h (until the solid disappeared). Excess thionyl chloride was removed *in vacuo* from the clear, bright yellow solution resulting in bright yellow solid. Then, the solution of **1** (0.46 g, 2.42 mmol) and triethylamine (0.70 mL, 5.02 mmol) in DCM (25.0 mL) was added to the *in situ* prepared acyl chloride and stirred for 12 h at RT. The dark orange solution was then extracted with water (3×50 mL). The combined organic layers were dried over MgSO_4 and gravity filtered, resulting in a transparent brownish-orange solution. After evaporation of the solvent, beige solid was formed. The compound was

purified by DCFC and the product was collected as dark orange wax from fractions 5 to 14 (0.34 g, 47% yield, pure): $R_f = 0.58$ (hexanes-EtOAc, 4:1).

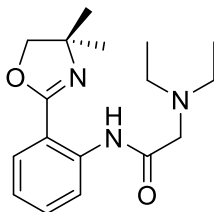
IR (KBr): 2969, 2779, 1677, 1645, 1581, 1532, 1447, 1291, 1208, 1053, 1044, 963, 877, 753, 689 cm^{-1} .

^1H NMR (400 MHz, CDCl_3): $\delta = 12.80$ (s, 1 H), 8.84 (d, $J = 12.0$ Hz, 1 H), 7.83 (dd, $J = 8.0$ Hz, $J = 4.0$ Hz, 1 H), 7.44 (t, $J = 8.0$ Hz, 1 H), 7.07 (t, $J = 8.0$ Hz, 1 H), 4.05 (s, 2 H), 3.16 (s, 2 H), 2.39 (s, 6 H), 1.40 (s, 6 H).

^{13}C NMR (100 MHz, CDCl_3): $\delta = 171.0$, 161.1, 139.5, 132.2, 129.0, 122.3, 119.8, 114.1, 77.7, 68.1, 64.5, 46.0, 28.6.

Anal. Calcd for $\text{C}_{15}\text{H}_{21}\text{N}_3\text{O}_2$: C, 65.43; H, 7.69; N, 15.26%. Found: C, 64.88; H, 7.66; N, 15.00%.

2-(Diethylamino)-*N*-(2-(4,4-dimethyl-4,5-dihydrooxazol-2-yl)phenyl)acetamide (3b)



Molecular weight: 303.41 g mol^{-1}

Compound **2** (1.27 g, 4.78 mmol) was added to the stirring solution of potassium carbonate (1.32 g, 9.55 mmol) and diethylamine (1.00 mL, 9.55 mmol) in MeCN (30.0 mL). An orange-coloured solution was then heated to reflux temperature ($\sim 80^\circ\text{C}$). The reaction progress was monitored by TLC, and the reflux was stopped after 24 h. The reaction mixture appeared dark brown with light brown precipitate. After it cooled down

to RT, it was gravity filtered and the solution was left to evaporate. After evaporation the compound appeared brown in colour and waxy in composition. The compound was purified by DCFC and the product was collected as yellow oil from fractions 8 to 18 (1.1 g, 69% yield, pure): $R_f = 0.59$ (hexanes-EtOAc, 4:1).

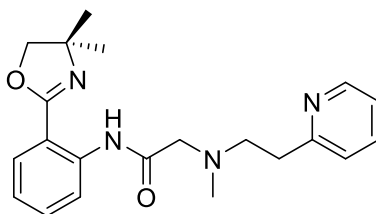
IR (NaCl): 2971, 1686, 1641, 1581, 1520, 1446, 1283, 1056, 1046, 773, 754 cm^{-1} .

^1H NMR (400 MHz, CDCl_3): $\delta = 12.64$ (s, 1 H), 8.88 (dd, $J = 8.8$ Hz, $J = 1.2$ Hz, 1 H), 7.85 (ddd, $J = 8.0$ Hz, $J = 1.6$ Hz, $J = 0.4$ Hz, 1 H), 7.44 (dddd, $J = 8.8$ Hz, $J = 7.2$ Hz, $J = 1.6$ Hz, $J = 0.4$ Hz, 1 H), 7.06 (ddd, $J = 7.6$ Hz, $J = 7.2$ Hz, $J = 1.2$ Hz, 1 H), 4.04 (s, 2 H), 3.24 (s, 2 H), 2.67 (q, $J = 7.2$ Hz, 4 H), 1.39 (s, 6 H), 1.09 (t, $J = 7.2$ Hz, 6 H).

^{13}C NMR (100 MHz, CDCl_3): $\delta = 172.8, 161.1, 139.6, 132.2, 129.3, 122.4, 120.1, 114.3, 77.8, 68.4, 58.2, 49.3, 28.7, 12.1$.

Anal. Calcd for $\text{C}_{17}\text{H}_{25}\text{N}_3\text{O}_2$: C, 67.30; H, 8.31; N, 13.85%. Found: C, 67.52; H, 8.20; N, 13.75%.

***N*-(2-(4,4-Dimethyl-4,5-dihydrooxazol-2-yl)phenyl)-2-(methyl(2-(pyridin-2-yl)ethyl)amino)acetamide (3c)**



Molecular weight: 366.46 g mol^{-1}

The compound was prepared similarly as for **3b** from 2-(2-methylaminoethyl)pyridine (0.50 mL, 3.60 mmol), **2** (0.48 g, 1.80 mmol) and potassium carbonate (0.50 g, 3.60 mmol) in MeCN (10 mL) for 23 h. The compound was purified by DCFC and the product

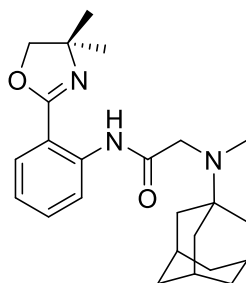
was collected as yellowish powder from fractions 20 to 34 (0.30 g, 45% yield, pure): R_f = 0.12 (hexanes-EtOAc, 3:2).

^1H NMR (400 MHz, CDCl_3): δ = 12.65 (s, 1 H), 8.84 (dd, J = 8.4 Hz, J = 1.2 Hz, 1 H), 8.50 (ddd, J = 4.8 Hz, J = 2.0 Hz, J = 0.8 Hz, 1 H), 7.84 (dd, J = 8.0 Hz, J = 1.6 Hz, 1 H), 7.54 (td, J = 7.6 Hz, J = 2.0 Hz, 1 H), 7.44 (ddd, J = 8.8 Hz, J = 7.6 Hz, J = 1.6 Hz, 1 H), 7.14 (dt, J = 8.0 Hz, J = 0.8 Hz, 1 H), 7.04-7.11 (m, 2 H), 4.02 (s, 2 H), 3.31 (s, 2 H), 2.95-3.10 (m, 4 H), 2.50 (s, 3 H), 1.38 (s, 6 H).

^{13}C NMR (100 MHz, CDCl_3): δ = 171.2, 161.2, 160.0, 149.4, 139.6, 136.5, 132.3, 129.2, 123.3, 122.5, 121.4, 120.1, 114.3, 77.8, 68.3, 62.2, 58.1, 43.6, 35.9, 28.8.

Anal. Calcd for $\text{C}_{21}\text{H}_{26}\text{N}_4\text{O}_2$: C, 68.83; H, 7.15; N, 15.29%. Found: C, 68.56; H, 7.14; N, 15.23%.

2-((3*S*,5*S*,7*S*)-Adamantan-1-yl(methyl)amino)-*N*-(2-(4,4-dimethyl-4,5-dihydrooxazol-2-yl)phenyl) acetamide (3d)



Molecular weight: 395.55 g mol⁻¹

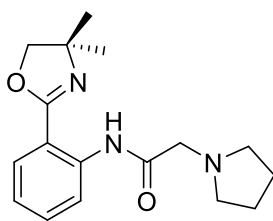
The compound was prepared similarly as for **3b** from *N*-methyldadamantylamine (0.17 g, 1.00 mmol), **2** (0.24 g, 0.90 mmol) and potassium carbonate (0.14 g, 1.00 mmol) in MeCN (20 mL) for 28 hours. The compound was recrystallized from DCM and hexanes as yellow wax (0.20 g, 56% yield, pure): R_f = 0.66 (hexanes-EtOAc, 4:1).

^1H NMR (400 MHz, CDCl_3): δ = 12.24 (s br, 1 H), 8.86 (dd, J = 8.4 Hz, J = 0.8 Hz, 1 H), 7.88 (dd, J = 7.6 Hz, J = 1.2 Hz, 1 H), 7.44 (ddd, J = 8.8 Hz, J = 7.6 Hz, J = 1.6 Hz, 1 H), 7.06 (ddd, J = 8.0 Hz, J = 7.6 Hz, J = 0.8 Hz, 1 H), 4.02, (s, 2 H), 3.31 (s, 2 H), 2.07-2.13 (m br, 3 H), 1.76 (d, J = 2.4 Hz, 6 H), 1.63 (q, J = 12.4 Hz, 6 H), 1.42 (s, 6 H).

^{13}C NMR (100 MHz, CDCl_3): δ = 173.6, 161.2, 139.6, 132.2, 129.6, 122.5, 120.5, 114.6, 77.8, 68.6, 56.0, 54.4, 38.7, 36.8, 36.2, 29.6, 28.7.

Anal. Calcd for $\text{C}_{24}\text{H}_{33}\text{N}_3\text{O}_2 \cdot \frac{1}{2}\text{H}_2\text{O}$: C, 71.25; H, 8.47; N, 10.39%. Found: C, 71.01; H, 8.49; N, 10.39%.

***N*-(2-(4,4-Dimethyl-4,5-dihydrooxazol-2-yl)phenyl)-2-(pyrrolidin-1-yl)acetamide (3e)**



Molecular weight: 301.39 g mol $^{-1}$

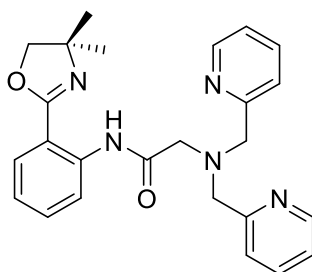
The compound was prepared similarly as for **3b** from pyrrolidine (0.58 mL, 6.95 mmol), **2** (1.20 g, 4.50 mmol) and potassium carbonate (1.24 g, 9.00 mmol) in MeCN (30 mL) for 7 h. The compound was recrystallized from DCM and hexane as beige solid (0.62 g, 73% yield, pure): Mp 106-108 °C; R_f = 0.28 (hexanes-EtOAc, 4:1).

^1H NMR (400 MHz, CDCl_3): δ = 12.47 (s, 1 H), 8.83 (dd, J = 8.4 Hz, J = 0.8 Hz, 1 H), 7.84 (ddd, J = 8.0 Hz, J = 2.0 Hz, J = 0.4 Hz, 1 H), 7.44 (dddd, J = 9.2 Hz, J = 7.2 Hz, J = 1.6 Hz, J = 0.4 Hz, 1 H), 7.07 (ddd, J = 8.0 Hz, J = 7.6 Hz, J = 1.2 Hz, 1 H), 4.04 (s, 2 H), 3.37 (s, 2 H), 2.68-2.76 (m, 4 H), 1.82-1.91 (m, 4 H), 1.39 (s, 6 H).

^{13}C NMR (100 MHz, CDCl_3): δ = 171.3, 161.3, 139.6, 132.3, 129.2, 122.5, 120.3, 114.3, 77.8, 68.3, 61.6, 54.7, 28.6, 24.5.

Anal. Calcd for $\text{C}_{17}\text{H}_{23}\text{N}_3\text{O}_2$: C, 67.75; H, 7.69; N, 13.94%. Found: C, 67.93; H, 7.66; N, 13.96%.

2-(Bis(pyridin-2-ylmethyl)amino)-*N*-(2-(4,4-dimethyl-4,5-dihydrooxazol-2-yl)phenyl)acetamide (3f)



Molecular weight: 429.52 g mol $^{-1}$

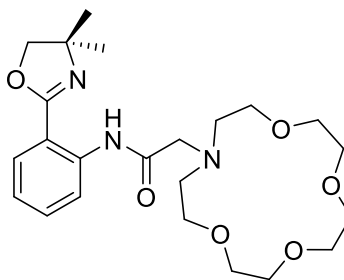
The compound was prepared similarly as for **3b** from 2,2'-dipicolylamine (0.20 mL, 1.12 mmol), **2** (0.30 g, 1.12 mmol) and potassium carbonate (0.31 g, 2.25 mmol) in MeCN (20 mL) for 24 h. The compound was purified by DCFC from fractions 29 to 38, then washed with Et_2O and collected as white solid (0.14 g, 30% yield, pure): R_f = 0.05 (hexanes-ETOAc, 1:1).

^1H NMR (400 MHz, CDCl_3): δ = 12.57 (s, 1 H), 8.76 (dd, J = 8.4 Hz, J = 0.8 Hz, 1 H), 8.55 (dt, J = 6.0 Hz, J = 1.2 Hz, 2 H), 7.88 (dd, J = 8.0 Hz, J = 2.0 Hz, 1 H), 7.45 (ddd, J = 8.8 Hz, J = 7.6 Hz, J = 2.0 Hz, 7.61-7.72 (m, 4 H), 7.18 (ddd, J = 6.8 Hz, J = 5.2 Hz, J = 2.4 Hz, 2 H), 7.10 (ddd, J = 8.0 Hz, J = 7.6 Hz, J = 1.2 Hz, 1 H), 4.12 (s, 4 H), 4.08 (s, 2 H), 3.49 (s, 2 H), 1.40 (s, 6 H).

^{13}C NMR (100 MHz, CDCl_3): δ = 170.6, 161.6, 157.9, 149.2, 139.4, 136.4, 132.3, 129.2, 123.6, 122.5, 122.2, 120.2, 114.1, 77.7, 68.3, 60.6, 57.9, 28.7.

Anal. Calcd for $\text{C}_{25}\text{H}_{27}\text{N}_5\text{O}_2$: C, 69.91; H, 6.34; N, 16.31%. Found: C, 69.88; H, 6.26; N, 16.13%.

***N*-(2-(4,4-Dimethyl-4,5-dihydrooxazol-2-yl)phenyl)-2-(1,4,7,10-tetraoxa-13-azacyclopentadecan-13-yl) acetamide (3g)**



Molecular weight: 449.55 g mol $^{-1}$

The compound was prepared similarly as for **3b** from 1-aza-15-crown-5 (0.22 g, 1.00 mmol), **2** (0.27 g, 1.00 mmol) and potassium carbonate (0.28 g, 2.00 mmol) in MeCN (25 mL) for 17 h. The compound was dissolved in CHCl_3 (30 mL) and extracted with H_2O (30 mL), and then brine (10 mL). Organic layer was dried over MgSO_4 . Collected as yellow wax (0.30 g, 67% yield, pure): R_f = 0.15 (hexanes-EtOAc, 1:1).

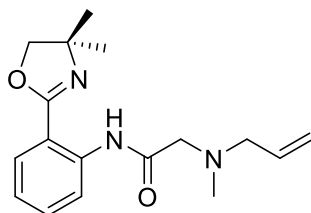
IR (KBr): 3089, 2867, 1683, 1636, 1582, 1520, 1446, 1355, 1284, 1127, 1057, 968, 934, 755 cm^{-1} .

^1H NMR (400 MHz, CDCl_3): δ = 12.52 (s br, 1 H), 8.82 (d, J = 8.4 Hz), 7.84 (d, J = 8.0 Hz, 1 H), 7.43 (t, J = 8.4 Hz, 1 H), 7.06 (t, J = 7.6 Hz, 1 H), 4.03 (s, 2 H), 3.72 (t, J = 6.0 Hz, 4 H), 3.60-3.68 (m, 12 H), 3.48 (s, 2 H), 3.04 (t, J = 6.0 Hz, 4 H), 1.40 (s, 6 H).

^{13}C NMR (100 MHz, CDCl_3): δ = 171.8, 161.2, 139.5, 132.2, 129.2, 122.4, 120.0, 114.1, 77.6, 70.9, 70.5, 70.4, 69.4, 68.2, 60.0, 54.5, 28.7.

Anal. Calcd for $C_{23}H_{35}N_3O_6$: C, 61.45; H, 7.85; N, 9.35%. Found: C, 61.38; H, 7.82; N, 9.52%.

2-(Allyl(methyl)amino)-*N*-(2-(4,4-dimethyl-4,5-dihydrooxazol-2-yl)phenyl)acetamide (3h)



Molecular weight: 301.39 g mol⁻¹

The compound was prepared similarly as for **3b** from allylmethylamine (0.30 mL, 3.10 mmol), **2** (0.80 g, 3.00 mmol) and potassium carbonate (0.71 g, 5.10 mmol) in MeCN (30 mL) for 48 h. The compound was purified by DCFC and the product was collected as yellowish oil from fractions 7 to 10 (0.37 g, 41% yield, pure): R_f = 0.53 (hexanes-EtOAc, 4:1).

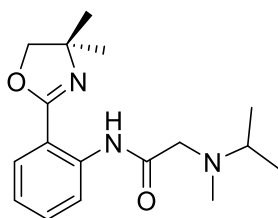
IR (KBr): 3083, 2971, 1683, 1643, 1582, 1520, 1447, 1354, 1293, 1209, 1056, 1046, 968, 926, 773, 754, 690 cm⁻¹.

¹H NMR (400 MHz, CDCl₃): δ = 12.71 (s, 1 H), 8.86 (dd, J = 8.4 Hz, J = 0.8 Hz, 1 H), 7.84 (ddd, J = 8.0 Hz, J = 1.6 Hz, J = 0.4 Hz, 1 H), 7.43 (dddd, J = 9.2 Hz, J = 7.6 Hz, J = 2.0 Hz, J = 0.4 Hz, 1 H), 7.06 (ddd, J = 7.6 Hz, J = 7.2 Hz, J = 1.2 Hz, 1 H), 5.95 (ddt, J = 16.8 Hz, J = 10.4 Hz, J = 6.8 Hz, 1 H), 5.23 (dq, J = 17.2 Hz, J = 1.6 Hz, 1 H), 5.16 (ddt, J = 10.0 Hz, J = 2.0 Hz, J = 0.8 Hz, 1 H), 4.03 (s, 2 H), 3.20 (s, 2 H), 3.16 (dt, J = 6.8 Hz, J = 1.6 Hz, 2 H), 2.38 (s, 3 H), 1.39 (s, 6 H).

^{13}C NMR (100 MHz, CDCl_3): δ = 171.4, 161.2, 139.6, 135.2, 132.2, 129.2, 122.4, 120.0, 118.4, 114.2, 77.7, 68.2, 61.4, 61.1, 43.7, 28.6.

Anal. Calcd for $\text{C}_{17}\text{H}_{23}\text{N}_3\text{O}_2$: C, 67.75; H, 7.69; N, 13.94%. Found: C, 67.96; H, 7.67; N, 13.73%.

***N*-(2-(4,4-Dimethyl-4,5-dihydrooxazol-2-yl)phenyl)-2-(isopropyl(methyl)amino)acetamide (3i)**



Molecular weight: 303.41 g mol $^{-1}$

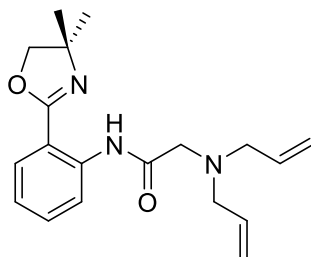
The compound was prepared similarly as for **3b** from *N*-isopropylmethylamine (1.04 g, 10.0 mmol), **2** (2.67 g, 10.0 mmol) and potassium carbonate (2.76 g, 20.0 mmol) in MeCN (50 mL) for 24 h. The compound was dissolved in DCM (30 mL) and extracted with H_2O (2×30 mL), and then brine (30 mL). Organic layer was dried over MgSO_4 . The product was collected as orange oil (2.00 g, 66% yield, pure): R_f = 0.14 (hexanes-ETOAc, 4:1).

^1H NMR (400 MHz, CDCl_3): δ = 12.63 (s br, 1 H), 8.88 (d, J = 8.4 Hz, 1 H), 7.84 (d, J = 7.6 Hz, 1 H), 7.43 (t, J = 8.4 Hz, 1 H), 7.05 (t, J = 7.6 Hz, 1 H), 4.02 (s, 2 H), 3.17 (s, 2 H), 2.93 (sept, J = 6.8 Hz, 1 H), 2.35 (s, 3 H), 1.38 (s, 6 H), 1.07 (d, J = 6.8 Hz, 6 H).

^{13}C NMR (100 MHz, CDCl_3): δ = 172.5, 161.0, 139.5, 132.1, 129.2, 122.3, 120.0, 114.3, 77.6, 68.2, 57.1, 54.3, 40.2, 28.5, 18.2.

Anal. Calcd for $C_{17}H_{25}N_3O_2$: C, 67.30; H, 8.31; N, 13.85%. Found: C, 67.18; H, 8.28; N, 13.96%.

2-(Diallylamino)-N-(2-(4,4-dimethyl-4,5-dihydrooxazol-2-yl)phenyl)acetamide (3j)



Molecular weight: 327.43 g mol⁻¹

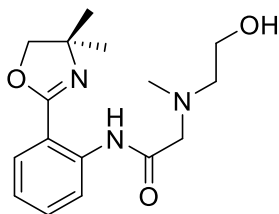
The compound was prepared similarly as for **3b** from diallylamine (0.43 mL, 3.50 mmol), **2** (0.80 g, 3.00 mmol) and potassium carbonate (0.83 g, 6.00 mmol) in MeCN (25 mL). The compound was recrystallized from petroleum ether as orange wax (0.72 g, 74% yield, pure): R_f = 0.67 (hexanes-EtOAc, 4:1).

¹H NMR (400 MHz, CDCl₃): δ = 12.61 (s, 1 H), 8.86 (d, J = 8.8 Hz, 1 H), 7.86 (dd, J = 1.6 Hz, J = 8.0 Hz, 1 H), 7.44 (dt, J = 1.6 Hz, J = 8.8 Hz, 1 H), 7.07 (t, J = 8.0 Hz, 1 H), 5.97 (tdd, J = 6.8 Hz, J = 10.4 Hz, J = 17.2 Hz, 2 H), 5.21 (d, J = 17.2 Hz, 2 H), 5.15 (d, J = 10.4 Hz, 2 H), 4.05 (s, 2 H), 3.27 (s, 2 H), 3.24 (d, J = 6.8 Hz, 4 H), 1.41 (s, 6 H).

¹³C NMR (100 MHz, CDCl₃): δ = 171.8, 161.2, 139.5, 134.8, 132.2, 129.2, 122.3, 119.9, 118.6, 114.1, 77.6, 68.3, 58.5, 57.6, 28.6.

Anal. Calcd for $C_{19}H_{25}N_3O_2 \cdot \frac{1}{4}H_2O$: C, 68.75; H, 7.74; N, 12.66%. Found: C, 68.46; H, 7.64; N, 12.43%.

***N*-(2-(4,4-Dimethyl-4,5-dihydrooxazol-2-yl)phenyl)-2-((2-hydroxyethyl)(methyl)amino)acetamide (3k)**



Molecular weight: 305.38 g mol⁻¹

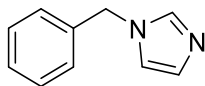
In a 50 mL three neck round bottom flask, **4** (0.22, 1.20 mmol) and K₂CO₃ (0.21 g, 1.50 mmol) were dissolved in MeCN (15 mL) under an atmosphere of nitrogen gas. The solution was stirred for 15 min. Then the solution of **2** (0.20 g, 0.75 mmol) in MeCN (10 mL) was transferred to the reaction flask. The mixture was stirred at reflux temperature (80 °C) for 18 h. After the reflux was complete, the solution was filtered and allowed to evaporate. The product was a light yellow wax (0.20 g, 88% calculated yield, crude).

¹H NMR (400 MHz, CDCl₃): δ = 12.22 (s br, 1 H), 8.80 (d, *J* = 8.0 Hz, 1 H), 7.80 (dd, *J* = 8.0 Hz, *J* = 1.6 Hz, 1 H), 7.42 (t, *J* = 8.0 Hz, 1 H), 7.05 (t, *J* = 8.0 Hz, 1 H), 4.03 (s, 2 H), 3.62 (t, *J* = 4.8 Hz, 2 H), 3.24 (s, 2 H), 2.66 (t, *J* = 4.8 Hz, 2 H), 2.43 (s, 3 H), 1.40 (s, 6 H).

¹³C NMR (100 MHz, CDCl₃): δ = 170.7, 162.2, 139.1, 132.6, 129.6, 122.8, 120.0, 114.3, 77.9, 68.6, 62.8, 60.8, 59.2, 44.2, 28.5.

Anal. Calcd for C₁₆H₂₃N₃O₃: C, 62.93; H, 7.59; N, 13.76%. Found: C, 62.56; H, 7.23; N, 12.06%.

Synthesis of 1-benzylimidazole⁶²

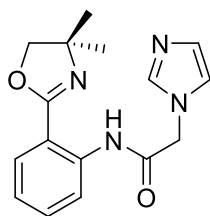


Molecular weight: 158.20 g mol⁻¹

Potassium carbonate (3.99 g, 28.8 mmol) and imidazole hydrochloride (1.00 g, 9.60 mmol) were dissolved in MeCN (30 mL). Benzyl bromide (1.25 mL, 10.6 mmol) was added dropwise to the stirring solution at RT. After 70 hours, the solution was concentrated and redissolved in DCM and extracted with H₂O (3 x 30 mL). Organic layer was dried over MgSO₄. The product was collected as off-white wax (0.63 g, 42% yield, pure).

¹H NMR matches reported literature values.⁶²

N-(2-(4,4-dimethyl-4,5-dihydrooxazol-2-yl)phenyl)-2-(1*H*-imidazol-1-yl)acetamide (2I)



Molecular weight: 298.35 g mol⁻¹

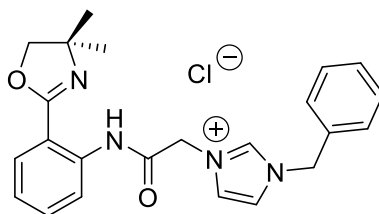
Imidazole (0.05 g, 0.750 mmol), **2** (0.22 g, 0.82 mmol) and K₂CO₃ (0.31 g, 2.25 mmol) were dissolved in MeCN (15.0 mL). The bright yellow reaction mixture was refluxed for 24 h. It was then cooled to RT, the reaction mixture was gravity filtered, and the filtrate was concentrated and then washed with Et₂O (3 × 5.0 mL). The compound was recrystallized from DCM and hexanes as white solid (0.12 g, 56% yield; pure): R_f = 0.18 (hexanes-EtOAc, 4:1).

^1H NMR (400 MHz, CDCl_3): δ = 12.40 (s, 1 H), 8.71 (d, J = 8.4 Hz, 1 H), 7.84 (d, J = 7.6 Hz, 1 H), 7.62 (s, 1 H), 7.46 (t, J = 7.6 Hz, 1 H), 7.16 (s, 1 H), 7.12 (t, J = 7.6 Hz, 1 H), 7.04 (s, 1 H), 4.80 (s, 2 H), 3.98 (s, 2 H), 1.30 (s, 6 H).

^{13}C NMR (100 MHz, CDCl_3): δ = 165.7, 161.7, 138.8, 138.3, 132.5, 130.4, 129.2, 123.3, 120.1, 120.0, 113.9, 77.9, 68.2, 51.4, 28.2.

Anal. Calcd for $\text{C}_{16}\text{H}_{18}\text{N}_4\text{O}_2$: C, 64.41; H, 6.08; N, 18.78%. Found: C, 64.53; H, 6.17; N, 16.32%.

1-Benzyl-3-(2-((2-(4,4-dimethyl-4,5-dihydrooxazol-2-yl)phenyl)amino)-2-oxoethyl)-1H-imidazol-3-ium chloride (3I)



Molecular weight: 424.93 g mol $^{-1}$

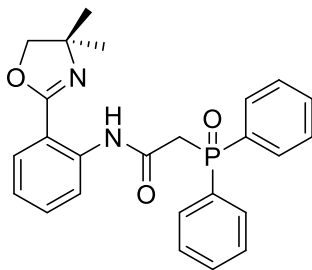
A solution of **2** (0.40 g, 1.50 mmol) and **1-benzylimidazole** (0.19 g, 1.20 mmol) in THF/MeCN (15/3 mL) was refluxed for 24 h. The solution was concentrated and then washed with Et_2O (10 mL total). The compound was collected as yellow wax (0.29 g, 57% yield, pure): R_f = 0.61 (hexanes-EtOAc, 4:1).

^1H NMR (400 MHz, CDCl_3): δ = 12.96 (s br, 1 H), 10.71 (s br, 1 H), 8.44 (d, J = 8.4 Hz, 1 H), 7.84 (d, J = 7.6 Hz, 1 H), 7.47 (s br, 1 H), 7.33-7.45 (m, 6 H), 7.21 (s br, 1 H), 7.12 (t, J = 7.6 Hz, 1 H), 5.54 (s, 2 H), 5.50 (s, 2 H), 4.08 (s, 2 H), 1.43 (s, 6 H).

^{13}C NMR (100 MHz, CDCl_3): δ = 162.6, 162.0, 139.1, 138.5, 132.6, 132.5, 129.6, 129.5, 129.2, 129.0, 123.6, 123.5, 120.8, 119.9, 114.0, 78.1, 68.2, 53.7, 52.3, 28.6.

Anal. Calcd for $C_{23}H_{25}ClN_4O_2 \cdot \frac{1}{2}H_2O$: C, 59.93; H, 6.34; N, 12.15%. Found: C, 59.86; H, 6.27; N, 11.03%.

***N*-(2-(4,4-Dimethyl-4,5-dihydrooxazol-2-yl)phenyl)-2-(diphenylphosphoryl)acetamide (3m•oxide)**



Molecular weight: 432.46 g mol⁻¹

Compound **2** (0.80 g, 3.00 mmol) was dissolved in dry THF (15.0 mL) and was placed into an ice bath at -84 °C (the mixture of EtOAc/liquid N₂). A 0.5 M solution of KPPH₂ in THF (6.00 mL, 3.00 mmol) was added dropwise to the stirring solution. After the solution was stirred for 24 h under N₂ at RT it was cannula transferred and the precipitate was discarded. The compound was recrystallized in air from DCM/Et₂O as yellow waxy solid (0.69 g, 55% yield, pure): R_f = 0.63 (hexanes-EtOAc, 4:1).

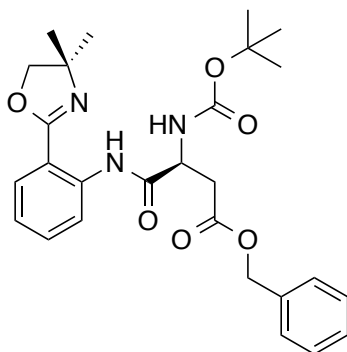
¹H NMR (400 MHz, CDCl₃): δ = 12.43 (s, 1 H), 8.45 (d, *J* = 8.4 Hz, 1 H), 7.82-7.90 (m, 4 H), 7.76 (dd, *J* = 7.6 Hz, *J* = 1.6 Hz, 1 H), 7.40-7.53 (m, 6 H), 7.34 (ddd, *J* = 8.8 Hz, *J* = 8.0 Hz, *J* = 1.6 Hz, 1 H), 7.03 (td, *J* = 8.0 Hz, *J* = 1.2 Hz, 1 H), 4.03 (s, 2 H), 3.56 (d, *J* = 15.6 Hz, 2 H), 1.38 (s, 6 H).

¹³C NMR (100 MHz, CDCl₃): δ = 162.7 (d, *J* (¹³C-³¹P) = 5.0 Hz), 161.8, 139.3, 132.4, 132.3, 132.2 (d, *J* (¹³C-³¹P) = 3.0 Hz), 131.5, 131.4, 131.3, 128.9, 128.7, 128.6, 122.8, 119.8, 113.7, 77.9, 68.0, 43.06 (d, *J* (¹³C-³¹P) = 61.0 Hz), 28.7.

³¹P{¹H} NMR (162 MHz, CDCl₃): δ = 28.49.

Anal. Calcd for $C_{25}H_{25}N_2O_3P \cdot \frac{1}{2}(H_2O) \cdot \frac{1}{2}CH_2Cl_2$: C, 63.29; H, 5.62; N, 5.79%. Found: C, 64.70; H, 5.92; N, 5.75%.

Synthesis of Boc-Bn-pincer (3n)



Molecular weight: 495.58 g mol⁻¹

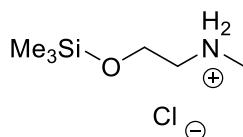
Boc-*L*-aspartic acid 4-benzyl ester (2.00 g, 6.30 mmol) and **1** (ox-NH₂, 1.00 g, 5.25 mmol) were dissolved in DCM (25.0 mL) and the solution was stirred in an ice bath for 5 min. Then DCC (1.62 g, 7.88 mmol) was added to the stirring solution. After the reaction was stirred for 24 h at RT, the white precipitate was filtered off (gravity filtration) and solvent was removed *in vacuo*. Recrystallization with DCM/hexanes (1:1) afforded compound as yellow wax (2.60 g, >99% yield; pure).

¹H NMR (400 MHz, CDCl₃): δ = 12.69 (s, 1 H), 8.65 (d, J = 8.4 Hz, 1 H), 7.83 (d, J = 7.6 Hz, 1 H), 7.45 (ddd, J = 8.8 Hz, J = 7.2 Hz, J = 1.6 Hz, 1 H), 7.35-7.31 (m, 1 H), 7.28-7.25 (m, 4 H), 7.10 (td, J = 8.0 Hz, J = 1.2 Hz, 1 H), 5.71 (d, J = 9.2 Hz, 1 H), 5.20-5.03 (m, 2 H), 4.90-4.70 (m, 1 H), 4.06-4.00 (m, 2 H), 3.30-2.80 (m, 2 H), 1.49-1.36 (m, 18 H).

^{13}C NMR (100 MHz, CDCl_3): δ = 171.3, 169.8, 161.8, 155.6, 139.4, 132.4, 129.1, 128.6, 128.3, 122.9, 120.3, 114.2, 80.6, 78.0, 68.1, 66.8, 52.5, 37.0, 34.8, 31.7, 28.7, 28.5, 25.4, 22.8, 14.3.

Anal. Calcd for $\text{C}_{27}\text{H}_{33}\text{N}_3\text{O}_6$: C, 65.44; H, 6.71; N, 8.48%. Found: C, 65.53; H, 6.91; N, 8.23%.

Synthesis of N-methyl-2-((trimethylsilyl)oxy)ethan-1-aminium chloride (4)



Molecular weight: 183.75 g mol $^{-1}$

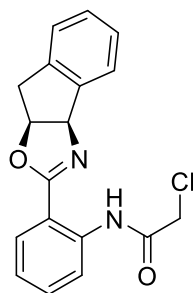
Dry Et_2O (30.0 mL) was obtained in a round bottom flask attached to a reflux condenser. 2-Methylaminoethanol (1.07 mL, 13.3 mmol) was added to the flask and the mixture was let to stir for 5 min under an atmosphere of N_2 . TMSCl (3.34 mL, 26.7 mmol) was then added dropwise to the reaction flask. The reaction was then refluxed for 3 h. After reflux, the solvent was evaporated *in vacuo* giving a white fluffy solid (1.98 g, 81% yield, pure).

^1H NMR (400 MHz, CDCl_3) δ = 9.43 (bs, 2H), 3.93 (t, J = 5.2 Hz, 2H), 3.08 (t, J = 5.2 Hz, 2H), 2.74 (t, J = 5.2 Hz, 3H), 0.14 (s, 9H).

^{13}C NMR (100 MHz, CDCl_3) δ = 57.7, 50.6, 33.3, -0.5.

Anal. Calcd for $\text{C}_6\text{H}_{18}\text{ClNOSi}\cdot\text{H}_2\text{O}$: C, 35.72; H, 9.99; N, 6.94%. Found: C, 35.56; H, 9.67; N, 9.02%.

2-chloro-*N*-(2-((3*aR*,8*aS*)-3*a*,8*a*-dihydro-8*H*-indeno[1,2-*d*]oxazol-2-yl)phenyl)acetamide (6)



Molecular weight: 326.78 g mol⁻¹

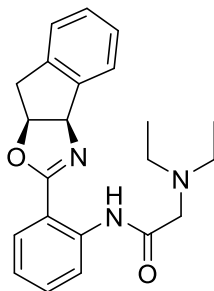
The solution of **5** (0.50 g, 2.00 mmol) and triethylamine (0.42 mL, 3.00 mmol) in DCM (25 mL) was placed into an ice bath and stirred for 30 min. 2-Chloroacetyl chloride (0.17 mL, 2.20 mmol) was then added dropwise for 5 min to the stirring solution. Upon the completion of addition, the contents of the reaction vessel were stirred for 24 h at RT. The colour of the solution changed from yellow to dark brown with white precipitate over the course of the reaction. The solution was gravity filtered. Hexanes (10 mL) and then Et₂O (5 mL) were used to crash the product out of DCM solution. The product was isolated as peachy crystalline solid after filtration (0.56 g, 86% yield; pure): *R_f* = 0.63 (hexanes-EtOAc, 4:1).

¹H NMR (400 MHz, CDCl₃): δ = 12.98 (s, 1 H), 8.72 (dd, *J* = 8.4 Hz, *J* = 0.8 Hz, 1 H), 7.89 (dd, *J* = 8.0 Hz, *J* = 1.6 Hz, 1 H), 7.51-7.57 (m, 1 H), 7.47 (ddd, *J* = 8.8 Hz, *J* = 7.6 Hz, *J* = 2.0 Hz, 1 H), 7.25-7.35 (m, 2 H), 7.13 (td, *J* = 7.6 Hz, *J* = 0.8 Hz, 1 H), 5.86 (d, *J* = 8.0, 1 H), 5.47 (ddd, *J* = 8.4 Hz, *J* = 7.2 Hz, *J* = 2.0 Hz, 1 H), 4.25 (q, *J* = 14.8 Hz, 2 H), 3.50-3.60 (m, 1 H), 3.35-3.45 (m, 1 H), 1.41 (t, *J* = 7.6 Hz, 1 H).

¹³C NMR (100 MHz, CDCl₃): δ = 165.8, 163.8, 141.4, 139.7, 139.0, 132.8, 129.5, 129.0, 127.8, 125.8, 125.6, 123.4, 120.3, 114.2, 82.4, 76.5, 43.7, 39.8.

Anal. Calcd for C₁₈H₁₅ClN₂O₂: C, 66.16; H, 4.63; N, 8.57%. Found: C, 65.88; H, 4.60; N, 8.50%.

Synthesis of *N*-methyl-2-((trimethylsilyl)oxy)ethan-1-aminium chloride (7)



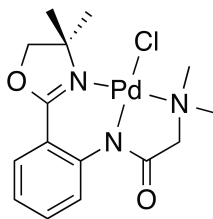
Molecular weight: 363.46 g mol⁻¹

Compound **6** (0.20 g, 0.61 mmol) was added to the stirring solution of K₂CO₃ (0.17 g, 1.22 mmol) and diethylamine (0.063 mL, 0.610 mmol) in MeCN (15.0 mL). An orange-coloured solution was then heated to reflux temperature (~80 °C). The reaction progress was monitored by TLC, and the reflux was stopped after 48 h. The reaction mixture appeared dark brown with light brown precipitate. After it cooled down to RT, it was gravity filtered and the solution was left to evaporate. After evaporation the compound appeared brown in colour and waxy in composition. The compound was purified by recrystallization with EtOAc (0.12 g, 55% yield, crude): R_f = 0.42 (hexanes-EtOAc, 4:1).

¹H NMR (400 MHz, CDCl₃): δ = 12.54 (s, 1 H), 8.81 (d, *J* = 8.4 Hz, 1 H), 7.85 (dd, *J* = 7.6 Hz, *J* = 1.2 Hz, 1 H), 7.51-7.38 (m, 2 H), 7.30-7.22 (m, 3 H), (t, *J* = 7.6 Hz, 1 H), 5.80 (d, *J* = 8.0 Hz, 1 H), 5.41 (td, *J* = 6.8 Hz, *J* = 1.6 Hz, 1 H), 3.56-3.47 (m, 1 H), 3.42-3.34 (m, 1 H), 3.27 (s, 2 H), 2.75 (q, *J* = 7.2 Hz, 4 H), 1.14 (t, *J* = 7.2 Hz, 6 H).

5.3 PALLADIUM COMPLEXES

Synthesis of 9a



Molecular weight: 416.21 g mol⁻¹

The solution of **3a** (0.10 g, 0.36 mmol) in MeOH (5.0 mL) was cooled in the ice bath for 5 min. Then the 0.1135 M solution of Li₂PdCl₄ (3.20 mL, 0.36 mmol) was added dropwise. The orange solution was stirred at RT for 24 h. The solvent was removed *in vacuo* and the orange compound was redissolved in DCM (5.0 mL) and filtered through Celite. The compound was isolated as orange solid (0.12 g, 82% yield; pure).

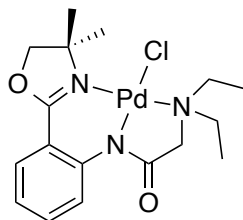
IR (KBr): 2956, 2911, 1646, 1611, 1488, 1362, 1273, 1167, 1086, 966, 865, 756 cm⁻¹.

¹H NMR (400 MHz, CDCl₃): δ = 8.34 (dd, *J* = 8.4 Hz, *J* = 0.8 Hz, 1 H), 7.70 (dd, *J* = 8.0 Hz, *J* = 1.6 Hz, 1 H), 7.40 (ddd, *J* = 8.8 Hz, *J* = 7.2 Hz, *J* = 1.6 Hz, 1 H), 6.99 (ddd, *J* = 8.0 Hz, *J* = 7.2 Hz, *J* = 0.8 Hz, 1 H), 4.21 (s, 2 H), 3.68 (s, 2 H), 2.70 (s, 6 H), 1.72 (s, 6 H).

¹³C NMR (100 MHz, CDCl₃): δ = 175.1, 162.6, 144.8, 133.2, 129.8, 123.4, 122.0, 116.5, 81.5, 71.2, 70.7, 52.2, 27.9.

Anal. Calcd for C₁₅H₂₀ClN₃O₂Pd: C, 43.29; H, 4.84; N, 10.10%. Found: C, 43.24; H, 4.92; N, 9.99%.

Synthesis of 9b



Molecular weight: 444.27 g mol⁻¹

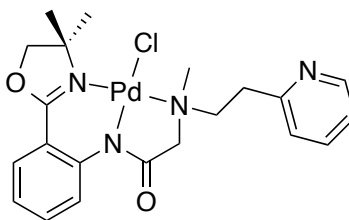
The compound was prepared and purified similarly as for **9a** from **3b** (0.24 g, 0.79 mmol) and 7.9×10⁻² M Li₂PdCl₄ (10.0 mL, 0.79 mmol). The compound was isolated as orange solid (0.18 g, 52% yield; pure).

¹H NMR (400 MHz, CDCl₃): δ = 8.30 (d, *J* = 8.4 Hz, 1 H), 7.65 (d, *J* = 7.6 Hz, 1 H), 7.37 (t, *J* = 7.6 Hz, 1 H), 6.96 (t, *J* = 7.6 Hz, 1 H), 4.21 (s, 2 H), 3.61 (s, 2 H), 3.23 (dq, *J* = 13.6 Hz, *J* = 6.8 Hz, 2 H), 2.43 (dq, *J* = 13.6 Hz, *J* = 6.8 Hz, 2 H), 1.73 (s, 6 H), 1.65 (t, *J* = 6.8 Hz, 6 H).

¹³C NMR (100 MHz, CDCl₃): δ = 177.3, 162.4, 144.7, 132.9, 129.4, 123.2, 121.6, 116.4, 81.6, 70.6, 63.6, 56.6, 27.9, 12.4.

Anal. Calcd for C₁₇H₂₄ClN₃O₂Pd·½(H₂O): C, 43.33; H, 5.77; N, 8.92%. Found: C, 43.57; H, 5.47; N, 8.52%.

Synthesis of 9c



Molecular weight: 507.33 g mol⁻¹

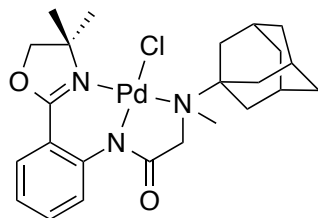
The compound was prepared and purified similarly as for **9a** from **3c** (0.34 g, 0.92 mmol) and 9.3×10^{-2} M Li₂PdCl₄ (10.0 mL, 0.92 mmol). The compound was purified using preparative TLC (% Acetone as eluent, R_f = 0.62) and isolated as orange solid (0.21 g, 45% yield; pure).

¹H NMR (400 MHz, CDCl₃): δ = 9.12 (d, J = 5.6 Hz, 1 H), 8.49 (d, J = 8.6 Hz, 1 H), 7.79-7.66 (m, 3 H), 7.48-7.32 (m, 2 H), 7.05-6.96 (m, 1 H), 5.22-5.09 (m, 1 H), 4.91-4.80 (m, 1 H), 4.79-4.69 (m, 1 H), 4.35-4.20 (m, 2 H), 3.82-3.73 (m, 1 H), 3.56-3.42 (m, 1 H), 3.16-3.06 (m, 1 H), 2.98 (s, 3 H), 1.83 (s, 3 H), 1.76 (s, 3 H).

¹³C NMR (100 MHz, CDCl₃): δ = 175.4, 162.6, 159.8, 153.1, 144.7, 138.9, 133.2, 129.5, 127.3, 123.7, 121.9, 116.4, 81.6, 70.7, 68.4, 62.3, 52.6, 51.3, 39.0, 28.1, 27.9.

Anal. Calcd for C₂₁H₂₅ClN₄O₂Pd·2(CH₂Cl₂): C, 40.79; H, 4.32; N, 8.27%. Found: C 41.34, H 4.53, N 8.69%.

Synthesis of 9d



Molecular weight: 536.41 g mol⁻¹

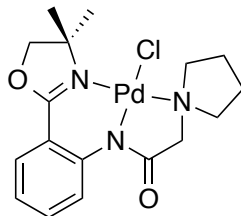
The compound was prepared and purified similarly as for **9a** from **3d** (0.03 g, 0.08 mmol) and 7.9×10^{-2} M Li₂PdCl₄ (0.96 mL, 0.08 mmol). The compound was isolated as orange solid (0.04 g, 80% yield; pure).

¹H NMR (400 MHz, CDCl₃): δ = 8.07 (d, J = 8.4 Hz, 1 H), 7.69 (d, J = 8.0 Hz, 1 H), 7.41 (t, J = 7.2 Hz, 1 H), 7.01 (t, J = 7.6 Hz, 1 H), 4.35-4.12 (m, 2 H), 3.91-3.84 (m, 2 H), 2.85 (s, 3 H), 2.23-2.08 (m, 7 H), 1.88 (s, 3 H), 1.70-1.56 (m, 15 H).

¹³C NMR (100 MHz, CDCl₃): δ = 177.0, 162.7, 144.7, 133.2, 129.4, 123.0, 121.7, 117.4, 82.0, 70.9, 67.1, 64.2, 47.7, 39.0, 36.1, 30.2, 28.7, 27.7.

Anal. Calcd for C₂₄H₃₂ClN₃O₂Pd·½(CH₂Cl₂): C, 46.14; H, 5.31; N, 6.33%. Found: C, 46.30; H, 5.48; N, 6.15%.

Synthesis of 9e



Molecular weight: 442.25 g mol⁻¹

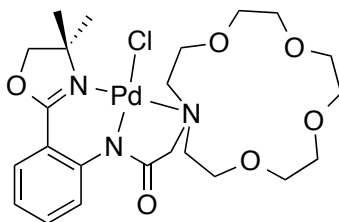
The compound was prepared and purified similarly as for **9a** from **3e** (0.20 g, 0.66 mmol) and 0.1135 M Li₂PdCl₄ (5.85 mL, 0.66 mmol). The compound was isolated as orange solid (0.18 g, 62% yield; pure).

¹H NMR (400 MHz, CDCl₃): δ = 8.27 (d, *J* = 8.4 Hz, 1 H), 7.70 (*J* = 8.0 Hz, *J* = 1.6 Hz, 1 H), 7.40 (ddd, *J* = 8.8 Hz, *J* = 7.2 Hz, *J* = 1.6 Hz, 1 H), 6.99 (dd, *J* = 7.6 Hz, *J* = 7.6 Hz, 1 H), 4.20 (s, 2 H), 3.83-3.71 (m, 4 H), 2.75-2.64 (m, 2 H), 2.12-2.01 (m, 2 H), 1.91-1.81 (m, 2 H), 1.72 (s, 6 H).

¹³C NMR (100 MHz, CDCl₃): δ = 175.2, 162.4, 144.6, 132.9, 129.6, 123.3, 121.7, 116.6, 81.4, 70.6, 68.0, 60.1, 27.8, 22.2.

Anal. Calcd for C₁₇H₂₂ClN₃O₂Pd: C, 45.25; H, 5.14; N, 9.31%. Found: C, 45.45; H, 4.97; N, 8.95%.

Synthesis of 9g



Molecular weight: 590.41 g mol⁻¹

The compound was prepared and purified similarly as for **9a** from **3g** (0.10 g, 0.20 mmol) and 0.1135 M Li₂PdCl₄ (1.75 mL, 0.20 mmol). The compound was isolated as orange solid (0.11 g, 93% yield; pure).

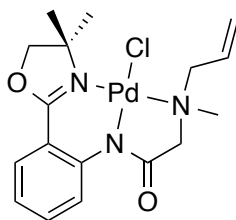
IR (KBr): 2871, 1636, 1617, 1364, 1272, 1125, 1085, 755, 732 cm⁻¹.

¹H NMR (400 MHz, CDCl₃): δ = 8.28 (dd, *J* = 8.4 Hz, *J* = 0.8 Hz, 1 H), 7.65 (dd, *J* = 8.0 Hz, *J* = 1.6 Hz, 1 H), 7.37 (ddd, *J* = 8.8 Hz, *J* = 7.2 Hz, *J* = 1.6 Hz, 1 H), 6.96 (ddd, *J* = 8.4 Hz, *J* = 7.2 Hz, *J* = 1.2 Hz, 1 H), 4.65 (s, 2 H), 4.35-4.25 (m, 2 H), 4.20 (s, 2 H), 4.12-4.02 (m, 2 H), 3.75-3.55 (m, 12 H), 3.42-3.35 (m, 4 H), 1.72 (s, 6 H).

¹³C NMR (100 MHz, CDCl₃): δ = 177.2, 162.6, 145.0, 133.0, 129.4, 123.7, 121.6, 116.5, 81.7, 71.0, 70.8, 70.6, 70.5, 68.8, 60.1, 28.0.

Anal. Calcd for C₂₃H₃₄ClN₃O₆Pd·½(CH₃OH): C, 46.54; H, 5.98; N, 6.93%. Found: C, 47.63; H, 6.38; N, 6.91%.

Synthesis of 9h



Molecular weight: 442.25 g mol⁻¹

The compound was prepared and purified similarly as for **9a** from **3h** (0.16 g, 0.51 mmol) and 0.1135 M Li₂PdCl₄ (4.53 mL, 0.51 mmol). The compound was isolated as orange solid (0.18 g, 78% yield; pure).

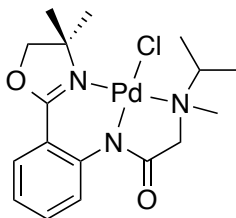
IR (KBr): 2954, 2918, 1636, 1618, 1486, 1356, 1324, 1271, 1085, 753 cm⁻¹.

¹H NMR (400 MHz, CDCl₃): δ = 8.31 (dd, *J* = 8.4 Hz, *J* = 0.8 Hz, 1 H), 7.67 (dd, *J* = 8.0 Hz, *J* = 1.6 Hz, 1 H), 7.38 (ddd, *J* = 8.8 Hz, *J* = 7.2 Hz, *J* = 1.6 Hz, 1 H), 6.97 (ddd, *J* = 8.4 Hz, *J* = 7.2 Hz, *J* = 1.2 Hz, 1 H), 6.64 (dddd, *J* = 17.2 Hz, *J* = 10.0 Hz, *J* = 8.4 Hz, *J* = 5.2 Hz, 1 H), 5.48 (d, *J* = 10.0 Hz, 1 H), 5.37 (dd, *J* = 17.2 Hz, *J* = 0.8 Hz, 1 H), 4.27-4.15 (m, 2 H), 3.99 (d, *J* = 16.0 Hz, 1 H), 3.89 (dd, *J* = 12.8 Hz, *J* = 5.2 Hz, 1 H), 3.31 (d, *J* = 16.0 Hz, 1 H), 2.78 (s, 3 H), 2.74 (dd, *J* = 12.8 Hz, *J* = 8.4 Hz, 1 H), 1.77 (s, 3 H), 1.68 (s, 3 H).

¹³C NMR (100 MHz, CDCl₃): δ = 175.9, 162.6, 144.8, 133.1, 131.5, 129.6, 123.4, 123.3, 121.9, 116.4, 81.6, 70.7, 66.9, 65.5, 50.8, 28.1, 27.8.

Anal. Calcd for C₁₇H₂₂ClN₃O₂Pd: C, 46.17; H, 5.01; N, 9.50%. Found: C, 46.30; H, 5.31; N, 9.32%.

Synthesis of 9i



Molecular weight: 444.27 g mol⁻¹

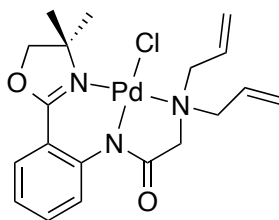
The compound was prepared and purified similarly as for **9a** from **3i** (0.06 g, 0.20 mmol) and 7.9×10⁻² M Li₂PdCl₄ (2.53 mL, 0.20 mmol). The compound was isolated as orange solid (0.07g, 77% yield; pure).

¹H NMR (400 MHz, CDCl₃): δ = 8.34 (dd, *J* = 8.8 Hz, *J* = 0.8 Hz, 1 H), 7.69 (*J* = 8.0 Hz, *J* = 1.6 Hz, 1 H), 7.41 (ddd, *J* = 8.8 Hz, *J* = 7.2 Hz, *J* = 1.6 Hz, 1 H), 7.00 (ddd, *J* = 8.0 Hz, *J* = 7.2 Hz, *J* = 0.8 Hz, 1 H), 4.28-4.20 (m, 2 H), 3.90-3.83 (m, 1 H), 3.60 (sept, *J* = 6.8 Hz, 1 H), 3.45-3.39 (m, 1 H), 2.84 (s, 3 H), 1.79 (s, 3 H), 1.74 (s, 3 H), 1.71 (d, *J* = 6.8 Hz, 3 H), 1.26 (d, *J* = 6.8 Hz, 3 H).

¹³C NMR (100 MHz, CDCl₃): δ = 176.8, 162.4, 144.6, 132.9, 129.4, 123.3, 121.7, 116.5, 81.5, 70.5, 62.3, 59.5, 47.6, 27.9, 27.7, 20.5, 15.7.

Anal. Calcd for C₁₇H₂₄ClN₃O₂Pd: C, 45.96; H, 5.45; N, 9.46%. Found: C, 46.56; H, 5.52; N, 9.26%.

Synthesis of 9j



Molecular weight: 468.29 g mol⁻¹

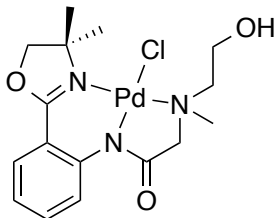
The compound was prepared and purified similarly as for **9a** from **3j** (0.21 g, 0.63 mmol) and 6.3×10^{-2} M Li₂PdCl₄ (10.0 mL, 0.63 mmol). The compound was isolated as orange solid (0.12 g, 42% yield; pure).

¹H NMR (400 MHz, CDCl₃): δ = 8.24 (dd, J = 8.8 Hz, J = 0.8 Hz, 1 H), 7.66 (dd, J = 8.0 Hz, J = 1.6 Hz, 1 H), 7.38 (ddd, J = 8.8 Hz, J = 7.2 Hz, J = 1.6 Hz, 1 H), 6.97 (ddd, J = 8.0 Hz, J = 7.2 Hz, J = 0.8 Hz, 1 H), 6.73 (dddd, J = 17.2 Hz, J = 10.4 Hz, J = 8.8 Hz, J = 5.6 Hz, 2 H), 5.47 (d, J = 10.0 Hz, 2 H), 5.39 (d, J = 17.2 Hz, 2 H), 4.23 (s, 2 H), 3.95 (dd, J = 12.8 Hz, J = 5.6 Hz, 2 H), 3.66 (s, 2 H), 2.89 (dd, J = 12.8 Hz, J = 8.8 Hz, 2 H), 1.75 (s, 6 H).

¹³C NMR (100 MHz, CDCl₃): δ = 176.8, 162.7, 144.7, 133.1, 131.6, 129.4, 123.3, 123.1, 121.7, 116.4, 81.7, 70.7, 64.9, 63.4, 28.0.

Anal. Calcd for C₁₉H₂₄ClN₃O₂Pd: C, 48.73; H, 5.17; N, 8.97%. Found: C, 48.33; H, 5.19; N, 8.80%.

Synthesis of 9k



Molecular weight: 446.24 g mol⁻¹

The compound was prepared and purified similarly as for **9a** from **3k** (0.063g, 0.206 mmol) and 7.9×10⁻² M Li₂PdCl₄ (2.60 mL, 0.205 mmol). The compound was isolated as orange solid (0.09 g, 95% yield; pure).

¹H NMR (400 MHz, CDCl₃): δ = 8.29 (dd, *J* = 8.8 Hz, *J* = 0.8 Hz, 1 H), 7.69 (dd, *J* = 8.0 Hz, *J* = 1.6 Hz, 1 H), 7.40 (ddd, *J* = 8.8 Hz, *J* = 7.2 Hz, *J* = 1.6 Hz, 1 H), 7.00 (ddd, *J* = 8.0 Hz, *J* = 7.2 Hz, *J* = 0.8 Hz, 1 H), 4.50-4.38 (m, 1 H), 4.30-4.12 (m, 3 H), 3.90-3.70 (m, 2 H), 3.52 (t, *J* = 6.8 Hz, 1 H), 2.92-2.82 (m, 1 H), 2.76 (s, 3 H), 2.75-2.70 (m, 1 H), 1.73 (s, 3 H), 1.67 (s, 3 H).

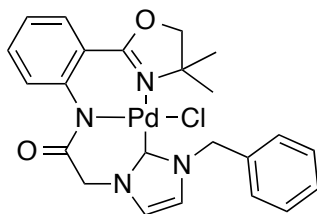
¹³C NMR (100 MHz, CDCl₃): δ = 174.8, 162.6, 144.4, 133.1, 129.6, 123.4, 122.0, 116.4, 81.5, 70.5, 70.2, 65.1, 60.2, 50.9, 27.9, 27.6.

Anal. Calcd for C₁₆H₂₂ClN₃O₃Pd·½ CH₂Cl₂: C, 40.55; H, 4.74; N, 8.60%. Found: C, 41.04; H, 4.40; N, 8.14%.

Synthesis of PdCl₂(MeCN)₂

PdCl₂ (0.51 g, 2.88 mmol) was dissolved in MeCN (60.0 mL) and refluxed for 1.5 h until the solution got saturated. The reaction mixture was hot gravity filtered and the bright orange filtrate was put on ice. Orange crystals crashed out of the solution and were vacuum filtered (0.65 g, 89% yield; pure). ¹H-NMR spectrum matches the literature.⁶⁹

Synthesis of 9l



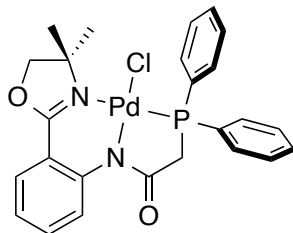
Molecular weight: 530.34 g mol⁻¹

Ag₂O (0.028 g, 0.12 mmol) and **3l** (0.100 g, 0.24 mmol) were dissolved in DCM (10.0 mL) and stirred at RT under N₂ atmosphere for 2 h. The reaction mixture was filtered through Celite. Then PdCl₂(MeCN)₂ (0.062g, 0.24 mmol) was added and the solution turned bright yellow milky colour after 2 min. The reaction was stirred at RT for 24 h under N₂. The opaque solution was gravity filtered and the solvent was removed *in vacuo*. Recrystallized from DCM/hexanes (1:1) mixture as yellow wax (0.12 g, 94% yield; pure).

¹H NMR (400 MHz, CDCl₃): δ = 7.67 (d, *J* = 7.6 Hz, 1 H), 7.45-7.24 (m, 7 H), 7.10-7.04 (m, 1 H), 7.01 (d, *J* = 1.8 Hz, 1 H), 6.71 (d, *J* = 1.8 Hz, 1 H), 5.78-5.70 (m, 1 H), 5.64-5.57 (m, 1 H), 5.52-5.44 (m, 1 H), 4.52-4.45 (m, 1 H), 4.39-4.33 (m, 1 H), 4.16-4.10 (m, 1 H), 1.79 (s, 3 H), 1.72 (s, 3 H).

¹³C NMR (100 MHz, CDCl₃): δ = 171.2, 163.3, 136.1, 132.1, 129.2, 128.8, 128.2, 127.8, 126.8, 122.8, 121.6, 121.2, 120.6, 81.8, 70.0, 60.4, 57.5, 53.9, 29.7, 28.6, 27.1, 24.4, 21.0, 14.2.

Synthesis of 9m



Molecular weight: 557.32 g mol⁻¹

Compound **2** (0.20 g, 0.75 mmol) was dissolved in dry THF (10.0 mL) and was placed into an ice bath at -84 °C (the mixture of EtOAc/liquid N₂). A 0.5 M solution of KPh₂ in THF (1.50 mL, 0.75 mmol) was added dropwise to the stirring solution. The solution was stirred under N₂ at RT for 24 h, and then it was cannula transferred into the flask containing the solution of PdCl₂(MeCN)₂ (0.195 g, 0.75 mmol) in MeCN:THF mixture (10:5 mL). Dark orange solution was stirred under N₂ at RT for 24 h. After 24 h the reaction mixture turned black, and was gravity filtered, giving bright orange filtrate with black precipitate. After the solvent was removed *in vacuo* the compound was retrieved as orange solid (0.12 g, 96% yield, crude). The pure compound was isolated by preparative TLC (R_f = 0.18; EtOAc-hexanes, 4:1) as orange waxy solid.

¹H NMR (400 MHz, CDCl₃): δ = 7.94-7.80 (m, 4 H), 7.71-7.62 (m, 2 H), 7.61-7.46 (m, 5 H), 7.28-7.19 (m, 1 H), 7.01 (t, *J* = 8.0 Hz, 1 H), 6.81 (d, *J* = 8.4 Hz, 1 H), 4.62 (dd, *J* = 20.0 Hz, *J* = 15.2 Hz, 1 H), 4.39-4.34 (m, 1 H), 4.14-4.12 (m, 1 H), 3.52 (d, *J* = 16.4 Hz, 1 H), 1.78 (s, 3 H), 1.66 (s, 3 H).

¹³C NMR (100 MHz, CDCl₃): δ = 165.1, 163.3, 145.6, 133.5, 132.6, 131.4, 129.4, 129.2, 128.2, 126.2, 122.9, 120.5, 82.2, 69.9, 53.4, 44.8, 44.2, 29.7, 28.0, 27.0.

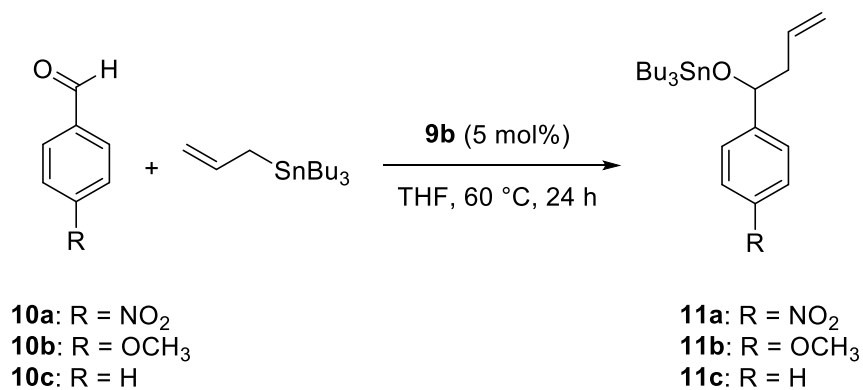
³¹P NMR (162 MHz, CDCl₃): δ = 50.45.

Anal. Calcd for $\text{C}_{25}\text{H}_{24}\text{ClN}_2\text{O}_2\text{PPd}\cdot 1(\text{CH}_2\text{Cl}_2)\cdot 1(\text{H}_2\text{O})$: C, 47.30; H, 4.27; N, 4.24%.

Found: C, 47.60; H, 4.21; N, 4.23%.

5.4 CATALYSIS

Allylation of aldehydes



Each respective aldehyde (0.15 mmol) and 9.0×10^{-3} M THF solution of **4b** (0.007 mmol; 5 mol%) were dissolved in 1.0 mL of THF. Allyltributyltin (56 μ L, 0.18 mmol) was added to the stirring solution at RT. The reaction was stirred at 60 $^\circ$ C for 24 h. The solvent was removed *in vacuo* and the residual material was analyzed by ^1H NMR spectroscopy.

CHAPTER 6 – CONCLUSION AND FUTURE WORK

A modular approach towards synthesis of novel asymmetric achiral and chiral pincer ligands of NNN, NNC and NNP types was developed. Fifteen novel pincer ligands have been synthesized following the method developed; showcasing the ease and the accessibility towards the presence of different functional groups. The investigation towards the complexation of these pincer ligands was performed with Pd and Ni metal centres. However, only Pd complexes were successfully synthesized from 42-98% yield and characterized by elemental analysis, and NMR spectroscopy. A catalytic study was performed using **9b** (5 mol%) in allylation of benzaldehyde, *p*-nitrobenzaldehyde, and *p*-methoxybenzaldehyde. The preliminary results showed successful conversion of up to 99%.

As part of the future work, both chiral and achiral pincer complexes can be screened for catalytic activity with the above described (allylation of aldehydes) and other types of reactions. Chiral derivatives of these ligands are of immense interest due to their ability to catalyze reactions with stereospecific products.

CHAPTER 7 – APPENDIX

7.1 NMR SPECTRA

Figure A1. ^1H -NMR Spectrum of **2** in CDCl_3

Figure A2. ^{13}C -NMR Spectrum of **2** in CDCl_3

Figure A3. ^1H -NMR Spectrum of **3a** in CDCl_3

Figure A4. ^{13}C -NMR Spectrum of **3a** in CDCl_3

Figure A5. ^1H -NMR Spectrum of **3b** in CDCl_3

Figure A6. ^{13}C -NMR Spectrum of **3b** in CDCl_3

Figure A7. ^1H -NMR Spectrum of **3c** in CDCl_3

Figure A8. ^{13}C -NMR Spectrum of **3c** in CDCl_3

Figure A9. ^1H -NMR Spectrum of **3d** in CDCl_3

Figure A10. ^{13}C -NMR Spectrum of **3d** in CDCl_3

Figure A11. ^1H -NMR Spectrum of **3e** in CDCl_3

Figure A12. ^{13}C -NMR Spectrum of **3e** in CDCl_3

Figure A13. ^1H -NMR Spectrum of **3f** in CDCl_3

Figure A14. ^{13}C -NMR Spectrum of **3f** in CDCl_3

Figure A15. ^1H -NMR Spectrum of **3g** in CDCl_3

Figure A16. ^{13}C -NMR Spectrum of **3g** in CDCl_3

Figure A17. ^1H -NMR Spectrum of **3h** in CDCl_3

Figure A18. ^{13}C -NMR Spectrum of **3h** in CDCl_3

Figure A19. ^1H -NMR Spectrum of **3i** in CDCl_3

Figure A20. ^{13}C -NMR Spectrum of **3i** in CDCl_3

Figure A21. ^1H -NMR Spectrum of **3j** in CDCl_3

Figure A22. ^{13}C -NMR Spectrum of **3j** in CDCl_3

Figure A23. ^1H -NMR Spectrum of **3k** in CDCl_3

Figure A24. ^{13}C -NMR Spectrum of **3k** in CDCl_3

Figure A25. ^1H -NMR Spectrum of **3l** in CDCl_3

Figure A26. ^{13}C -NMR Spectrum of **3l** in CDCl_3

Figure A27. ^1H -NMR Spectrum of **3m•oxide** in CDCl_3

Figure A28. ^{13}C -NMR Spectrum of **3m•oxide** in CDCl_3

Figure A29. ^{31}P -NMR Spectrum of **3m•oxide** in CDCl_3

Figure A30. ^1H -NMR Spectrum of **3n** in CDCl_3

Figure A31. ^{13}C -NMR Spectrum of **3n** in CDCl_3

Figure A32. ^1H -NMR Spectrum of **4** in CDCl_3

Figure A33. ^{13}C -NMR Spectrum of **4** in CDCl_3

Figure A34. ^1H -NMR Spectrum of **6** in CDCl_3

Figure A35. ^{13}C -NMR Spectrum of **6** in CDCl_3

Figure A36. ^1H -NMR Spectrum of **7** in CDCl_3

Figure A37. ^1H -NMR Spectrum of **9a** in CDCl_3

Figure A38. ^{13}C -NMR Spectrum of **9a** in CDCl_3

Figure A39. ^1H -NMR Spectrum of **9b** in CDCl_3

Figure A40. ^{13}C -NMR Spectrum of **9b** in CDCl_3

Figure A41. ^1H -NMR Spectrum of **9c** in CDCl_3

Figure A42. ^{13}C -NMR Spectrum of **9c** in CDCl_3

Figure A43. ^1H -NMR Spectrum of **9d** in CDCl_3

Figure A44. ^{13}C -NMR Spectrum of **9d** in CDCl_3

Figure A45. ^1H -NMR Spectrum of **9e** in CDCl_3

Figure A46. ^{13}C -NMR Spectrum of **9e** in CDCl_3

Figure A47. ^1H -NMR Spectrum of **9g** in CDCl_3

Figure A48. ^{13}C -NMR Spectrum of **9g** in CDCl_3

Figure A49. ^1H -NMR Spectrum of **9h** in CDCl_3

Figure A50. ^{13}C -NMR Spectrum of **9h** in CDCl_3

Figure A51. ^1H -NMR Spectrum of **9i** in CDCl_3

Figure A52. ^{13}C -NMR Spectrum of **9i** in CDCl_3

Figure A53. ^1H -NMR Spectrum of **9j** in CDCl_3

Figure A54. ^{13}C -NMR Spectrum of **9j** in CDCl_3

Figure A55. ^1H -NMR Spectrum of **9k** in CDCl_3

Figure A56. ^{13}C -NMR Spectrum of **9k** in CDCl_3

Figure A57. ^1H -NMR Spectrum of **9l** in CDCl_3

Figure A58. ^{13}C -NMR Spectrum of **9l** in CDCl_3

Figure A59. ^1H -NMR Spectrum of **9m** in CDCl_3

Figure A60. ^{13}C -NMR Spectrum of **9m** in CDCl_3

Figure A61. ^{31}P -NMR Spectrum of **9m** in CDCl_3

Figure A62. ^1H -NMR Spectra of the **11a-c** conversion after 24 h in CDCl_3

Figure A1. ^1H -NMR Spectrum of **2** in CDCl_3

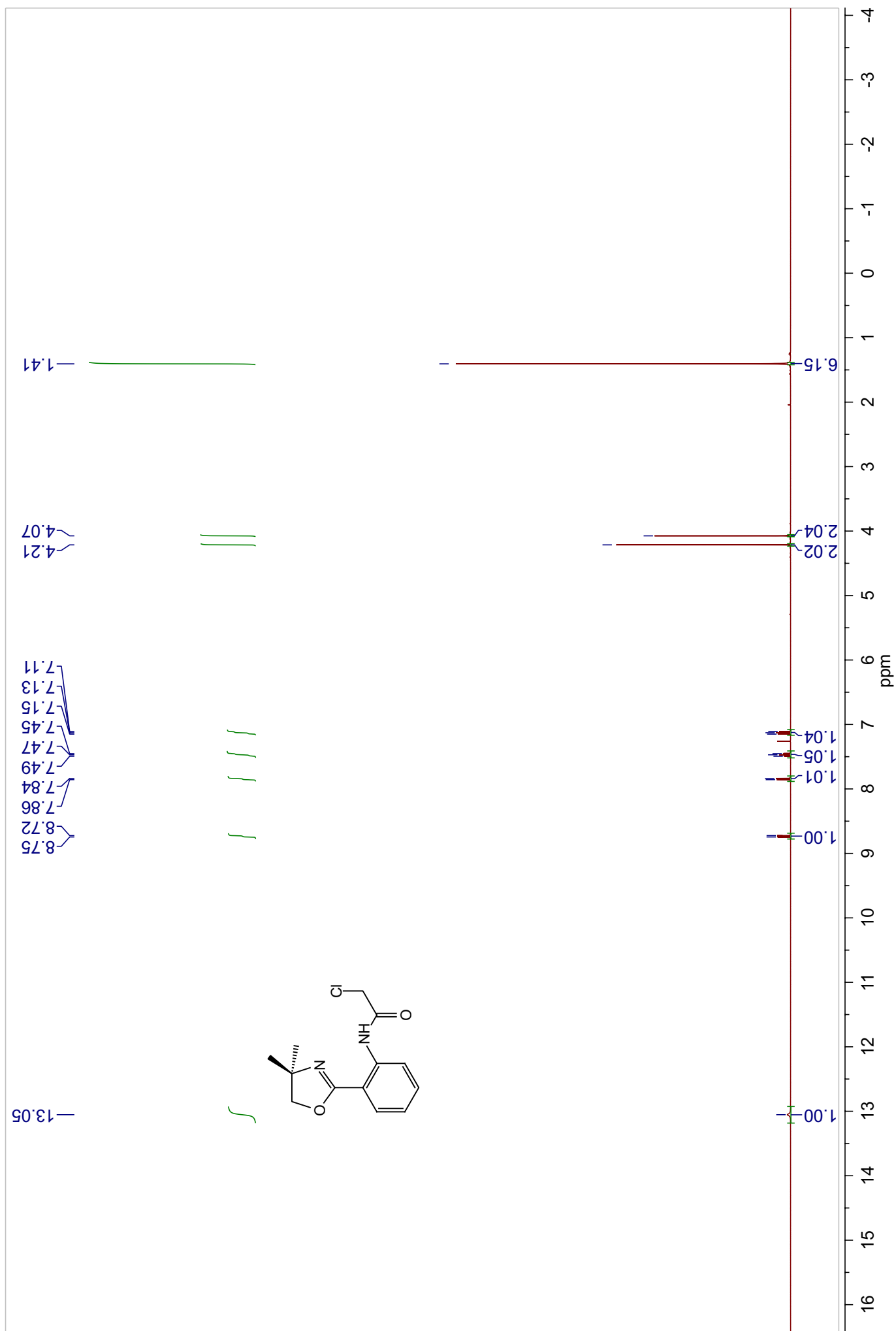


Figure A2. ^{13}C -NMR Spectrum of **2** in CDCl_3

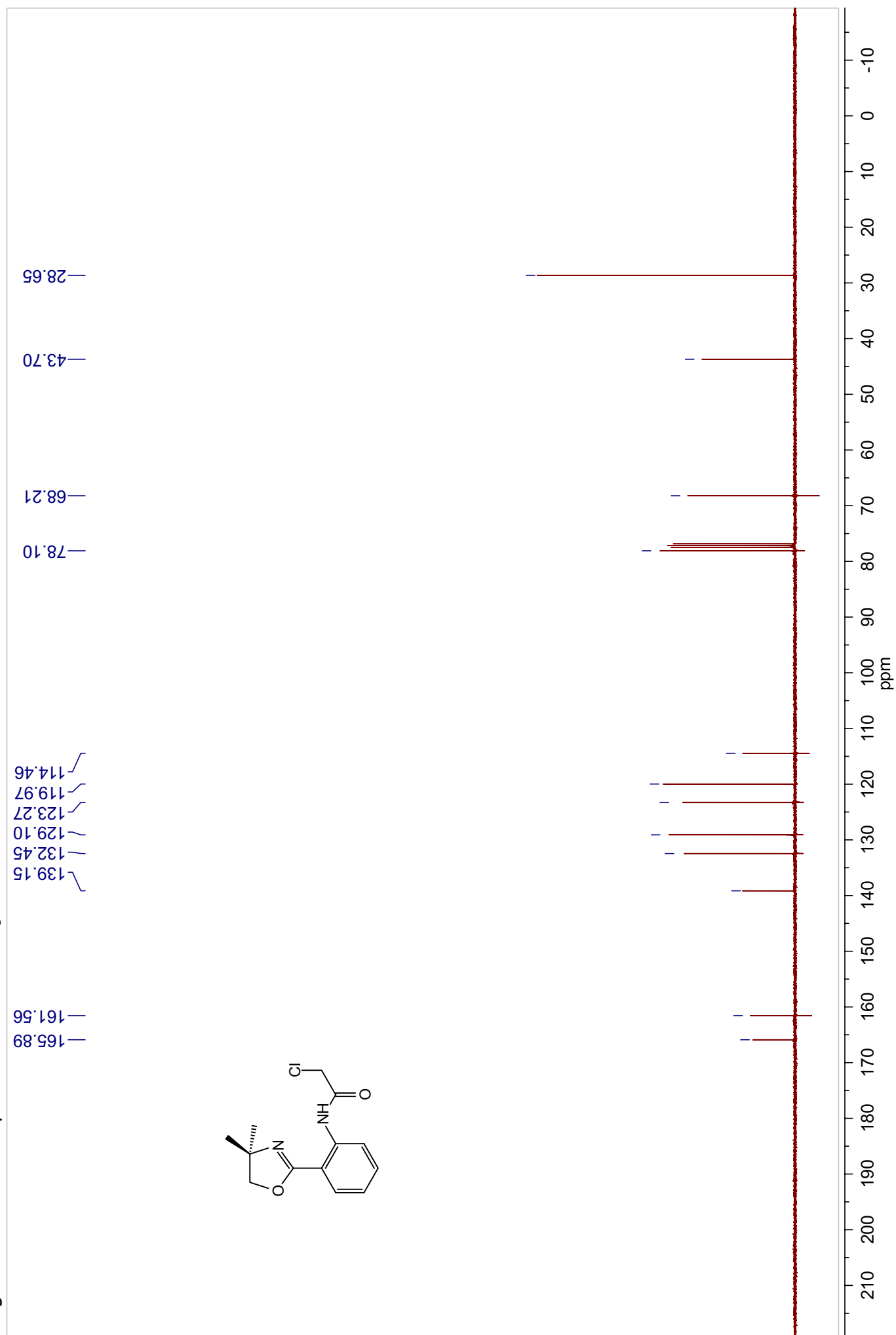


Figure A3. ^1H -NMR Spectrum of **3a** in CDCl_3

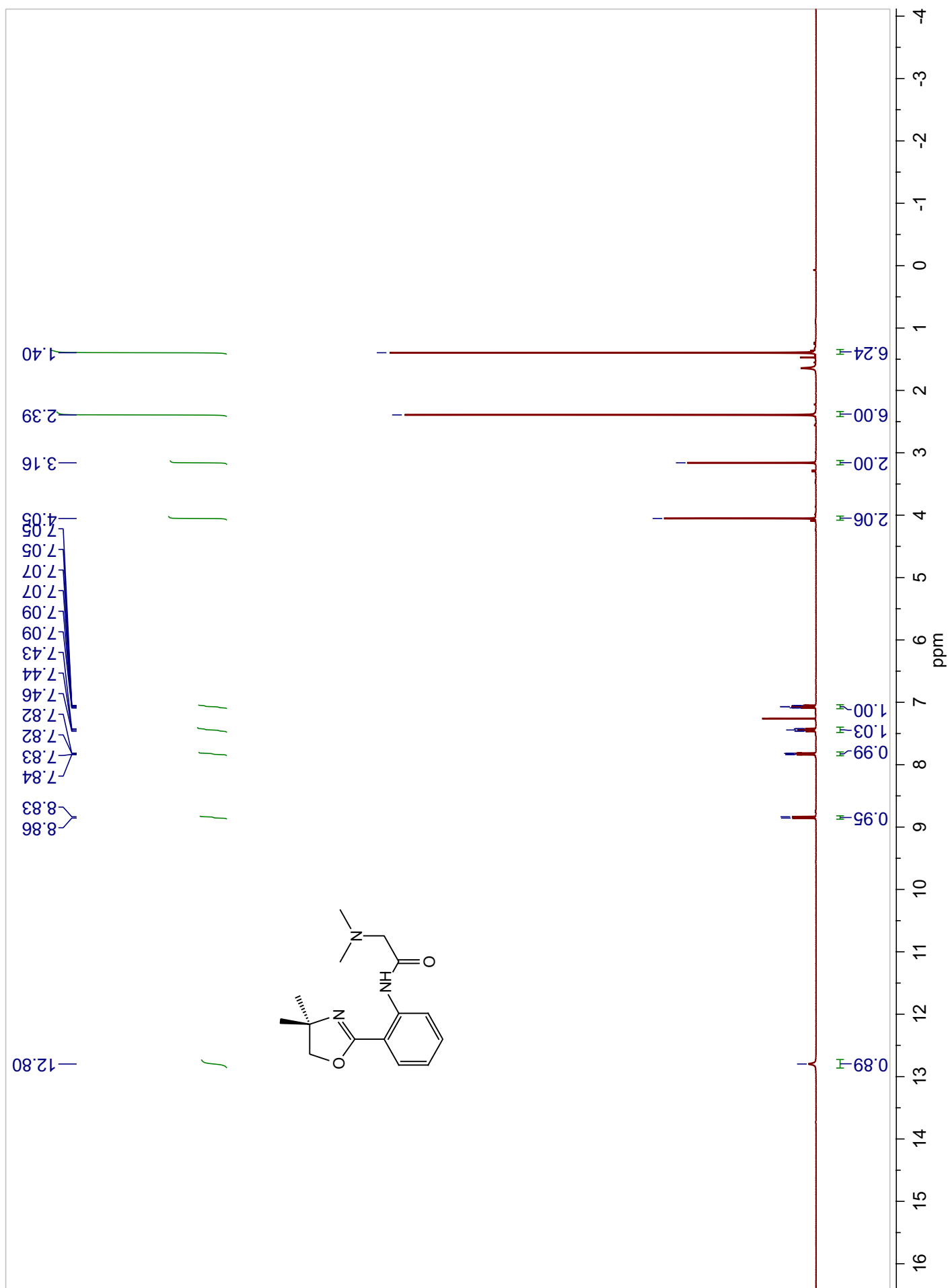


Figure A4. ^{13}C -NMR Spectrum of **3a** in CDCl_3

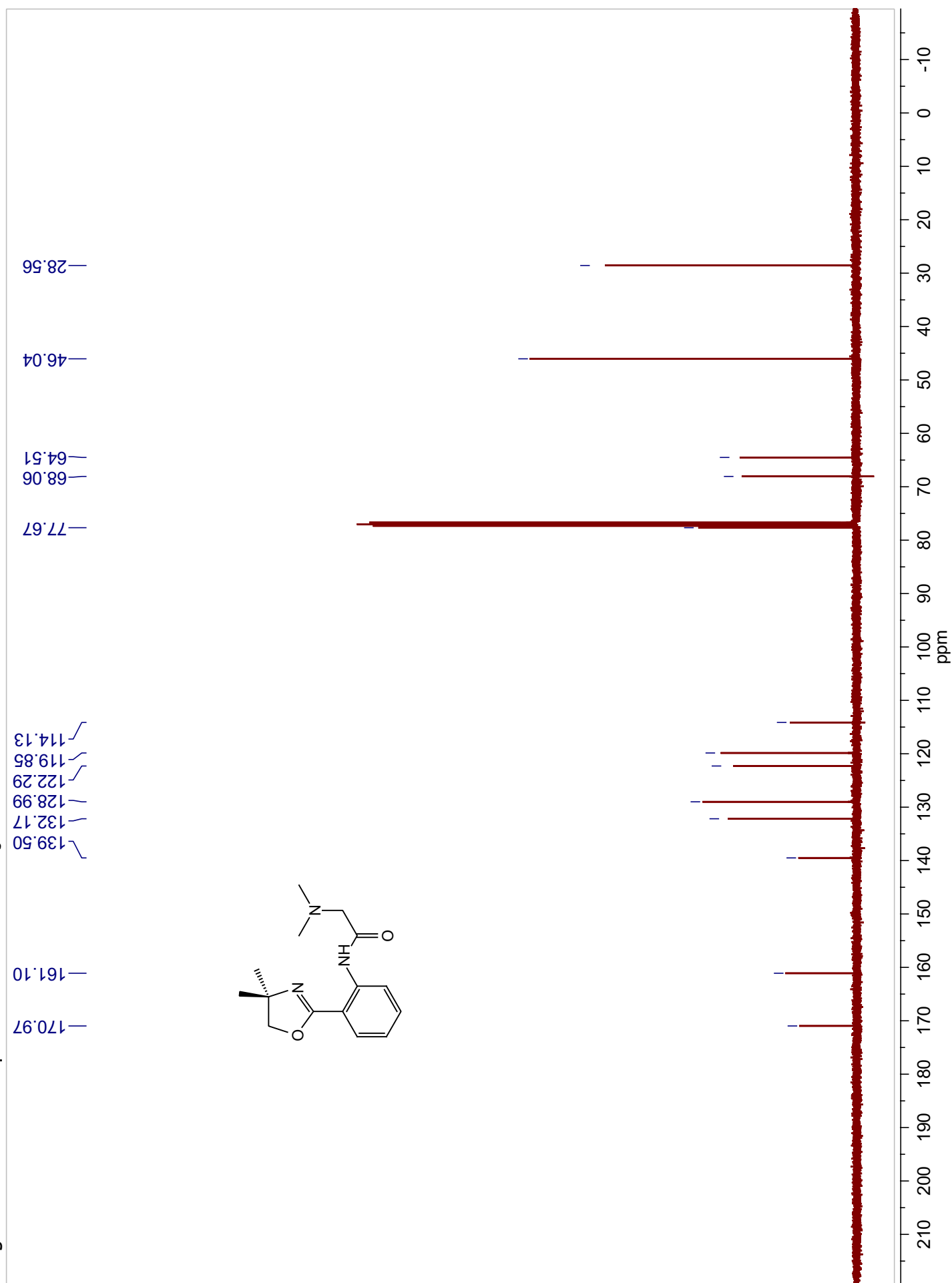


Figure A5. ^1H -NMR Spectrum of **3b** in CDCl_3

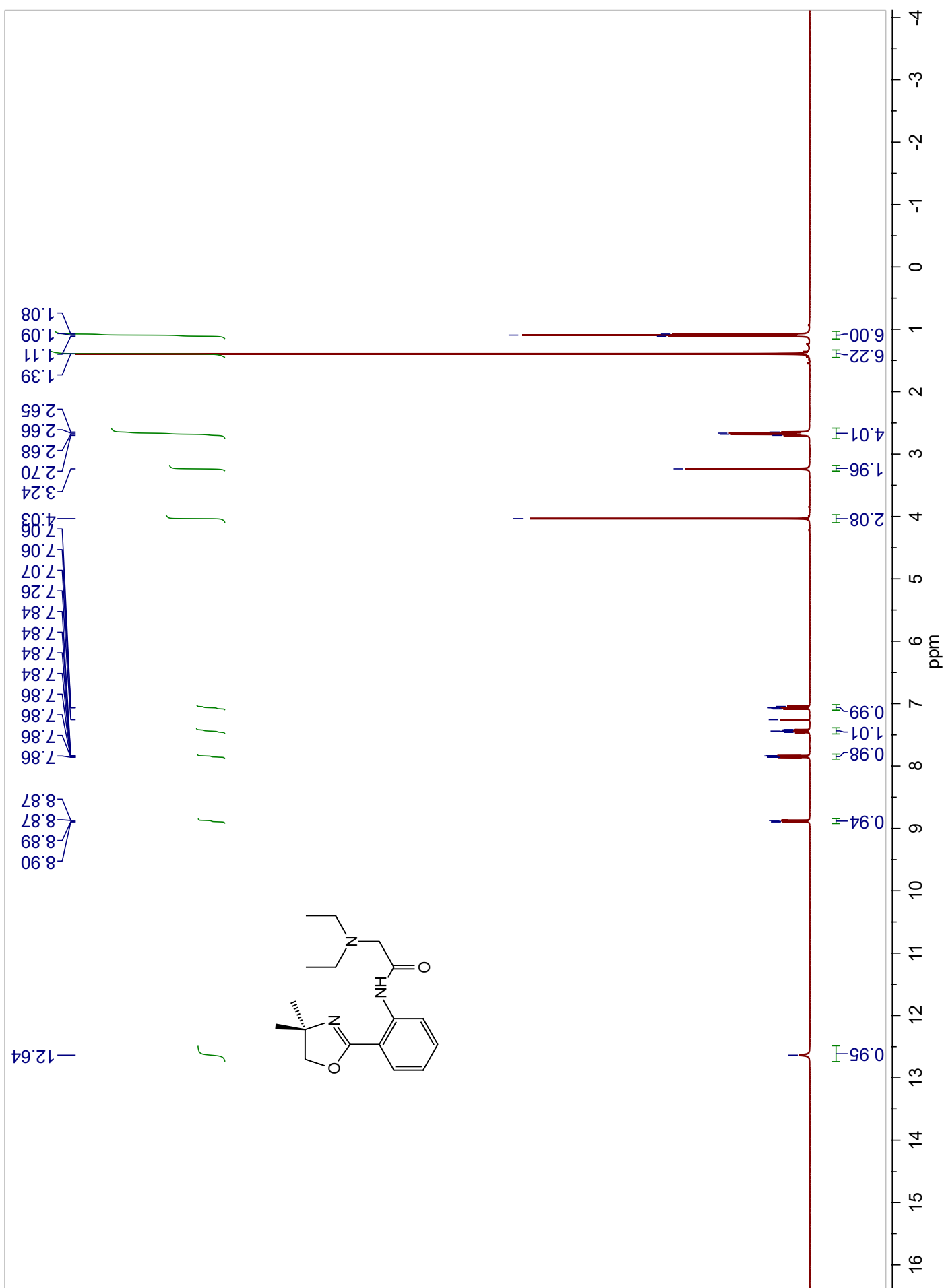


Figure A6. ^{13}C -NMR Spectrum of **3b** in CDCl_3

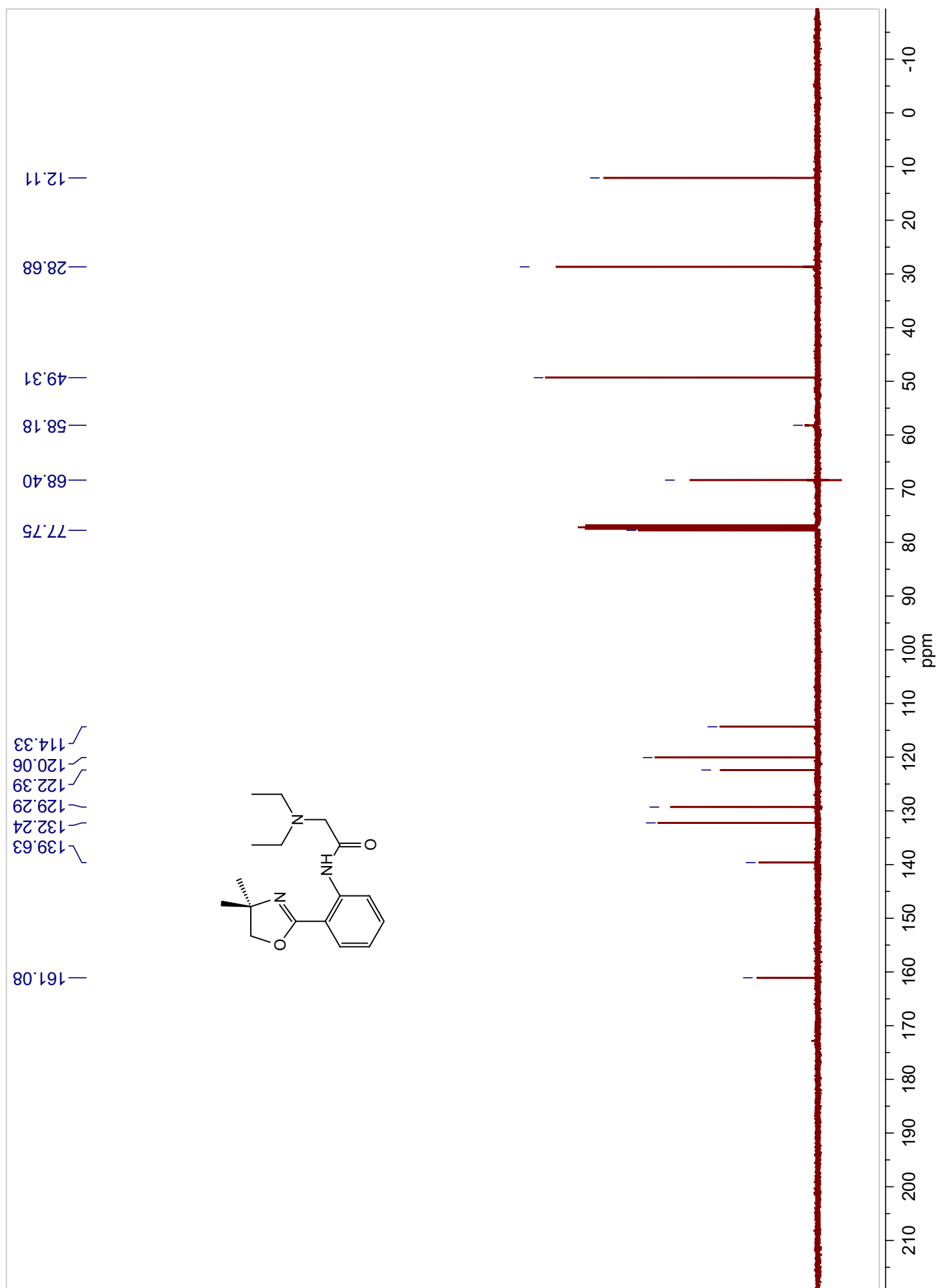


Figure A7. ^1H -NMR Spectrum of **3c** in CDCl_3

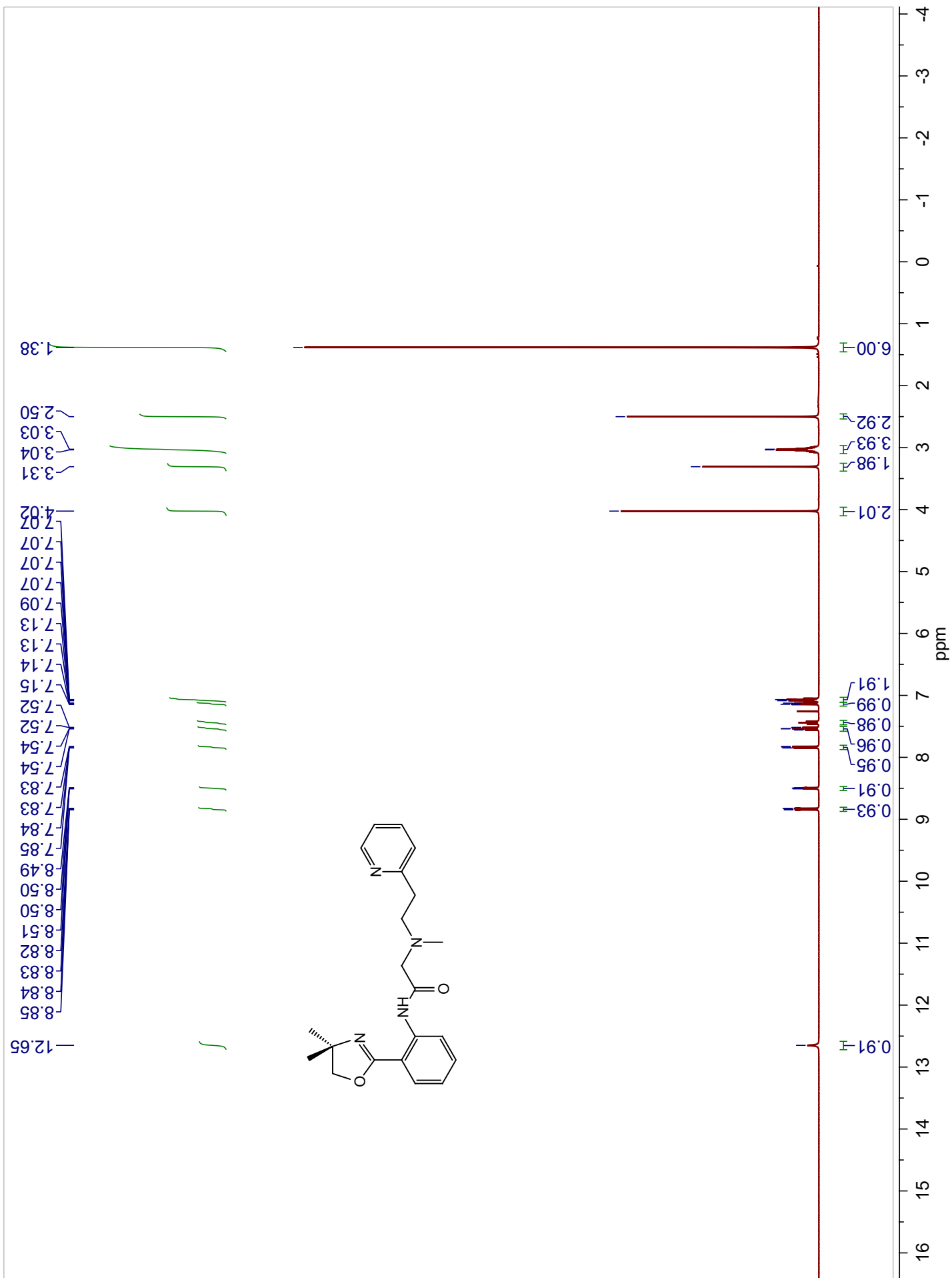


Figure A8. ^{13}C -NMR Spectrum of **3c** in CDCl_3

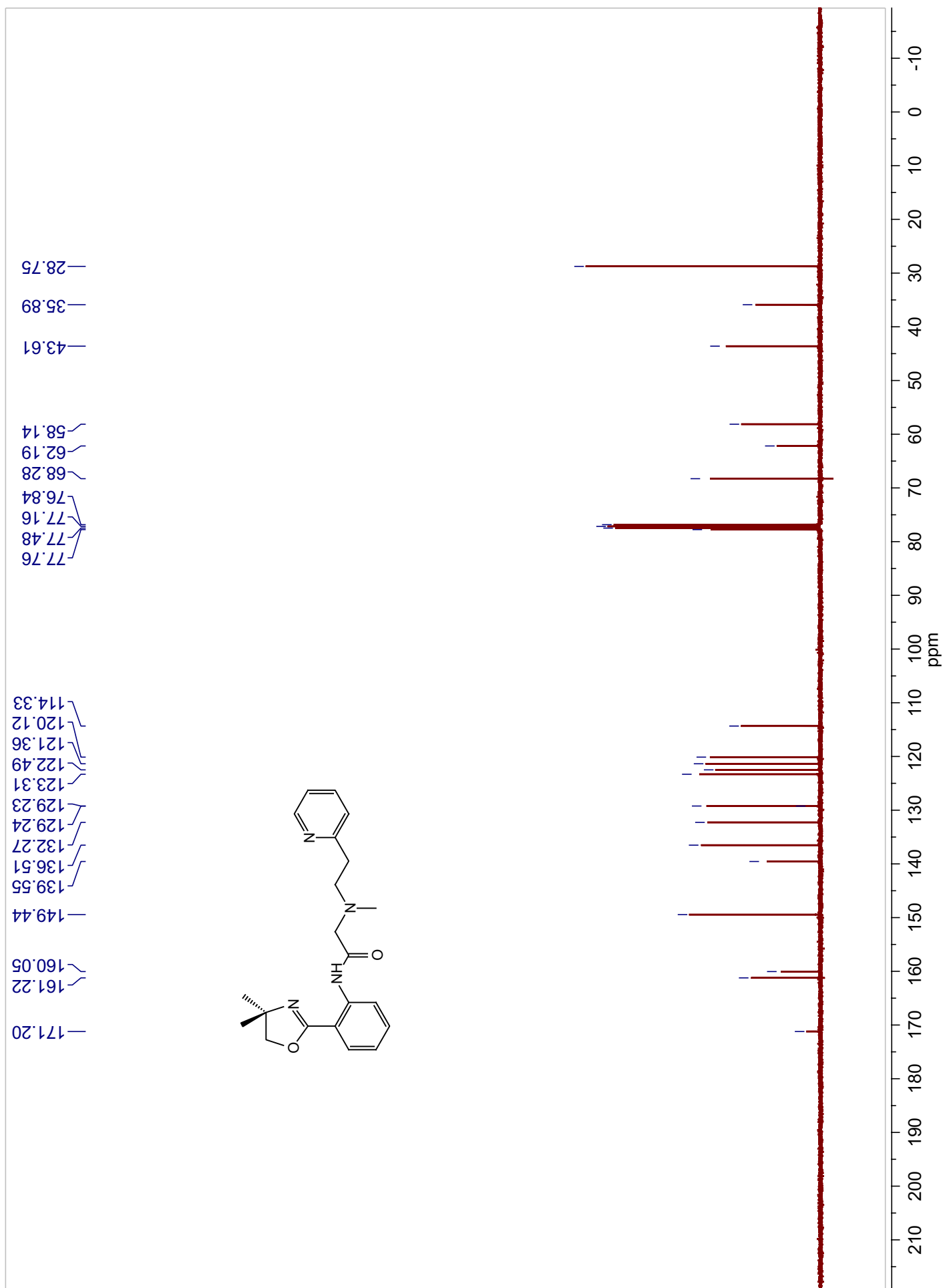


Figure A9. ^1H -NMR Spectrum of **3d** in CDCl_3

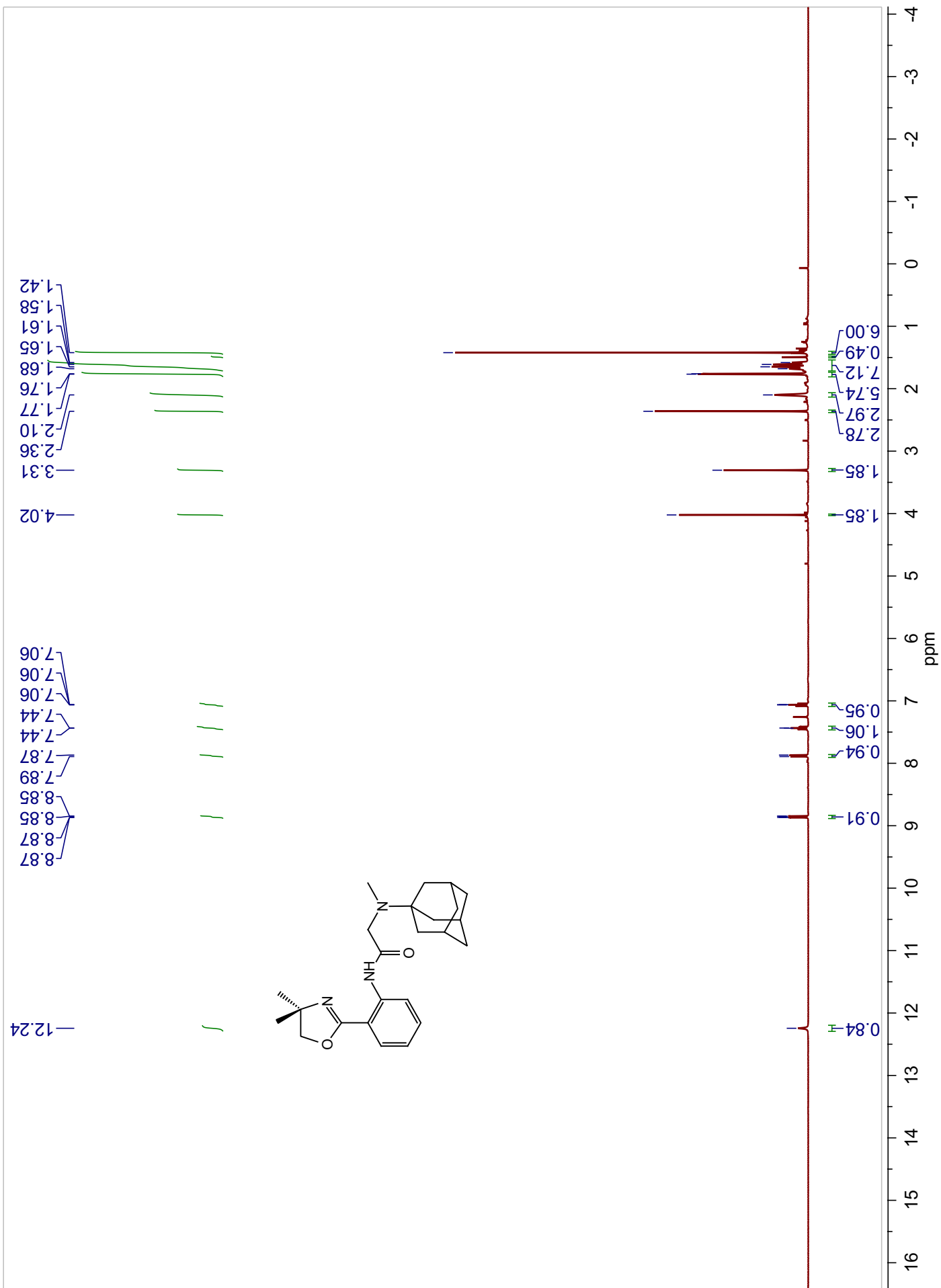


Figure A 10. ^{13}C -NMR Spectrum of **3d** in CDCl_3

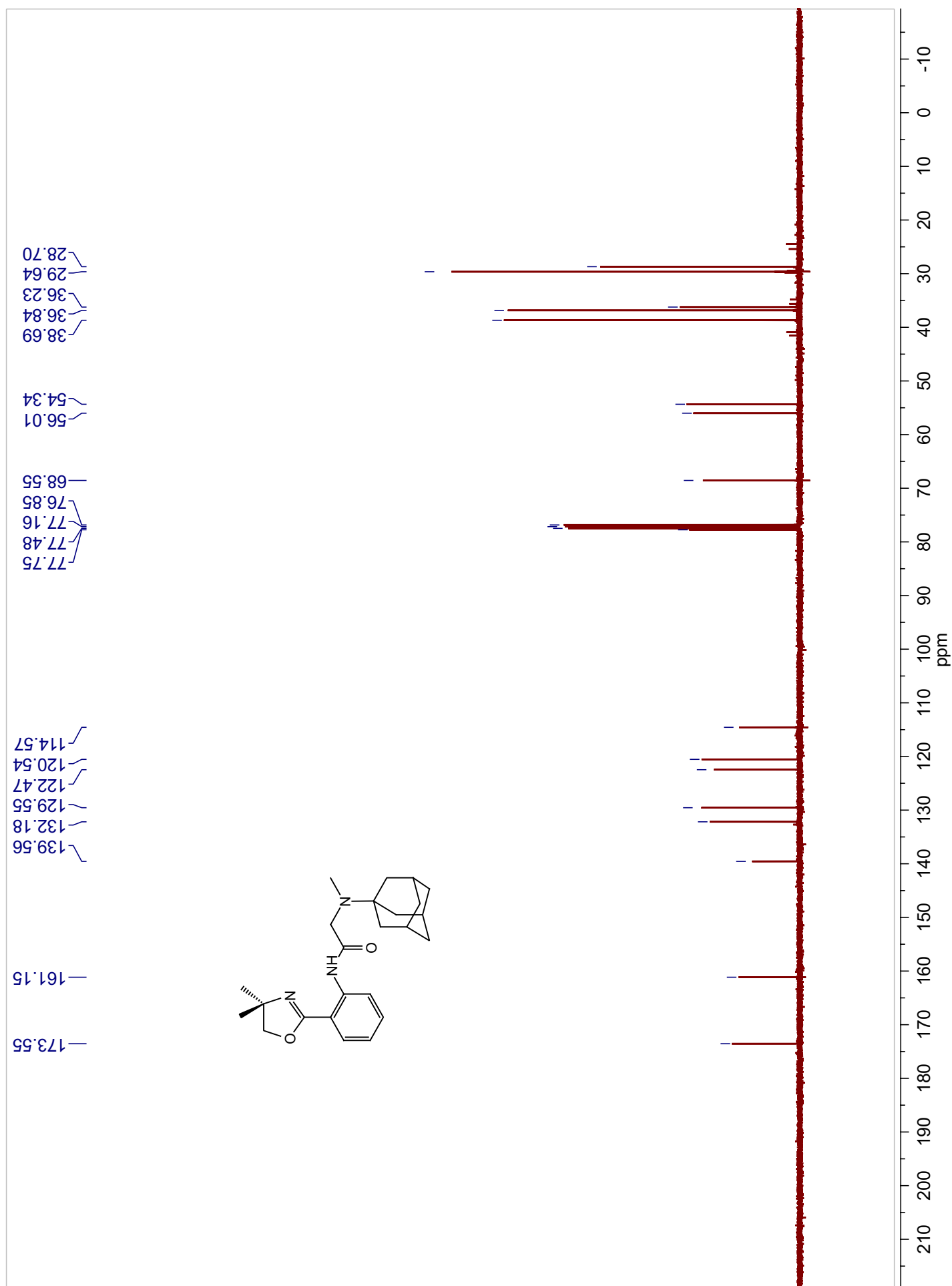


Figure A11. ^1H -NMR Spectrum of **3e** in CDCl_3

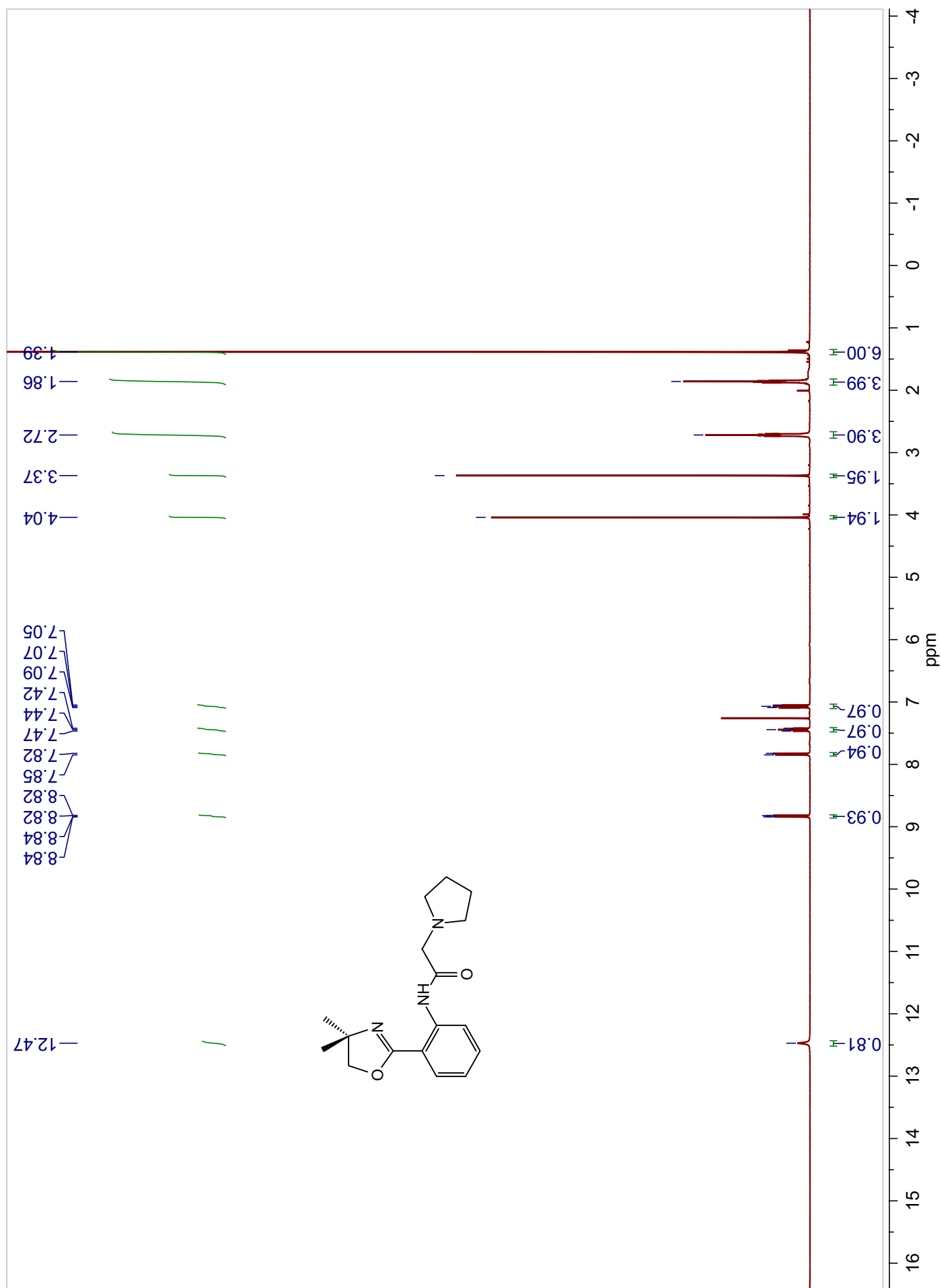


Figure A 12. ^{13}C -NMR Spectrum of **3e** in CDCl_3

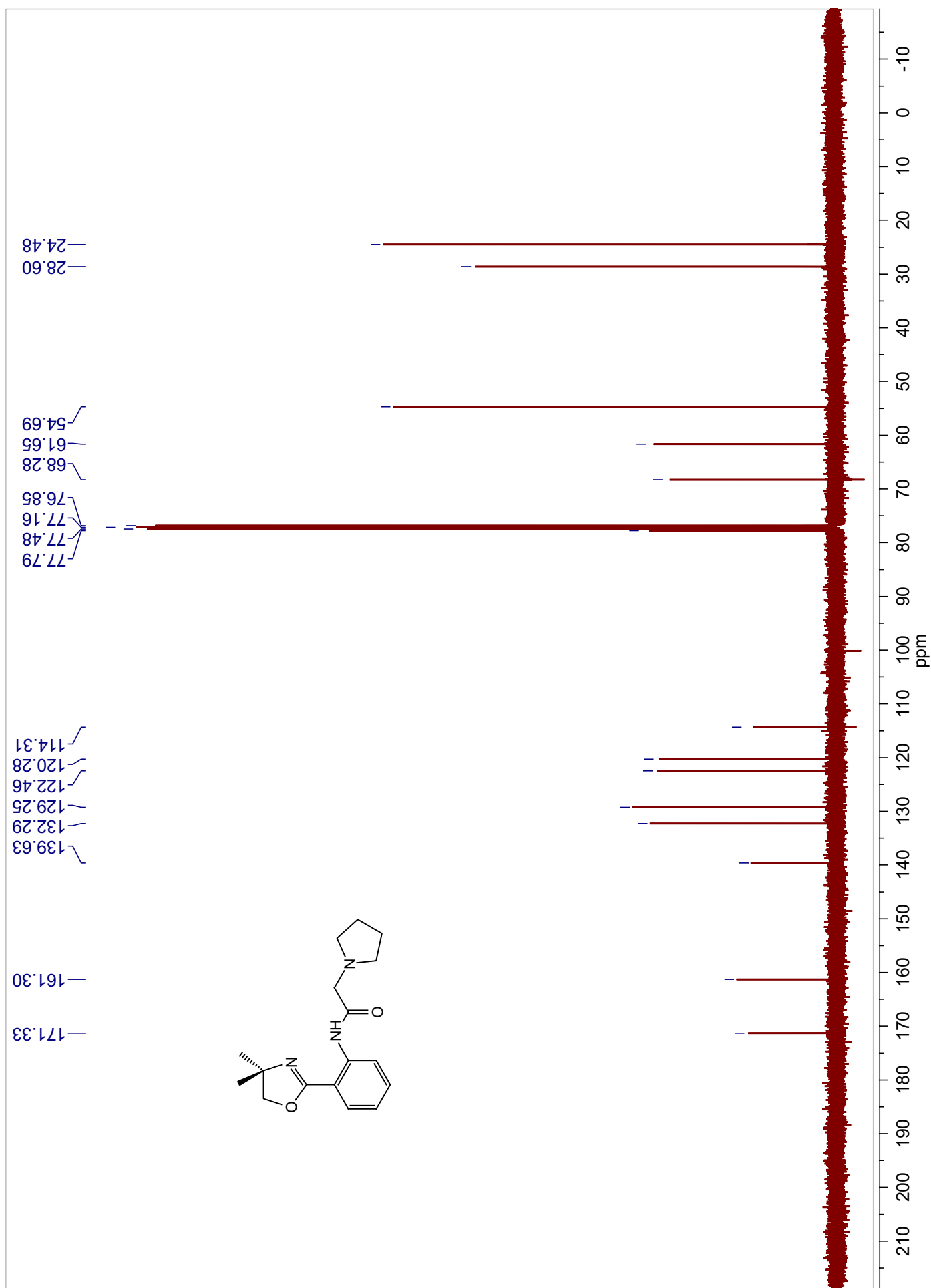


Figure A13. ^1H -NMR Spectrum of **3f** in CDCl_3

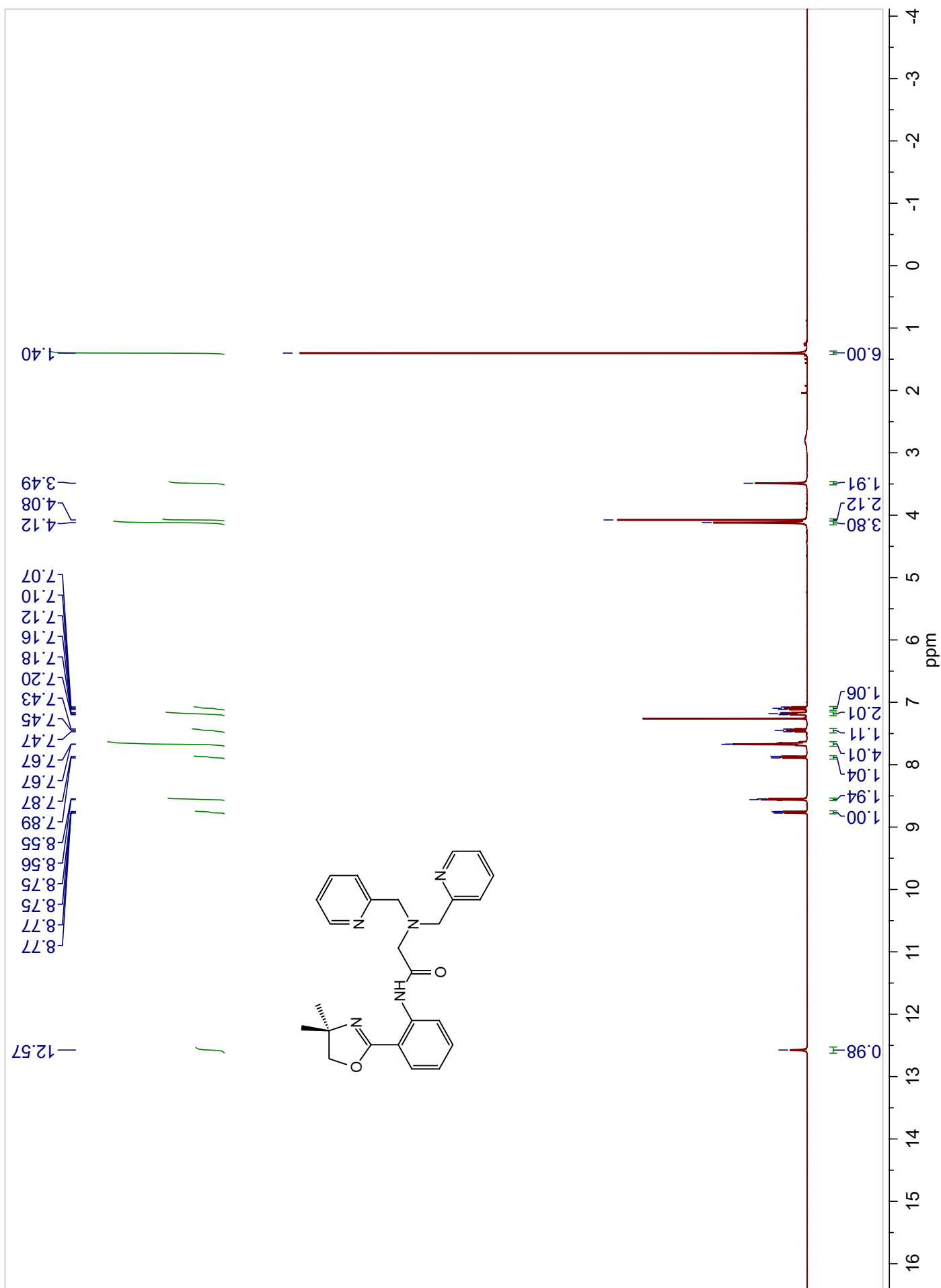


Figure A14. ^{13}C -NMR Spectrum of **3f** in CDCl_3

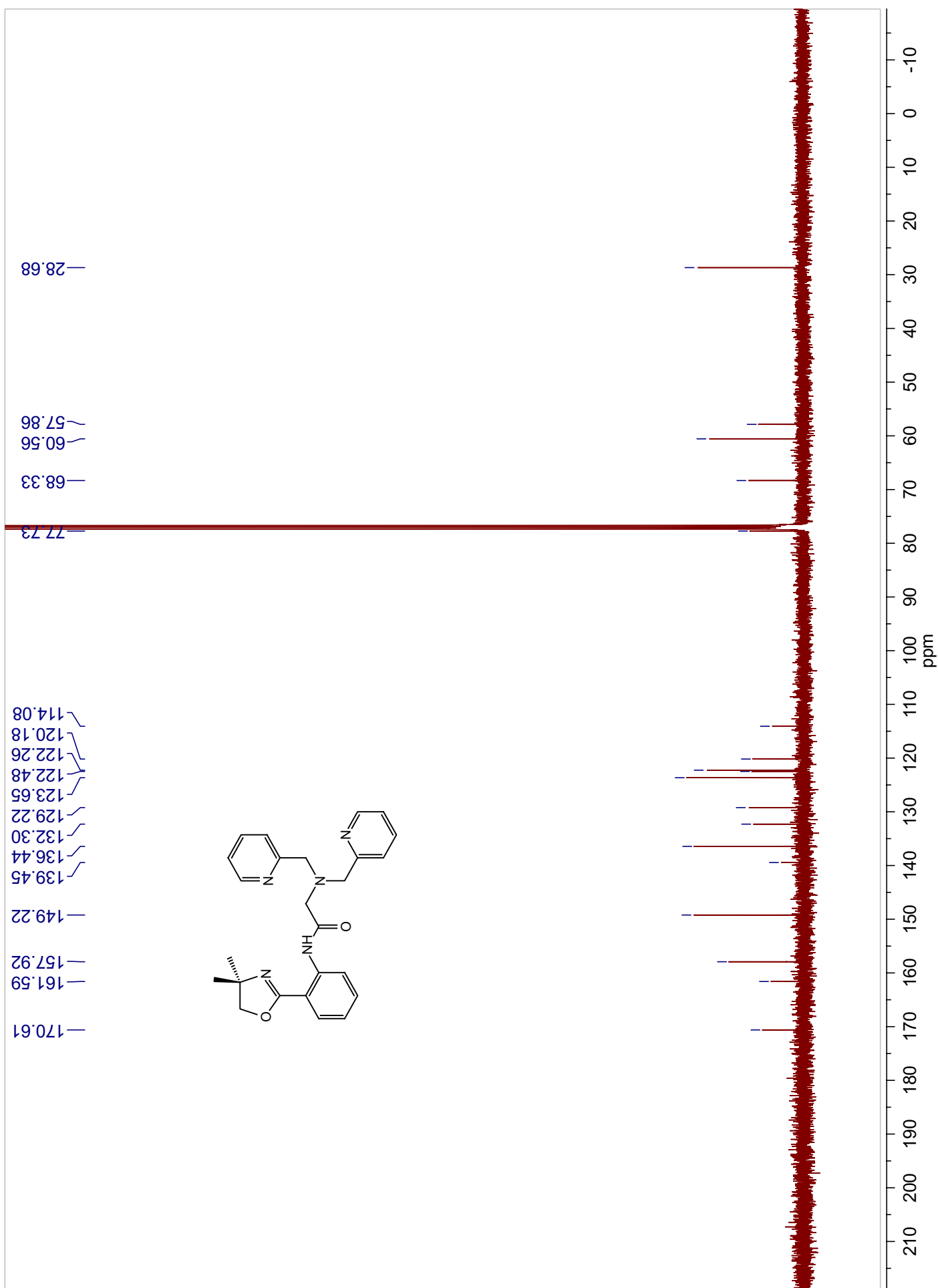


Figure A15. ^1H -NMR Spectrum of **3g** in CDCl_3

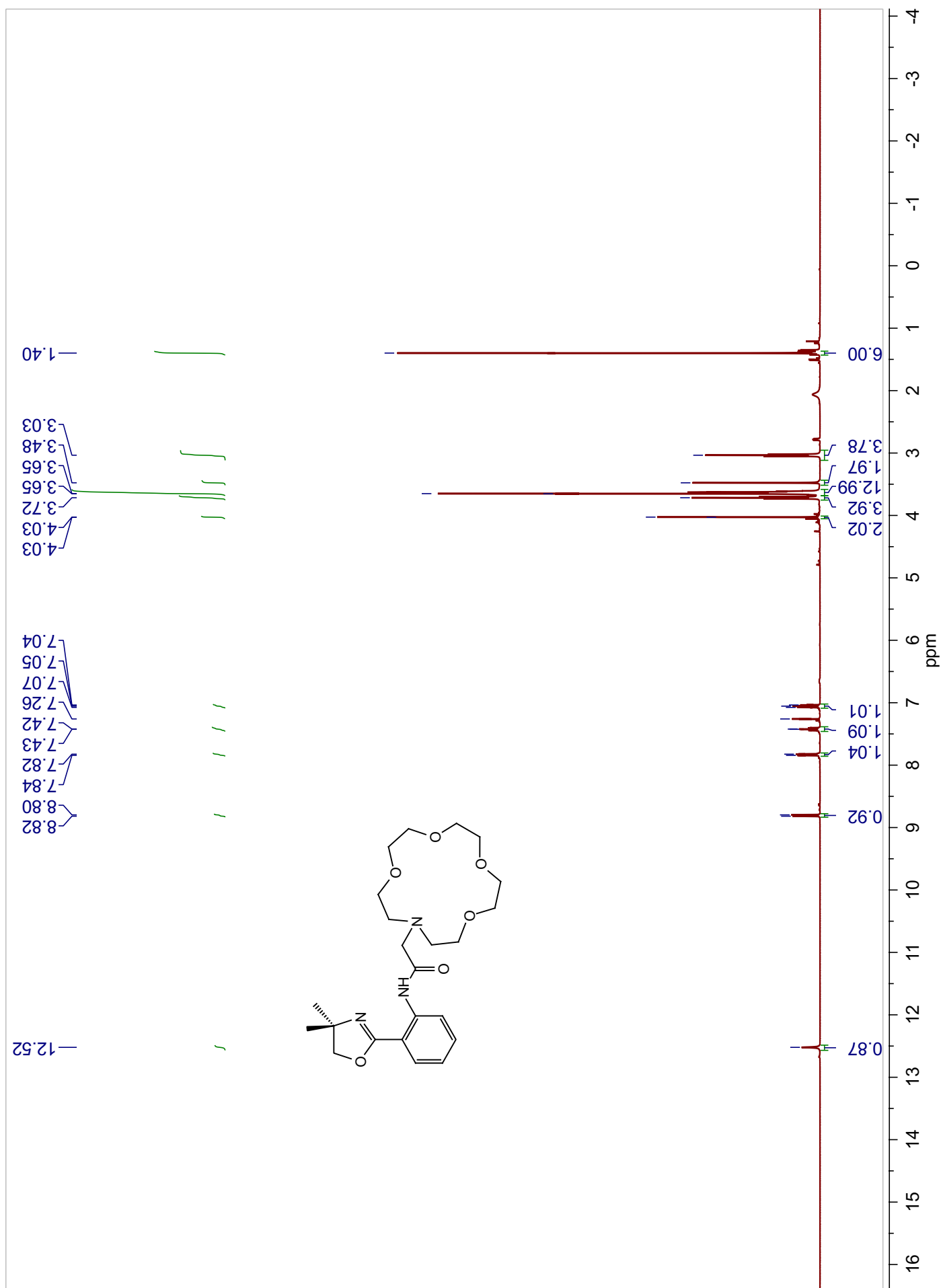


Figure A16. ^{13}C -NMR Spectrum of **3g** in CDCl_3

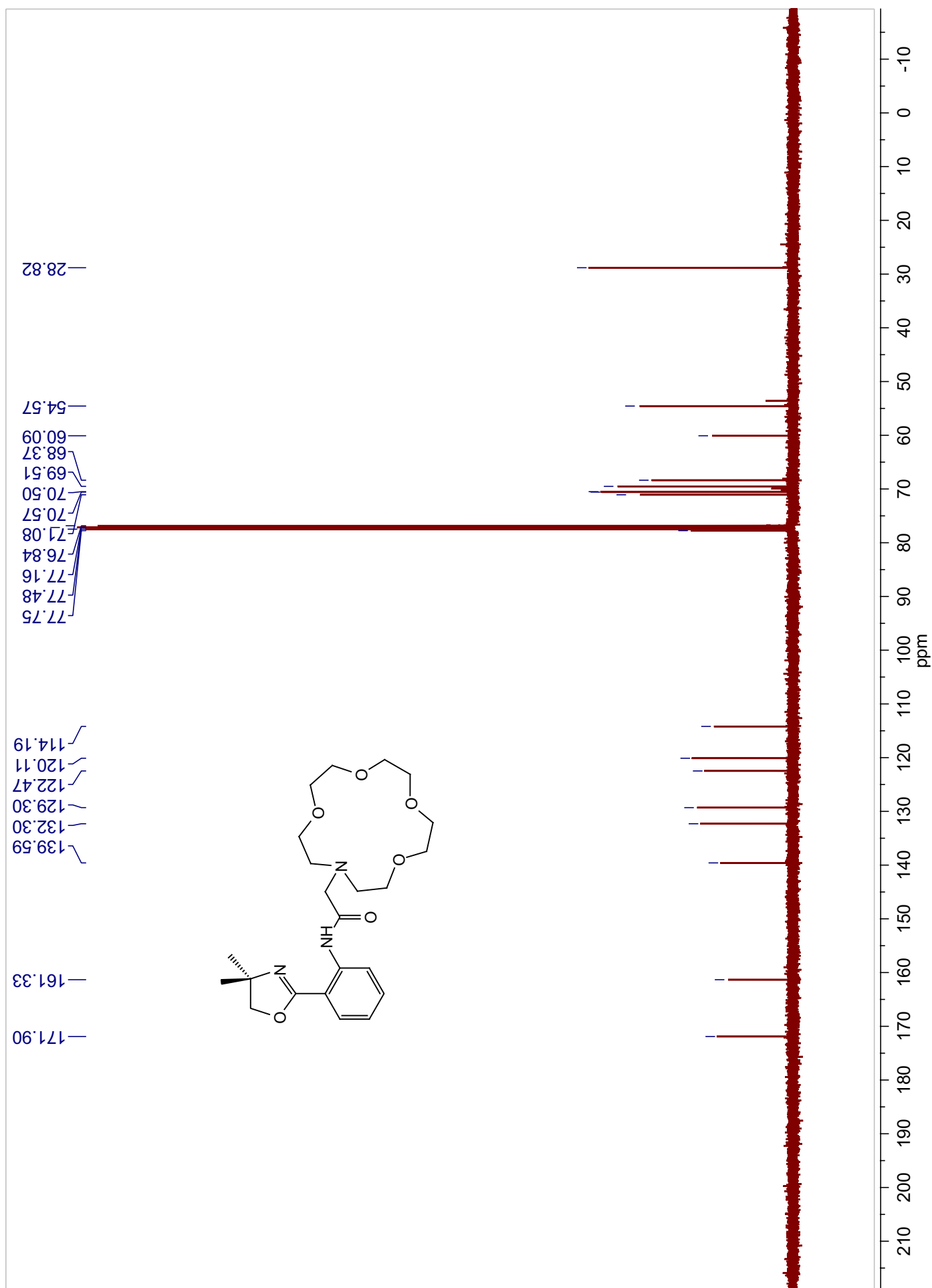


Figure A17. ^1H -NMR Spectrum of **3h** in CDCl_3

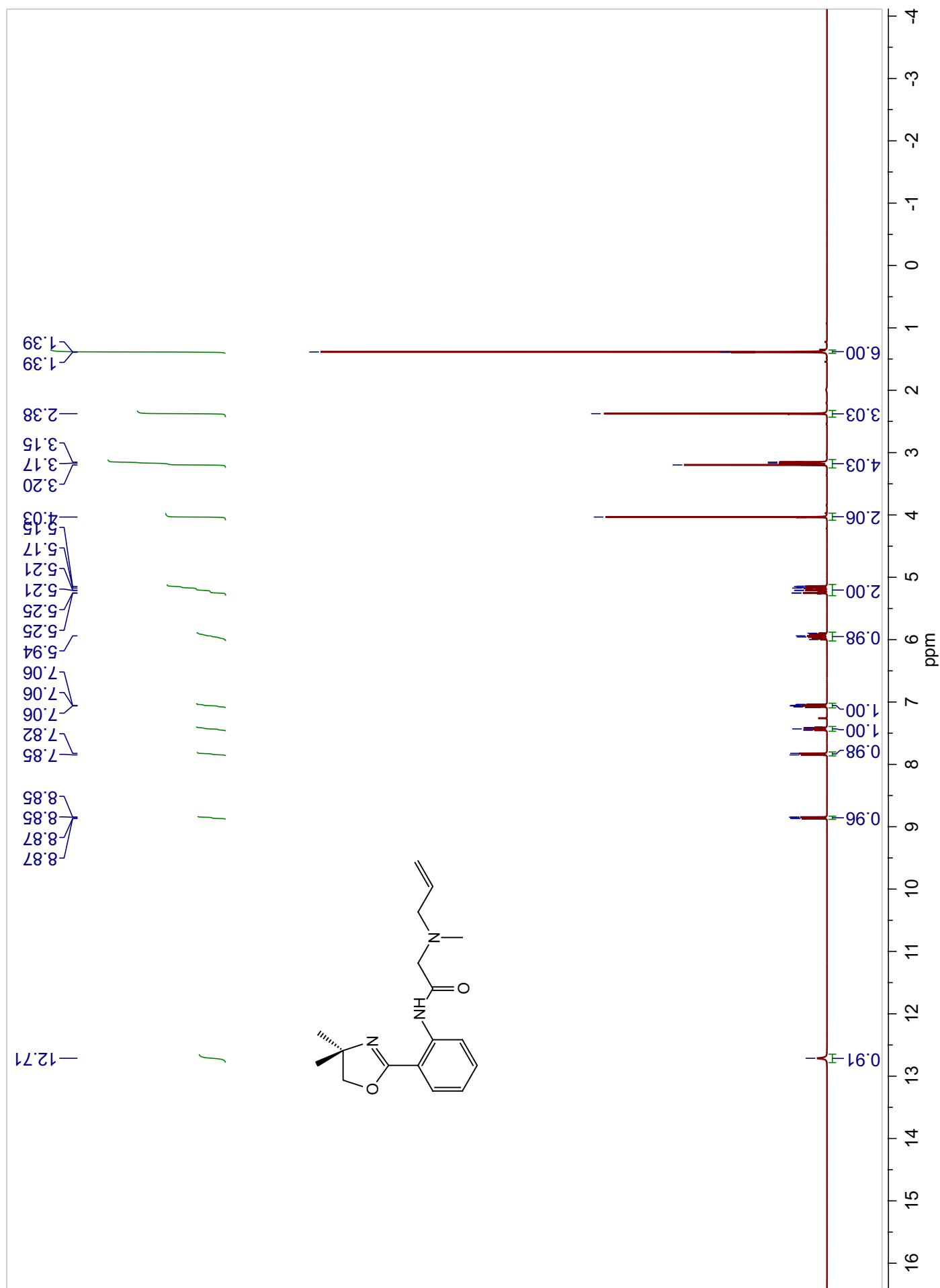


Figure A18. ^{13}C -NMR Spectrum of **3h** in CDCl_3

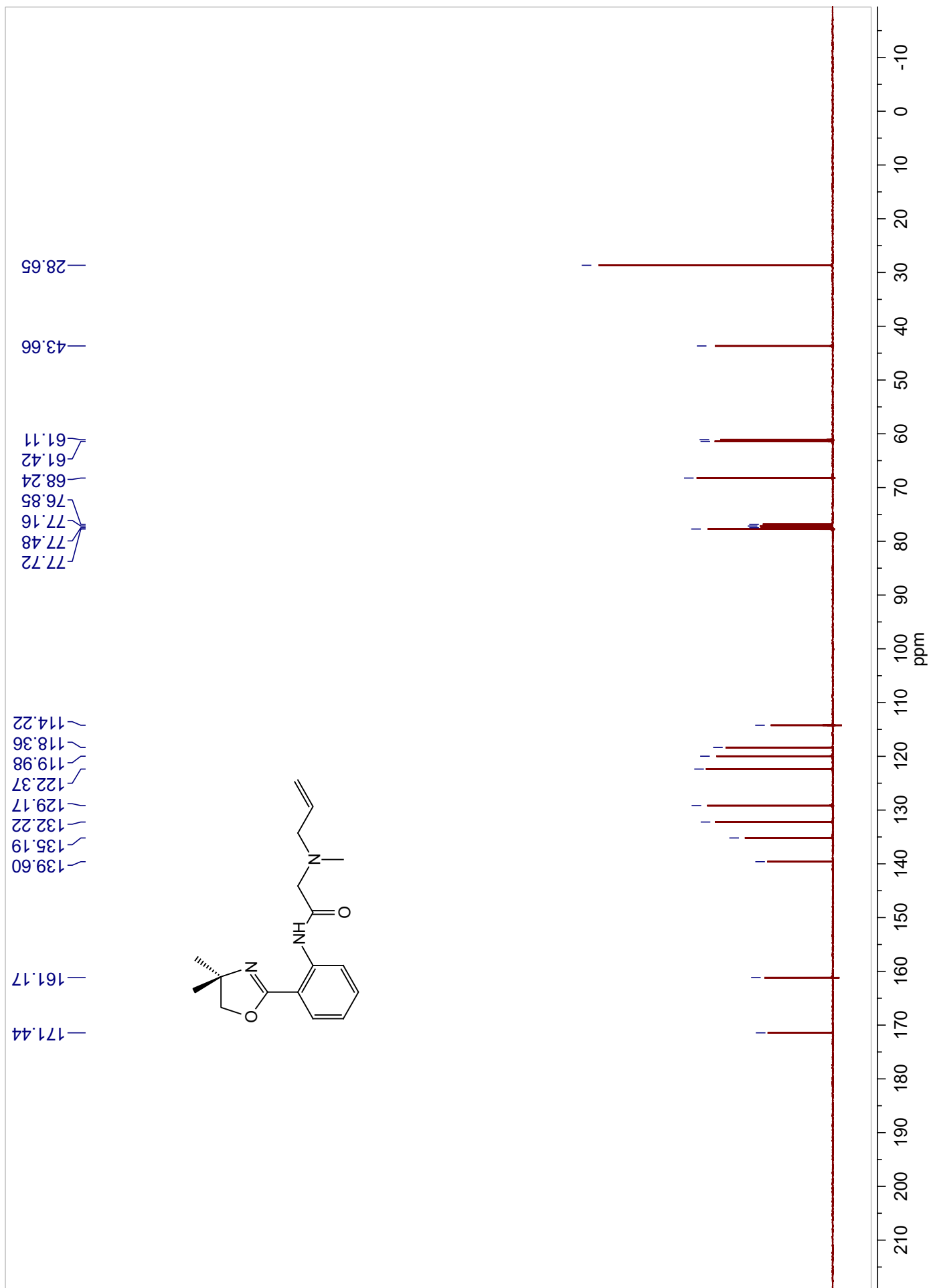


Figure A19. ^1H -NMR Spectrum of **3i** in CDCl_3

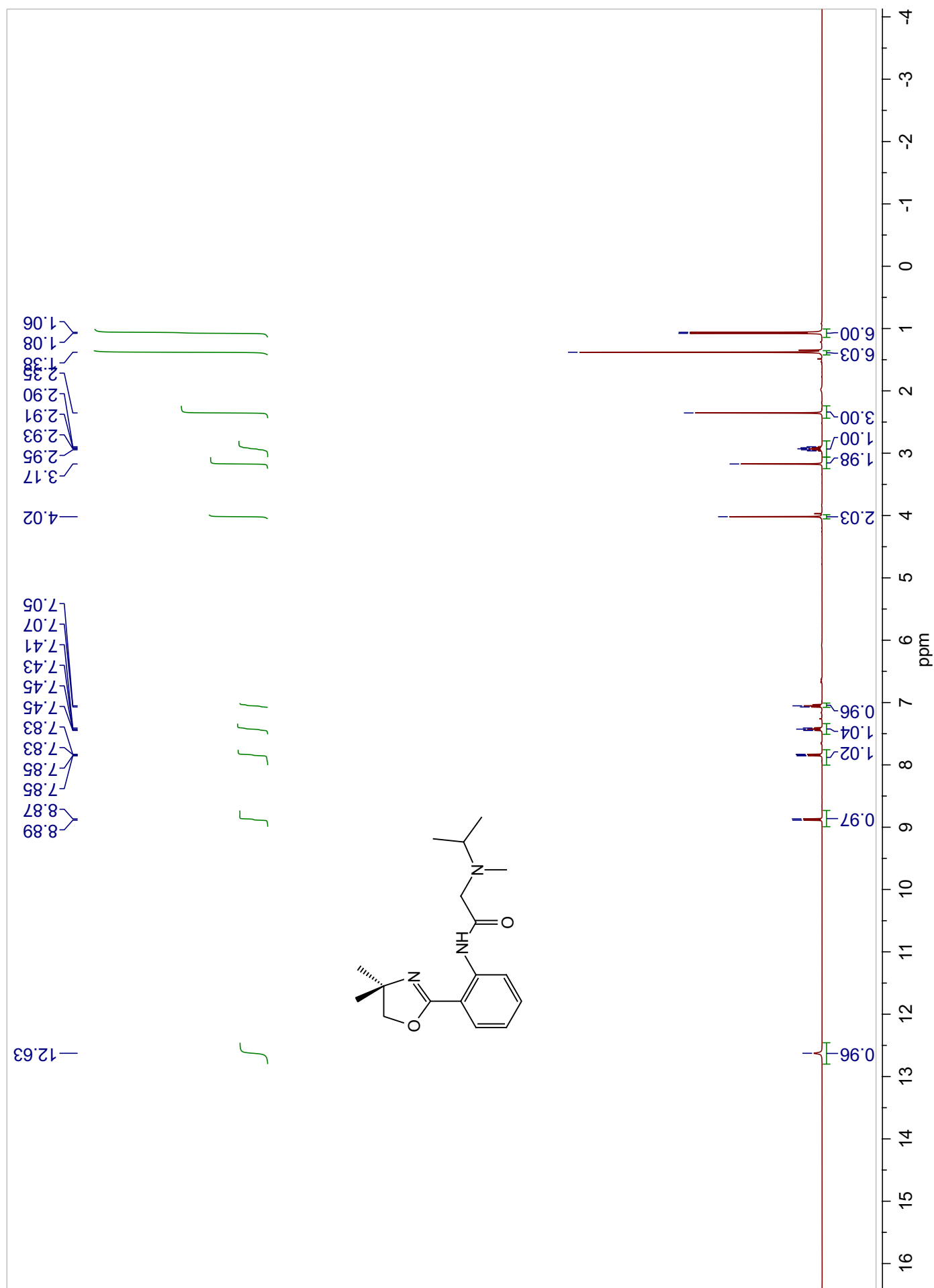


Figure A20. ^{13}C -NMR Spectrum of **3i** in CDCl_3

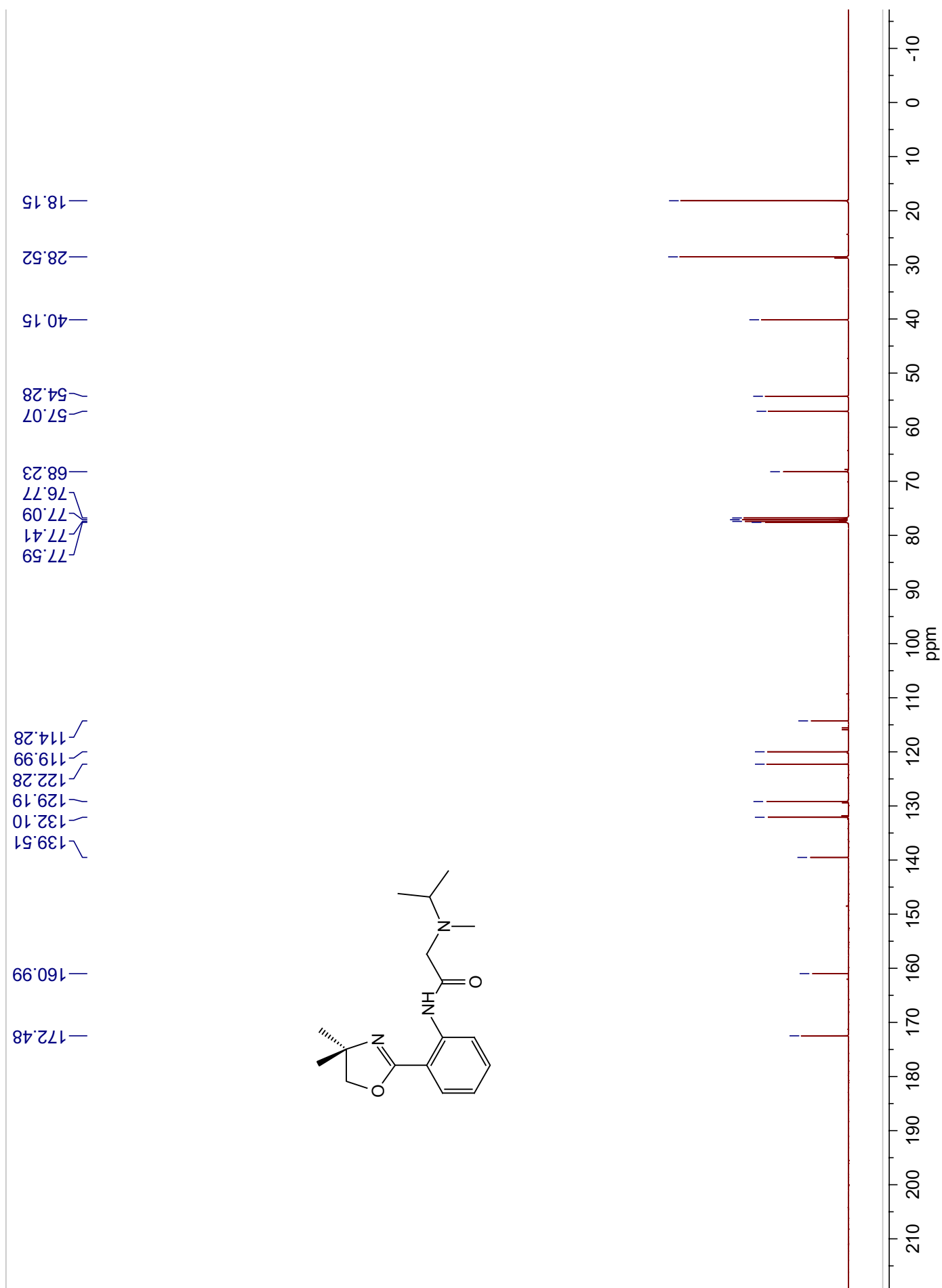


Figure A21. ^1H -NMR Spectrum of **3j** in CDCl_3

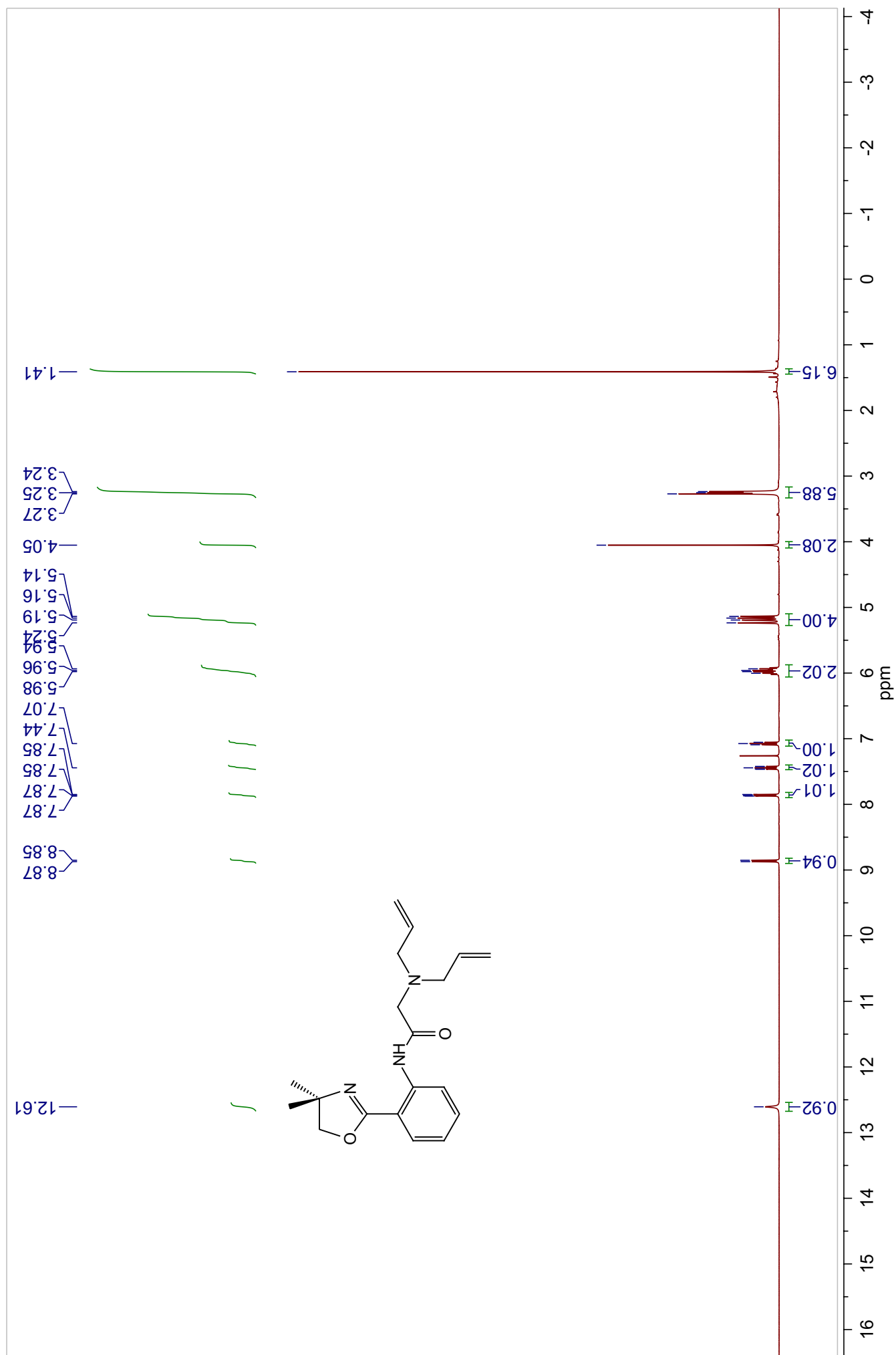
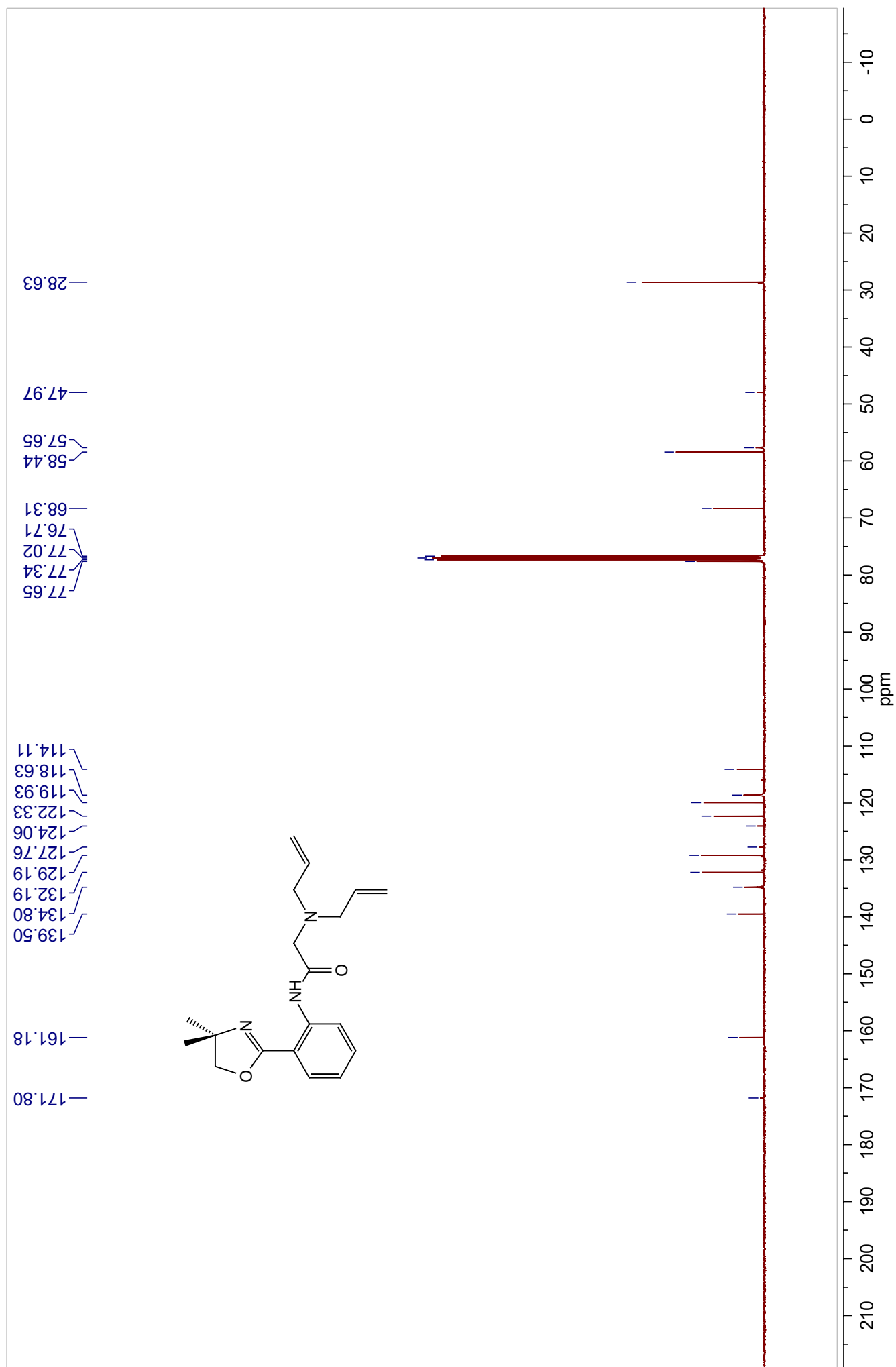


Figure A22. ^{13}C -NMR Spectrum of **3j** in CDCl_3



CN(C)CC(=O)Nc1ccccc1C2=CN(C[C@H]2C)O

Chemical Structure: CN(C)CC(=O)Nc1ccccc1C2=CN(C[C@H]2C)O

¹H NMR Data (ppm):

- 12.22 (broad, 1H, integration 0.93)
- 8.81, 8.79, 8.81 (multiplet, 1H, integration 0.95)
- 7.82, 7.81, 7.80, 7.79, 7.44, 7.42, 7.40, 7.07, 7.07, 7.05, 7.03 (multiplet, 7H, integration 1.11, 1.14, 1.08)
- 3.63, 3.62, 3.61, 3.24, 2.67, 2.66, 2.65, 2.43 (multiplet, 6H, integration 6.00)
- 2.90, 2.11, 1.97, 1.95 (multiplet, 6H, integration 6.00)

Figure A24. ^{13}C -NMR Spectrum of **3k** in CDCl_3

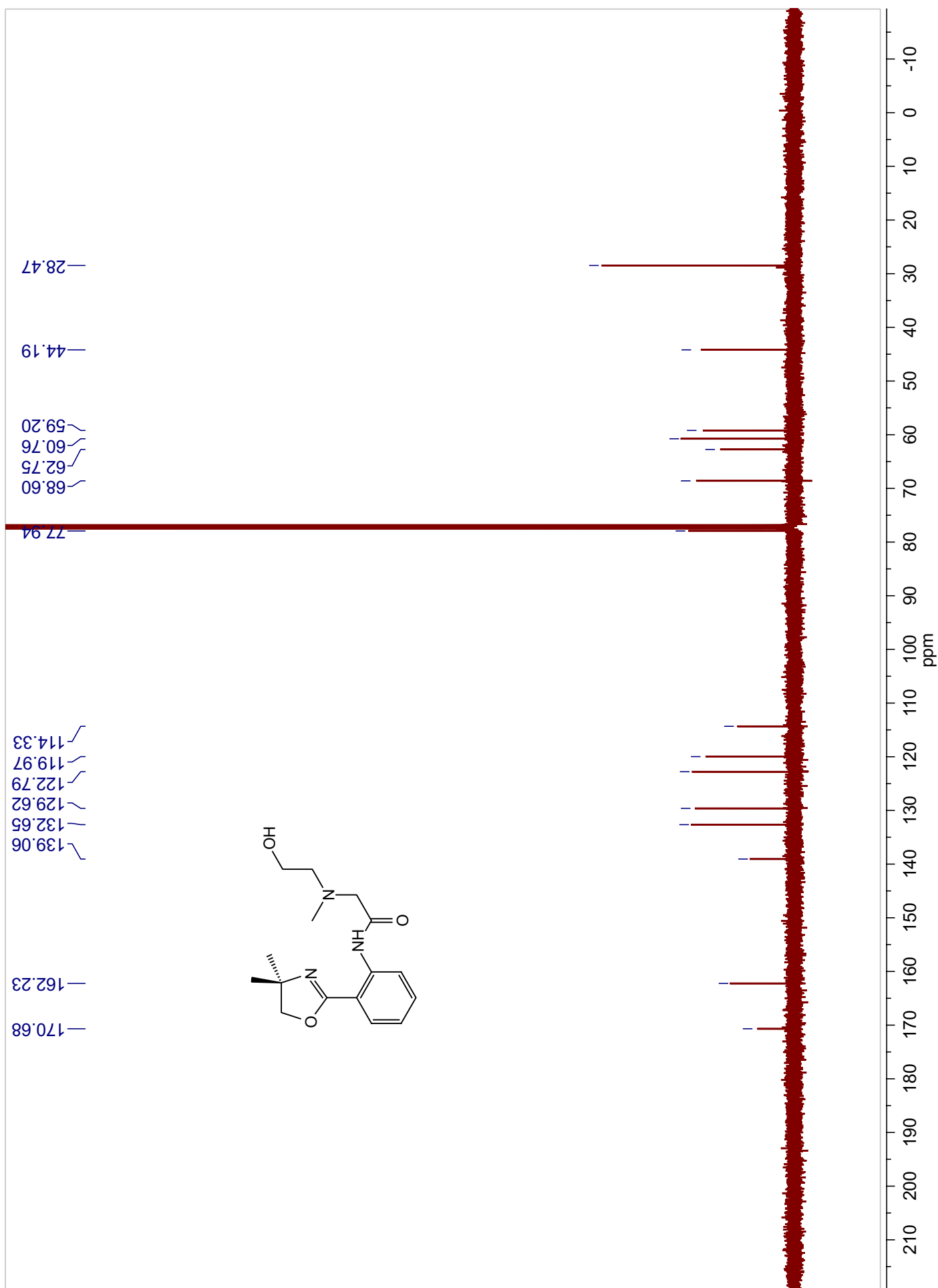


Figure A25. ^1H -NMR Spectrum of **31** in CDCl_3

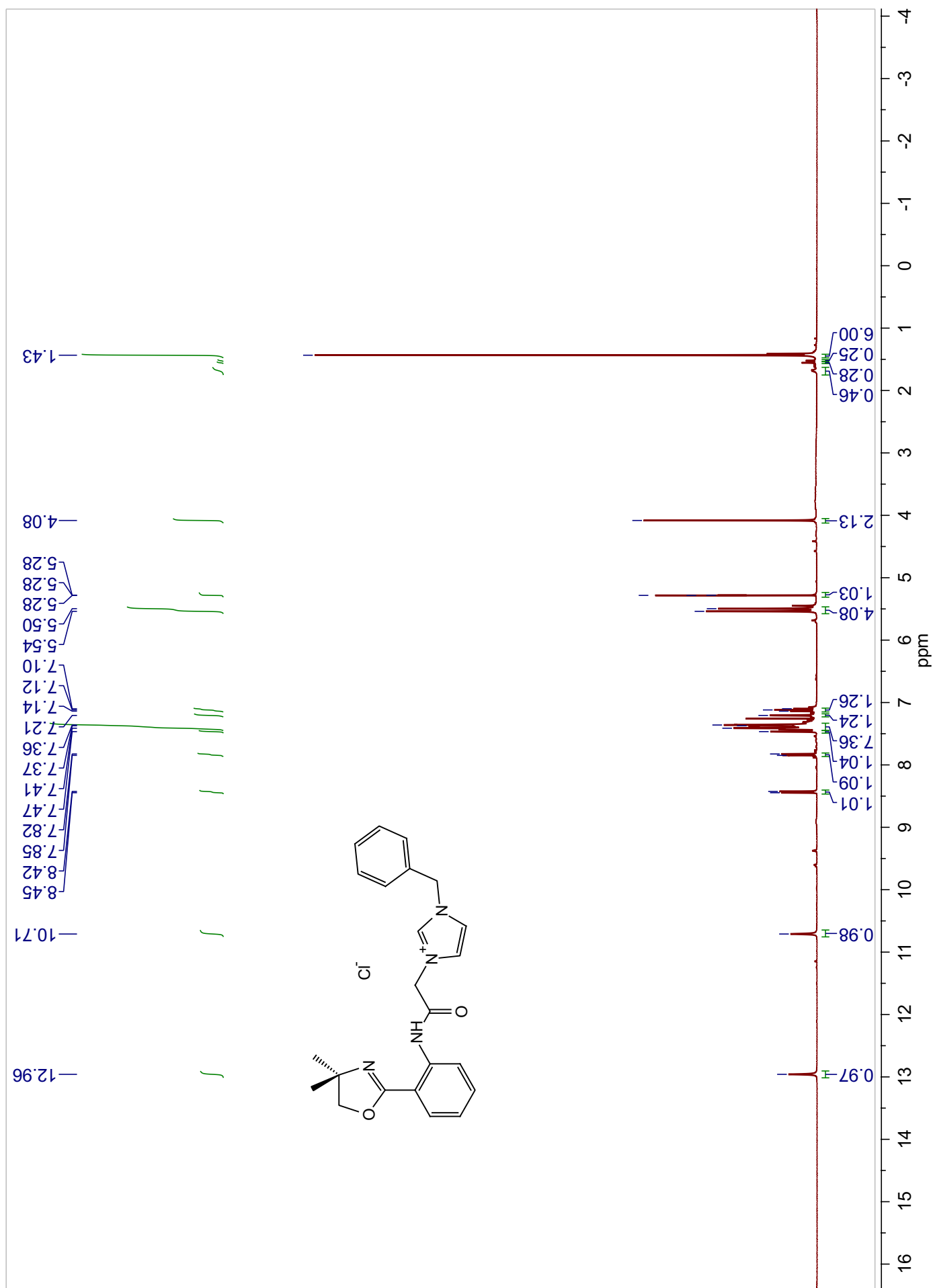


Figure A26. ^{13}C -NMR Spectrum of **3I** in CDCl_3

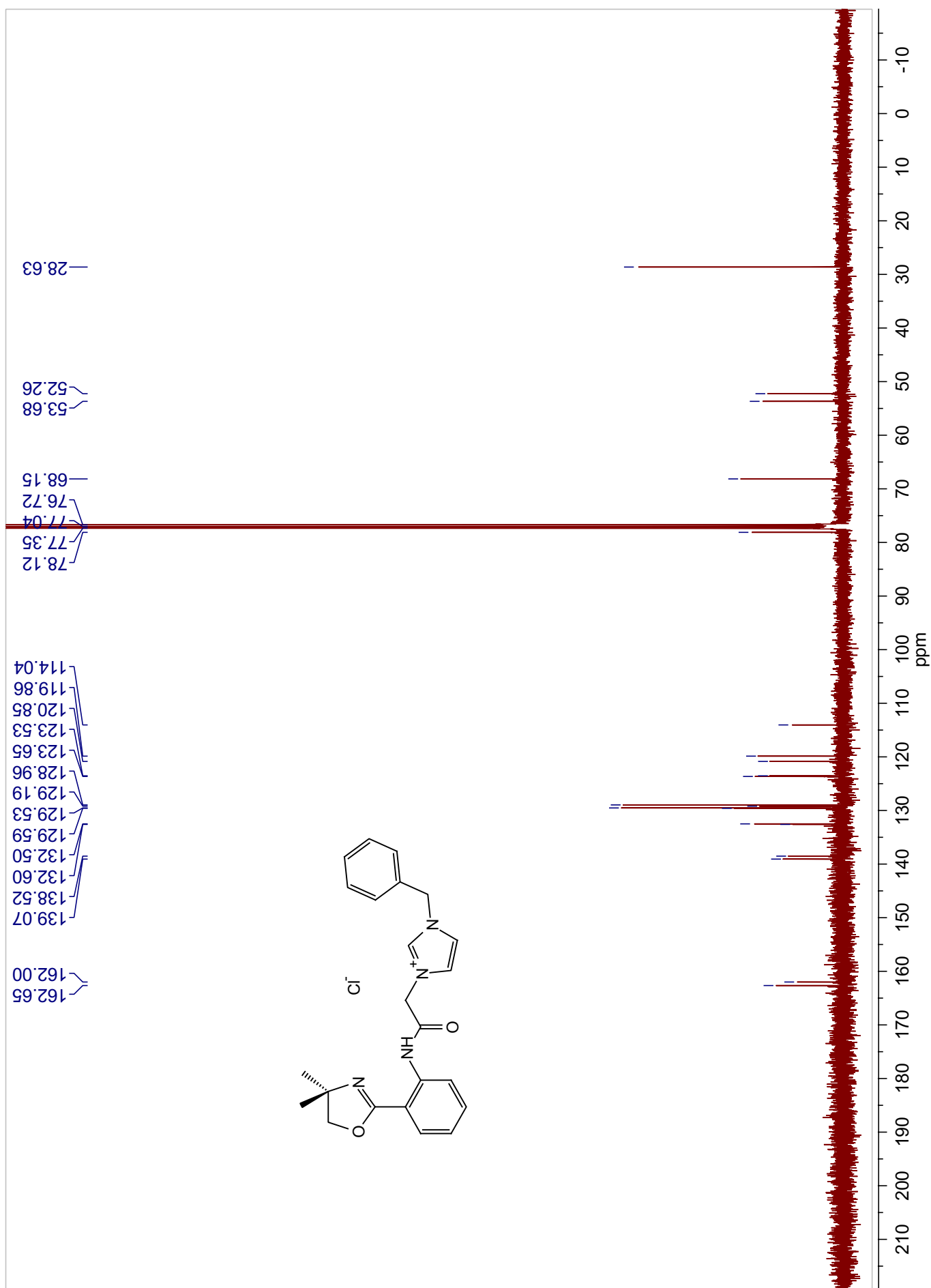


Figure A27. ^1H -NMR Spectrum of **3m•oxide** in CDCl_3

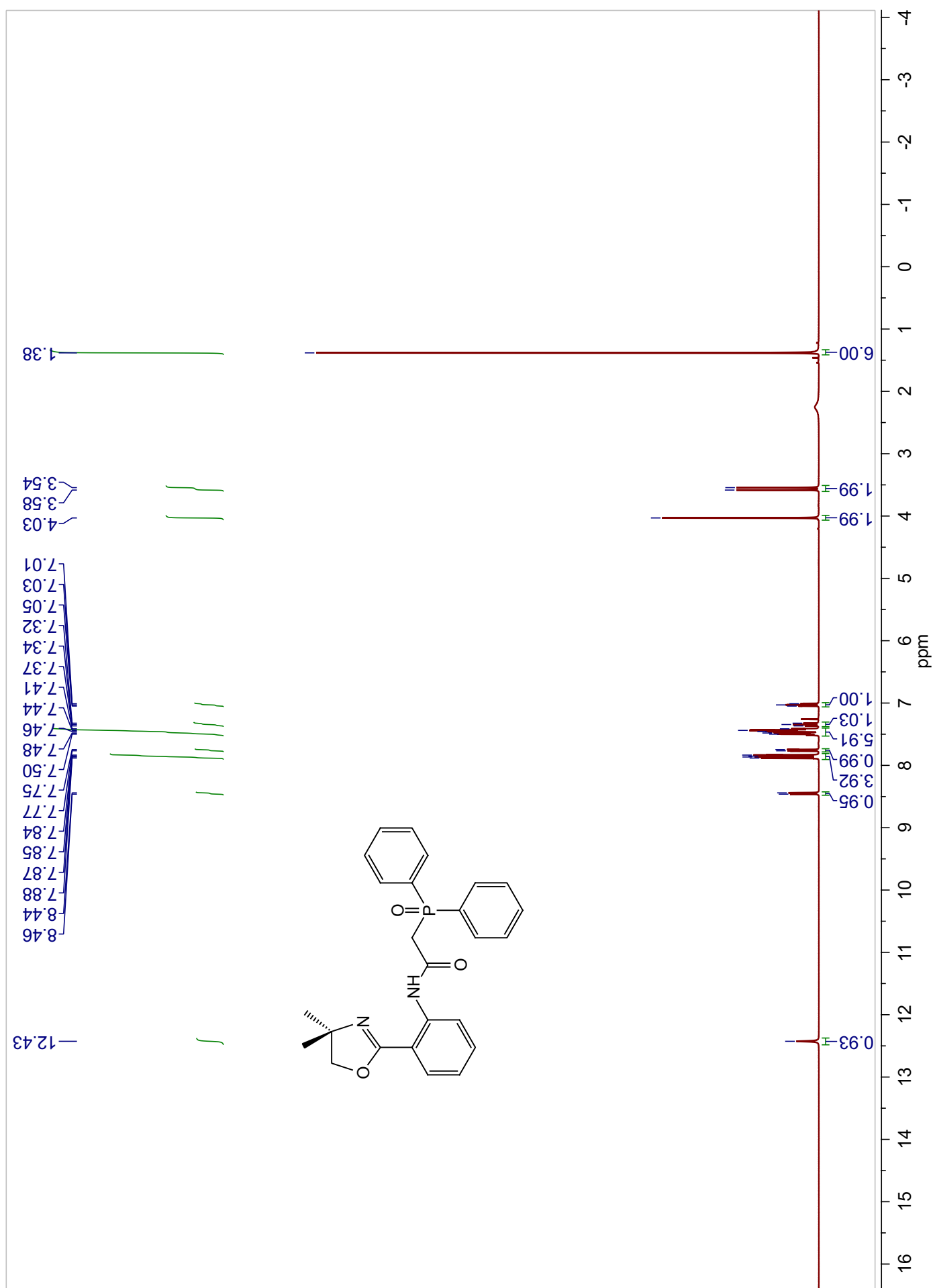


Figure A28. ^{13}C -NMR Spectrum of **3m-oxide** in CDCl_3

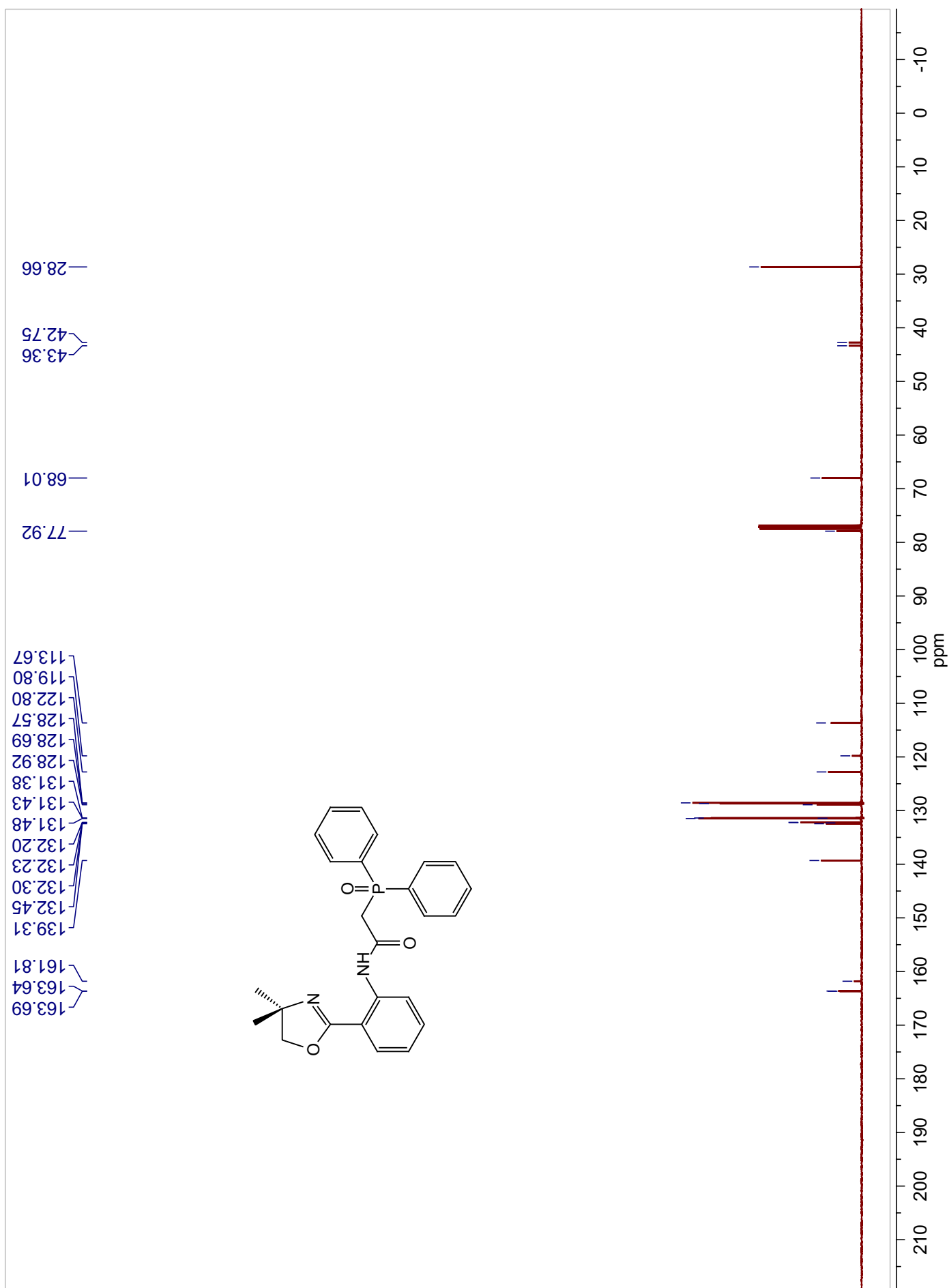


Figure A29. ^{31}P -NMR Spectrum of **3m•oxide** in CDCl_3

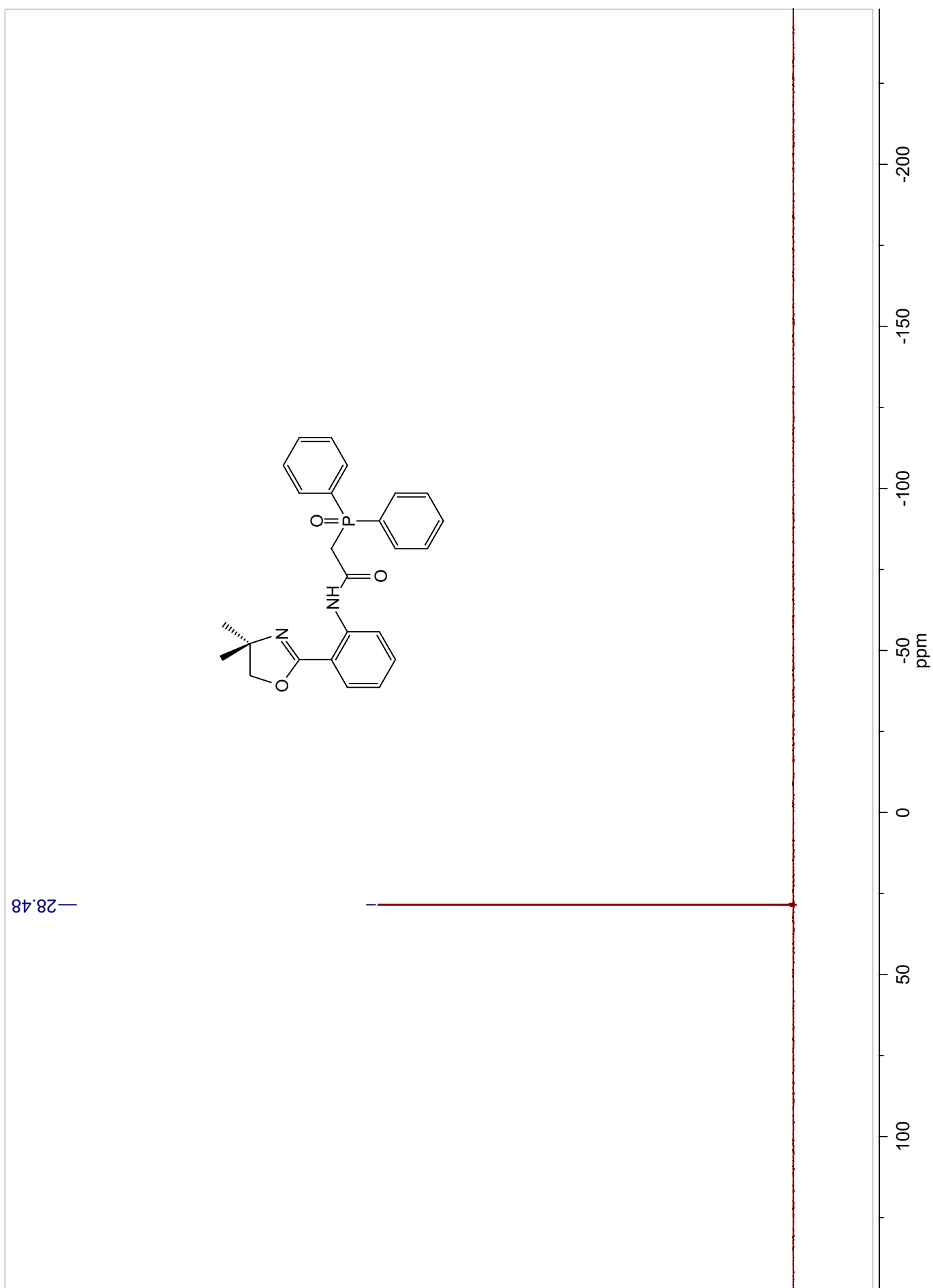


Figure A30. ^1H -NMR Spectrum of **3n** in CDCl_3

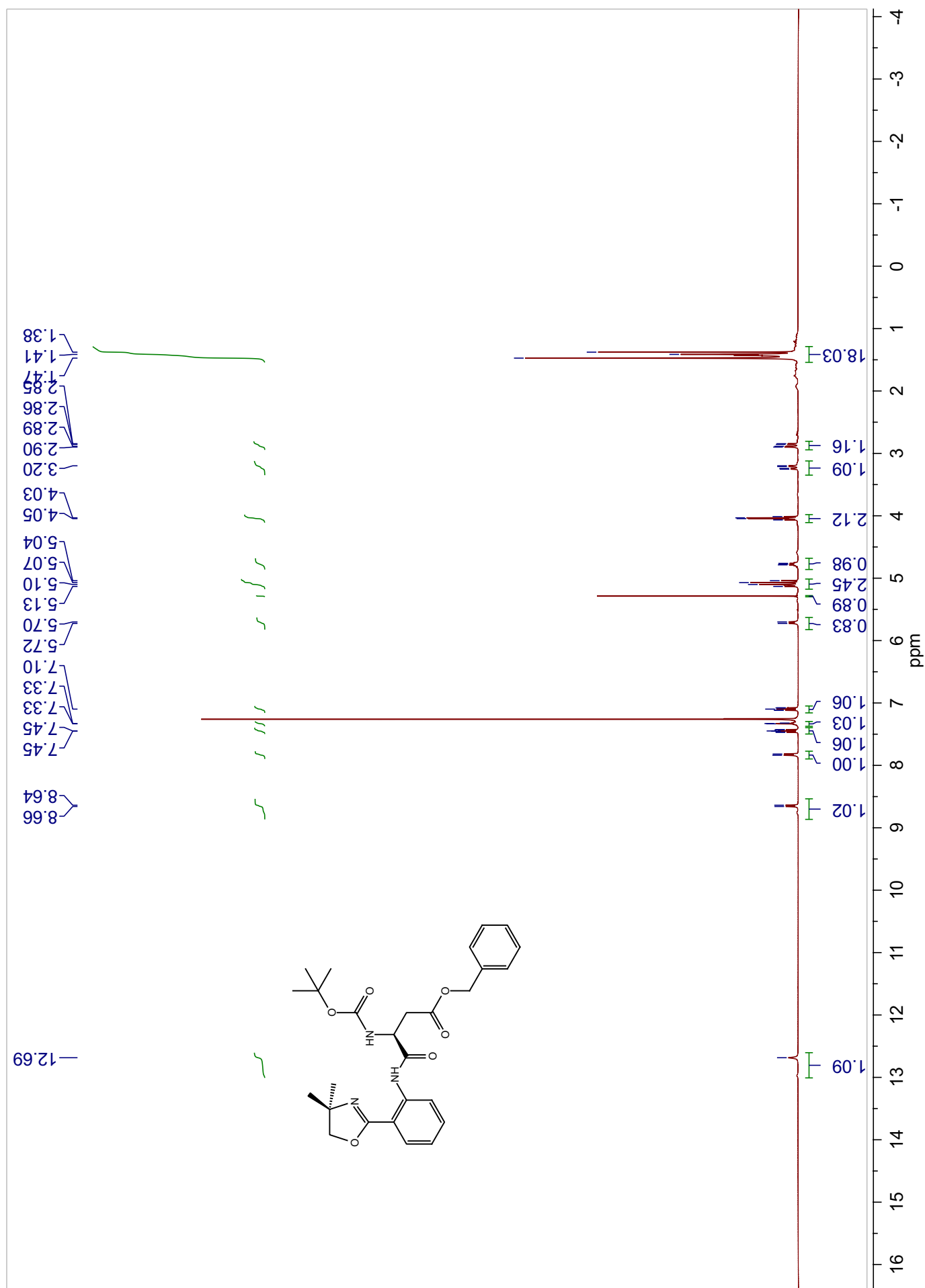


Figure A31. ^{13}C -NMR Spectrum of **3n** in CDCl_3

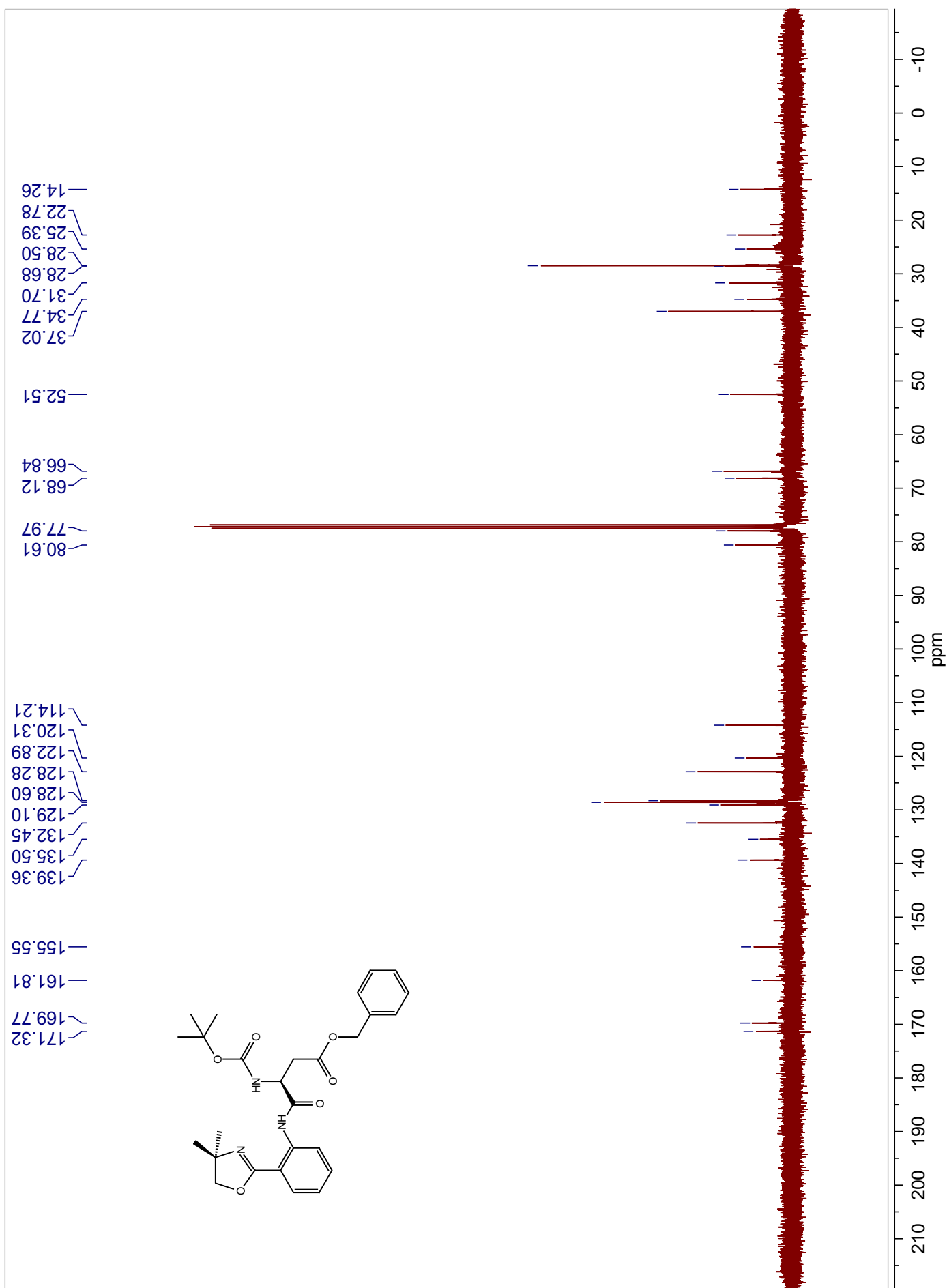


Figure A32. ^1H -NMR Spectrum of **4** in CDCl_3

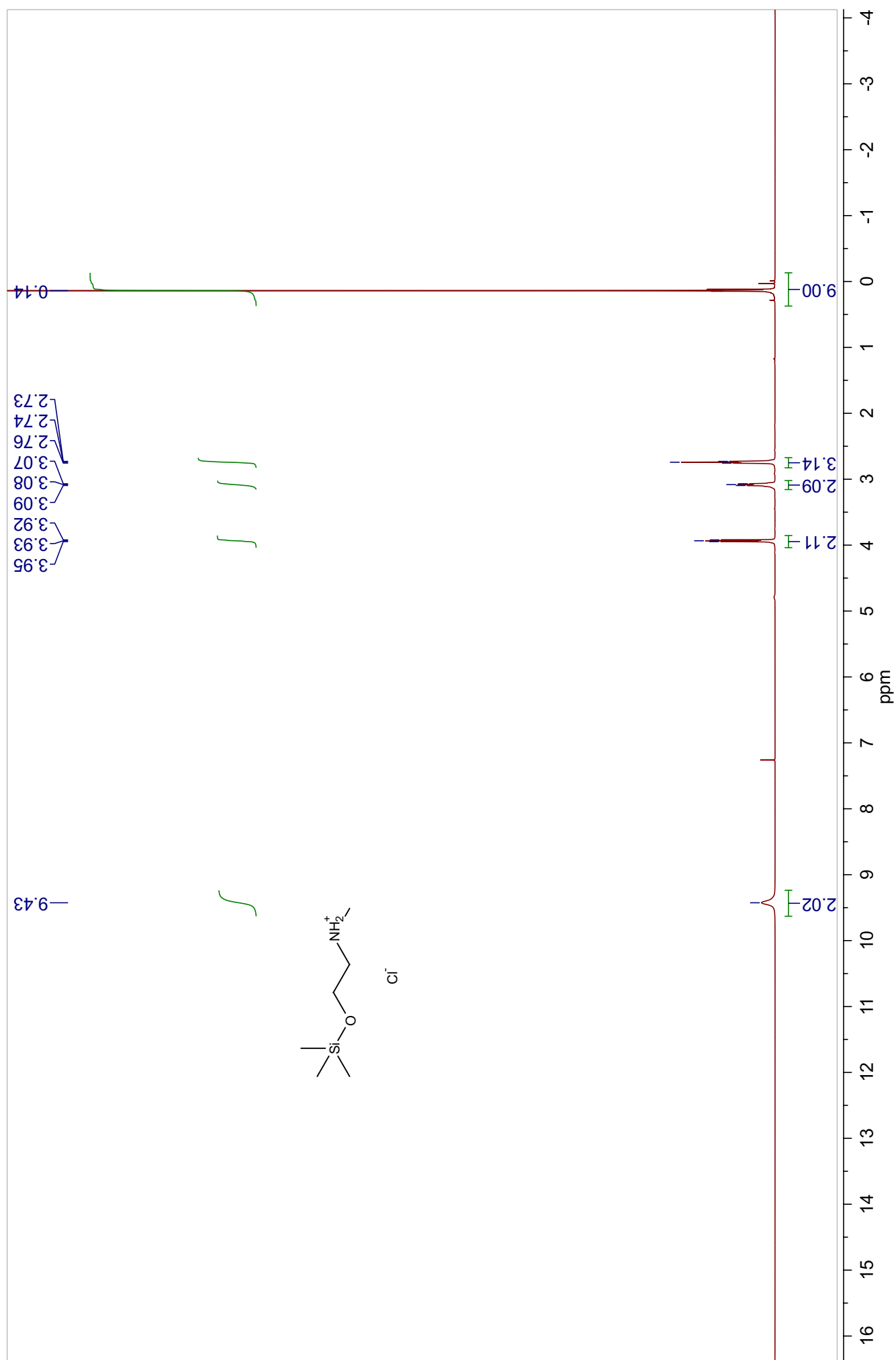


Figure A33. ^{13}C -NMR Spectrum of **4** in CDCl_3

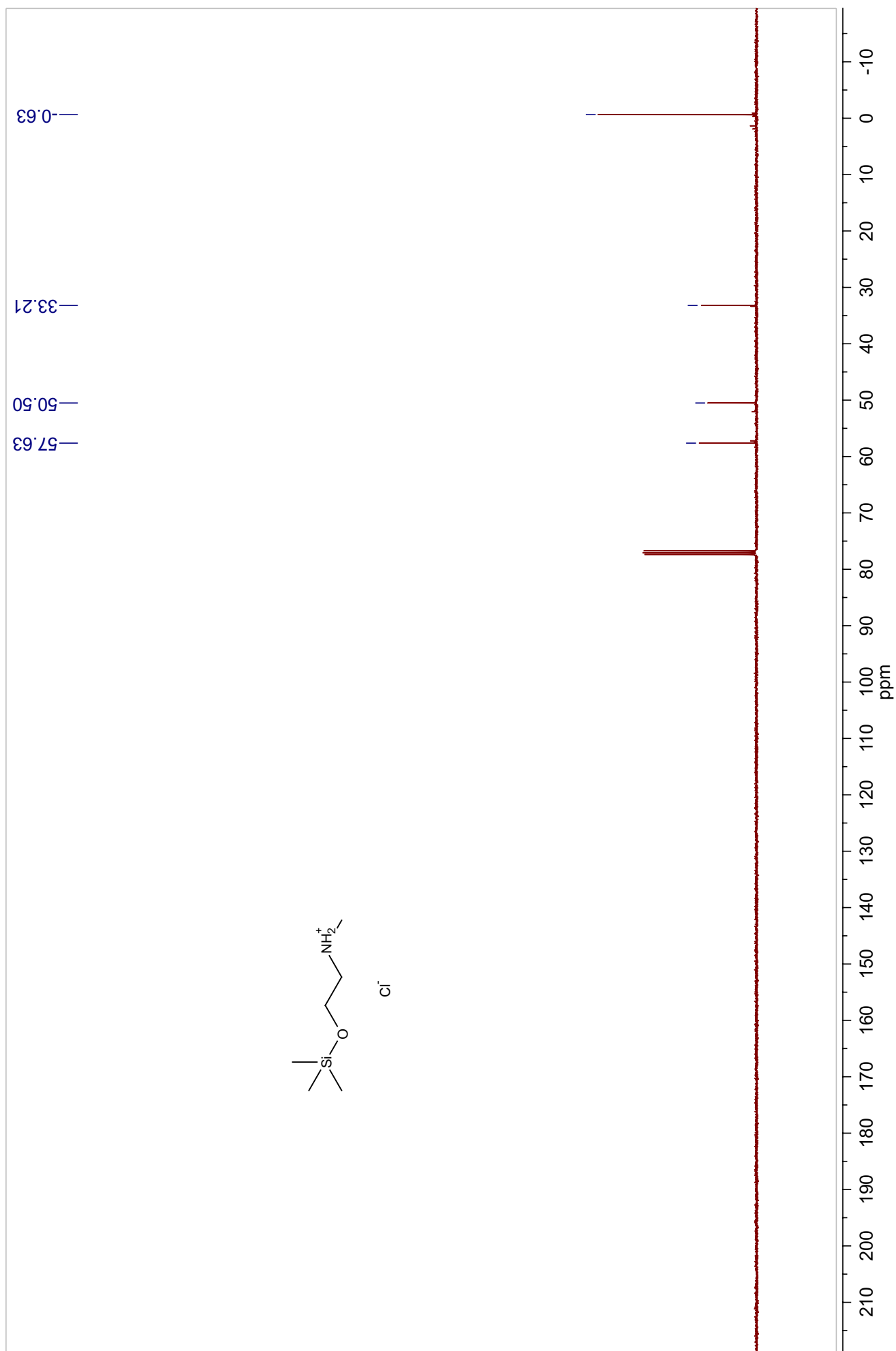


Figure A34. ^1H -NMR Spectrum of **6** in CDCl_3

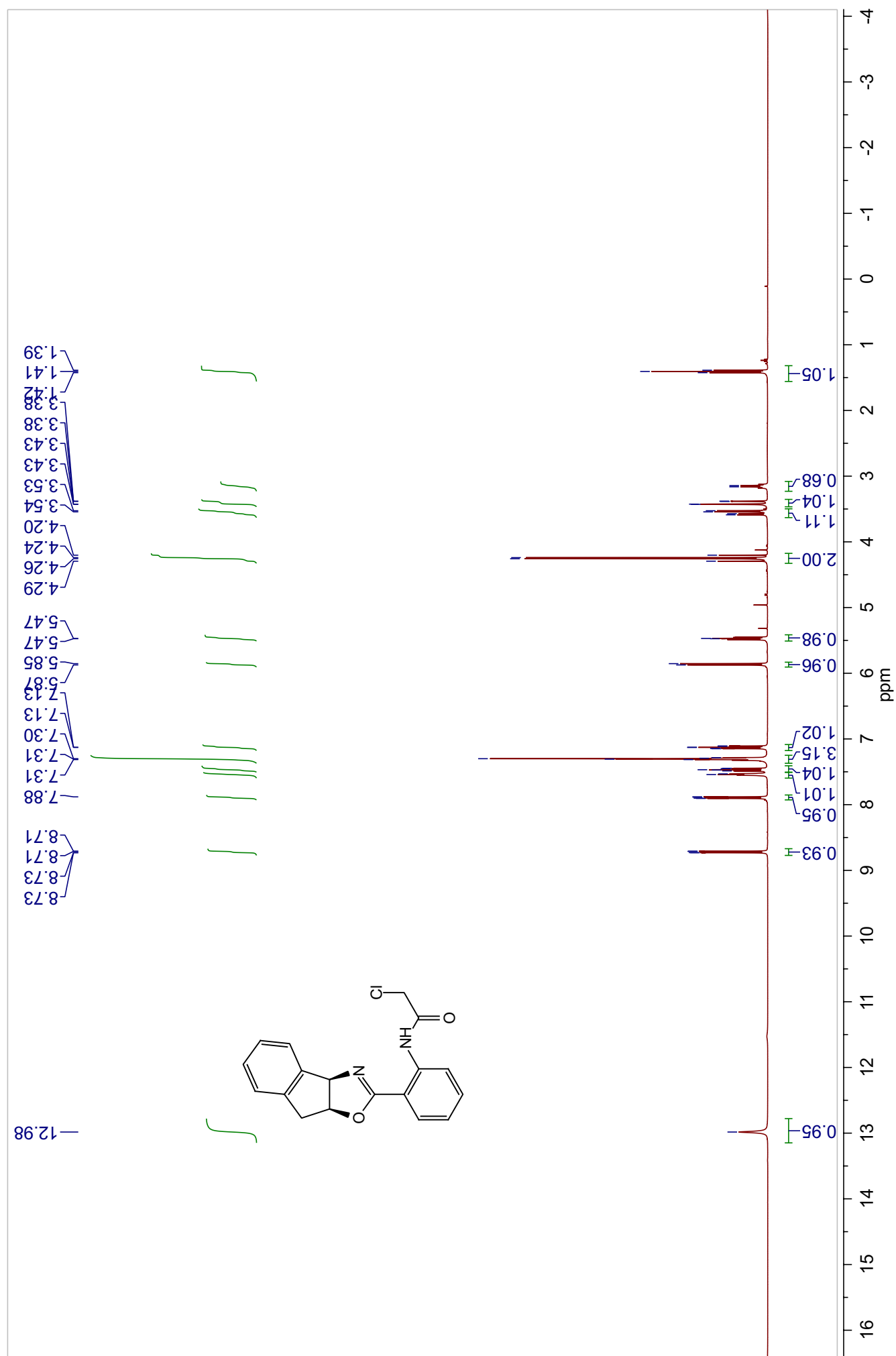


Figure A35. ^{13}C -NMR Spectrum of **6** in CDCl_3

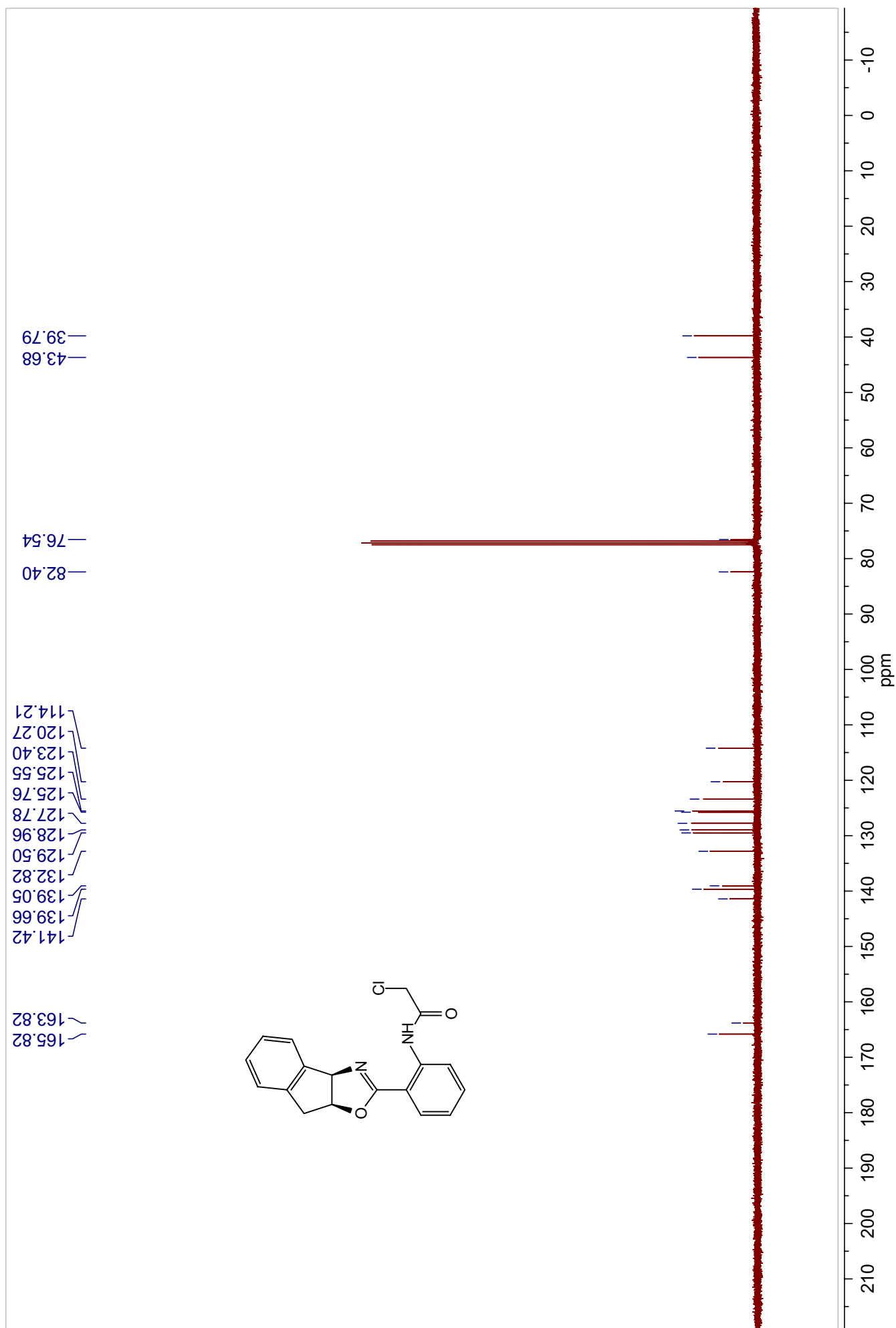


Figure A36. ^1H -NMR Spectrum of **7** in CDCl_3

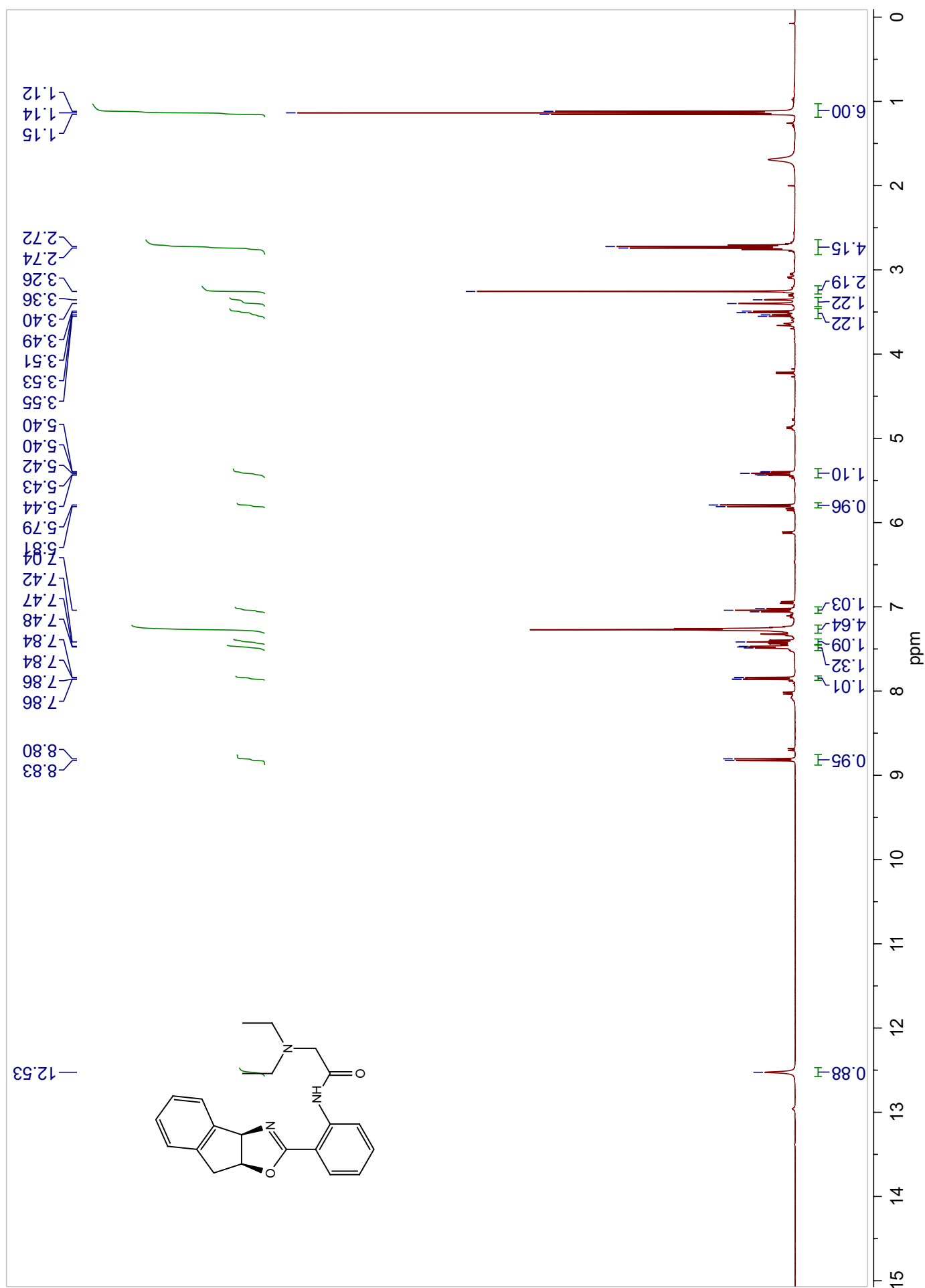


Figure A37. ^1H -NMR Spectrum of **9a** in CDCl_3

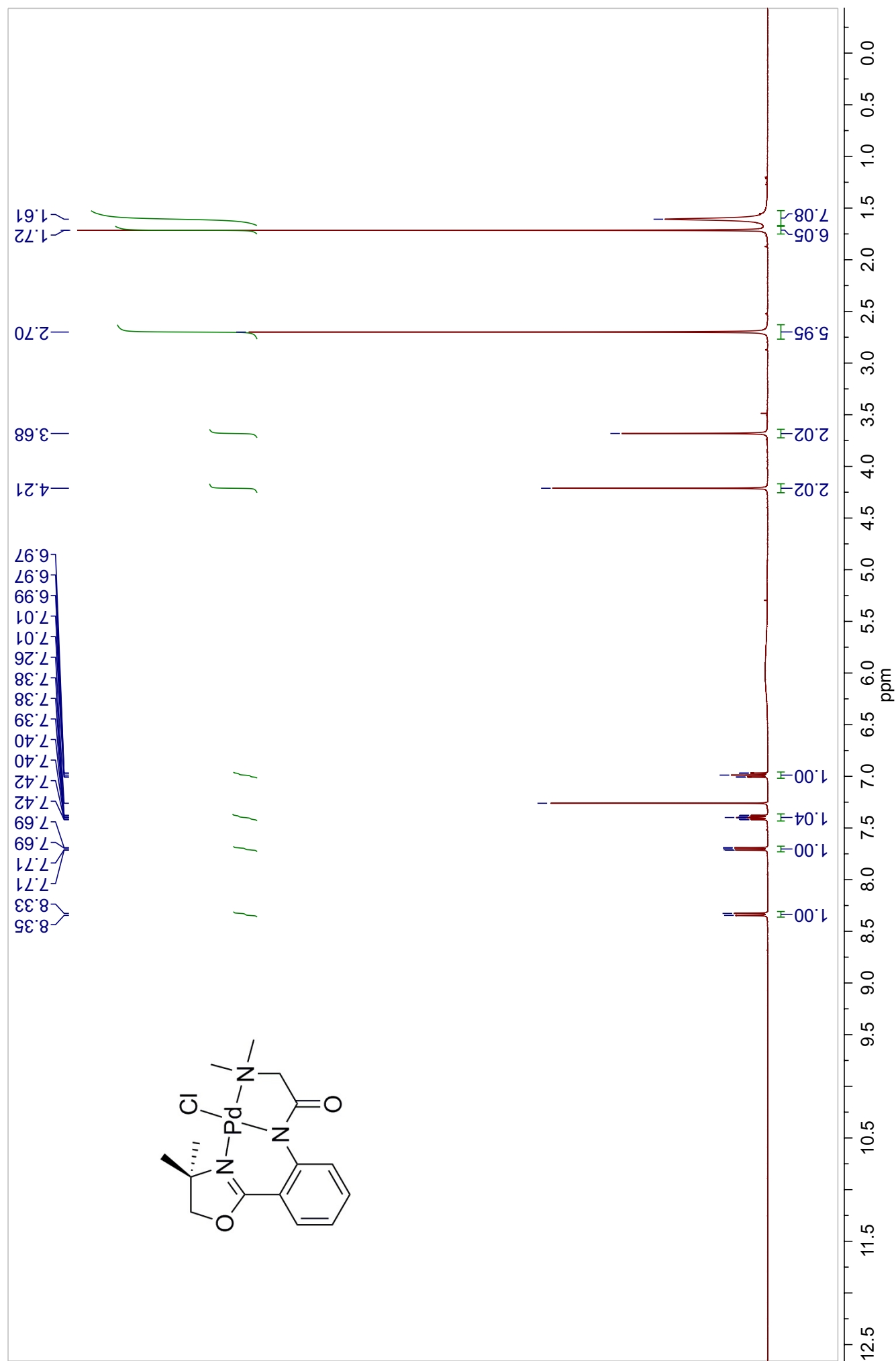


Figure A38. ^{13}C -NMR Spectrum of **9a** in CDCl_3

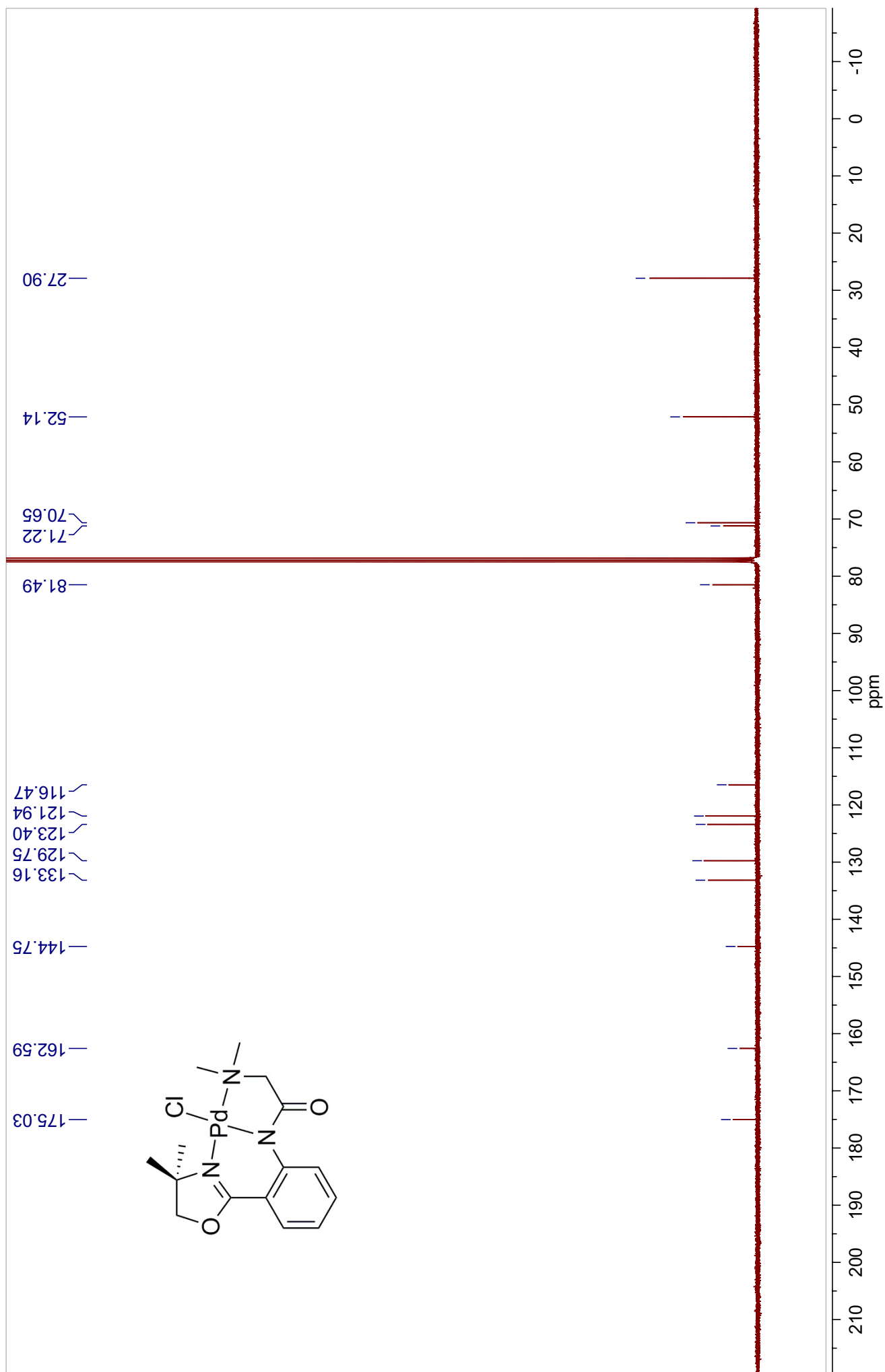


Figure A39. ^1H -NMR Spectrum of **9b** in CDCl_3

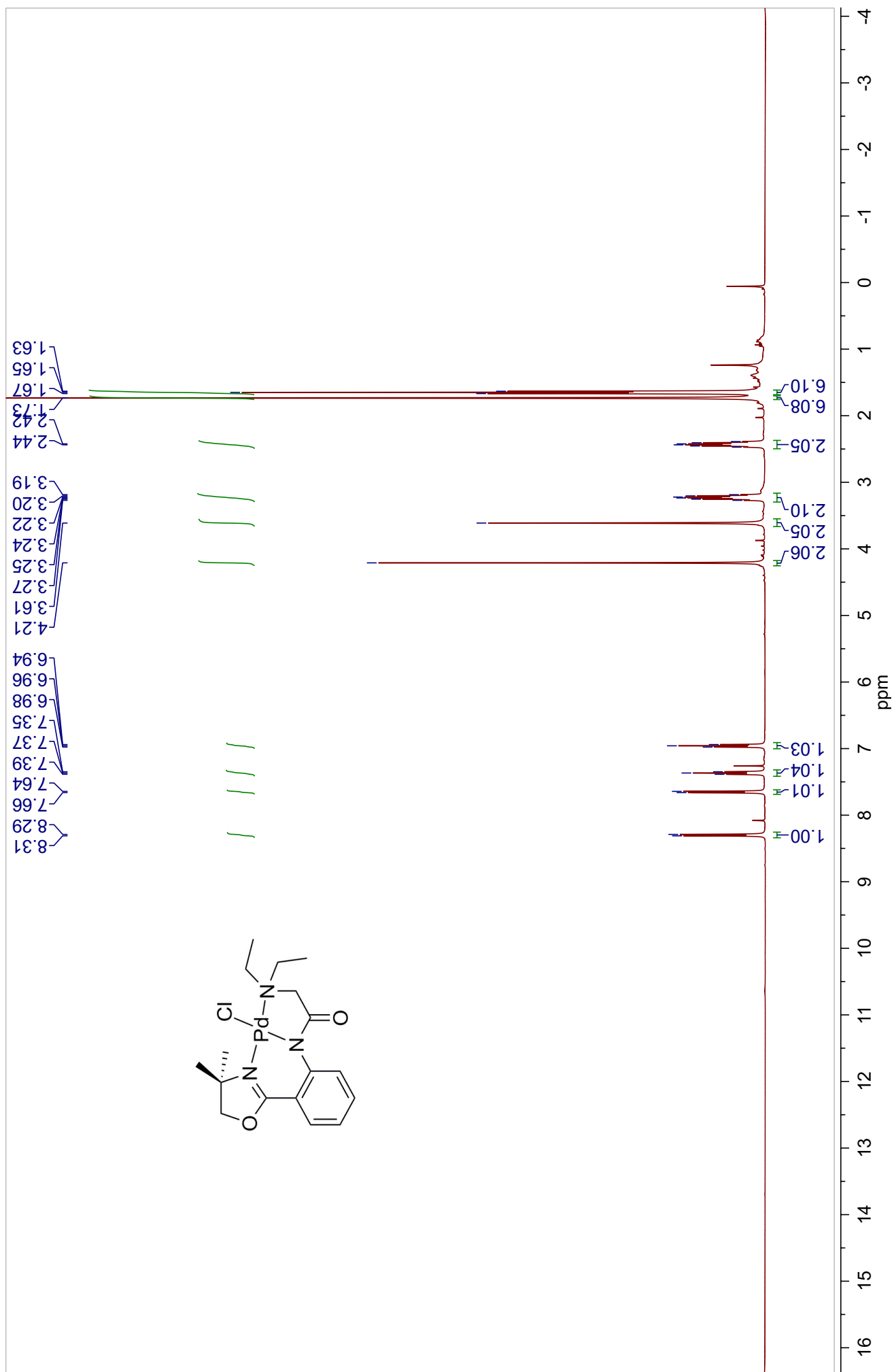


Figure A40. ^{13}C -NMR Spectrum of **9b** in CDCl_3

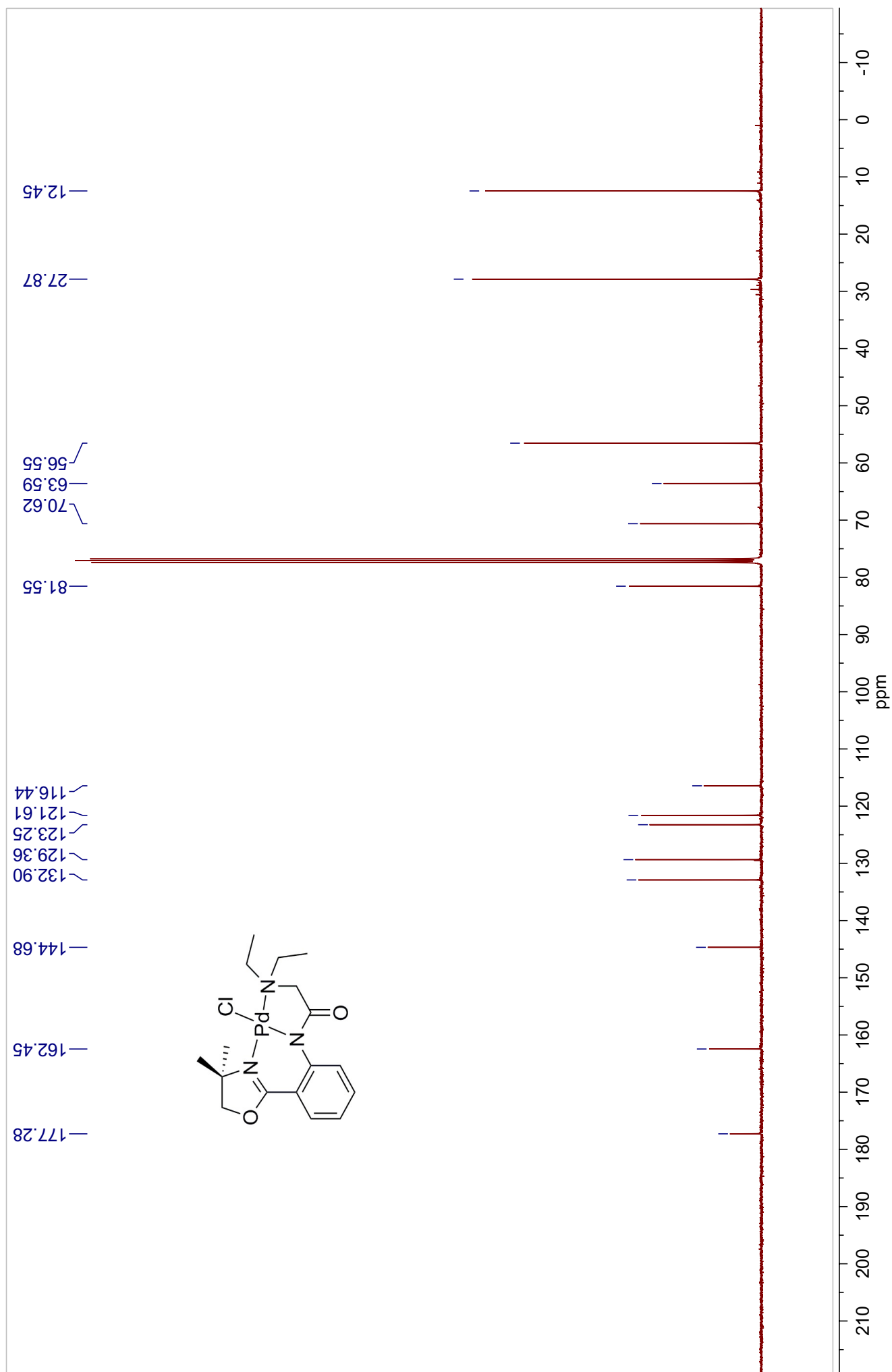


Figure A41. ^1H -NMR Spectrum of **9c** in CDCl_3

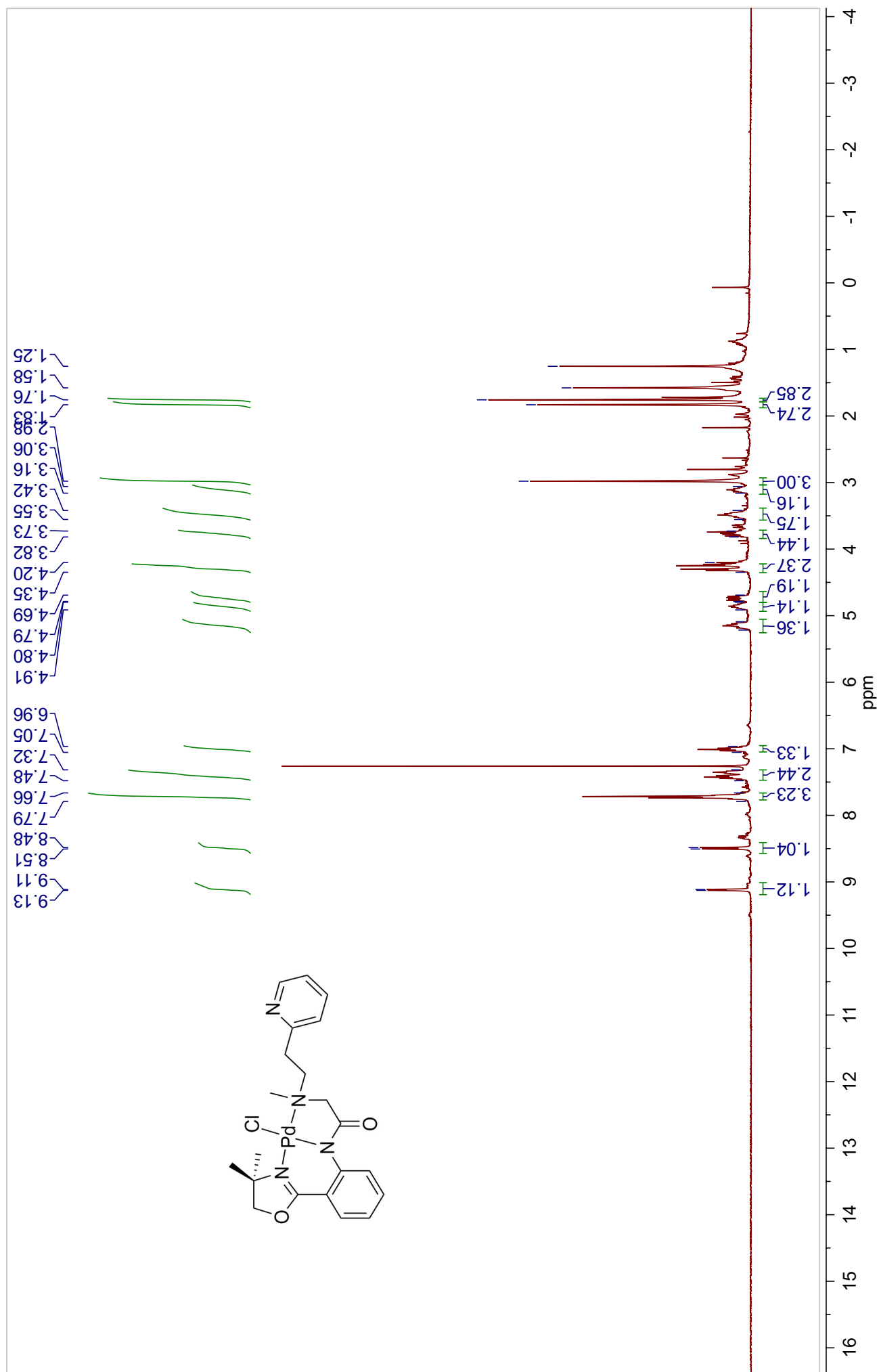


Figure A42. ^{13}C -NMR Spectrum of **9c** in CDCl_3

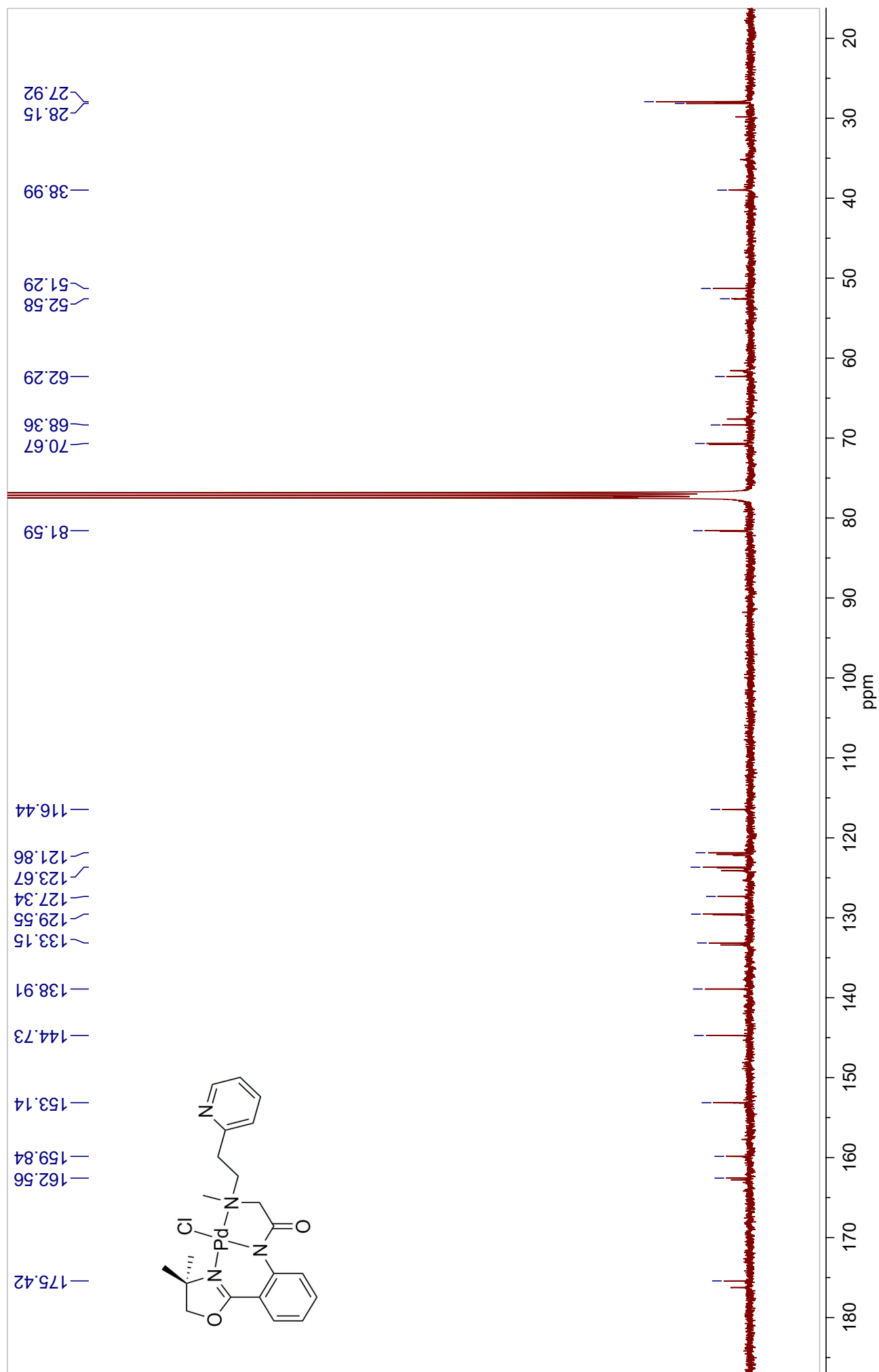


Figure A43. ^1H -NMR Spectrum of **9d** in CDCl_3

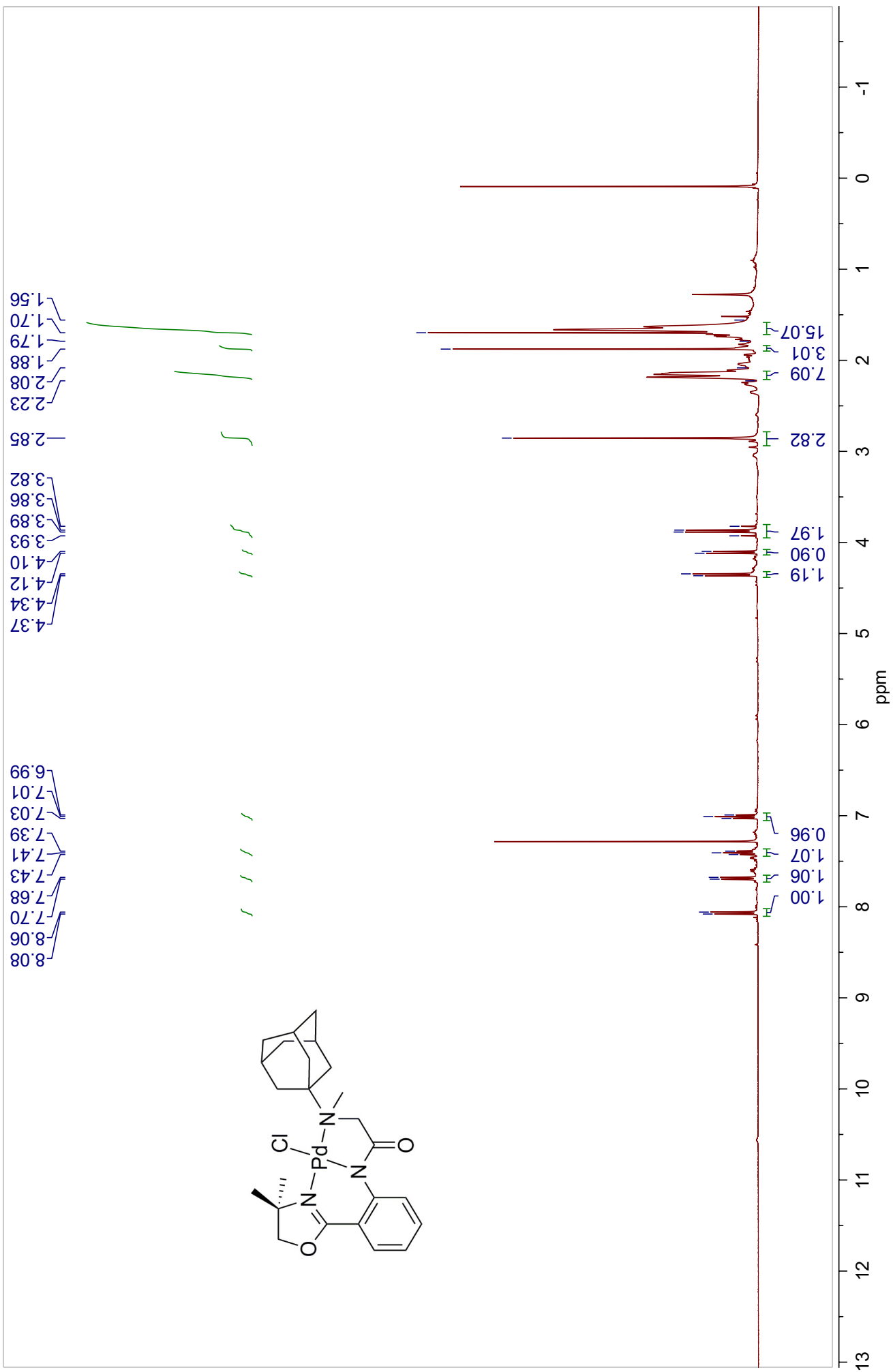


Figure A44. ^{13}C -NMR Spectrum of **9d** in CDCl_3

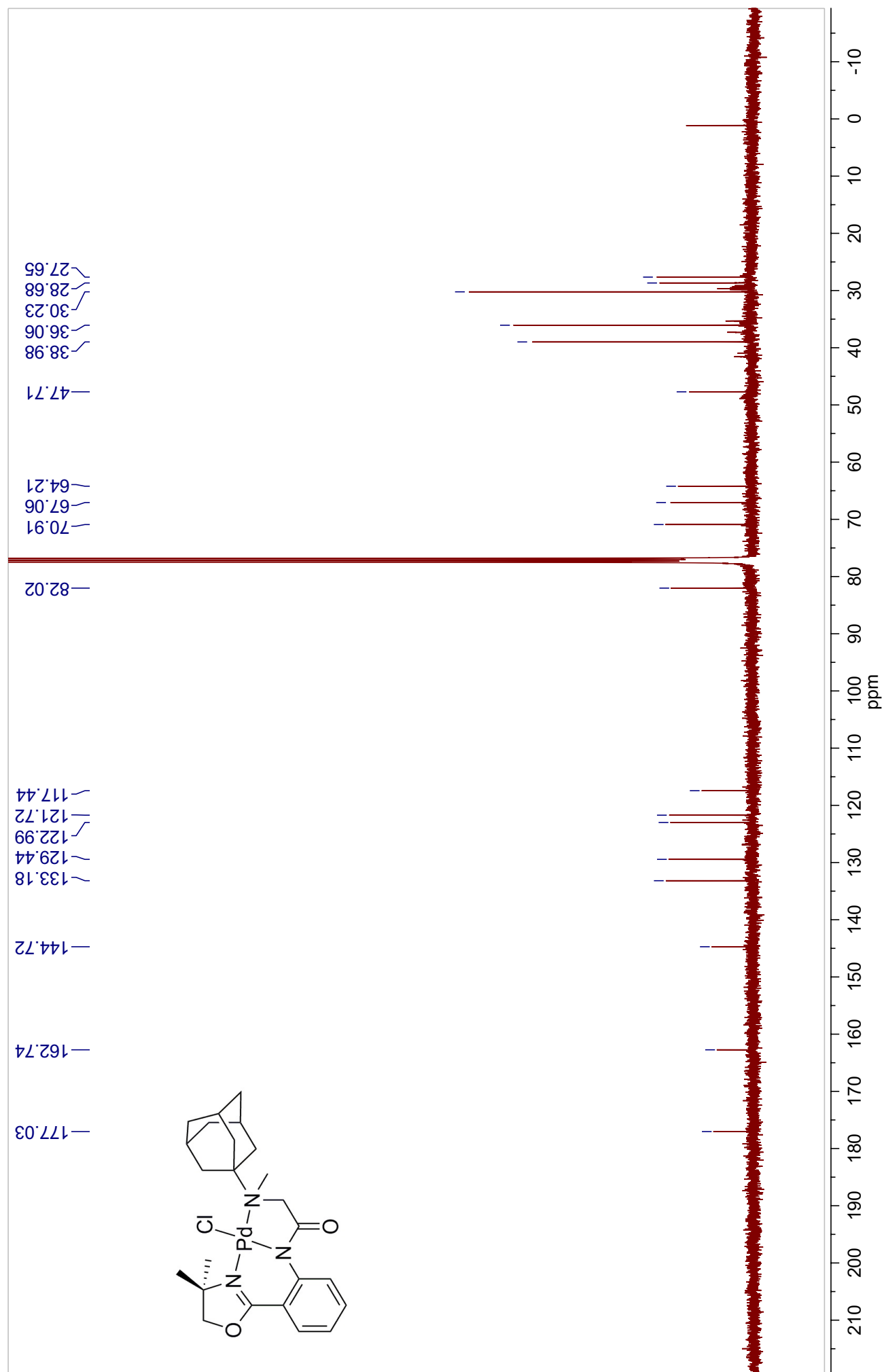


Figure A45. ^1H -NMR Spectrum of **9e** in CDCl_3

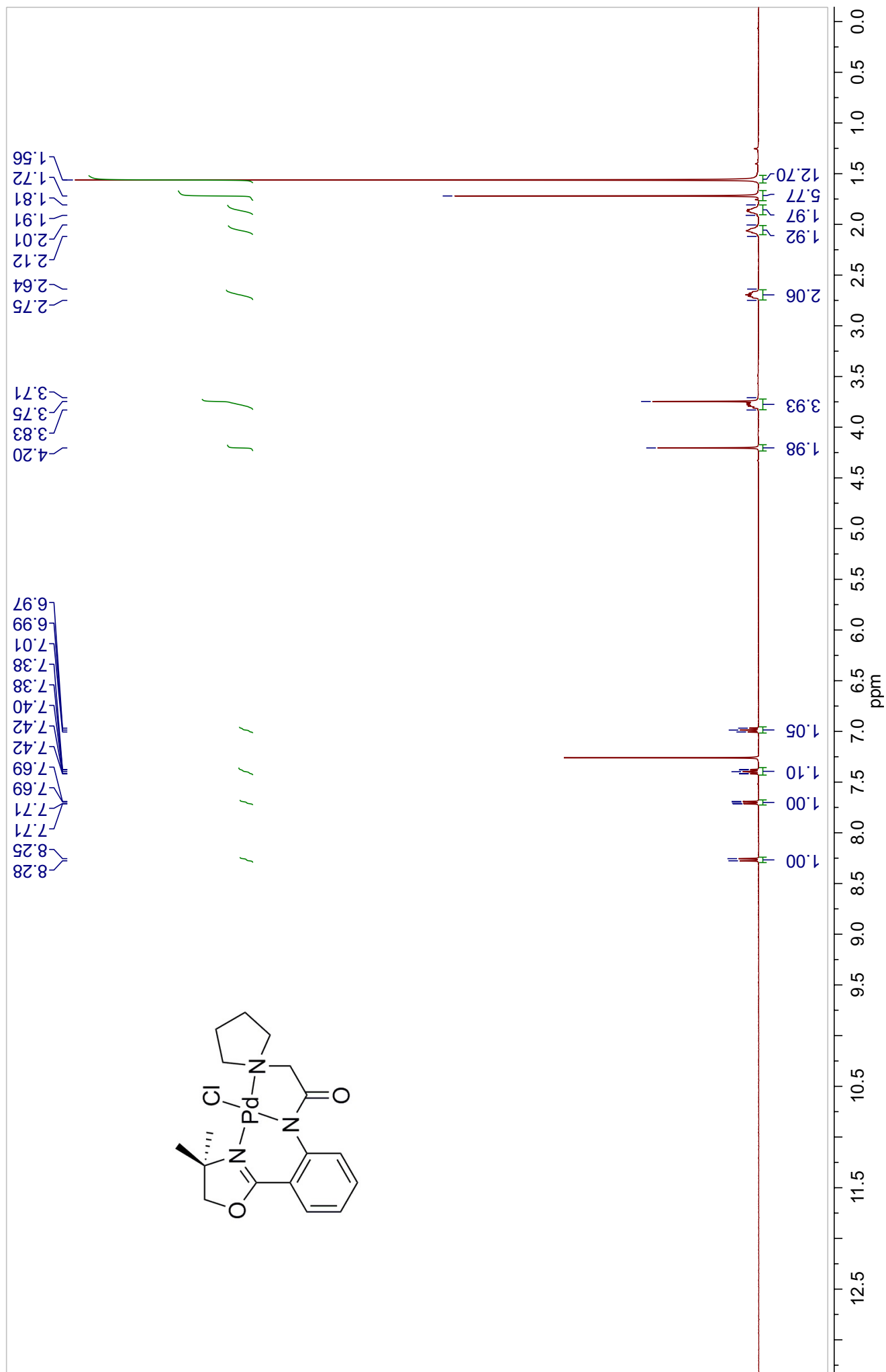


Figure A46. ^{13}C -NMR Spectrum of **9e** in CDCl_3

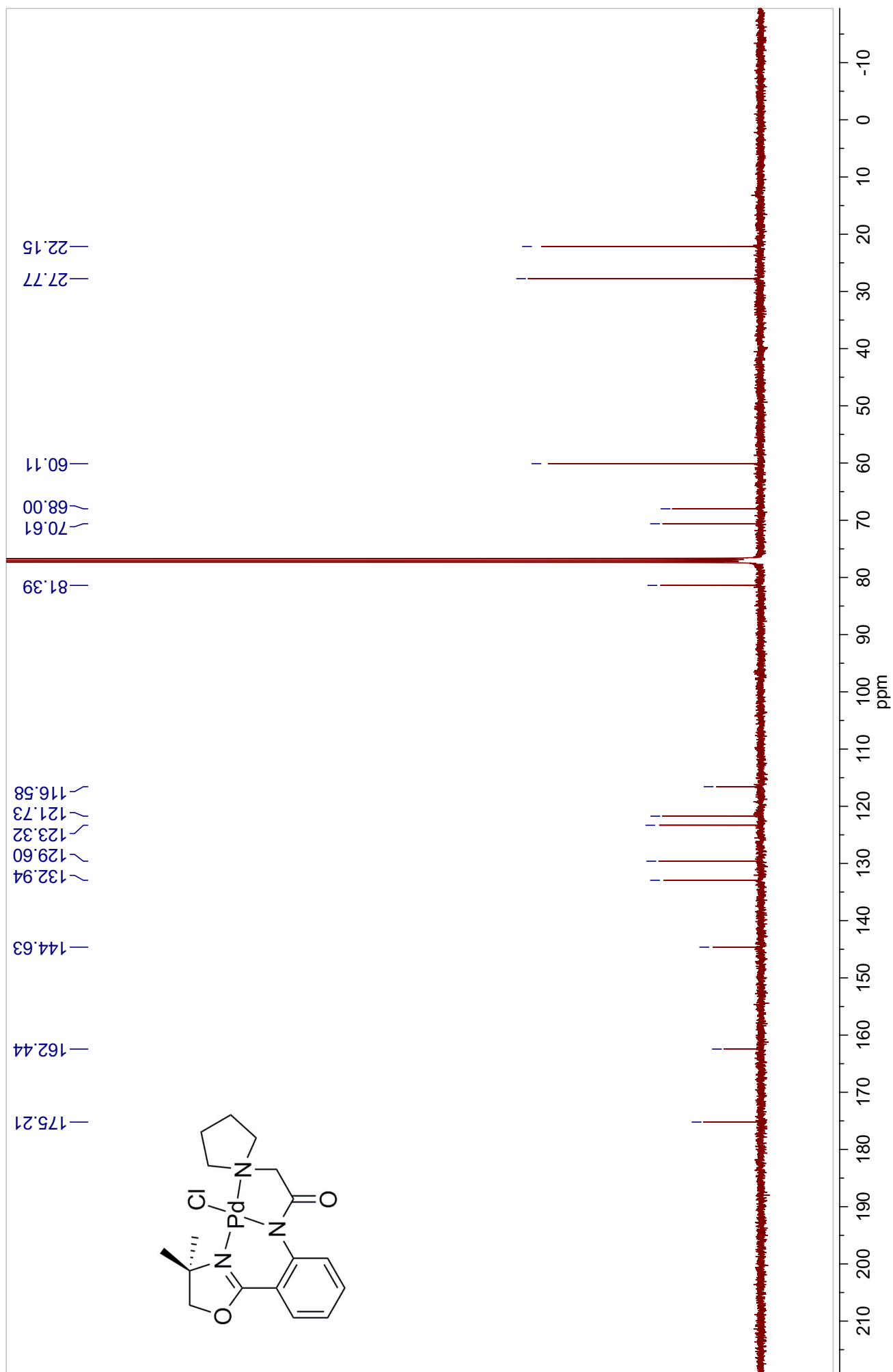


Figure A47. ^1H -NMR Spectrum of **9g** in CDCl_3

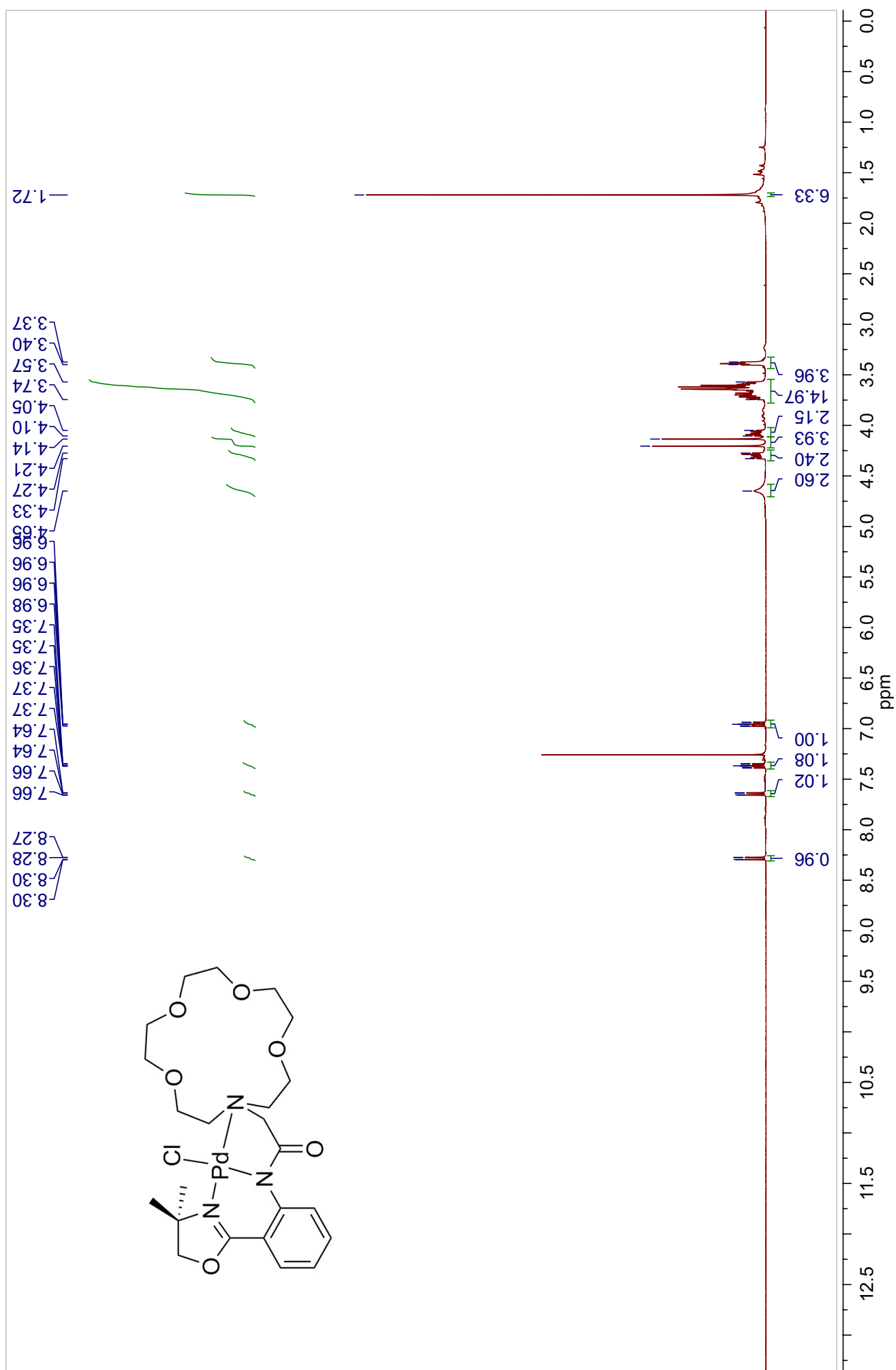


Figure A48. ^{13}C -NMR Spectrum of **9g** in CDCl_3

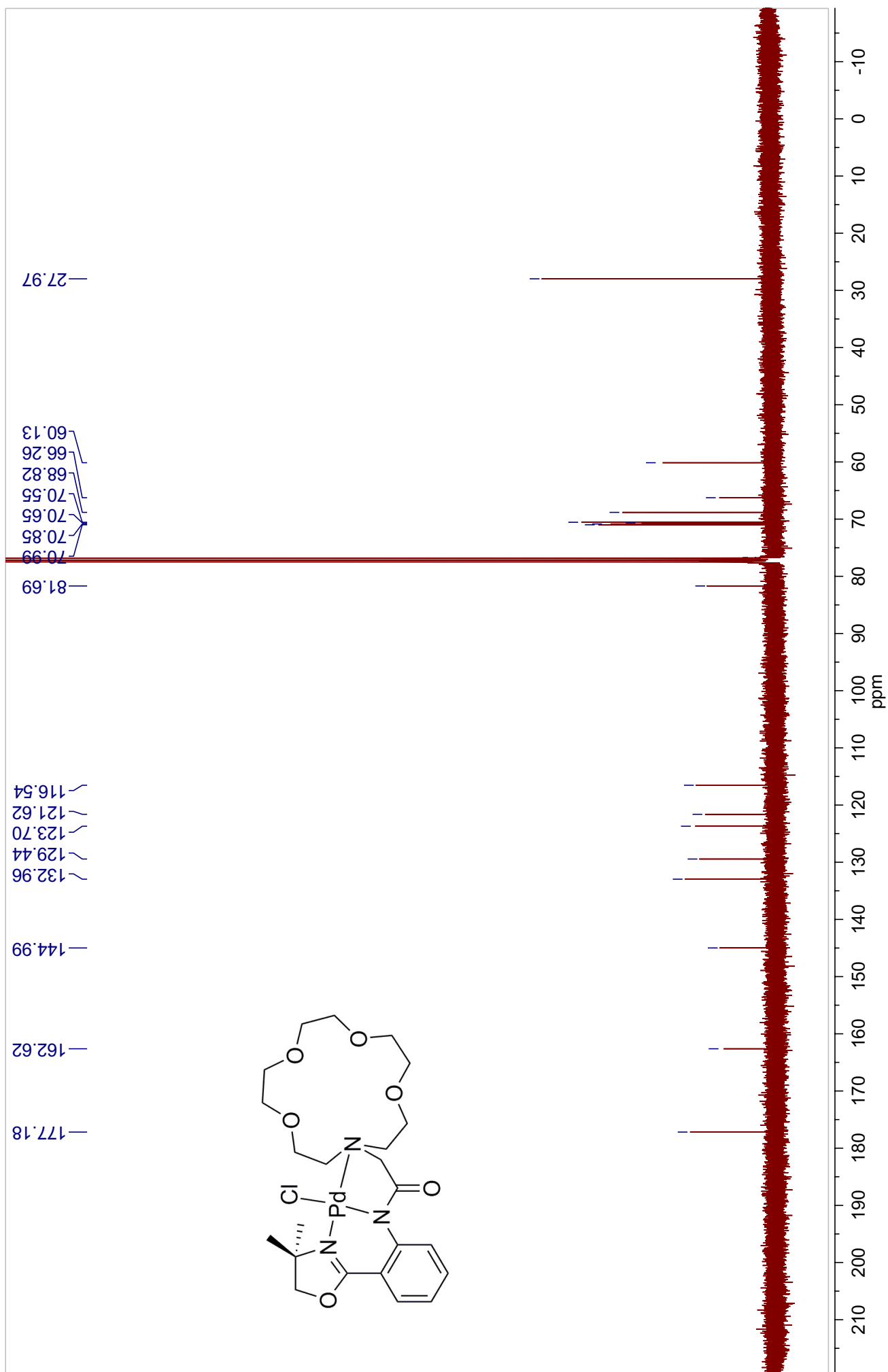


Figure A49. ^1H -NMR Spectrum of **9h** in CDCl_3

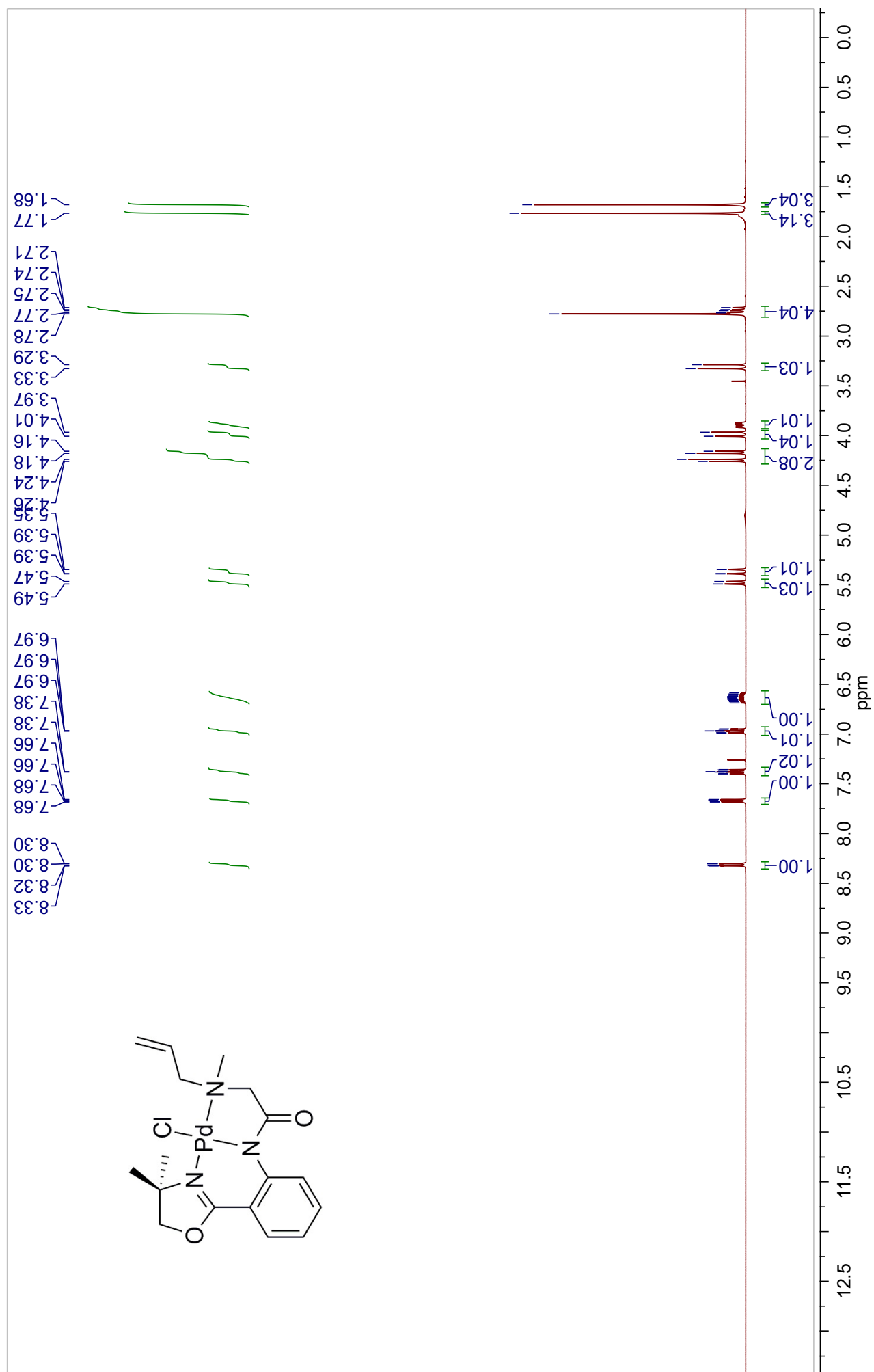


Figure A50. ^{13}C -NMR Spectrum of **9h** in CDCl_3

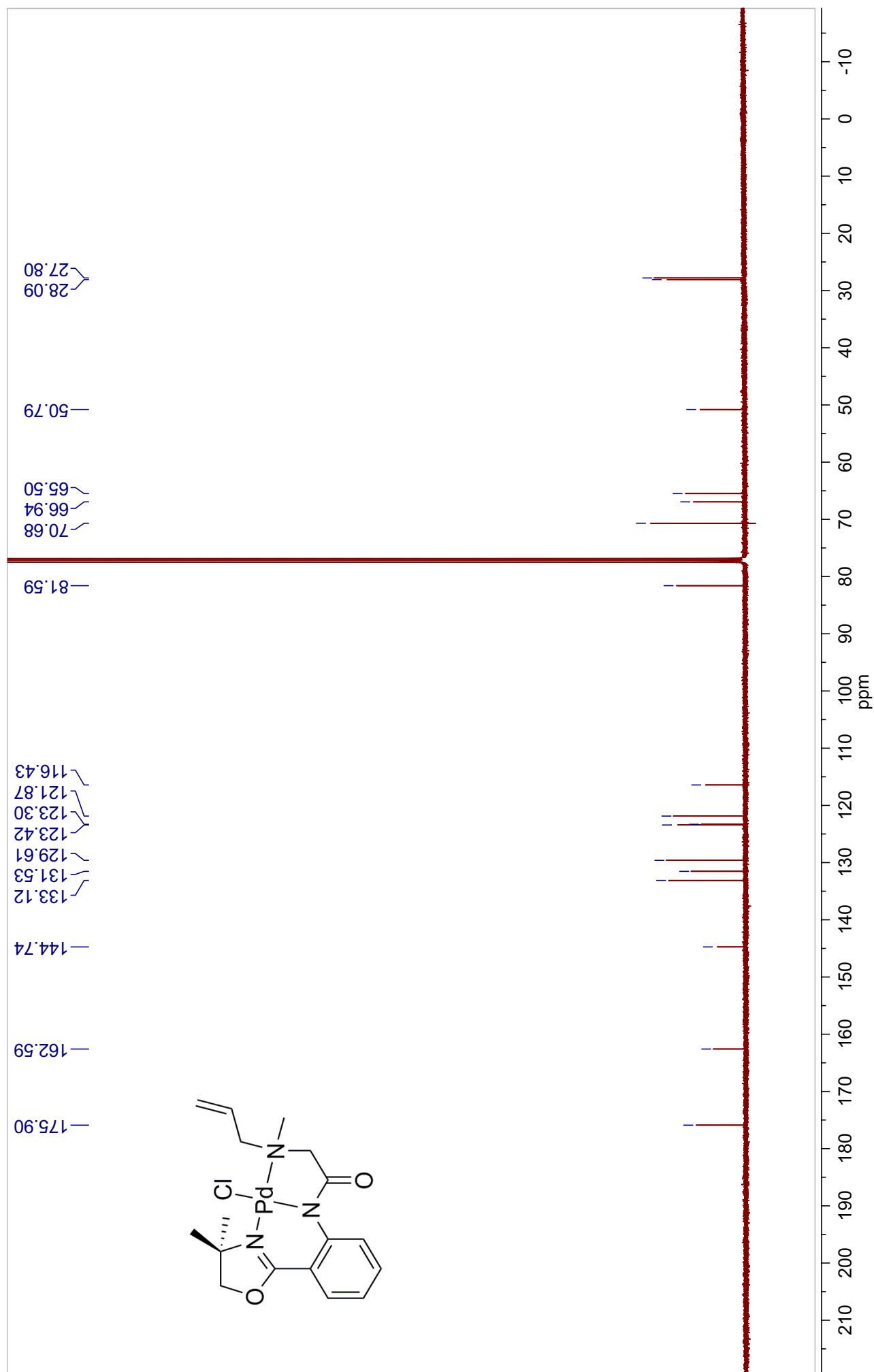


Figure A51. ^1H -NMR Spectrum of **9i** in CDCl_3

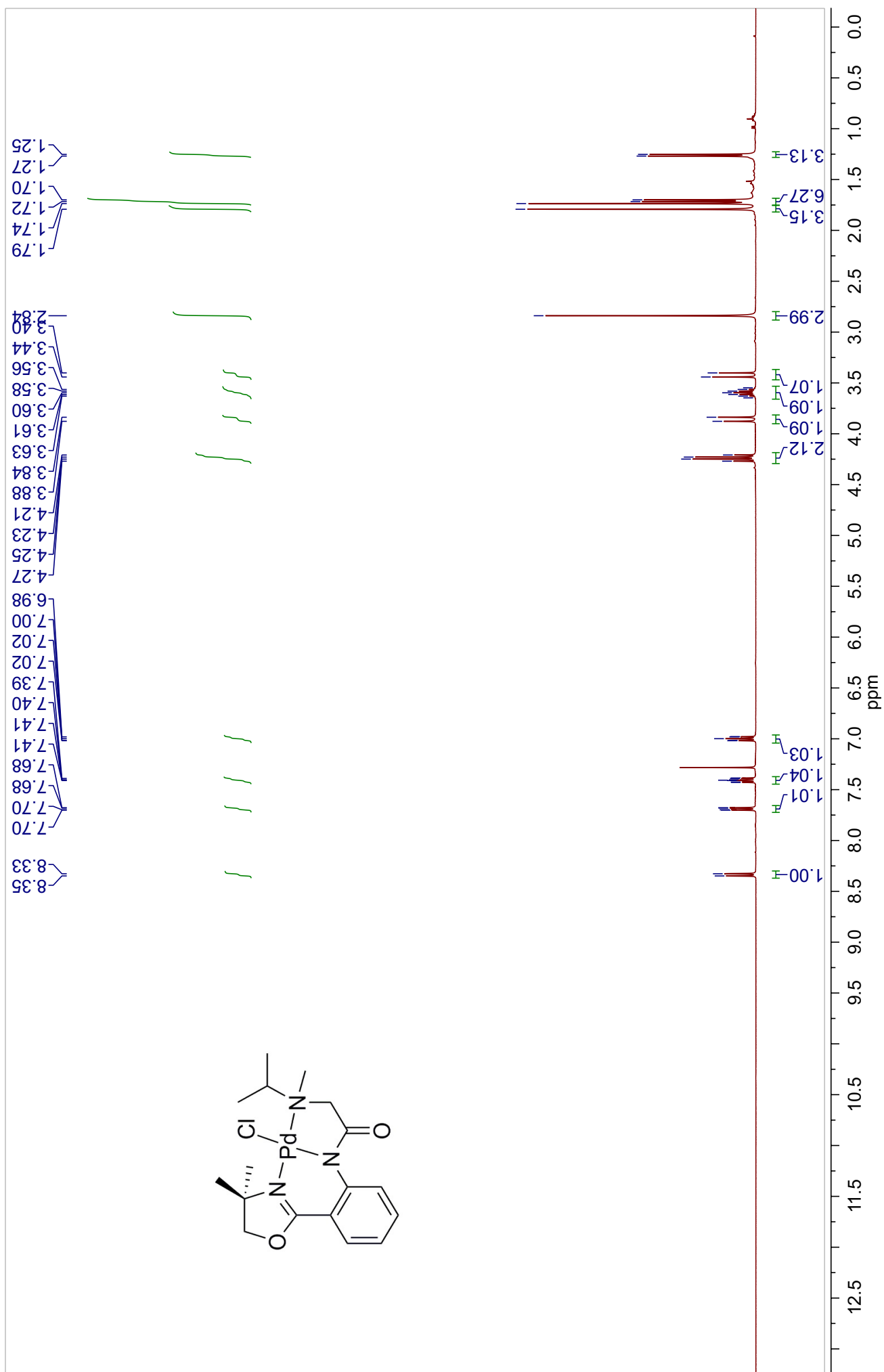


Figure A52. ^{13}C -NMR Spectrum of **9i** in CDCl_3

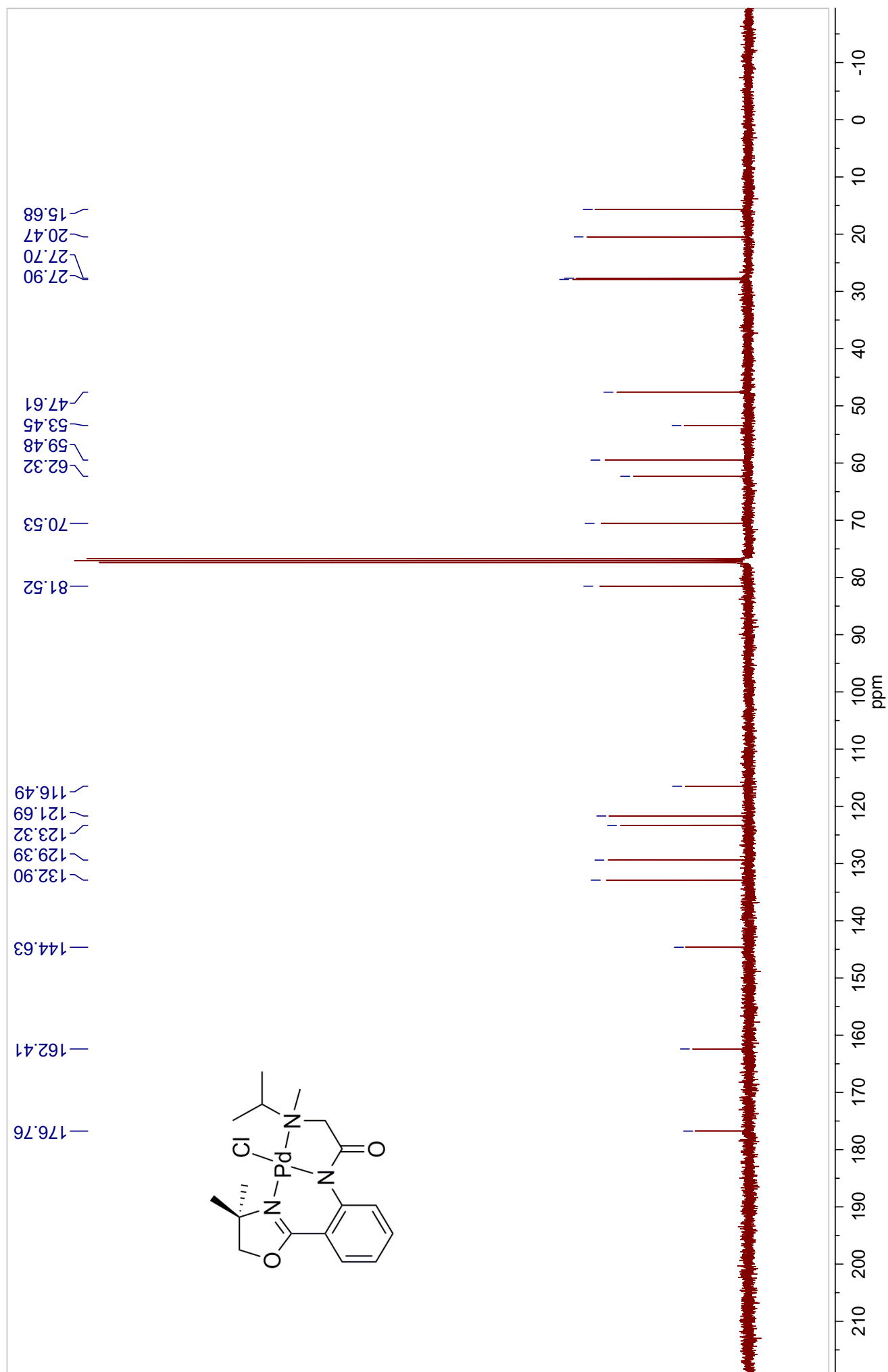


Figure A53. ^1H -NMR Spectrum of **9j** in CDCl_3

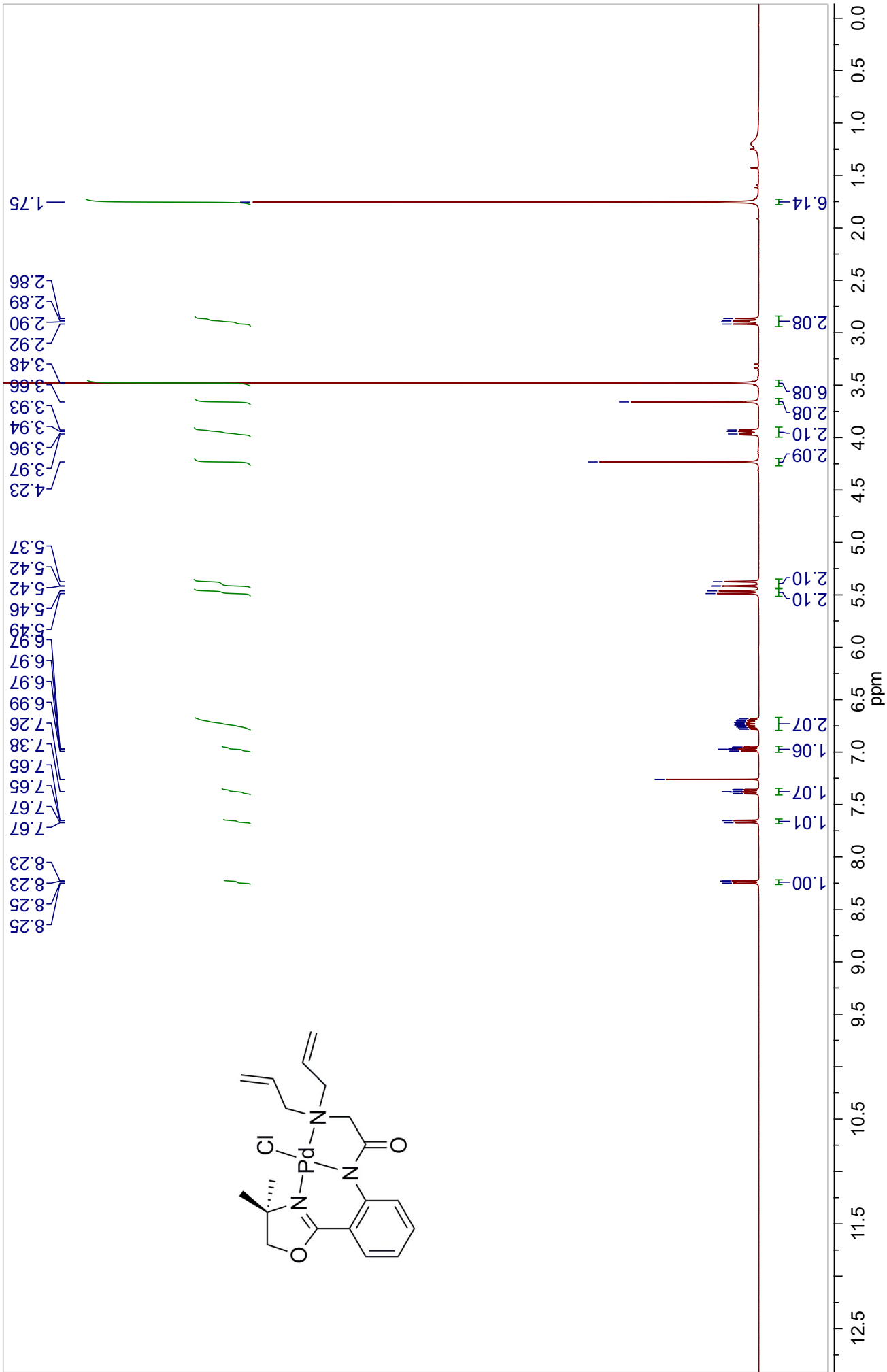


Figure A54. ^{13}C -NMR Spectrum of **9j** in CDCl_3

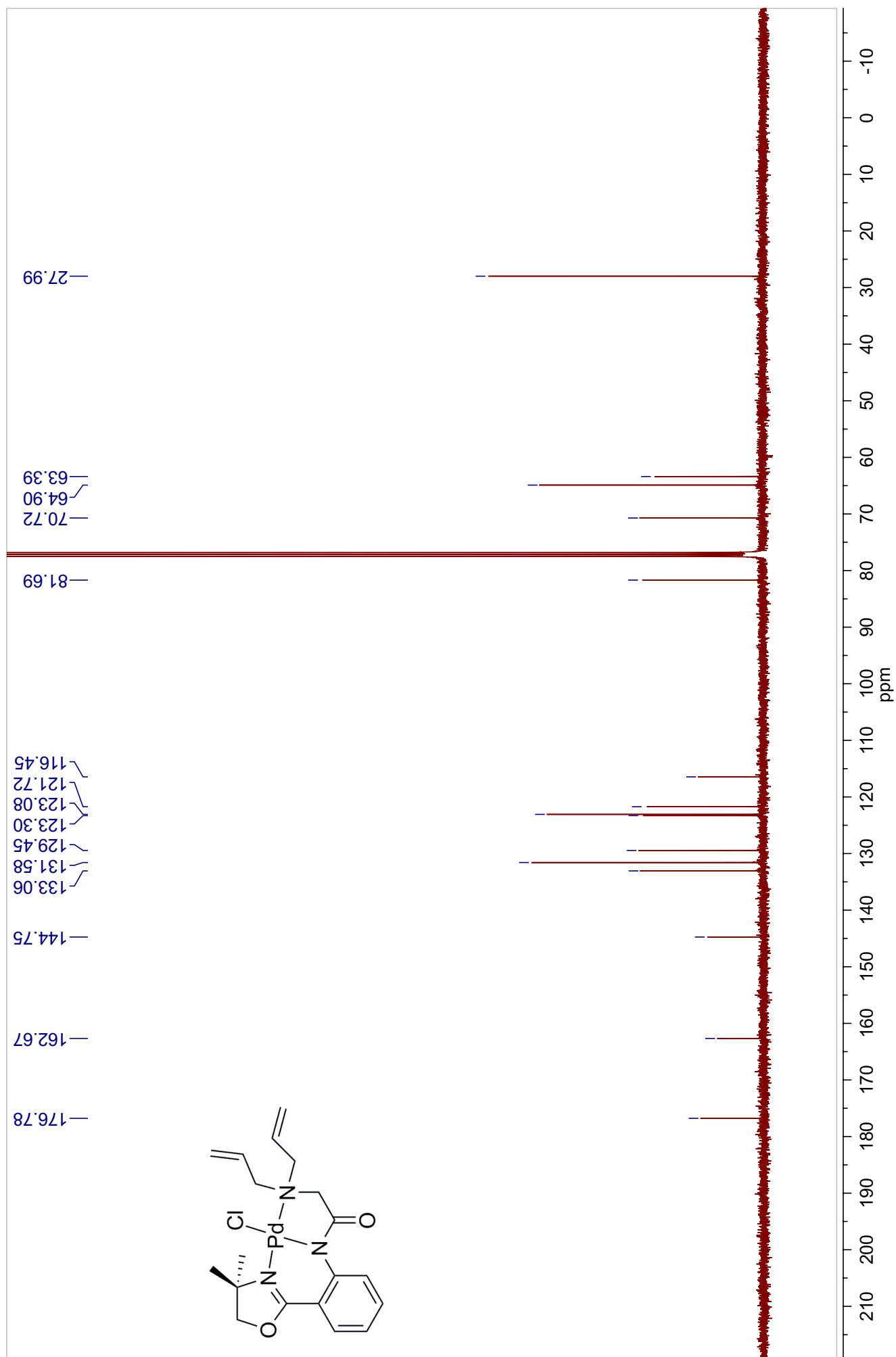


Figure A55. ^1H -NMR Spectrum of **9k** in CDCl_3

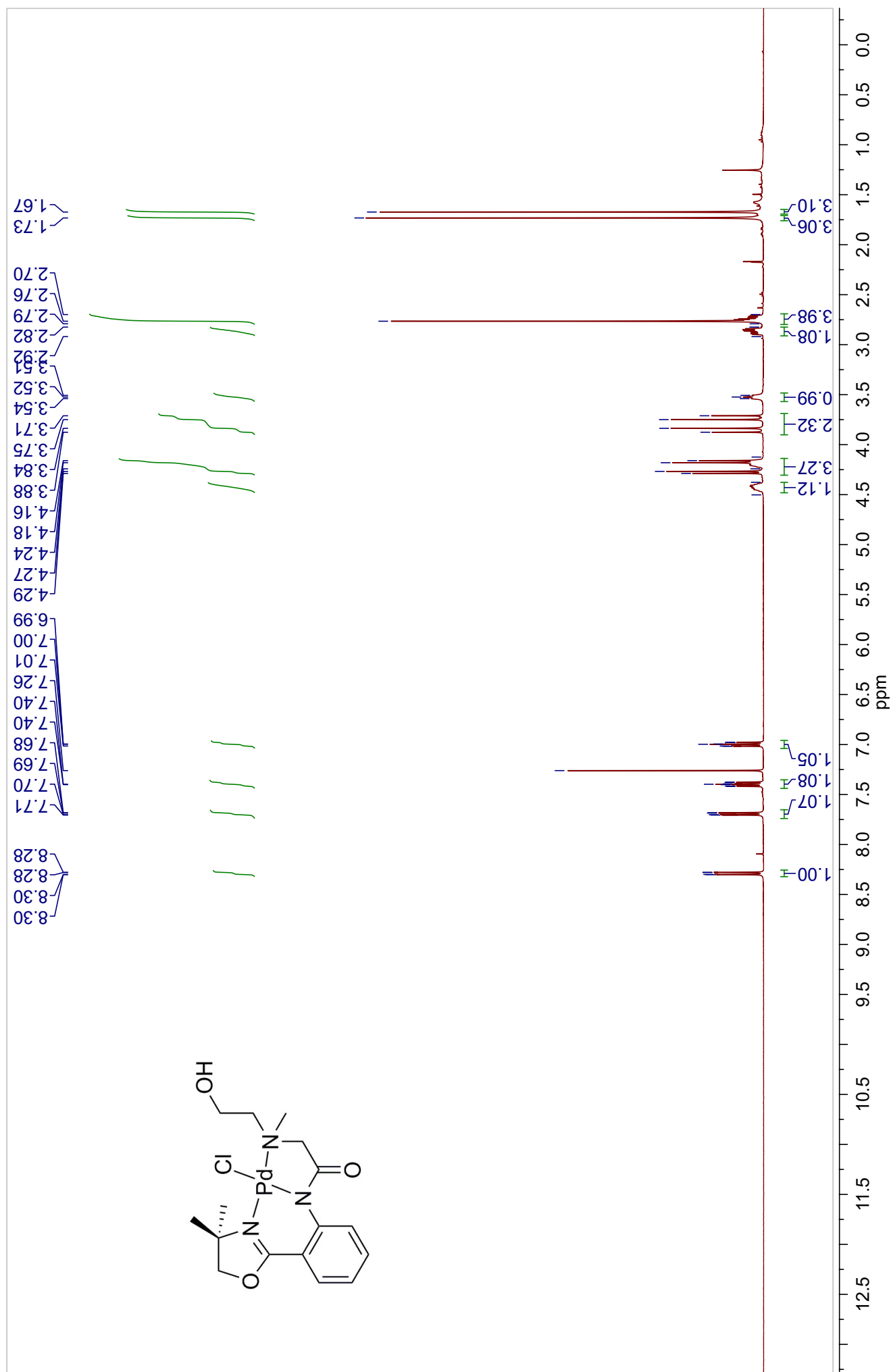
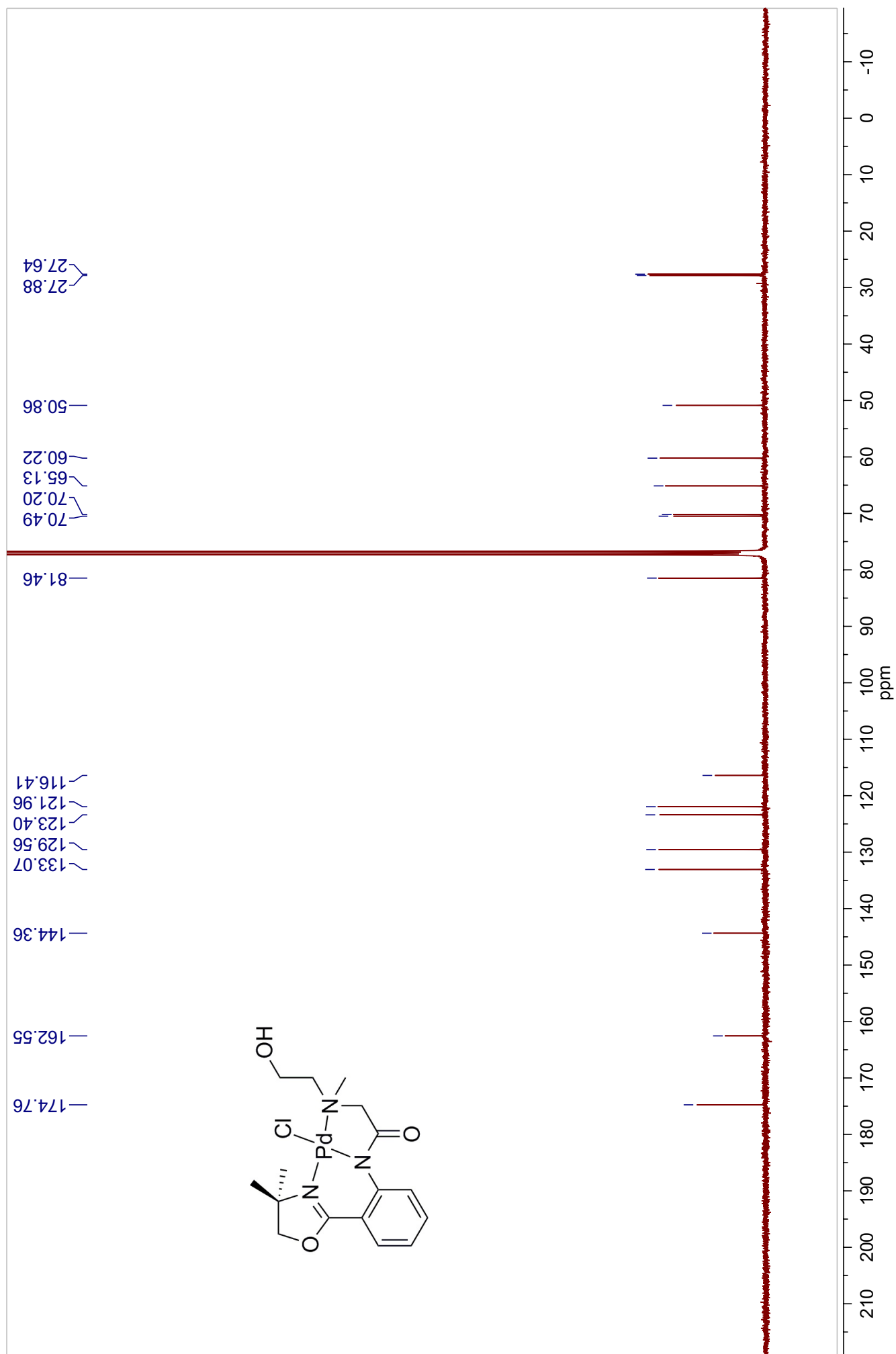


Figure A56. ^{13}C -NMR Spectrum of **9k** in CDCl_3



C[C@H]1CN(C(=O)CCN2C=CCN(C2Cc3ccccc3)C1)c4ccccc4

¹H NMR spectrum (CDCl₃) of compound 10. The x-axis represents chemical shift in ppm from 0.0 to 12.5. The spectrum shows several peaks: a multiplet at 7.24-7.68 ppm (aromatic protons), a multiplet at 5.46-5.76 ppm (CH₂ protons), a multiplet at 4.37-4.51 ppm (CH₂ protons), a multiplet at 1.72-1.79 ppm (CH₃ protons), and a small peak at 3.02 ppm (residual solvent). Integration values are provided for each peak group.

Chemical Shift (ppm)	Integration
7.24-7.68	1.03, 0.95, 0.84, 1.03
5.46-5.76	1.00, 1.05, 0.96
4.37-4.51	1.07, 1.10, 1.02
1.72-1.79	2.72, 3.02

Figure A58. ^{13}C -NMR Spectrum of **9I** in CDCl_3

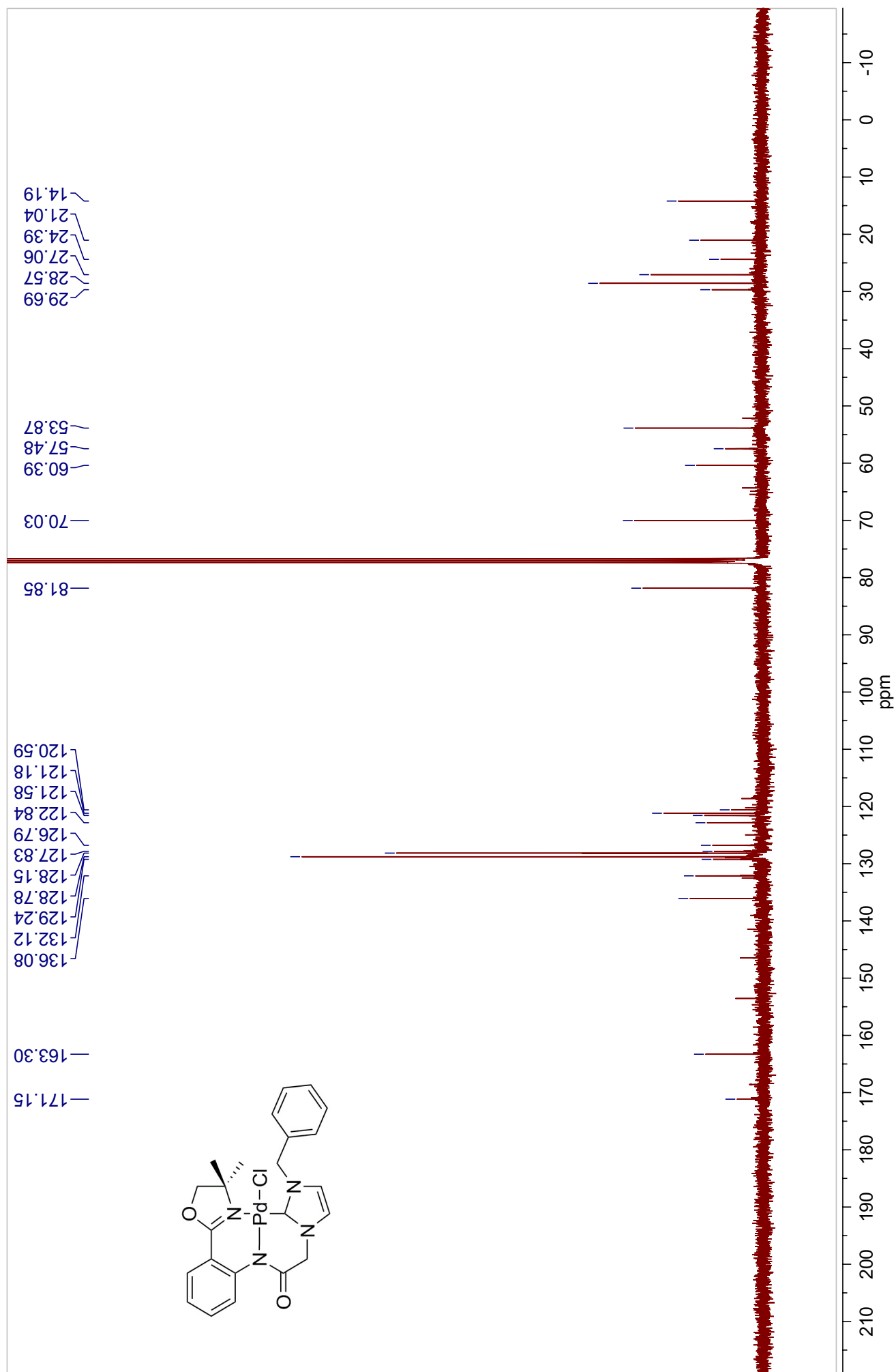


Figure A59. ^1H -NMR Spectrum of **9m** in CDCl_3

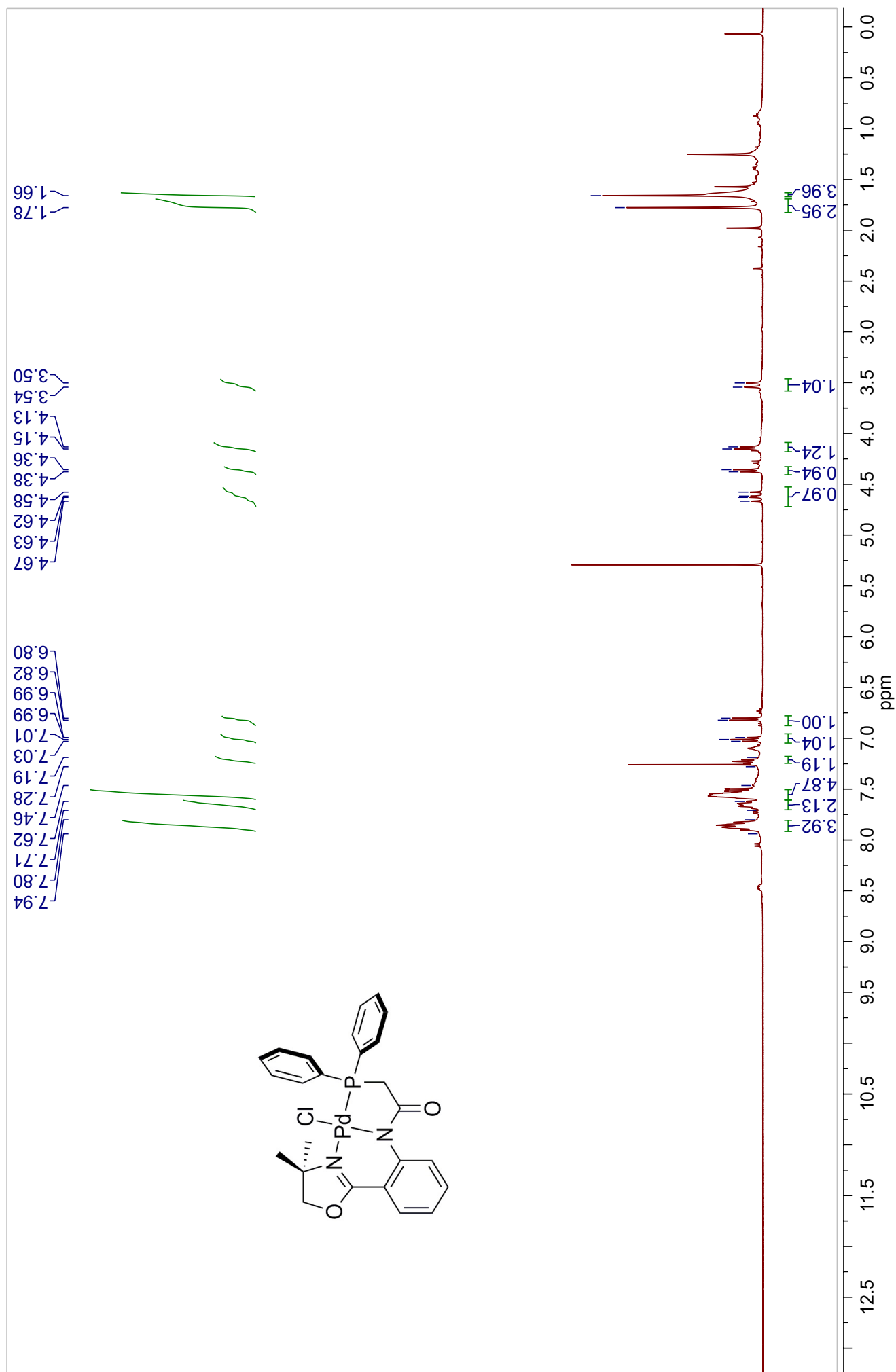
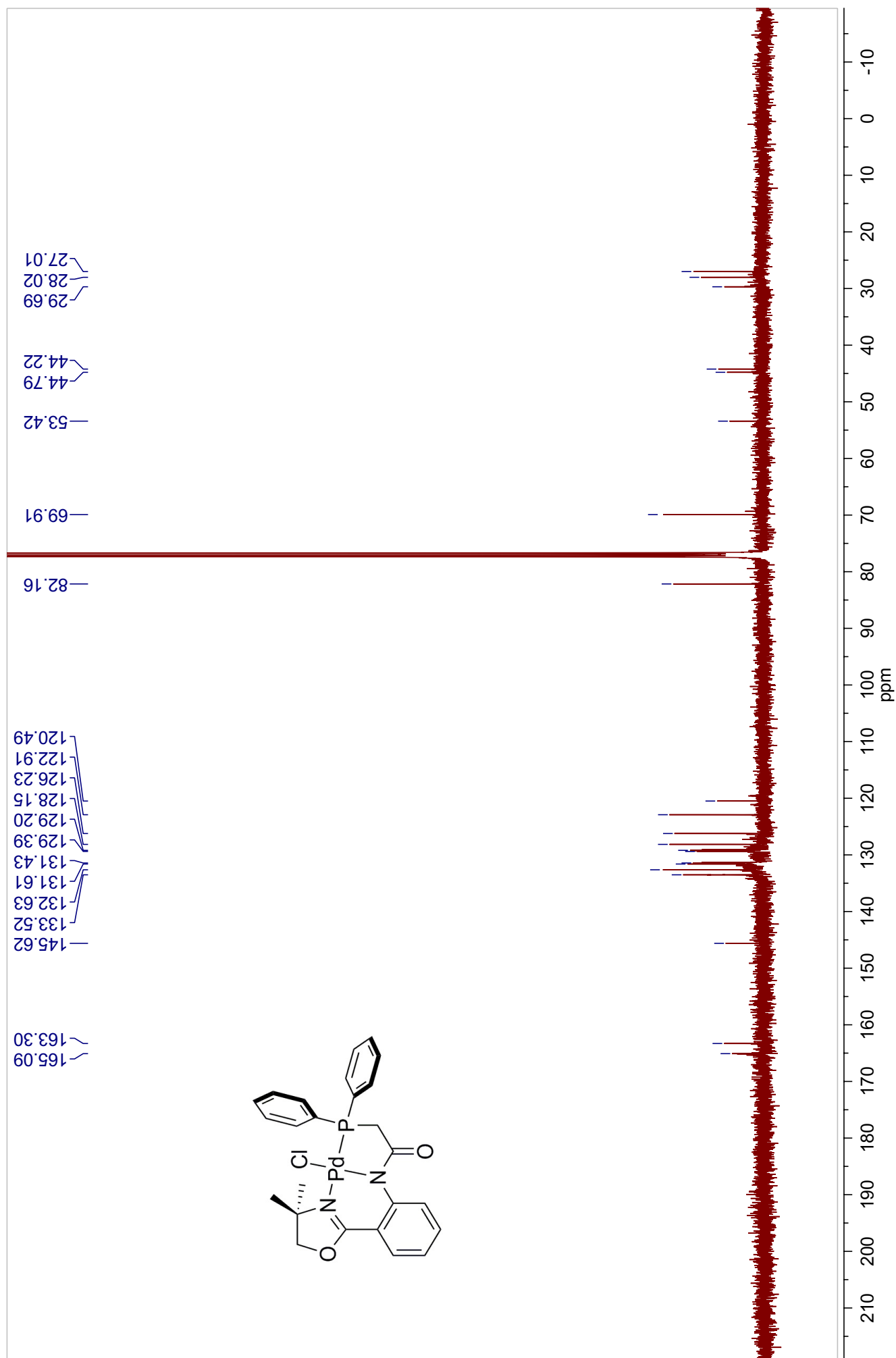
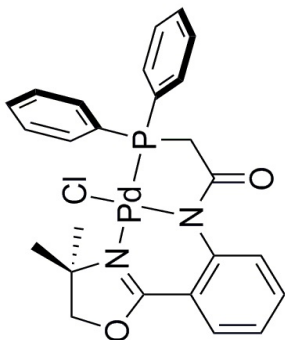


Figure A60. ^{13}C -NMR Spectrum of **9m** in CDCl_3



—50.46



7.2 X-RAY CRYSTALLOGRAPHY DATA

Table A1. Crystal data and structure refinement for **2**.

Table A2. Bond lengths [Å] and angles [°] for **2**.

Table A3. Torsion angles [°] for **2**

Table A4. Hydrogen bonds for **2** [Å and °].

Table A5. Bond lengths [Å] for **3m•oxide**

Table A6. Angles [°] for **3m•oxide**

Table A7. Torsion angles [°] for **3m•oxide**

Table A8. Bond lengths [Å] for **6**

Table A9. Angles [°] for **6**

Table A10. Torsion angles [°] for **6**

Table A11. Bond lengths [Å] for **9a**

Table A12. Angles [°] for **9a**

Table A13. Torsion angles [°] for **9a**

Crystallographic data for **9h** is pending.

Table A1. Crystal data and structure refinement for **2**.

Empirical formula	C13 H15 Cl N2 O2	
Formula weight	266.72	
Temperature	150(1) K	
Wavelength	0.71073 Å	
Crystal system	Triclinic	
Space group	P -1	
Unit cell dimensions	a = 8.3982(12) Å	a = 80.500(3)°.
	b = 8.9541(12) Å	b = 72.754(3)°.
	c = 9.4632(13) Å	g = 71.727(3)°.
Volume	643.31(15) Å ³	
Z	2	
Density (calculated)	1.377 Mg/m ³	
Absorption coefficient	0.293 mm ⁻¹	
F(000)	280	
Crystal size	0.28 x 0.21 x 0.15 mm ³	
Theta range for data collection	2.26 to 26.03°.	
Index ranges	-10 ≤ h ≤ 10, -11 ≤ k ≤ 10, -11 ≤ l ≤ 5	
Reflections collected	4099	
Independent reflections	2464 [R(int) = 0.0190]	
Completeness to theta = 25.24°	97.6 %	
Absorption correction	Semi-empirical from equivalents	
Max. and min. transmission	0.9574 and 0.9226	
Refinement method	Full-matrix least-squares on F ²	
Data / restraints / parameters	2464 / 0 / 169	
Goodness-of-fit on F ²	1.035	
Final R indices [I > 2σ(I)]	R1 = 0.0368, wR2 = 0.0895	
R indices (all data)	R1 = 0.0456, wR2 = 0.0955	
Largest diff. peak and hole	0.261 and -0.288 e.Å ⁻³	

Table A2. Bond lengths [Å] and angles [°] for **2**.

Cl(1)-C(13)	1.7828(17)
O(1)-C(7)	1.3667(19)
O(1)-C(8)	1.4539(19)
O(2)-C(12)	1.218(2)
N(1)-C(12)	1.357(2)
N(1)-C(1)	1.407(2)
N(1)-H(1N)	0.853(19)
N(2)-C(7)	1.268(2)
N(2)-C(9)	1.489(2)
C(1)-C(2)	1.397(2)
C(1)-C(6)	1.415(2)
C(2)-C(3)	1.385(3)
C(2)-H(2A)	0.9500
C(3)-C(4)	1.383(3)
C(3)-H(3A)	0.9500
C(4)-C(5)	1.380(2)
C(4)-H(4A)	0.9500
C(5)-C(6)	1.393(2)
C(5)-H(5A)	0.9500
C(6)-C(7)	1.472(2)
C(8)-C(9)	1.541(2)
C(8)-H(8A)	0.9900
C(8)-H(8B)	0.9900
C(9)-C(11)	1.516(3)
C(9)-C(10)	1.518(3)
C(10)-H(10A)	0.9800
C(10)-H(10B)	0.9800
C(10)-H(10C)	0.9800
C(11)-H(11A)	0.9800
C(11)-H(11B)	0.9800
C(11)-H(11C)	0.9800
C(12)-C(13)	1.510(2)
C(13)-H(13B)	0.9900
C(13)-H(13A)	0.9900

C(7)-O(1)-C(8)	104.67(12)
C(12)-N(1)-C(1)	127.77(14)
C(12)-N(1)-H(1N)	116.4(13)
C(1)-N(1)-H(1N)	115.7(13)
C(7)-N(2)-C(9)	107.79(13)
C(2)-C(1)-N(1)	122.62(15)
C(2)-C(1)-C(6)	118.52(16)
N(1)-C(1)-C(6)	118.86(14)
C(3)-C(2)-C(1)	120.66(16)
C(3)-C(2)-H(2A)	119.7
C(1)-C(2)-H(2A)	119.7
C(4)-C(3)-C(2)	120.81(16)
C(4)-C(3)-H(3A)	119.6
C(2)-C(3)-H(3A)	119.6
C(5)-C(4)-C(3)	119.30(17)
C(5)-C(4)-H(4A)	120.4
C(3)-C(4)-H(4A)	120.4
C(4)-C(5)-C(6)	121.21(16)
C(4)-C(5)-H(5A)	119.4
C(6)-C(5)-H(5A)	119.4
C(5)-C(6)-C(1)	119.49(15)
C(5)-C(6)-C(7)	118.88(14)
C(1)-C(6)-C(7)	121.55(15)
N(2)-C(7)-O(1)	117.67(14)
N(2)-C(7)-C(6)	126.94(14)
O(1)-C(7)-C(6)	115.31(14)
O(1)-C(8)-C(9)	104.49(13)
O(1)-C(8)-H(8A)	110.9
C(9)-C(8)-H(8A)	110.9
O(1)-C(8)-H(8B)	110.9
C(9)-C(8)-H(8B)	110.9
H(8A)-C(8)-H(8B)	108.9
N(2)-C(9)-C(11)	111.07(14)
N(2)-C(9)-C(10)	108.01(14)
C(11)-C(9)-C(10)	111.29(16)
N(2)-C(9)-C(8)	101.67(13)

C(11)-C(9)-C(8)	112.84(16)
C(10)-C(9)-C(8)	111.49(15)
C(9)-C(10)-H(10A)	109.5
C(9)-C(10)-H(10B)	109.5
H(10A)-C(10)-H(10B)	109.5
C(9)-C(10)-H(10C)	109.5
H(10A)-C(10)-H(10C)	109.5
H(10B)-C(10)-H(10C)	109.5
C(9)-C(11)-H(11A)	109.5
C(9)-C(11)-H(11B)	109.5
H(11A)-C(11)-H(11B)	109.5
C(9)-C(11)-H(11C)	109.5
H(11A)-C(11)-H(11C)	109.5
H(11B)-C(11)-H(11C)	109.5
O(2)-C(12)-N(1)	125.94(17)
O(2)-C(12)-C(13)	116.52(15)
N(1)-C(12)-C(13)	117.54(14)
C(12)-C(13)-Cl(1)	117.10(12)
C(12)-C(13)-H(13B)	108.0
Cl(1)-C(13)-H(13B)	108.0
C(12)-C(13)-H(13A)	108.0
Cl(1)-C(13)-H(13A)	108.0
H(13B)-C(13)-H(13A)	107.3

Table A3. Torsion angles [°] for **2**

C(12)-N(1)-C(1)-C(2)	-3.5(3)
C(12)-N(1)-C(1)-C(6)	176.50(16)
N(1)-C(1)-C(2)-C(3)	179.30(17)
C(6)-C(1)-C(2)-C(3)	-0.7(3)
C(1)-C(2)-C(3)-C(4)	-0.6(3)
C(2)-C(3)-C(4)-C(5)	0.9(3)
C(3)-C(4)-C(5)-C(6)	0.0(3)
C(4)-C(5)-C(6)-C(1)	-1.3(2)

C(4)-C(5)-C(6)-C(7)	175.61(15)
C(2)-C(1)-C(6)-C(5)	1.6(2)
N(1)-C(1)-C(6)-C(5)	-178.42(15)
C(2)-C(1)-C(6)-C(7)	-175.18(15)
N(1)-C(1)-C(6)-C(7)	4.8(2)
C(9)-N(2)-C(7)-O(1)	-3.8(2)
C(9)-N(2)-C(7)-C(6)	172.90(15)
C(8)-O(1)-C(7)-N(2)	-9.1(2)
C(8)-O(1)-C(7)-C(6)	173.84(14)
C(5)-C(6)-C(7)-N(2)	-161.25(17)
C(1)-C(6)-C(7)-N(2)	15.6(3)
C(5)-C(6)-C(7)-O(1)	15.5(2)
C(1)-C(6)-C(7)-O(1)	-167.67(15)
C(7)-O(1)-C(8)-C(9)	17.04(17)
C(7)-N(2)-C(9)-C(11)	134.32(17)
C(7)-N(2)-C(9)-C(10)	-103.38(17)
C(7)-N(2)-C(9)-C(8)	14.04(18)
O(1)-C(8)-C(9)-N(2)	-18.69(17)
O(1)-C(8)-C(9)-C(11)	-137.72(15)
O(1)-C(8)-C(9)-C(10)	96.18(16)
C(1)-N(1)-C(12)-O(2)	-2.8(3)
C(1)-N(1)-C(12)-C(13)	177.11(15)
O(2)-C(12)-C(13)-Cl(1)	-178.63(13)
N(1)-C(12)-C(13)-Cl(1)	1.5(2)

Table A4. Hydrogen bonds for **2** [Å and °].

D-H...A	d(D-H)	d(H...A)	d(D...A)	<(DHA)
N(1)-H(1N)...N(2)	0.853(19)	2.03(2)	2.732(2)	138.9(17)
N(1)-H(1N)...Cl(1)	0.853(19)	2.468(19)	2.9746(15)	118.9(16)

Table A5. Bond lengths [Å] for **3m•oxide**

C1	H1A	0.970(2)
C1	H1B	0.971(1)
C1	C2	1.517(2)
C1	P1	1.816(2)
C2	N1	1.351(2)
C2	O2	1.227(2)
C3	C4	1.398(3)
C3	C8	1.409(2)
C3	N1	1.405(2)
C4	H4	0.930(2)
C4	C5	1.384(3)
C5	H5	0.930(2)
C5	C6	1.384(3)
C6	H6	0.930(2)
C6	C7	1.382(3)
C7	H7	0.931(2)
C7	C8	1.393(3)
C8	C9	1.472(3)
C9	N2	1.256(3)
C9	O3	1.324(4)
C10	H10A	0.970(3)
C10	H10B	0.970(4)
C10	C11	1.532(5)
C10	O3	1.450(5)
C11	C12	1.498(4)
C11	C13	1.504(3)
C11	N2	1.471(3)
C12	H12A	0.959(3)
C12	H12B	0.960(4)
C12	H12C	0.960(3)
C13	H13A	0.960(3)
C13	H13B	0.960(3)
C13	H13C	0.961(3)
C20	C21	1.396(2)
C20	C25	1.397(2)
C20	P1	1.804(2)
C21	H21	0.930(1)
C21	C22	1.387(3)
C22	H22	0.930(2)
C22	C23	1.384(2)
C23	H23	0.930(2)

C23	C24	1.386(3)
C24	H24	0.930(1)
C24	C25	1.387(3)
C25	H25	0.930(2)
C30	C31	1.393(2)
C30	C35	1.396(2)
C30	P1	1.803(2)
C31	H31	0.930(2)
C31	C32	1.387(3)
C32	H32	0.930(2)
C32	C33	1.383(2)
C33	H33	0.930(2)
C33	C34	1.388(2)
C34	H34	0.930(2)
C34	C35	1.383(3)
C35	H35	0.930(2)
N1	H1	0.87(2)
O1	P1	1.489(1)
O40	H40A	0.91(2)
O40	H40B	0.92(2)

Table A6. Angles [°] for **3m•oxide**

H1A	C1	H1B	107.9(2)
H1A	C1	C2	109.1(1)
H1A	C1	P1	109.1(1)
H1B	C1	C2	109.1(1)
H1B	C1	P1	109.1(1)
C2	C1	P1	112.5(1)
C1	C2	N1	113.7(1)
C1	C2	O2	121.2(1)
N1	C2	O2	125.1(1)
C4	C3	C8	119.2(1)
C4	C3	N1	123.5(1)
C8	C3	N1	117.3(1)
C3	C4	H4	119.9(2)
C3	C4	C5	120.3(2)
H4	C4	C5	119.8(2)
C4	C5	H5	119.7(2)
C4	C5	C6	120.5(2)
H5	C5	C6	119.8(2)
C5	C6	H6	120.1(2)

C5	C6	C7	119.8(2)
H6	C6	C7	120.1(2)
C6	C7	H7	119.5(2)
C6	C7	C8	120.9(2)
H7	C7	C8	119.6(2)
C3	C8	C7	119.3(2)
C3	C8	C9	121.9(2)
C7	C8	C9	118.7(2)
C8	C9	N2	127.8(2)
C8	C9	O3	115.3(2)
N2	C9	O3	116.9(2)
H10A	C10	H10B	108.9(4)
H10A	C10	C11	110.9(3)
H10A	C10	O3	110.9(3)
H10B	C10	C11	110.9(3)
H10B	C10	O3	110.9(3)
C11	C10	O3	104.2(3)
C10	C11	C12	113.4(2)
C10	C11	C13	111.6(2)
C10	C11	N2	102.2(2)
C12	C11	C13	110.2(2)
C12	C11	N2	109.9(2)
C13	C11	N2	109.2(2)
C11	C12	H12A	109.5(3)
C11	C12	H12B	109.4(3)
C11	C12	H12C	109.5(3)
H12A	C12	H12B	109.5(3)
H12A	C12	H12C	109.5(3)
H12B	C12	H12C	109.5(3)
C11	C13	H13A	109.5(2)
C11	C13	H13B	109.5(2)
C11	C13	H13C	109.4(2)
H13A	C13	H13B	109.5(3)
H13A	C13	H13C	109.5(3)
H13B	C13	H13C	109.4(3)
C21	C20	C25	119.3(1)
C21	C20	P1	117.7(1)
C25	C20	P1	122.9(1)
C20	C21	H21	119.9(2)
C20	C21	C22	120.1(2)
H21	C21	C22	120.0(2)
C21	C22	H22	119.9(2)
C21	C22	C23	120.2(2)

H22	C22	C23	119.9(2)
C22	C23	H23	120.0(2)
C22	C23	C24	120.1(2)
H23	C23	C24	119.9(2)
C23	C24	H24	120.0(2)
C23	C24	C25	120.2(2)
H24	C24	C25	119.9(2)
C20	C25	C24	120.1(2)
C20	C25	H25	119.9(2)
C24	C25	H25	120.0(2)
C31	C30	C35	119.4(2)
C31	C30	P1	118.4(1)
C35	C30	P1	122.2(1)
C30	C31	H31	120.0(2)
C30	C31	C32	120.0(2)
H31	C31	C32	120.0(2)
C31	C32	H32	119.8(2)
C31	C32	C33	120.3(2)
H32	C32	C33	119.9(2)
C32	C33	H33	120.0(2)
C32	C33	C34	120.0(2)
H33	C33	C34	120.0(2)
C33	C34	H34	120.0(2)
C33	C34	C35	120.0(2)
H34	C34	C35	120.0(2)
C30	C35	C34	120.3(2)
C30	C35	H35	119.8(2)
C34	C35	H35	119.9(2)
C2	N1	C3	129.2(1)
C2	N1	H1	118(1)
C3	N1	H1	112(1)
C9	N2	C11	109.5(2)
C9	O3	C10	107.2(3)
C1	P1	C20	104.28(7)
C1	P1	C30	108.06(8)
C1	P1	O1	112.64(7)
C20	P1	C30	106.33(7)
C20	P1	O1	113.09(7)
C30	P1	O1	111.92(7)
H40A	O40	H40B	103(2)

Table A7. Torsion angles [°] for **3m•oxide**

H1A	C1	C2	N1	-15.8(2)
H1A	C1	C2	O2	163.0(1)
H1B	C1	C2	N1	-133.4(2)
H1B	C1	C2	O2	45.4(2)
P1	C1	C2	N1	105.4(1)
P1	C1	C2	O2	-75.8(2)
H1A	C1	P1	C20	-57.7(1)
H1A	C1	P1	C30	-170.5(1)
H1A	C1	P1	O1	65.3(1)
H1B	C1	P1	C20	59.9(1)
H1B	C1	P1	C30	-52.9(1)
H1B	C1	P1	O1	-177.1(1)
C2	C1	P1	C20	-178.9(1)
C2	C1	P1	C30	68.3(1)
C2	C1	P1	O1	-55.9(1)
C1	C2	N1	C3	174.1(2)
C1	C2	N1	H1	-3(1)
O2	C2	N1	C3	-4.6(3)
O2	C2	N1	H1	179(1)
C8	C3	C4	H4	178.8(2)
C8	C3	C4	C5	-1.2(2)
N1	C3	C4	H4	-1.6(3)
N1	C3	C4	C5	178.4(2)
C4	C3	C8	C7	1.2(2)
C4	C3	C8	C9	179.4(2)
N1	C3	C8	C7	-178.5(2)
N1	C3	C8	C9	-0.3(2)
C4	C3	N1	C2	9.8(3)
C4	C3	N1	H1	-173(1)
C8	C3	N1	C2	-170.5(2)
C8	C3	N1	H1	6(1)
C3	C4	C5	H5	-179.6(2)
C3	C4	C5	C6	0.3(3)
H4	C4	C5	H5	0.4(3)
H4	C4	C5	C6	-179.7(2)
C4	C5	C6	H6	-179.5(2)
C4	C5	C6	C7	0.6(3)
H5	C5	C6	H6	0.5(3)
H5	C5	C6	C7	-179.4(2)
C5	C6	C7	H7	179.3(2)
C5	C6	C7	C8	-0.7(3)

H6	C6	C7	H7	-0.6(3)
H6	C6	C7	C8	179.4(2)
C6	C7	C8	C3	-0.2(3)
C6	C7	C8	C9	-178.5(2)
H7	C7	C8	C3	179.8(2)
H7	C7	C8	C9	1.4(3)
C3	C8	C9	N2	-6.3(3)
C3	C8	C9	O3	175.7(2)
C7	C8	C9	N2	171.9(2)
C7	C8	C9	O3	-6.0(3)
C8	C9	N2	C11	-178.6(2)
O3	C9	N2	C11	-0.7(3)
C8	C9	O3	C10	178.8(2)
N2	C9	O3	C10	0.6(3)
H10A	C10	C11	C12	1.1(4)
H10A	C10	C11	C13	-124.1(3)
H10A	C10	C11	N2	119.3(3)
H10B	C10	C11	C12	122.3(3)
H10B	C10	C11	C13	-2.9(4)
H10B	C10	C11	N2	-119.5(3)
O3	C10	C11	C12	-118.3(3)
O3	C10	C11	C13	116.5(3)
O3	C10	C11	N2	-0.1(3)
H10A	C10	O3	C9	-119.7(3)
H10B	C10	O3	C9	119.1(3)
C11	C10	O3	C9	-0.3(3)
C10	C11	C12	H12A	-68.7(4)
C10	C11	C12	H12B	171.3(3)
C10	C11	C12	H12C	51.4(4)
C13	C11	C12	H12A	57.3(3)
C13	C11	C12	H12B	-62.7(3)
C13	C11	C12	H12C	177.4(3)
N2	C11	C12	H12A	177.7(2)
N2	C11	C12	H12B	57.7(3)
N2	C11	C12	H12C	-62.3(3)
C10	C11	C13	H13A	66.8(3)
C10	C11	C13	H13B	-53.2(3)
C10	C11	C13	H13C	-173.2(2)
C12	C11	C13	H13A	-60.2(3)
C12	C11	C13	H13B	179.8(2)
C12	C11	C13	H13C	59.9(3)
N2	C11	C13	H13A	179.0(2)
N2	C11	C13	H13B	59.0(3)

N2	C11	C13	H13C	-60.9(3)
C10	C11	N2	C9	0.4(2)
C12	C11	N2	C9	121.1(2)
C13	C11	N2	C9	-117.9(2)
C25	C20	C21	H21	-179.7(2)
C25	C20	C21	C22	0.4(2)
P1	C20	C21	H21	-2.0(2)
P1	C20	C21	C22	178.0(1)
C21	C20	C25	C24	-0.1(2)
C21	C20	C25	H25	179.9(2)
P1	C20	C25	C24	-177.5(1)
P1	C20	C25	H25	2.5(3)
C21	C20	P1	C1	144.4(1)
C21	C20	P1	C30	-101.5(1)
C21	C20	P1	O1	21.7(2)
C25	C20	P1	C1	-38.1(2)
C25	C20	P1	C30	76.0(2)
C25	C20	P1	O1	-160.8(1)
C20	C21	C22	H22	179.7(2)
C20	C21	C22	C23	-0.3(3)
H21	C21	C22	H22	-0.3(3)
H21	C21	C22	C23	179.7(2)
C21	C22	C23	H23	180.0(2)
C21	C22	C23	C24	-0.0(3)
H22	C22	C23	H23	-0.0(3)
H22	C22	C23	C24	180.0(2)
C22	C23	C24	H24	-179.6(2)
C22	C23	C24	C25	0.3(3)
H23	C23	C24	H24	0.4(3)
H23	C23	C24	C25	-179.7(2)
C23	C24	C25	C20	-0.3(3)
C23	C24	C25	H25	179.7(2)
H24	C24	C25	C20	179.7(2)
H24	C24	C25	H25	-0.3(3)
C35	C30	C31	H31	179.8(2)
C35	C30	C31	C32	-0.2(3)
P1	C30	C31	H31	3.3(3)
P1	C30	C31	C32	-176.6(1)
C31	C30	C35	C34	0.3(3)
C31	C30	C35	H35	-179.7(2)
P1	C30	C35	C34	176.7(1)
P1	C30	C35	H35	-3.3(2)
C31	C30	P1	C1	-132.0(1)

C31	C30	P1	C20	116.5(1)
C31	C30	P1	O1	-7.4(2)
C35	C30	P1	C1	51.6(2)
C35	C30	P1	C20	-59.8(2)
C35	C30	P1	O1	176.2(1)
C30	C31	C32	H32	-180.0(2)
C30	C31	C32	C33	0.0(3)
H31	C31	C32	H32	0.1(3)
H31	C31	C32	C33	-180.0(2)
C31	C32	C33	H33	180.0(2)
C31	C32	C33	C34	-0.0(3)
H32	C32	C33	H33	-0.0(3)
H32	C32	C33	C34	180.0(2)
C32	C33	C34	H34	-179.7(2)
C32	C33	C34	C35	0.2(3)
H33	C33	C34	H34	0.3(3)
H33	C33	C34	C35	-179.8(2)
C33	C34	C35	C30	-0.4(3)
C33	C34	C35	H35	179.6(2)
H34	C34	C35	C30	179.5(2)
H34	C34	C35	H35	-0.5(3)

Table A8. Bond lengths [Å] for **6**

Cl1	C17	1.782(3)
N1	HN1	0.879(2)
N1	C11	1.408(3)
N1	C16	1.354(3)
C10	C18	1.470(3)
C10	C11	1.415(3)
C10	C15	1.397(3)
O1	C16	1.218(3)
O2	C18	1.360(3)
O2	C8	1.456(3)
C18	N2	1.279(3)
C11	C12	1.398(3)
C16	C17	1.518(3)
C15	H15	0.950(3)
C15	C14	1.379(4)
N2	C9	1.477(3)

C5	C9	1.493(3)
C5	C6	1.387(3)
C5	C4	1.387(4)
C9	H9	1.000(3)
C9	C8	1.548(4)
C6	C1	1.386(4)
C6	C7	1.510(4)
C13	H13	0.949(3)
C13	C12	1.386(3)
C13	C14	1.378(4)
C12	H12	0.950(2)
C1	H1	0.950(3)
C1	C2	1.385(4)
C3	H3	0.950(3)
C3	C2	1.388(4)
C3	C4	1.391(4)
C14	H14	0.950(3)
C17	H17A	0.990(2)
C17	H17B	0.990(3)
C8	H8	1.000(2)
C8	C7	1.537(4)
C7	H7A	0.990(3)
C7	H7B	0.990(3)
C2	H2	0.949(3)
C4	H4	0.950(3)

Table A9. Select angles [°] for **6**

HN1	N1	C11	116.6(2)
HN1	N1	C16	116.7(2)
C11	N1	C16	126.7(2)
C18	C10	C11	122.4(2)
C18	C10	C15	118.2(2)
C11	C10	C15	119.4(2)
C18	O2	C8	106.5(2)
C10	C18	O2	115.4(2)
C10	C18	N2	126.7(2)
O2	C18	N2	117.9(2)
N1	C11	C10	118.8(2)
N1	C11	C12	122.6(2)

C10	C11	C12	118.6(2)
N1	C16	O1	125.8(2)
N1	C16	C17	118.1(2)
O1	C16	C17	116.1(2)
C10	C15	H15	119.4(2)
C10	C15	C14	121.0(2)
H15	C15	C14	119.6(2)
C18	N2	C9	107.4(2)
C9	C5	C6	111.5(2)
C9	C5	C4	128.3(2)
C6	C5	C4	120.2(2)
N2	C9	C5	113.0(2)
N2	C9	H9	111.5(2)
N2	C9	C8	104.2(2)
C5	C9	H9	111.4(2)
C5	C9	C8	104.8(2)
H9	C9	C8	111.4(2)
C5	C6	C1	120.4(2)
C5	C6	C7	111.6(2)
C1	C6	C7	128.0(2)
H13	C13	C12	119.5(2)
H13	C13	C14	119.5(3)
C12	C13	C14	121.0(2)
C11	C12	C13	120.4(2)
C11	C12	H12	119.8(2)
C13	C12	H12	119.8(2)
C6	C1	H1	120.6(3)
C6	C1	C2	118.9(2)
H1	C1	C2	120.5(3)
H3	C3	C2	120.5(3)
H3	C3	C4	120.5(3)
C2	C3	C4	119.0(3)
C15	C14	C13	119.5(2)
C15	C14	H14	120.2(3)
C13	C14	H14	120.3(3)
Cl1	C17	C16	116.5(2)
Cl1	C17	H17A	108.2(2)
Cl1	C17	H17B	108.2(2)
C16	C17	H17A	108.2(2)
C16	C17	H17B	108.1(2)
H17A	C17	H17B	107.3(2)
O2	C8	C9	103.9(2)
O2	C8	H8	111.2(2)

O2	C8	C7	111.5(2)
C9	C8	H8	111.2(2)
C9	C8	C7	107.6(2)
H8	C8	C7	111.2(2)
C6	C7	C8	104.4(2)
C6	C7	H7A	110.9(2)
C6	C7	H7B	110.9(2)
C8	C7	H7A	110.9(2)
C8	C7	H7B	110.9(2)
H7A	C7	H7B	108.9(2)
C1	C2	C3	121.5(3)
C1	C2	H2	119.3(3)
C3	C2	H2	119.2(3)
C5	C4	C3	120.0(2)
C5	C4	H4	120.0(3)
C3	C4	H4	120.0(3)

Table A10. Select torsion angles [°] for **6**

HN1	N1	C11	C10	-7.3(3)
HN1	N1	C11	C12	172.0(2)
C16	N1	C11	C10	172.7(2)
C16	N1	C11	C12	-7.9(4)
HN1	N1	C16	O1	-179.0(2)
HN1	N1	C16	C17	2.1(3)
C11	N1	C16	O1	1.0(4)
C11	N1	C16	C17	-177.9(2)
C11	C10	C18	O2	-169.4(2)
C11	C10	C18	N2	11.8(4)
C15	C10	C18	O2	12.0(3)
C15	C10	C18	N2	-166.8(2)
C18	C10	C11	N1	1.0(3)
C18	C10	C11	C12	-178.4(2)
C15	C10	C11	N1	179.6(2)
C15	C10	C11	C12	0.2(3)
C18	C10	C15	H15	-1.6(4)
C18	C10	C15	C14	178.5(2)
C11	C10	C15	H15	179.8(2)
C11	C10	C15	C14	-0.1(4)
C8	O2	C18	C10	179.1(2)

C8	O2	C18	N2	-2.0(3)
C18	O2	C8	C9	3.4(2)
C18	O2	C8	H8	123.1(2)
C18	O2	C8	C7	-112.2(2)
C10	C18	N2	C9	178.3(2)
O2	C18	N2	C9	-0.6(3)
N1	C11	C12	C13	-179.6(2)
N1	C11	C12	H12	0.4(4)
C10	C11	C12	C13	-0.3(3)
C10	C11	C12	H12	179.7(2)
N1	C16	C17	Cl1	-5.1(3)
N1	C16	C17	H17A	-127.1(2)
N1	C16	C17	H17B	116.9(2)
O1	C16	C17	Cl1	175.9(2)
O1	C16	C17	H17A	53.9(3)
O1	C16	C17	H17B	-62.1(3)
C10	C15	C14	C13	0.1(4)
C10	C15	C14	H14	-179.9(2)
H15	C15	C14	C13	-179.8(2)
H15	C15	C14	H14	0.1(4)
C18	N2	C9	C5	115.9(2)
C18	N2	C9	H9	-117.6(2)
C18	N2	C9	C8	2.7(2)
C6	C5	C9	N2	-109.4(2)
C6	C5	C9	H9	124.1(2)
C6	C5	C9	C8	3.5(3)
C4	C5	C9	N2	70.5(3)
C4	C5	C9	H9	-56.0(3)
C4	C5	C9	C8	-176.6(2)
C9	C5	C6	C1	179.1(2)
C9	C5	C6	C7	-1.2(3)
C4	C5	C6	C1	-0.8(4)
C4	C5	C6	C7	178.9(2)
C9	C5	C4	C3	-178.9(2)
C9	C5	C4	H4	1.1(4)
C6	C5	C4	C3	1.0(4)
C6	C5	C4	H4	-179.0(2)
N2	C9	C8	O2	-3.6(2)
N2	C9	C8	H8	-123.3(2)
N2	C9	C8	C7	114.6(2)
C5	C9	C8	O2	-122.6(2)
C5	C9	C8	H8	117.7(2)
C5	C9	C8	C7	-4.4(3)

H9	C9	C8	O2	116.7(2)
H9	C9	C8	H8	-3.0(3)
H9	C9	C8	C7	-125.0(2)
C5	C6	C1	H1	180.0(2)
C5	C6	C1	C2	-0.0(4)
C7	C6	C1	H1	0.4(4)
C7	C6	C1	C2	-179.6(2)
C5	C6	C7	C8	-1.6(3)
C5	C6	C7	H7A	-121.1(2)
C5	C6	C7	H7B	117.8(2)
C1	C6	C7	C8	178.0(3)
C1	C6	C7	H7A	58.5(4)
C1	C6	C7	H7B	-62.5(4)
H13	C13	C12	C11	-179.7(2)
H13	C13	C12	H12	0.3(4)
C14	C13	C12	C11	0.3(4)
C14	C13	C12	H12	-179.7(2)
H13	C13	C14	C15	179.8(2)
H13	C13	C14	H14	-0.2(4)
C12	C13	C14	C15	-0.2(4)
C12	C13	C14	H14	179.8(2)
C6	C1	C2	C3	0.6(4)
C6	C1	C2	H2	-179.4(3)
H1	C1	C2	C3	-179.4(3)
H1	C1	C2	H2	0.7(4)
H3	C3	C2	C1	179.6(3)
H3	C3	C2	H2	-0.4(5)
C4	C3	C2	C1	-0.4(4)
C4	C3	C2	H2	179.6(3)
H3	C3	C4	C5	179.6(3)
H3	C3	C4	H4	-0.5(5)
C2	C3	C4	C5	-0.4(4)
C2	C3	C4	H4	179.6(3)
O2	C8	C7	C6	116.9(2)
O2	C8	C7	H7A	-123.6(2)
O2	C8	C7	H7B	-2.5(3)
C9	C8	C7	C6	3.7(3)
C9	C8	C7	H7A	123.2(2)
C9	C8	C7	H7B	-115.8(2)
H8	C8	C7	C6	-118.4(2)
H8	C8	C7	H7A	1.1(3)
H8	C8	C7	H7B	122.2(2)

Table A11. Bond lengths [Å] for **9a**

H1A	C1	H1B	109.4(7)
H1A	C1	H1C	109.6(7)
H1A	C1	N1	109.5(6)
H1B	C1	H1C	109.5(7)
H1B	C1	N1	109.4(6)
H1C	C1	N1	109.5(6)
H2A	C2	H2B	109.5(7)
H2A	C2	H2C	109.4(7)
H2A	C2	N1	109.4(7)
H2B	C2	H2C	109.5(7)
H2B	C2	N1	109.5(7)
H2C	C2	N1	109.4(7)
H3A	C3	H3B	107.8(6)
H3A	C3	C4	109.1(6)
H3A	C3	N1	109.2(6)
H3B	C3	C4	109.1(6)
H3B	C3	N1	109.1(6)
C4	C3	N1	112.3(5)
C3	C4	N2	112.7(6)
C3	C4	O1	119.5(6)
N2	C4	O1	127.8(6)
C6	C5	C10	117.2(6)
C6	C5	N2	122.0(6)
C10	C5	N2	120.7(5)
C5	C6	H6	119.1(6)
C5	C6	C7	121.7(6)
H6	C6	C7	119.2(6)
C6	C7	H7	119.6(7)
C6	C7	C8	120.8(6)
H7	C7	C8	119.6(7)
C7	C8	H8	120.4(7)
C7	C8	C9	119.0(6)
H8	C8	C9	120.6(7)
C8	C9	H9	119.7(6)
C8	C9	C10	120.7(6)
H9	C9	C10	119.7(6)
C5	C10	C9	120.6(6)
C5	C10	C11	122.3(6)
C9	C10	C11	117.1(6)
C10	C11	N3	129.9(6)
C10	C11	O2	114.5(5)

N3	C11	O2	115.6(6)
H12A	C12	H12B	108.7(6)
H12A	C12	C13	110.5(6)
H12A	C12	O2	110.4(6)
H12B	C12	C13	110.5(6)
H12B	C12	O2	110.4(6)
C13	C12	O2	106.3(5)
C12	C13	C14	110.9(5)
C12	C13	C15	110.8(5)
C12	C13	N3	100.9(5)
C14	C13	C15	112.5(5)
C14	C13	N3	112.2(5)
C15	C13	N3	109.1(5)
C13	C14	H14A	109.5(6)
C13	C14	H14B	109.4(6)
C13	C14	H14C	109.5(6)
H14A	C14	H14B	109.5(6)
H14A	C14	H14C	109.5(6)
H14B	C14	H14C	109.4(6)
C13	C15	H15A	109.5(6)
C13	C15	H15B	109.5(6)
C13	C15	H15C	109.5(6)
H15A	C15	H15B	109.3(6)
H15A	C15	H15C	109.4(6)
H15B	C15	H15C	109.6(6)
C1	N1	C2	109.0(5)
C1	N1	C3	110.8(5)
C1	N1	Pd1	107.5(4)
C2	N1	C3	108.3(5)
C2	N1	Pd1	117.4(4)
C3	N1	Pd1	103.7(4)
C4	N2	C5	120.0(6)
C4	N2	Pd1	115.2(4)
C5	N2	Pd1	124.7(4)
C11	N3	C13	108.7(5)
C11	N3	Pd1	121.3(4)
C13	N3	Pd1	129.9(4)
C11	O2	C12	106.1(5)
N1	Pd1	N2	80.7(2)
N1	Pd1	N3	171.2(2)
N1	Pd1	Cl1	92.5(1)
N2	Pd1	N3	90.7(2)
N2	Pd1	Cl1	172.5(2)

N3	Pd1	Cl1	96.1(1)
H16A	C16	H16B	109.4(7)
H16A	C16	H16C	109.6(7)
H16A	C16	N4	109.5(6)
H16B	C16	H16C	109.4(7)
H16B	C16	N4	109.5(6)
H16C	C16	N4	109.5(6)
H17A	C17	H17B	109.4(6)
H17A	C17	H17C	109.5(6)
H17A	C17	N4	109.4(6)
H17B	C17	H17C	109.5(6)
H17B	C17	N4	109.4(6)
H17C	C17	N4	109.5(6)
H18A	C18	H18B	107.9(6)
H18A	C18	C19	109.0(6)
H18A	C18	N4	109.1(6)
H18B	C18	C19	109.1(6)
H18B	C18	N4	109.0(6)
C19	C18	N4	112.6(5)
C18	C19	N5	112.6(5)
C18	C19	O3	119.5(6)
N5	C19	O3	127.8(6)
C21	C20	C25	117.4(6)
C21	C20	N5	121.6(6)
C25	C20	N5	121.0(5)
C20	C21	H21	119.2(7)
C20	C21	C22	121.7(6)
H21	C21	C22	119.1(7)
C21	C22	H22	119.5(7)
C21	C22	C23	121.1(7)
H22	C22	C23	119.4(7)
C22	C23	H23	120.6(7)
C22	C23	C24	118.7(6)
H23	C23	C24	120.6(7)
C23	C24	H24	119.5(6)
C23	C24	C25	120.9(6)
H24	C24	C25	119.5(6)
C20	C25	C24	120.0(6)
C20	C25	C26	122.9(5)
C24	C25	C26	117.0(5)
C25	C26	N6	129.8(5)
C25	C26	O4	114.1(5)
N6	C26	O4	116.2(5)

H27A	C27	H27B	108.7(6)
H27A	C27	C28	110.7(6)
H27A	C27	O4	110.7(6)
H27B	C27	C28	110.7(6)
H27B	C27	O4	110.6(6)
C28	C27	O4	105.4(5)
C27	C28	C29	110.4(5)
C27	C28	C30	110.0(5)
C27	C28	N6	100.7(5)
C29	C28	C30	114.0(5)
C29	C28	N6	111.7(5)
C30	C28	N6	109.4(5)
C28	C29	H29A	109.5(6)
C28	C29	H29B	109.5(6)
C28	C29	H29C	109.5(6)
H29A	C29	H29B	109.4(6)
H29A	C29	H29C	109.5(6)
H29B	C29	H29C	109.5(6)
C28	C30	H30A	109.5(6)
C28	C30	H30B	109.5(6)
C28	C30	H30C	109.5(6)
H30A	C30	H30B	109.4(7)
H30A	C30	H30C	109.5(7)
H30B	C30	H30C	109.4(7)
C16	N4	C17	108.8(5)
C16	N4	C18	107.7(5)
C16	N4	Pd2	118.5(4)
C17	N4	C18	110.0(5)
C17	N4	Pd2	108.1(4)
C18	N4	Pd2	103.4(4)
C19	N5	C20	120.5(5)
C19	N5	Pd2	113.4(4)
C20	N5	Pd2	126.0(4)
C26	N6	C28	108.1(5)
C26	N6	Pd2	123.2(4)
C28	N6	Pd2	128.6(4)
C26	O4	C27	106.6(5)
N4	Pd2	N5	81.6(2)
N4	Pd2	N6	172.0(2)
N4	Pd2	Cl2	91.2(1)
N5	Pd2	N6	90.4(2)
N5	Pd2	Cl2	172.5(1)
N6	Pd2	Cl2	96.8(1)

Table A12. Angles [°] for **9a**

H1A	C1	H1B	109.4(7)
H1A	C1	H1C	109.6(7)
H1A	C1	N1	109.5(6)
H1B	C1	H1C	109.5(7)
H1B	C1	N1	109.4(6)
H1C	C1	N1	109.5(6)
H2A	C2	H2B	109.5(7)
H2A	C2	H2C	109.4(7)
H2A	C2	N1	109.4(7)
H2B	C2	H2C	109.5(7)
H2B	C2	N1	109.5(7)
H2C	C2	N1	109.4(7)
H3A	C3	H3B	107.8(6)
H3A	C3	C4	109.1(6)
H3A	C3	N1	109.2(6)
H3B	C3	C4	109.1(6)
H3B	C3	N1	109.1(6)
C4	C3	N1	112.3(5)
C3	C4	N2	112.7(6)
C3	C4	O1	119.5(6)
N2	C4	O1	127.8(6)
C6	C5	C10	117.2(6)
C6	C5	N2	122.0(6)
C10	C5	N2	120.7(5)
C5	C6	H6	119.1(6)
C5	C6	C7	121.7(6)
H6	C6	C7	119.2(6)
C6	C7	H7	119.6(7)
C6	C7	C8	120.8(6)
H7	C7	C8	119.6(7)
C7	C8	H8	120.4(7)
C7	C8	C9	119.0(6)
H8	C8	C9	120.6(7)
C8	C9	H9	119.7(6)
C8	C9	C10	120.7(6)
H9	C9	C10	119.7(6)
C5	C10	C9	120.6(6)
C5	C10	C11	122.3(6)
C9	C10	C11	117.1(6)
C10	C11	N3	129.9(6)
C10	C11	O2	114.5(5)

N3	C11	O2	115.6(6)
H12A	C12	H12B	108.7(6)
H12A	C12	C13	110.5(6)
H12A	C12	O2	110.4(6)
H12B	C12	C13	110.5(6)
H12B	C12	O2	110.4(6)
C13	C12	O2	106.3(5)
C12	C13	C14	110.9(5)
C12	C13	C15	110.8(5)
C12	C13	N3	100.9(5)
C14	C13	C15	112.5(5)
C14	C13	N3	112.2(5)
C15	C13	N3	109.1(5)
C13	C14	H14A	109.5(6)
C13	C14	H14B	109.4(6)
C13	C14	H14C	109.5(6)
H14A	C14	H14B	109.5(6)
H14A	C14	H14C	109.5(6)
H14B	C14	H14C	109.4(6)
C13	C15	H15A	109.5(6)
C13	C15	H15B	109.5(6)
C13	C15	H15C	109.5(6)
H15A	C15	H15B	109.3(6)
H15A	C15	H15C	109.4(6)
H15B	C15	H15C	109.6(6)
C1	N1	C2	109.0(5)
C1	N1	C3	110.8(5)
C1	N1	Pd1	107.5(4)
C2	N1	C3	108.3(5)
C2	N1	Pd1	117.4(4)
C3	N1	Pd1	103.7(4)
C4	N2	C5	120.0(6)
C4	N2	Pd1	115.2(4)
C5	N2	Pd1	124.7(4)
C11	N3	C13	108.7(5)
C11	N3	Pd1	121.3(4)
C13	N3	Pd1	129.9(4)
C11	O2	C12	106.1(5)
N1	Pd1	N2	80.7(2)
N1	Pd1	N3	171.2(2)
N1	Pd1	Cl1	92.5(1)
N2	Pd1	N3	90.7(2)
N2	Pd1	Cl1	172.5(2)

N3	Pd1	Cl1	96.1(1)
H16A	C16	H16B	109.4(7)
H16A	C16	H16C	109.6(7)
H16A	C16	N4	109.5(6)
H16B	C16	H16C	109.4(7)
H16B	C16	N4	109.5(6)
H16C	C16	N4	109.5(6)
H17A	C17	H17B	109.4(6)
H17A	C17	H17C	109.5(6)
H17A	C17	N4	109.4(6)
H17B	C17	H17C	109.5(6)
H17B	C17	N4	109.4(6)
H17C	C17	N4	109.5(6)
H18A	C18	H18B	107.9(6)
H18A	C18	C19	109.0(6)
H18A	C18	N4	109.1(6)
H18B	C18	C19	109.1(6)
H18B	C18	N4	109.0(6)
C19	C18	N4	112.6(5)
C18	C19	N5	112.6(5)
C18	C19	O3	119.5(6)
N5	C19	O3	127.8(6)
C21	C20	C25	117.4(6)
C21	C20	N5	121.6(6)
C25	C20	N5	121.0(5)
C20	C21	H21	119.2(7)
C20	C21	C22	121.7(6)
H21	C21	C22	119.1(7)
C21	C22	H22	119.5(7)
C21	C22	C23	121.1(7)
H22	C22	C23	119.4(7)
C22	C23	H23	120.6(7)
C22	C23	C24	118.7(6)
H23	C23	C24	120.6(7)
C23	C24	H24	119.5(6)
C23	C24	C25	120.9(6)
H24	C24	C25	119.5(6)
C20	C25	C24	120.0(6)
C20	C25	C26	122.9(5)
C24	C25	C26	117.0(5)
C25	C26	N6	129.8(5)
C25	C26	O4	114.1(5)
N6	C26	O4	116.2(5)

H27A	C27	H27B	108.7(6)
H27A	C27	C28	110.7(6)
H27A	C27	O4	110.7(6)
H27B	C27	C28	110.7(6)
H27B	C27	O4	110.6(6)
C28	C27	O4	105.4(5)
C27	C28	C29	110.4(5)
C27	C28	C30	110.0(5)
C27	C28	N6	100.7(5)
C29	C28	C30	114.0(5)
C29	C28	N6	111.7(5)
C30	C28	N6	109.4(5)
C28	C29	H29A	109.5(6)
C28	C29	H29B	109.5(6)
C28	C29	H29C	109.5(6)
H29A	C29	H29B	109.4(6)
H29A	C29	H29C	109.5(6)
H29B	C29	H29C	109.5(6)
C28	C30	H30A	109.5(6)
C28	C30	H30B	109.5(6)
C28	C30	H30C	109.5(6)
H30A	C30	H30B	109.4(7)
H30A	C30	H30C	109.5(7)
H30B	C30	H30C	109.4(7)
C16	N4	C17	108.8(5)
C16	N4	C18	107.7(5)
C16	N4	Pd2	118.5(4)
C17	N4	C18	110.0(5)
C17	N4	Pd2	108.1(4)
C18	N4	Pd2	103.4(4)
C19	N5	C20	120.5(5)
C19	N5	Pd2	113.4(4)
C20	N5	Pd2	126.0(4)
C26	N6	C28	108.1(5)
C26	N6	Pd2	123.2(4)
C28	N6	Pd2	128.6(4)
C26	O4	C27	106.6(5)
N4	Pd2	N5	81.6(2)
N4	Pd2	N6	172.0(2)
N4	Pd2	Cl2	91.2(1)
N5	Pd2	N6	90.4(2)
N5	Pd2	Cl2	172.5(1)
N6	Pd2	Cl2	96.8(1)

Table A13. Torsion angles [°] for **9a**

H1A	C1	N1	C2	-63.4(7)
H1A	C1	N1	C3	177.4(6)
H1A	C1	N1	Pd1	64.8(6)
H1B	C1	N1	C2	176.7(6)
H1B	C1	N1	C3	57.5(8)
H1B	C1	N1	Pd1	-55.1(7)
H1C	C1	N1	C2	56.7(8)
H1C	C1	N1	C3	-62.4(7)
H1C	C1	N1	Pd1	-175.1(5)
H2A	C2	N1	C1	61.6(8)
H2A	C2	N1	C3	-177.7(6)
H2A	C2	N1	Pd1	-60.8(7)
H2B	C2	N1	C1	-58.4(8)
H2B	C2	N1	C3	62.2(8)
H2B	C2	N1	Pd1	179.1(5)
H2C	C2	N1	C1	-178.5(6)
H2C	C2	N1	C3	-57.8(8)
H2C	C2	N1	Pd1	59.0(7)
H3A	C3	C4	N2	101.3(7)
H3A	C3	C4	O1	-76.9(8)
H3B	C3	C4	N2	-141.1(6)
H3B	C3	C4	O1	40.7(9)
N1	C3	C4	N2	-19.9(8)
N1	C3	C4	O1	161.9(6)
H3A	C3	N1	C1	161.4(6)
H3A	C3	N1	C2	41.9(7)
H3A	C3	N1	Pd1	-83.5(6)
H3B	C3	N1	C1	43.7(7)
H3B	C3	N1	C2	-75.7(7)
H3B	C3	N1	Pd1	158.8(5)
C4	C3	N1	C1	-77.4(7)
C4	C3	N1	C2	163.1(5)
C4	C3	N1	Pd1	37.7(6)
C3	C4	N2	C5	164.9(6)
C3	C4	N2	Pd1	-10.9(7)
O1	C4	N2	C5	-17(1)
O1	C4	N2	Pd1	167.2(6)
C10	C5	C6	H6	-178.4(6)
C10	C5	C6	C7	1.7(9)
N2	C5	C6	H6	4(1)
N2	C5	C6	C7	-175.9(6)

C6	C5	C10	C9	-0.7(9)
C6	C5	C10	C11	179.9(6)
N2	C5	C10	C9	176.8(6)
N2	C5	C10	C11	-2.5(9)
C6	C5	N2	C4	-26.7(9)
C6	C5	N2	Pd1	148.6(5)
C10	C5	N2	C4	155.8(6)
C10	C5	N2	Pd1	-28.9(8)
C5	C6	C7	H7	177.8(7)
C5	C6	C7	C8	-2(1)
H6	C6	C7	H7	-2(1)
H6	C6	C7	C8	177.9(7)
C6	C7	C8	H8	-178.4(7)
C6	C7	C8	C9	2(1)
H7	C7	C8	H8	2(1)
H7	C7	C8	C9	-178.3(7)
C7	C8	C9	H9	179.2(7)
C7	C8	C9	C10	-1(1)
H8	C8	C9	H9	-1(1)
H8	C8	C9	C10	179.3(6)
C8	C9	C10	C5	0(1)
C8	C9	C10	C11	179.6(6)
H9	C9	C10	C5	-179.7(6)
H9	C9	C10	C11	-0(1)
C5	C10	C11	N3	23(1)
C5	C10	C11	O2	-158.4(6)
C9	C10	C11	N3	-155.9(7)
C9	C10	C11	O2	22.3(8)
C10	C11	N3	C13	173.9(6)
C10	C11	N3	Pd1	-8.9(9)
O2	C11	N3	C13	-4.3(7)
O2	C11	N3	Pd1	172.8(4)
C10	C11	O2	C12	175.4(5)
N3	C11	O2	C12	-6.1(7)
H12A	C12	C13	C14	-14.3(8)
H12A	C12	C13	C15	-139.9(6)
H12A	C12	C13	N3	104.7(6)
H12B	C12	C13	C14	106.0(6)
H12B	C12	C13	C15	-19.6(8)
H12B	C12	C13	N3	-135.0(6)
O2	C12	C13	C14	-134.1(5)
O2	C12	C13	C15	100.2(6)
O2	C12	C13	N3	-15.1(6)

H12A	C12	O2	C11	-106.3(6)
H12B	C12	O2	C11	133.4(6)
C13	C12	O2	C11	13.5(6)
C12	C13	C14	H14A	63.9(7)
C12	C13	C14	H14B	-56.0(7)
C12	C13	C14	H14C	-176.0(5)
C15	C13	C14	H14A	-171.4(5)
C15	C13	C14	H14B	68.7(7)
C15	C13	C14	H14C	-51.3(7)
N3	C13	C14	H14A	-48.0(7)
N3	C13	C14	H14B	-168.0(5)
N3	C13	C14	H14C	72.1(7)
C12	C13	C15	H15A	-173.2(5)
C12	C13	C15	H15B	66.9(7)
C12	C13	C15	H15C	-53.3(7)
C14	C13	C15	H15A	62.0(7)
C14	C13	C15	H15B	-57.8(7)
C14	C13	C15	H15C	-178.0(6)
N3	C13	C15	H15A	-63.0(7)
N3	C13	C15	H15B	177.1(5)
N3	C13	C15	H15C	56.9(7)
C12	C13	N3	C11	12.0(6)
C12	C13	N3	Pd1	-164.8(4)
C14	C13	N3	C11	130.0(6)
C14	C13	N3	Pd1	-46.7(7)
C15	C13	N3	C11	-104.7(6)
C15	C13	N3	Pd1	78.5(6)
C1	N1	Pd1	N2	83.6(4)
C1	N1	Pd1	N3	99(1)
C1	N1	Pd1	Cl1	-93.1(4)
C2	N1	Pd1	N2	-153.2(5)
C2	N1	Pd1	N3	-138(1)
C2	N1	Pd1	Cl1	30.1(5)
C3	N1	Pd1	N2	-33.8(4)
C3	N1	Pd1	N3	-19(1)
C3	N1	Pd1	Cl1	149.5(4)
C4	N2	Pd1	N1	26.2(5)
C4	N2	Pd1	N3	-151.5(5)
C4	N2	Pd1	Cl1	52(2)
C5	N2	Pd1	N1	-149.3(5)
C5	N2	Pd1	N3	33.0(5)
C5	N2	Pd1	Cl1	-123(1)
C11	N3	Pd1	N1	-30(2)

C11	N3	Pd1	N2	-14.7(5)
C11	N3	Pd1	Cl1	162.3(5)
C13	N3	Pd1	N1	147(1)
C13	N3	Pd1	N2	161.8(5)
C13	N3	Pd1	Cl1	-21.2(5)
H16A	C16	N4	C17	53.0(7)
H16A	C16	N4	C18	172.2(5)
H16A	C16	N4	Pd2	-71.0(7)
H16B	C16	N4	C17	-66.9(7)
H16B	C16	N4	C18	52.3(7)
H16B	C16	N4	Pd2	169.1(4)
H16C	C16	N4	C17	173.2(5)
H16C	C16	N4	C18	-67.6(7)
H16C	C16	N4	Pd2	49.2(7)
H17A	C17	N4	C16	174.8(5)
H17A	C17	N4	C18	57.0(7)
H17A	C17	N4	Pd2	-55.3(6)
H17B	C17	N4	C16	54.9(7)
H17B	C17	N4	C18	-62.9(7)
H17B	C17	N4	Pd2	-175.2(4)
H17C	C17	N4	C16	-65.1(7)
H17C	C17	N4	C18	177.1(5)
H17C	C17	N4	Pd2	64.8(6)
H18A	C18	C19	N5	103.4(6)
H18A	C18	C19	O3	-73.9(8)
H18B	C18	C19	N5	-139.0(6)
H18B	C18	C19	O3	43.7(8)
N4	C18	C19	N5	-17.8(7)
N4	C18	C19	O3	164.9(6)
H18A	C18	N4	C16	42.9(7)
H18A	C18	N4	C17	161.3(5)
H18A	C18	N4	Pd2	-83.4(5)
H18B	C18	N4	C16	-74.7(6)
H18B	C18	N4	C17	43.8(7)
H18B	C18	N4	Pd2	159.0(5)
C19	C18	N4	C16	164.1(5)
C19	C18	N4	C17	-77.5(6)
C19	C18	N4	Pd2	37.8(6)
C18	C19	N5	C20	168.4(5)
C18	C19	N5	Pd2	-13.4(6)
O3	C19	N5	C20	-15(1)
O3	C19	N5	Pd2	163.6(6)
C25	C20	C21	H21	178.4(6)

C25	C20	C21	C22	-2(1)
N5	C20	C21	H21	-1(1)
N5	C20	C21	C22	178.8(6)
C21	C20	C25	C24	1.4(9)
C21	C20	C25	C26	178.3(6)
N5	C20	C25	C24	-178.9(6)
N5	C20	C25	C26	-2.0(9)
C21	C20	N5	C19	-25.7(9)
C21	C20	N5	Pd2	156.4(5)
C25	C20	N5	C19	154.6(6)
C25	C20	N5	Pd2	-23.3(8)
C20	C21	C22	H22	179.9(7)
C20	C21	C22	C23	-0(1)
H21	C21	C22	H22	-0(1)
H21	C21	C22	C23	180.0(7)
C21	C22	C23	H23	-178.2(7)
C21	C22	C23	C24	2(1)
H22	C22	C23	H23	2(1)
H22	C22	C23	C24	-178.2(7)
C22	C23	C24	H24	178.1(7)
C22	C23	C24	C25	-2(1)
H23	C23	C24	H24	-2(1)
H23	C23	C24	C25	178.1(6)
C23	C24	C25	C20	0(1)
C23	C24	C25	C26	-176.9(6)
H24	C24	C25	C20	-179.7(6)
H24	C24	C25	C26	3.2(9)
C20	C25	C26	N6	17(1)
C20	C25	C26	O4	-163.4(6)
C24	C25	C26	N6	-166.2(6)
C24	C25	C26	O4	13.6(8)
C25	C26	N6	C28	-179.6(6)
C25	C26	N6	Pd2	-3.6(9)
O4	C26	N6	C28	0.7(7)
O4	C26	N6	Pd2	176.7(4)
C25	C26	O4	C27	168.4(5)
N6	C26	O4	C27	-11.8(7)
H27A	C27	C28	C29	-14.4(8)
H27A	C27	C28	C30	-141.0(6)
H27A	C27	C28	N6	103.7(6)
H27B	C27	C28	C29	106.3(6)
H27B	C27	C28	C30	-20.3(8)
H27B	C27	C28	N6	-135.6(5)

O4	C27	C28	C29	-134.1(5)
O4	C27	C28	C30	99.3(6)
O4	C27	C28	N6	-16.0(6)
H27A	C27	O4	C26	-102.5(6)
H27B	C27	O4	C26	136.9(6)
C28	C27	O4	C26	17.2(6)
C27	C28	C29	H29A	54.3(7)
C27	C28	C29	H29B	-65.6(7)
C27	C28	C29	H29C	174.3(5)
C30	C28	C29	H29A	178.6(6)
C30	C28	C29	H29B	58.7(7)
C30	C28	C29	H29C	-61.3(7)
N6	C28	C29	H29A	-56.8(7)
N6	C28	C29	H29B	-176.7(5)
N6	C28	C29	H29C	63.2(7)
C27	C28	C30	H30A	-177.0(6)
C27	C28	C30	H30B	63.1(7)
C27	C28	C30	H30C	-56.9(7)
C29	C28	C30	H30A	58.5(8)
C29	C28	C30	H30B	-61.5(8)
C29	C28	C30	H30C	178.5(6)
N6	C28	C30	H30A	-67.3(7)
N6	C28	C30	H30B	172.7(5)
N6	C28	C30	H30C	52.8(7)
C27	C28	N6	C26	9.8(6)
C27	C28	N6	Pd2	-165.9(4)
C29	C28	N6	C26	126.9(5)
C29	C28	N6	Pd2	-48.8(7)
C30	C28	N6	C26	-106.0(6)
C30	C28	N6	Pd2	78.3(6)
C16	N4	Pd2	N5	-154.1(5)
C16	N4	Pd2	N6	-147(1)
C16	N4	Pd2	Cl2	28.1(4)
C17	N4	Pd2	N5	81.6(4)
C17	N4	Pd2	N6	89(1)
C17	N4	Pd2	Cl2	-96.2(4)
C18	N4	Pd2	N5	-35.0(4)
C18	N4	Pd2	N6	-28(2)
C18	N4	Pd2	Cl2	147.1(3)
C19	N5	Pd2	N4	28.6(4)
C19	N5	Pd2	N6	-150.4(4)
C19	N5	Pd2	Cl2	45(1)
C20	N5	Pd2	N4	-153.3(5)

C20	N5	Pd2	N6	27.6(5)
C20	N5	Pd2	Cl2	-137(1)
C26	N6	Pd2	N4	-21(2)
C26	N6	Pd2	N5	-14.2(5)
C26	N6	Pd2	Cl2	163.8(4)
C28	N6	Pd2	N4	154(1)
C28	N6	Pd2	N5	160.9(5)
C28	N6	Pd2	Cl2	-21.1(5)

CHAPTER 8 – REFERENCES

- (1) Bhattacharya, P.; Guan, H. Synthesis and catalytic applications of iron pincer complexes. *Comments Inorg. Chem.* **2011**, 32, 88-112.
- (2) Constable, E. C.; Housecroft, C. E. Coordination chemistry: the scientific legacy of Alfred Werner. *Chem. Soc. Rev.* **2013**, 42, 1429-1439.
- (3) Miessler, G. L.; Tarr, D. A. Inorganic Chemistry, 3rd ed.; Prentice Hall: New Jersey, **2003**.
- (4) Gwynne, E. A.; Stephan, D. W. Nickel(II) and Palladium(II) bis-aminophosphine pincer complexes. *Organometallics* **2011**, 30, 4128-4135.
- (5) Zargarian, D.; Castronguay, A.; Spasyuk, D. M. ECE-type pincer complexes of nickel. *Top. Organomet. Chem.* **2013**, 40, 131-173.
- (6) Morales-Morales, D. Pincer complexes. Applications in catalysis. *Rev. Soc. Quim. Mex.* **2004**, 48, 338-346.
- (7) Motoyama, Y.; Shimozone, K.; Nishiyama, H. Novel (oxazolinyl)phenyl phosphine pincer ligand: development of the first non-symmetrical, PCN type chiral palladium and platinum complexes. *Inorg. Chim. Acta*, **2006**, 359, 1725-1730.
- (8) Vicente, J.; Arcas, A.; Julia-Hernandez, F. Organometallic complexes of palladium(II) derived from 2,6-diacetylpyridine dimethylketal. *Organometallics* **2010**, 29, 3066-3076.
- (9) Ito, J.; Ujiie, S.; Nishiyama, H. Chiral bis(oxazolinyl)phenyl Ru^{II} catalysts for highly enantioselective cyclopropanation. *Chem. Eur. J.* **2010**, 16, 4986-4990.
- (10) Konrad, F.; Fillol, J. L.; Rettenmeier, C.; Wadepohl, H.; Gade, L. H. Bis(oxazolinylmethyl) derivatives of C₄H₄E heterocycles (E = NH, O, S) as C₂-

- chiral meridionally coordinating ligands for nickel and chromium. *Eur. J. Inorg. Chem.* **2009**, 4950-4961.
- (11) El-Zaria, M. E.; Arii, H.; Nakamura, H. *m*-Carborane based chiral NBN pincer-metal complexes: synthesis, structure, and application in asymmetric catalysis. *Inorg. Chem.* **2011**, *50*, 4149-4161.
- (12) Polukeev, A. V.; Kuklin, S. A.; Petrovskii, P. V.; Peregudova, S. M.; Smol'yakov, A. F.; Dolgushin, F. M.; Koridze, A. A. Synthesis and characterization of fluorophenylpalladium pincer complexes: electronic properties of some pincer ligands evaluated by multinuclear NMR spectroscopy and electrochemical studies. *Dalton Trans.* **2011**, *40*, 7201-7209.
- (13) Gossage, R. A. Pincer oxazolines: emerging tools in coordination chemistry and catalysis – where to next? *Dalton Trans.* **2011**, *40*, 8755-8759.
- (14) Hollas, A. M.; Gu, W.; Bhuvanesh, N.; Ozerov, O. V. Synthesis and characterization of Pd complexes of a carbazoyl/bis(imine) NNN pincer ligand. *Inorg. Chem.* **2011**, *50*, 3673-3679.
- (15) Kumar, S.; Mani, G.; Mondal, S.; Chattaraj, P. K. Pyrrole-based new diphosphines: Pd and Ni complexes bearing the PNP pincer ligand. *Inorg. Chem.* **2012**, *51*, 12527-12539.
- (16) Vabre, B.; Canac, Y.; Duhayon, C.; Chauvin, R.; Zargarian, D. Nickel(II) complexes of the new pincer-type unsymmetrical ligands PIMCOP, PIMIOCOP, and NHCCOP: versatile binding motifs. *Chem. Commun.* **2012**, *48*, 10446-10448.

- (17) Herbert, D. E.; Miller, A. D.; Ozerov, O. V. Phosphorus(III) cations supported by a PNP pincer ligand and sub-stoichiometric generation of P₄ from thermolysis of a nickel insertion product. *Chem. Eur. J.* **2012**, *18*, 7696-7704.
- (18) Castonguay, A.; Sui-Seng, C.; Zargarian, D.; Beauchamp, A. L. Synthesis and reactivities of new PC_{sp3}P pincer complexes of nickel. *Organometallics* **2006**, *25*, 602-608.
- (19) Ruddy, A. J.; Mitton, S. J.; McDonald, R.; Turculet, L. 'Hemilabile' silyl pincer ligation: platinum group PSiN complexes and triple C-H activation to form a (PSiC) Ru carbene complex. *Chem. Commun.* **2012**, *48*, 1159-1161.
- (20) Lindner, R.; van den Bosch, B.; Lutz, M.; Reek, J. N. H.; van der Vlugt, J. I. Tunable hemilabile ligands for adoptive transition metal complexes. *Organometallics* **2011**, *30*, 499-510.
- (21) van Koten, G. The monoanionic ECE-pincer ligand: a versatile privileged ligand platform – general considerations. *Top. Organomet. Chem.* **2013**, *40*, 1-20.
- (22) Zhang, J.; Pattacini, R.; Braunstein, P. Tridentate assembling ligands based on oxazoline and phosphorus donors in dinuclear Pd(I)-Pd(I) complexes. *Inorg. Chem.* **2009**, *48*, 11954-11962.
- (23) Gossage, R. A.; Jenkins, H. A.; Yadav, P. N. Application of an air stable Pd oxazoline complex for Heck, Suzuki, Sonogashira and related C-C bond-forming reactions. *Tetrahedron Lett.* **2004**, *45*, 7689-7691 (Corrigendum: **2005**, *46*, 5243).
- (24) Button, K. M.; Gossage, R. A.; Phillips, R. K. R. A simple large scale synthesis of 1,3-bis(4,4-dimethyl-2-oxazoliny)benzene. *Synth. Commun.* **2002**, *32*, 363-368.

- (25) Fossey, J. S.; Richards, C. J. Synthesis of 2,6-bis(2-oxazoliny)phenylplatinum(II) NCN pincer complexes by direct cyclometalation. Catalysts for carbon-carbon bond formation. *Organometallics* **2004**, *23*, 367-373.
- (26) Younus, H. A.; Ahmad, N.; Su, W.; Verpoort, F. Ruthenium pincer complexes: Ligand design and complex synthesis. *Coord. Chem. Rev.* **2014**, *276*, 112-152.
- (27) Ito, J.; Nishiyama, H. Synthetic utility of chiral bis(oxazoliny)phenyl transition-metal complexes. *Synlett*, **2012**, 509-523.
- (28) Nishiyama, H. Synthesis and use of bisoxazoliny-phenyl pincers. *Chem. Soc. Rev.* **2007**, *36*, 1133-1141.
- (29) Ito, J.; Nishiyama, H. Recent topics of transfer hydrogenation. *Tetrahedron Lett.* **2014**, *55*, 3153-3166.
- (30) Toda, T.; Kuwata, S.; Ikariya, T. Unsymmetrical pincer-type ruthenium complex containing β -protic pyrazole and *N*-heterocyclic carbene arms: comparison of brønsted acidity of NH groups in second coordination sphere. *Chem. Eur. J.* **2014**, *20*, 9539-9542.
- (31) Ebeling, G.; Meneghetti, M. R.; Rominger, F.; Dupont, J. The trans-chlorometalation of hetero-substituted alkynes: A facile entry to unsymmetrical palladium YCY' (Y, Y' = NR₂, PPh₂, OPPh₂, and SR) "pincer" complexes *Organometallics* **2002**, *21*, 3221-3227.
- (32) Dietrich, B. L.; Egbert, J.; Morris, A. M.; Wicholas, M. Cd(II), Zn(II), and Pd(II) complexes of an isoindoline pincer ligand: consequences of steric crowding. *Inorg. Chem.* **2005**, *44*, 6476-6481.

- (33) Schaub, T.; Radius, U.; Diskin-Posner, Y.; Leitus, G.; Shimon, L. J. W.; Milstein, D. Pyridine-based sulfoxide pincer complexes of Rhodium and Iridium. *Organometallics* **2008**, *27*, 1892-1901.
- (34) Liu, A.; Zhang, X.; Chen, W. New pincer CC'C complexes of Nickel(II) via chloronickelation of alkyne-bearing *N*-heterocyclic carbenes. *Organometallics* **2009**, *28*, 4868-4871.
- (35) Lien, Y.-L.; Chang, Y.-C.; Chuang, N.-T.; Datta, A.; Chen, S.-J.; Hu, C.-H.; Huang, W.-Y.; Lin, C.-H.; Huang, J.-H. A new type of asymmetric tridentate pyrrolyl-linked pincer ligand and its aluminum dihydride complexes. *Inorg. Chem.* **2010**, *49*, 136-143.
- (36) Shibue, M.; Hirotsu, M.; Nishioka, T.; Kinoshita, I. Ruthenium and Rhodium complexes with thiolate-containing pincer ligands produced by C-S bond cleavage of pyridyl-substituted dibenzothiophenes. *Organometallics* **2008**, *27*, 4475-4483.
- (37) Juliá-Hernández, F.; Arcas, A.; Vicente, J. *Chem. Eur. J.* **2012**, *18*, 7780.
- (38) Pozo del, C.; Corma, A.; Iglesias, M.; Sánchez, F. Recyclable mesoporous silica-supported chiral ruthenium-(NHC)NN-pincer catalysts for asymmetric reactions. *Green Chem.* **2011**, *13*, 2471-2481.
- (39) Baratta, W.; Benedetti, F.; Zotto, A. D.; Fanfoni, L.; Felluga, F.; Magnolia, S.; Putignano, E.; Rigo, P. Chiral pincer ruthenium and osmium complexes for the fast and efficient hydrogen transfer reduction of ketones. *Organometallics* **2010**, *29*, 3563-3570.

- (40) Du, W.; Wang, L.; Wu, P.; Yu, Z. A versatile ruthenium(II)-NNC complex catalyst for transfer hydrogenation of ketones and oppenauer-type oxidation of alcohols. *Chem. Eur. J.* **2012**, *18*, 11550-11554.
- (41) Boronat, M.; Corma, A.; Gornález-Arellano, C.; Iglesias, M.; Sánchez, F. Synthesis of electron-rich CNN-pincer complexes, with *N*-heterocyclic carbene and (S)-proline moieties and application to asymmetric hydrogenation. *Organometallics* **2010**, *29*, 134-141.
- (42) Bröring, M.; Kleeberg, C.; Köhler, S. Palladium(II) complexes of unsymmetrical CNN pincer ligands. *Inorg. Chem.* **2008**, *47*, 6404-6412.
- (43) Zeng, G.; & Li, S. Insights into dehydrogenative coupling of alcohols and amines catalyzed by a (PNN)-Ru(II) hydride complex: unusual metal-ligand cooperation. *Inorg. Chem.* **2011**, *50*, 10572-10580.
- (44) Zhang, J.; Balaraman, E.; Leitus, G.; Milstein, D. Electron-rich PNP- and PNN-type ruthenium(II) hydrido borohydride pincer complexes. Synthesis, structure, and catalytic dehydrogenation of alcohols and hydrogenation of esters. *Organometallics* **2011**, *30*, 5716-5724.
- (45) He, L.-P.; Chen, T.; Gong, D.; Lai, Z.; Huang, K.-W. Enhanced reactivities toward amines by introducing an imine arm to the pincer ligand: direct coupling of two amines to form an imine without oxidant. *Organometallics* **2012**, *31*, 5208-5211.
- (46) Decken, A.; Gossage, R. A.; Yadav, P. N. Oxazoline Chemistry—Part VIII: Synthesis and characterisation of a new class of pincer ligands derived from the 2-(o-aniliny)-2-oxazoline skeleton: applications to the synthesis of group X transition metal catalysts. *Can. J. Chem.* **2005**, *83*, 1185-1189.

- (47) Taghvaei, M. Group XI Pincer Oxazoline Complexes. *MSc Thesis*, **2012**, Ryerson University.
- (48) Durran, S. E.; Elsegood, M. R. J.; Hammond, S. R.; Smith, M. B. Flexible κ^4 -PNN'O-tetradentate ligands: synthesis, complexation and structural studies. *Dalton Trans.* **2010**, 39, 7136-7146.
- (49) Button, K. M.; Gossage, R. A. Oxazoline chemistry part III. Synthesis and characterization of [2-(2'-aniliny)-2-oxazolines] and some related compounds. *J. Heterocyclic Chem.* **2003**, 40, 513-517.
- (50) Hornback, J. M. *Organic Chemistry*, 2nd Ed. Brooks/Cole: Belmont, 2006.
- (51) Kunishima, M.; Kawachi, C.; Morita, J.; Terao, K.; Iwasaki, F.; Tani, S. 4-(4,6-Dimethyl-1,3,5-triazin-2-yl)-4-methyl-morpholinium chloride: an efficient condensing agent leading to the formation of amides and esters. *Tetrahedron* **1999**, 55, 13159-13170.
- (52) Jarrold, M. F. Peptides and proteins in the vapor phase. *Annu. Rev. Phys. Chem.* **2000**, 51, 179-207.
- (53) Lesarri, A.; Cocinero, E. J.; Lopez, J. C.; Alonso, J. L. Gas-phase structure of *N,N*-dimethylglycine. *Chem. Phys. Chem.* **2005**, 6, 1559-1566.
- (54) Herasymchuk, K. Novel pincer ligands derived from 2-(2'-aniliny)-4,4-dimethyl-2-oxazoline skeleton. *BSc Thesis*. **2012**, Ryerson University.
- (55) Yella, R. Chloroacetylchloride: A Versatile Reagent in Heterocyclic Synthesis. *Synlett*. **2010**, 835-836.
- (56) Raycroft, M. A. R.; Maxwell, C. I.; Oldham, R. A. A.; Andrea, A. S.; Neverov, A. A.; Brown, R. S. Trifunctional metal ion-catalyzed solvolysis: Cu(II)-promoted

- methanolysis of *N,N*-bis(2-picolyl) benzamides involves unusual lewis acid activation of substrate, delivery of coordinated nucleophile, powerful assistance of the leaving group departure. *Inorg. Chem.* **2012**, *51*, 10325-10333.
- (57) Xu, S.; Held, I.; Kempf, B.; Mayr, H.; Steglich, W.; Zipse, H. The DMAP-Catalyzed Acetylation of Alcohols—A Mechanistic Study (DMAP=4-(Dimethylamino)pyridine). *Chem. Eur. J.* **2005**, *11*, 4751–4757.
- (58) Ghorbani-Choghamarani, A.; Norouzi, M. Protection of hydroxyl groups as a trimethylsilyl ether by 1,1,1,3,3,3-hexamethyldisilazane promoted by aspartic acid as an efficient organocatalyst. *Chin. J. Chem.* **2011**, *32*, 595-598.
- (59) Wuts, P. G. M.; Greene, T. W. *Greene's Protective Groups in Organic Synthesis*, 4th Ed. John Wiley & Sons, United States: New Jersey, 2007.
- (60) Huynh, J. Optimization of the novel pincer ligand derived from 2-(2'-aniliny)-2-oxazolines. *BSc Thesis*. **2014**, Ryerson University.
- (61) Reich, H. J. Chemical Shift. www.chem.wisc.edu/areas/reich/nmr/notes-5-hmr-2-shift.pdf, (accessed August 2, 2014).
- (62) Bara, J. E. Versatile and Scalable Method for Producing *N*-Functionalized Imidazoles. *Ind. Eng. Chem. Res.* **2011**, *50*, 13614-13619.
- (63) Stankevič, M.; Włodarczyk, A.; Jaklińska, M.; Parcheta, R.; Pietrusiewicz, K. M. Sodium in liquid ammonia – a versatile tool in modifications of arylphosphine oxides. *Tetrahedron* **2011**, *67*, 8671-8678.
- (64) Rohlik, Z.; Holzhauser, P.; Kotek, J.; Rudovsky, J.; Nemec, I.; Hermann, P.; Lukes, I. Synthesis and coordination properties of palladium(II) and platinum(II)

- complexes with phosphonated triphenylphosphine derivatives. *J. Organomet. Chem.* **2006**, 691, 2409-2423.
- (65) Dornhaus, F.; Bolte, M.; Lerner, H.-W.; Wagner, M. Phosphanylborohydrides: first assessment of the relative lewis basicities of $[\text{BH}_3\text{PPh}_2]^-$, CH_3PPh_2 , and HPPH_2 . *Eur. J. Inorg. Chem.* **2006**, 1777-1785.
- (66) Pavia, D. L.; Lampman, G. M.; Kriz, G. S.; Vyvyan, J. R. *Introduction to spectroscopy*, 4th Ed. Saunders Brooks/Cole Thompson Learning, United States: Belmont, 2009.
- (67) Schmid, T. E.; Jones, D. C.; Songis, O.; Diebolt, O.; Furst, M. R. L.; Slawin, A. M. Z.; Cazin, C. S. J. Mixed phosphine/*N*-heterocyclic carbene palladium complexes: synthesis, characterization and catalytic use in aqueous Suzuki-Miyaura reactions. *Dalton Trans.*, **2013**, 42, 7345-7353.
- (68) Tessin, U. I.; Bantreil, X.; Songis, O.; Cazin, C. S. J. Highly active $[\text{Pd}(\mu\text{-Cl})\text{Cl}(\text{NHC})]_2$ complexes in the Mizoroki-Heck reaction. *Eur. J. Inorg. Chem.* **2013**, 2007-2010.
- (69) Boronat, M.; Corma, A.; Gornález-Arellano, C.; Iglesias, M.; Sánchez, F. Synthesis of electron-rich CNN-pincer complexes, with *N*-heterocyclic carbene and (*S*)-proline moieties and application to asymmetric hydrogenation. *Organometallics* **2010**, 29, 134-141.
- (70) Tu, T.; Malineni, J.; Dötz, K. H. A novel pyridine-bridged bis-benzimidazolylidene pincer palladium complex: synthesis and catalytic properties. *Adv. Synth. Catal.* **2008**, 350, 1791-1795.

- (71) Santoro, O.; Collado, A.; Slawin, A. M. Z.; Nolan, S. P.; Cazin, C. S. J. A general synthetic route to [Cu(X)(NHC)] (NHC = *N*-heterocyclic carbene, X = Cl, Br, I) complexes. *Chem. Commun.* **2013**, 49, 10483-10485.
- (72) Egbert, J. D.; Cazin, C. S. J.; Nolan, S. P. Copper *N*-heterocyclic carbene complexes in catalysis. *Catal. Sci., Technol.*, **2013**, 3, 912-926.
- (73) Gruger, N.; Rodriguez, L.-I.; Wadeh, H.; Gade, L. H. Achiral and chiral PNP-pincer ligands with a carbazole backbone: coordination chemistry with d⁸ transition metals. *Inorg. Chem.* **2013**, 52, 2050-2059.
- (74) Gao, R.; Zhang, T.; Wang, F.; Sun, W.-H. Nickel(II) complexes chelated by 2-arylimino-6-benzoxazolylpyridine: synthesis, characterization and ethylene oligomerization. *Organometallics* **2008**, 27, 5641-5648.
- (75) Peters, J. C.; Harkins, S. B.; Brown, S. D.; Day, M. W. Pincer-like amido complexes of platinum, palladium and nickel. *Inorg. Chem.* **2001**, 40, 5083-5091.
- (76) [Liu](#), N.; [Wang](#), L.; [Wang](#), Z.-X. Room-temperature nickel-catalyzed cross-couplings of aryl chlorides with arylzincs. *Chem. Commun.* **2011**, 47, 1598-1600.
- (77) Solin, N.; Kjellgren, J.; Szabó, K. J. Pincer complex-catalyzed allylation of aldehyde and imine substrates via nucleophilic η^1 -allyl palladium intermediates. *J. Am. Chem. Soc.* **2004**, 126, 7026-7033.
- (78) Solin, N.; Kjellgren, J.; Szabó, K. J. Palladium-catalyzed electrophilic substitution via monoallylpalladium intermediates. *Angew. Chem. Int. Ed.* **2003**, 42, 3656-3658.
- (79) Yao, Q.; Sheets, M. A SeCSe-Pd(II) pincer complex as a highly efficient catalyst for allylation of aldehydes with allyltributyltin. *J. Org. Chem.* **2006**, 71, 5384-5387.

- (80) Selander, N.; Sebelius, S.; Estay, C.; Szabó, K. J. Highly selective and robust palladium-catalyzed carbon-carbon coupling between allyl alcohols and aldehydes via transient allylboronic acids. *Eur. J. Org. Chem.* **2006**, 4085-4087.
- (81) Selander, N.; Willy, B.; Szabó, K. J. Selective C-H borylation of alkenes by palladium pincer complex catalyzed oxidative functionalization. *Angew. Chem. Int. Ed.* **2010**, *49*, 4051-4053.
- (82) Nakamura, H.; Iwama, H.; Yamamoto, Y. Palladium- and platinum-catalyzed addition of aldehydes and imines with allylstannanes. Chemoselective allylation of imines in the presence of aldehydes. *J. Am. Chem. Soc.* **1996**, *118*, 6641-6647.
- (83) Pilarski, L.; Szabó, K. J. Palladium pincer complex catalyzed functionalization of electrophiles. *Curr. Org. Chem* **2011**, *15*, 3389-3414.
- (84) Aydin, J.; Szabó, K. J. Palladium-pincer complex catalyzed C-C coupling of allyl nitriles with tosyl imines via regioselective allylic C-H bond functionalization. *Org. Lett.* **2008**, *10*, 2881-2884.
- (85) Aydin, J.; Selander, N.; Szabó, K. J. Strategies for fine-tuning the catalytic activity of pincer-complexes. *Tetrahedron Lett.* **2006**, *47*, 8999-9001.
- (86) Selander, N.; Szabó, K. J. Catalysis by palladium pincer complexes. *Chem. Rev.* **2011**, *111*, 2048-2076.